Bioelectrical corrosion of iron by lithotrophic sulfate-reducing bacteria

DISSERTATION

zur

Erlangung des Grades eines

Doktors der Naturwissenschaften

− Dr. rer. nat. –

dem Fachbereich Biologie/Chemie der

Universität Bremen vorgelegt von

Dennis R. Enning

aus Duisburg

Bremen 2012

Die vorliegende Arbeit wurde in der Zeit von Mai 2008 bis Mai 2012 am Max-Planck-Institut für marine Mikrobiologie in Bremen angefertigt.

1. Gutachter: Prof. Dr. Friedrich Widdel, Universität Bremen

2. Gutachter: Prof. Dr. Karl-Heinz Blotevogel, Universität Bremen

Tag des Promotionskolloquiums: 14.06.2012

To my parents

Table of contents

List of abbreviations

(very common abbreviations are not listed)

ASW	Artificial seawater medium
CE	Counter electrode
CMIC	Chemical microbially influenced corrosion
CPE	Constant phase element
DIC	Dissolved inorganic carbon
EBSD	Electron backscatter diffraction analysis
EDX	Energy-dispersive X-ray spectroscopy
EIS	Electrochemical impedance spectroscopy
EMIC	Electrical microbially influenced corrosion
EPS	Extracellular polymeric substances
FISH	Fluorescent *in situ* hybridization
GDP	Gross domestic product
GNP	Gross national product
H_2ase	Hydrogenase
ICP-OES	Inductively coupled plasma optical emission spectroscopy
LSV	Linear sweep voltammetry
MEC	Microbial electrolysis cell
MFC	Microbial fuel cell
MIC	Microbially influenced corrosion
NR-SOB	Nitrate-reducing sulfide-oxidizing bacteria
ppm	Parts per million
ppmv	Parts per million (volume)
PWRI	Produced water re-injection
RE	Reference electrode
SEM	Scanning electron microscopy
SHE	Standard hydrogen electrode
SRB	Sulfate-reducing bacteria
SRR	Sulfate reduction rate
TEAP	Terminal electron-accepting process
WE	Working electrode
XRD	X-ray diffraction analysis

Symbols used in equations

(very common symbols and units are not listed)

a	Area (cm^2)
a_{H^+}	Activity of H_3O^+
$a_{Fe^{2+}}$	Activity of Fe^{2+}
a_{H_2S}	Activity of H_2S
$a_{SO_4^{2-}}$	Activity of SO_4^{2-}
$E_{average}$	Average redox potential for the multi-step reduction of SO_4^{2-} to H_2S (V vs. SHE)
E_{corr}	Free corrosion potential (V vs. SHE)
E_{Fe^{2+}/Fe^0}	Redox equilibrium potential of Fe^{2+}/Fe^0 (V vs. SHE)
$E^{O}_{Fe^{2+}/Fe^0}$	Redox equilibrium potential of Fe^{2+}/Fe^0 at standard conditions (V vs. SHE)
$E^{O'}_{2H^+/H_2}$	Redox equilibrium potential of $2H^+/H_2$ at *pH* 7, but otherwise standard conditions (V vs. SHE)
$E^{O'}_{O_2/H_2O}$	Redox equilibrium potential of O_2/H_2O at *pH* 7, but otherwise standard conditions (V vs. SHE)
ΔG^{O}	Gibbs free energy at standard conditions (kJ mol^{-1})
$\Delta G^{O'}$	Gibbs free energy at standard conditions, except $a_{H^+} = 1$ (kJ mol^{-1})
i	Current density (µA cm^{-2})
$n_{Fe(II)}$	Amount of total ferrous iron formed (mol)
n_{MIC}	Total amount of Fe^0 oxidized by MIC (mol)
n_{FeEMIC}	Amount of Fe^0 oxidized by EMIC (mol)
n_{FeS}	Amount of sulfidic iron (mol)
p_{H_2}	Partial pressure of molecular hydrogen (atm)
q_{Anab}	Quotient iron oxidized for biosynthesis per total iron oxidized by EMIC
q_{EMIC}	Quotient iron oxidized by EMIC per total iron oxidized by MIC
$q_{FeS/Fe(II)}$	Molar share of iron sulfide in total corroded iron
σ	Electrical conductivity (S m^{-1})

List of equations used in Part A and B

(in numerical order)

$$2\ e^- + Fe^{2+} \rightleftarrows Fe^0 \quad (1)$$

$$4\ e^- + O_2 + 4\ H^+ \rightleftarrows 2\ H_2O \quad (2)$$

$$2\ Fe^0 + O_2 + 2\ H_2O \rightarrow 2\ Fe(OH)_2 \quad (3)$$

$$2\ e^- + 2\ H^+ \rightleftarrows H_2 \quad (4)$$

$$Fe^0 + 2\ H^+ \rightarrow Fe^{2+} + H_2 \quad (5)$$

$$4\ FeS + 3\ O_2 + 2\ H_2O \rightarrow 4\ S^0 + 4\ FeOOH \quad (6)$$

$$Fe^0 + S^0 \rightarrow FeS \quad (7)$$

$$2\ CH_3CHOHCOO^- + SO_4^{2-} \rightarrow 2\ CH_3COO^- + 2\ HCO_3^- + HS^- + H^+ \quad (8)$$

$$CH_3COO^- + SO_4^{2-} \rightarrow 2\ HCO_3^- + HS^- \quad (9)$$

$$4\ H_2 + SO_4^{2-} + H^+ \rightarrow HS^- + 4\ H_2O \quad (10)$$

$$Fd_{red}^{2-} + 2\ H^+ \rightleftarrows Fd_{ox} + H_2 + \Delta\mu_{H^+} \quad (11)$$

$$CH_3CHOHCOO^- + H_2O \rightarrow CH_3COO^- + CO_2 + H_2 \quad (12)$$

$$4\ Fe^0 + SO_4^{2-} + 2\ H_2O + 2\ H^+ \rightarrow FeS + 3\ Fe(OH)_2 \quad (13)$$

$$Fe^0 + HS^-_{ads} \rightarrow FeHS^-_{ads} \quad (14)$$

$$FeHS^-_{ads} \rightarrow FeHS^+_{ads} + 2\ e^- \quad (15)$$

$$FeHS^+_{ads} \rightarrow Fe^{2+} + HS^- \quad (16)$$

$$FeHS^+_{ads} \rightarrow FeS + H^+ \quad (17)$$

$$Fe^{2+} + HS^- \rightarrow FeS + H^+ \quad (18)$$

$$Fe^0 + H_2S \rightarrow FeS + H_2 \tag{19}$$

$$Fe^0 + 2\,H^+ \xrightarrow{FeS} Fe^{2+} + H_2 \tag{20}$$

$$8\,e^- + SO_4^{2-} + 10\,H^+ \rightarrow H_2S + 4\,H_2O \tag{21}$$

$$4\,Fe^0 + SO_4^{2-} + 3\,HCO_3^- + 5\,H^+ \rightarrow FeS + 3\,FeCO_3 + 4\,H_2O \tag{22}$$

$$4\,Fe^0 + 5\,HCO_3^- + 5\,H^+ \rightarrow 4\,FeCO_3 + CH_4 + 3\,H_2O \tag{23}$$

$$H^+ \rightarrow (H^+)_* \tag{24}$$

$$(H^+)_* + e^- \rightarrow H_{ads} \tag{25}$$

$$H_{ads} + H_{ads} \rightarrow H_2 \tag{26}$$

$$H_{ads} + (H^+)_* + e^- \rightarrow H_2 \tag{27}$$

$$FeCO_3 + HS^- \rightarrow FeS + HCO_3^- \tag{28}$$

$$q_{EMIC} = \frac{n_{FeEMIC}}{n_{FeMIC}} = \frac{4\,(1 - n_{FeS} / n_{Fe(II)})}{3 + q_{Anab}} \tag{29}$$

Summary

Iron (Fe^0), a technological material of prime importance, deteriorates by interaction with its abiotic and biotic environment. While the corrosion of iron in oxic environments is, to our present knowledge, a largely chemical (abiotic) process, corrosion in anoxic environments is heavily affected by microbial activity. In technology, this is referred to as microbially influenced corrosion (MIC). Contrary to the more prominent rusting of iron with oxygen, MIC usually is a hidden process occurring in places such as closed cooling water systems or buried pipelines. The inferred economic costs are tremendous.

Sulfate-reducing bacteria (SRB) are the suspected main culprits; MIC usually is most severe in sulfate-containing environments, and iron sulfides (FeS), the characteristic product of SRB-induced corrosion, are ubiquitously found at the affected sites. Metal destruction by SRB is conventionally attributed to three effects, (i) the chemical aggressiveness of their metabolic product sulfide (H_2S, HS^-), (ii) a facilitated cathodic reduction of H^+-ions to molecular hydrogen at deposited iron sulfides and (iii) the microbial consumption of cathodic hydrogen from the iron or iron sulfides. Recently, another mechanism, i.e. direct electron uptake from metallic iron, has been discovered in specialized lithotrophic SRB that were isolated from enrichment cultures with iron as the only source of electrons (Dinh *et al*., 2004).

In the present study we investigated the suggested mechanisms of SRB-induced corrosion with particular emphasis on the latter, 'bioelectrical' process. This was achieved by a combination of kinetic and electrochemical studies in axenic SRB microcosms, and the physicochemical analysis of the formed corrosion products. Little or no corrosion resulted from galvanically coupled iron sulfides and microbial consumption of hydrogen, respectively. However, the specialized lithotrophic SRB corroded metallic iron severely and formed large amounts of an electroconductive mineral crust. Their corrosiveness results from the formation of a galvanic element between the iron anode and the bacterial cathode. Electrons flow from the iron ($4\,Fe^0 \rightarrow 4\,Fe^{2+} + 8\,e^-$) through the sulfidic crust to the crust-attached bacteria reducing sulfate ($8\,e^- + SO_4^{2-} + 10\,H^+ \rightarrow H_2S + 4\,H_2O$). The biological cathodic reaction controls the rate and, with appropriately adjusted cultivation conditions, such bioelectrical corrosion progressed at technologically highly relevant rates in long-term incubations.

The direct corrosion of iron through electron uptake is here referred to as electrical microbially influenced corrosion (EMIC). This mechanism is fundamentally different from the indirect corrosive effect of SRB owing to the excretion of the chemical hydrogen sulfide (chemical microbially influenced corrosion, CMIC). CMIC is also known to progress at high rates in laboratory cultures. Hence, we intended to unravel the relative contribution of EMIC

and CMIC to total microbial corrosion in natural sulfate-rich environments. Careful chemical analysis of corrosion products combined with knowledge of the fundamental differences of the two corrosion mechanisms allowed such quantitative assessment. In a marine tidal mud flat, studied as an example of a sulfate-rich environment possibly favoring MIC, severe metal corrosion could indeed be observed and exclusively attributed to EMIC, i.e. bioelectrical corrosion by lithotrophic SRB. A better understanding of microbial corrosion mechanisms as well as their quantitative contribution to corrosion damage is expected to aid in the development of more effective MIC prevention and mitigation strategies.

The striking physiological ability of the organisms to corrode iron by direct electron uptake apparently has polyphyletic origin; it was found in several phylogenetically unrelated bacterial isolates. However, the ecological role of such microorganisms in their natural (metal-free) habitat is currently unknown. Interestingly, we detected high numbers of directly corrosive SRB in marine anoxic sediment, despite obvious absence of man-made iron constructions. It is hypothesized that anaerobic biocorrosion is due to the promiscuous use of an ecophysiologically relevant catabolic trait for uptake of external electrons from natural abiotic and biotic sources.

Zusammenfassung

Das technisch bedeutsamste Metall Eisen korrodiert im wässrigen Milieu als Folge chemischer, aber auch biologischer Abläufe. Die Korrosion metallischen Eisens (Fe^0) mit Luftsauerstoff ist, nach derzeitigem Kenntnisstand, ein überwiegend chemisches (abiotisches) Phänomen. Ganz anders ist dies in sauerstofffreien Umgebungen, in denen Eisen mitunter sehr schnell und als Folge mikrobieller Aktivität korrodiert. Hierfür hat sich der technische Begriff mikrobiell beeinflusste Korrosion (Englisch: microbially influenced corrosion, MIC) etabliert. Anders als das bekannte Rosten von Eisen mit Sauerstoff, ist die mikrobielle Korrosion ein Prozess der überwiegend im Verborgenen, etwa in Kühlwasserkreisläufen oder an vergrabenen Pipelines, stattfindet. Die wirtschaftlichen Kosten der resultierende Materialzerstörung sind enorm.

Einer der wichtigsten biologischen Faktoren in der Korrosion von Eisen ist vermutlich die Aktivität von sulfatreduzierenden Bakterien. Diese Vermutung begründet sich durch die Beobachtung, dass die anaerobe (sauerstofffreie) Korrosion besonders gravierende Ausmaße in sulfathaltigen Gewässern annimmt und dass Eisensulfid (FeS), das charakteristische Korrosionsprodukt der SRB, fast immer mit solch schweren Korrosionsschäden assoziiert vorliegt. Die beobachtete Materialzerstörung durch sulfatreduzierende Bakterien wird üblicherweise drei sich ergänzenden Wirkungsmechanismen zugeschrieben. Dies ist erstens, die hohe Reaktivität des durch SRB gebildeten Sulfids (H_2S, HS^-) gegenüber Eisen. Zweitens, schreibt man dem daraus resultierenden FeS eine oberflächenkatalytische Wirkung zu, welche die Reduktion von Protonen (aus Wasser) zu molekularem Wasserstoff beschleunigt. Drittens, vermutet man eine Beschleunigung der Korrosion durch die mikrobielle Oxidation des kathodischen Wasserstoffs am Eisen oder an den Eisensulfiden. Kürzlich wurde an spezialisierten, lithotrophen Neuisolaten aus Anreicherungskulturen mit metallischem Eisen als einzigem Elektronendonator noch ein weiterer Mechanismus entdeckt (Dinh *et al*., 2004). Hierbei handelt es sich um die direkte Elektronenaufnahme vom Metall durch SRB.

In der vorliegenden Arbeit wurden die oben genannten Korrosionsmechanismen mit Schwerpunkt auf dem neuen, „bioelektrischen“ Prozess eingehend untersucht. Dies geschah durch eine Kombination kinetischer und elektrochemischer Untersuchungen unter genau definierten Bedingungen in SRB Reinkulturen sowie in abiotischen Referenzsystemen. Des Weiteren galt der physikochemischen Analyse der biogenen Korrosionsprodukte besondere Bedeutung. Im Rahmen der vorliegenden Untersuchungen wurde die Korrosion durch biogenes FeS und den mikrobiellen Verbrauch des kathodischen Wasserstoffs als geringfügig eingeschätzt bzw. ausgeschlossen. Die neuen, lithotrophen Stämme hingegegen korrodierten

Eisen massiv und bildeten dabei elektrisch leitfähige, mineralische Krusten auf dem Metall. Ihre Wirkung wird durch die Etablierung eines galvanischen Elements erklärt, wobei Eisen die Anode darstellt während die Zellen die kathodische Reaktion katalysieren und damit direkt die Rate der Eisenauflösung beeinflussen. Der Elektronenfluss verläuft entsprechend vom Metall ($4\,Fe^0 \rightarrow 4\,Fe^{2+} + 8\,e^-$) durch die überwiegend mineralische Korrosionskruste zu den mineral-assoziierten SRB ($8\,e^- + SO_4^{2-} + 10\,H^+ \rightarrow H_2S + 4\,H_2O$). Bei entsprechend angepassten Kultivierungsbedingungen konnten technisch hoch relevante Raten dieser bioelektrischen Korrosion gezeigt werden.

Die Korrosion von Eisen durch direkte, mikrobielle Elektronenaufnahme wird in dieser Studie als elektrisch mikrobiell beeinflusste Korrosion benannt (Englisch: electrical microbially influenced corrosion, EMIC). Diese ist mechanistisch grundsätzlich verschieden von der Materialzerstörung, die aus der chemischen Reaktion biogenen Schwefelwasserstoffs mit Eisen resultiert (Englisch: chemical microbially influenced corrosion, CMIC). CMIC kann in Labortests bekanntermaßen ebenfalls gravierende Schäden an Eisen verursachen. Im Rahmen dieser Studie sollte daher der relative Einfluss der beiden Mechanismen auf die Korrosion von Eisen in einem natürlichen sulfathaltigen Ökosystem untersucht werden. Die vorsichtige Beprobung sowie die chemische Analyse der Korrosionsprodukte von im Wattenmeer vergrabenen Stahlcoupons erlaubte eine quantitative Aussage zu dieser Fragestellung. Überraschenderweise war die mikrobielle Korrosion unter diesen Bedingungen ausschließlich bioelektrischer Natur, d.h. EMIC stellte die alleinige Ursache für den beobachteten Korrosionsschaden dar. Ein besseres Verständnis mikrobieller Korrosionsmechanismen sowie deren relativer Bedeutung für die Materialzerstörung sollte mittelfristig zur Entwicklung besserer Präventionsrichtlinien sowie gezielter Gegenmaßnahmen beitragen.

Die außergewöhnliche Fähigkeit spezieller anaerober Mikroorganismen zur direkten Korrosion ist anscheinend polyphyletischen Ursprungs, da sie in mehreren, phylogenetisch nicht verwandten Isolaten nachgewiesen werden konnte. Die ökologische Bedeutung dieser Fähigkeit ist hingegen unbekannt. Interessanterweise konnten in kultur-basierten Experimenten sehr hohe Zahlen dieser Organismen in einem vollkommen Eisen (Fe^0)-freien anoxischen Sediment nachgewiesen werden. In der vorliegenden Arbeit wird die Hypothese aufgestellt, dass die anaerobe Biokorrosion auf die Aktivität spezieller, „elektrotropher“ Mikroorganismen zurückzuführen ist, die unter natürlichen Bedingungen, d.h. in der Abwesenheit metallischen Eisens, noch weitgehend unbekannte biologische sowie abiotische Elektronenquellen nutzen.

Part A: Introduction to the topic and goals of the present work

A.1 Economic and environmental implications of iron corrosion

The advent of the first man-made iron dates back roughly 4000 years. Today, iron and steel are major and indispensible materials in transportation, infrastructure, and manufacturing. No other metal is produced on a comparable scale (Fig. 1). Corrosion of iron constructions, i.e. their progressive deterioration, requires costly maintenance operations and ultimately the replacement of failed equipment, and hence causes economic damages. Several studies have addressed the costs due to metal (iron + other) corrosion, the most comprehensive ones collecting data for the United States (Kruger, 2011). Here, a recent report provided direct costs due to metal corrosion of $276 billions, which is 3.1% of U.S. GDP (Koch *et al.*, 2001). Indirect costs to the user were conservatively estimated to be similar, so that total costs due to corrosion to society may be as high as 6% of U.S. GDP. Similarly, costs of metallic corrosion in other developed countries have been estimated to range between 2 and 3% of GNP (see Kruger, 2011 for review). As iron is the by far most widely used metal and particularly prone to corrosion, the calculated costs due to metal corrosion are to a large extent those of iron corrosion.

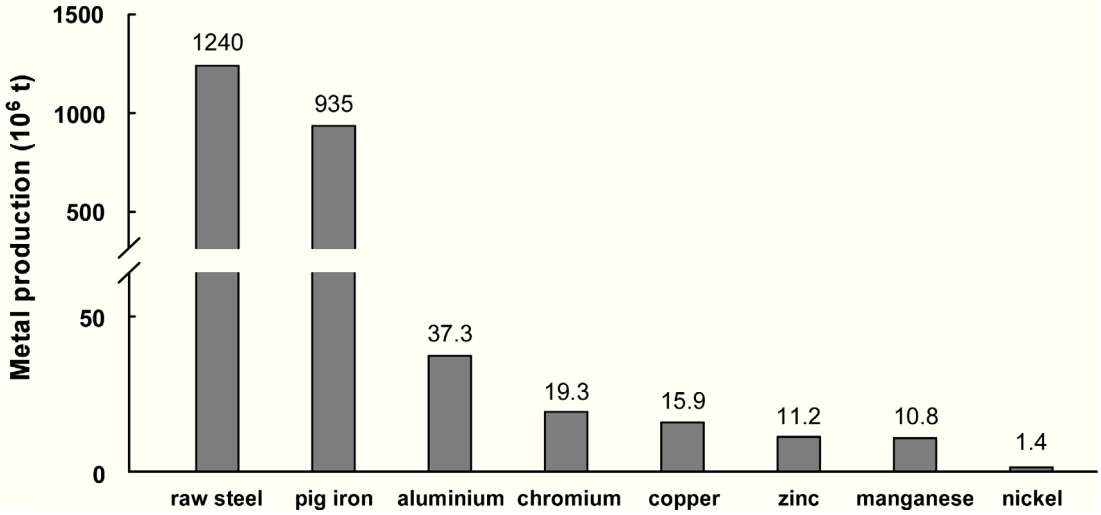

Fig. 1. Global production of the most widely used metallic materials (in million metric tons in 2009). Data from U.S. Geological Survey (2011).

While in most instances corrosion proceeds as the abiotic reaction of iron with oxygen and water, there are particular situations in which corrosion is influenced by microbial activity. This so-called microbially influenced corrosion (MIC) or biocorrosion is most pronounced in environments with no or limited access to oxygen. Consequently, MIC usually is a 'hidden'

process, found in places such as buried pipelines (Fig. 2), closed cooling water systems or at ship hulls in stagnant water. The industries most affected by MIC include the oil and gas industries, public utility companies, the nuclear power generating sector and the navigation industry (Hamilton, 1985; Flemming, 1994; Coetser and Cloete, 2005). The physical extent of iron constructions exposed to anoxic environments is vast, e.g. in the United States pipeline networks for the transmission and gathering of gas, oil and other hazardous liquid comprise in excess of 780,000 kilometers (Beavers and Thompson, 2006). Corrosion costs to the U.S. pipeline transmission industry are approximately $5.4 to $8.6 billion annually, 20 to 30% of which originate from MIC (Beavers and Thompson, 2006). Microbial activity was identified as the single most important cause of gas pipe corrosion (Pope, 1991; Li *et al.*, 2000). There is generally much agreement that microbial corrosion accounts for a large share of total corrosion costs (Booth, 1964; Flemming, 1994; Beech and Sunner, 2007) and hence billions of dollars annually, but estimates vary widely and lack a computed basis, so that definite numbers cannot be given with certainty.

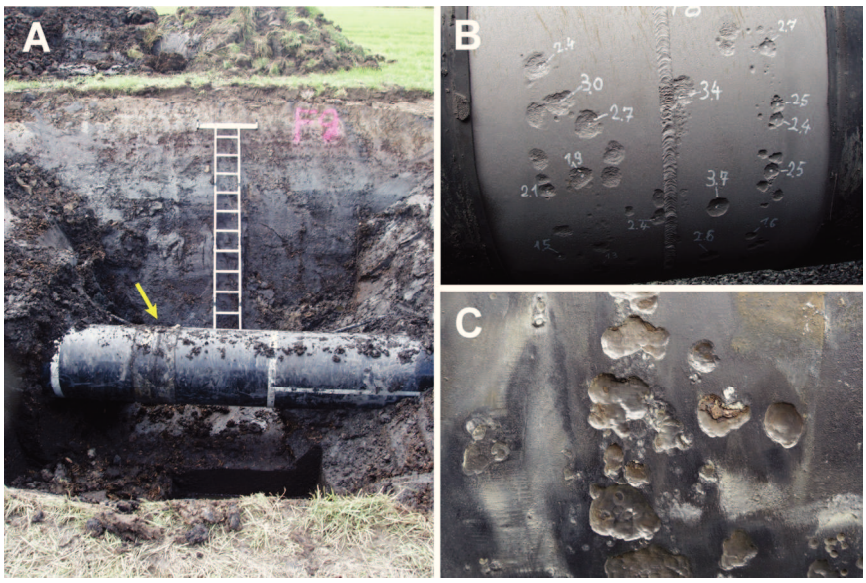

Fig. 2. External corrosion on buried gas transmission pipeline in bog-soil of Northern Germany.
A. Trench with insulated carbon steel gas pipeline. External corrosion has occurred under disbanded coating at welding sites (arrow).
B. Welding site with corrosion pits (disbonded asphalt coating and corrosion products removed). Numbers indicate pit depth in millimeters.
C. Higher magnification of corrosion pits from a different site of the same pipeline.

An ecological implication of corrosion is the loss of potable water from deteriorated water distribution systems (Volk *et al.*, 2000). However, serious environmental degradation arises from the corrosion of steel pipelines that carry hazardous freight. Pipeline incidents account

for a large fraction of oil spills, and globally an estimated three million barrels have been released to the environment between 1990 and 1999 (Etkin, 2001). Corrosion-related structural failures are the most common cause of U.S. pipeline spills (Etkin, 2001; Beavers and Thompson, 2006), e.g. the 2006 Prudhoe Bay release on Alaska's North Slope (Duncan *et al.*, 2009). In Nigeria, which suffers from a particularly high frequency of pipeline incidents, corrosion ranks second as a cause of oil spills (Adebayo and Dada, 2008; Aroh *et al.*, 2010).

A.2 Characteristics of iron and steel

Iron is the fourth most abundant element in the continental crust (Kato *et al.*, 2010), where it occurs mainly as a mineral, prominent examples of which include iron (hydr)oxides, iron silicates and the iron sulfides. In these compounds iron is present in the +II or +III redox state. Natural deposits of zero-valent, metallic iron (Fe^0) are scarce; Fe^0 appears in rare minerals originating from the deep subsurface (Deutsch *et al.*, 1977; Haggerty and Toft, 1985) or in certain meteorites and their debris (Cabanillas and Palacios, 2006). Vast amounts of metallic iron, on the other hand, have been produced from iron ore (e.g. Fe_2O_3) by human activity. However, Fe^0 is not the sole constituent of iron metal; other elements, particularly carbon (as FeC), are usual remains from the production process and profoundly affect the physical and mechanical properties of iron. Iron with an engineered carbon content between 0.01 and 2.1% is referred to as (carbon) steel. Alloying of iron with elements such as chromium, nickel or molybdenum yields stainless steels of superior corrosion resistance.

Due to its low cost and excellent mechanical properties, carbon steel is used where vast amounts of structural material are required, e.g. in oil and gas pipelines (Sun *et al*., 2011a). In the present study, a low carbon steel (>99.6% Fe; <0.1% C) was chosen for most experiments with MIC (Fig. 3).

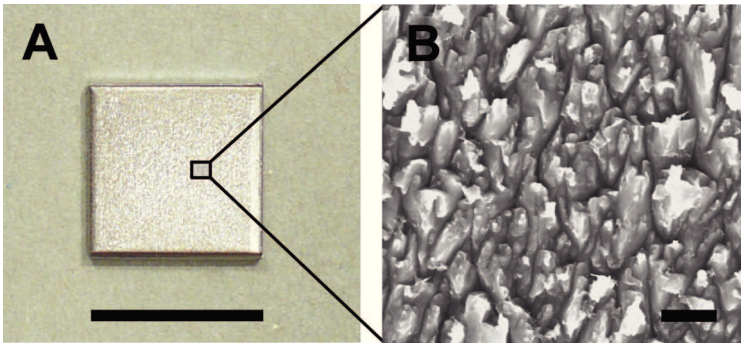

Fig. 3. Low carbon steel.
A. Piece of metal (1 mm thick) as used in this study (EN 1.0330; Fe ≥ 99.6%; <0.1% C). Bar, 1 cm.
B. Scanning electron micrograph of steel surface. Bar, 1 µm.

Metallic iron and steel are allotropic polycrystalline metals composed of individual crystals (grains) with different orientation and a typical size between 10 and 20 µm. In most technical materials their crystal structure is either body-centered cubic (ferrite, α-iron) or face-centered cubic (austenite, γ-iron). Interatomic cohesion is achieved by metallic bonding, i.e. positively charged iron atoms occupy lattice positions while valence electrons are shared among the lattice and move freely (electron 'sea' or 'gas'). Metallic bonding accounts for many of the physical characteristics of iron, including its excellent electrical and thermal conductivity and its luster (Binnewies *et al.*, 2004). Iron as a base metal is very reactive towards a variety of chemical compounds; most commonly it combines with abundant oxygen and water which results in deposition of iron (hydr)oxides at the metal surface (Fig. 4).

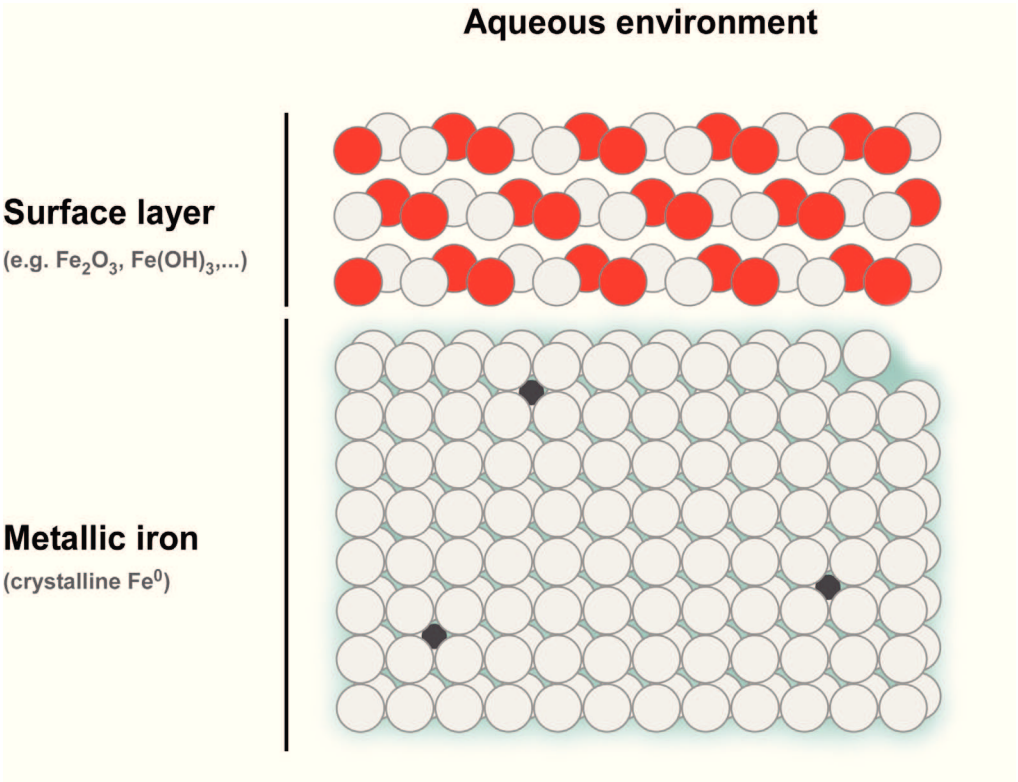

Fig. 4. Schematic illustration of metallic iron with ultra-structure and mineral surface layer. Ferrous cations (grey) occupy lattice positions in the face- or body-centered cubic crystal (grain depicted without indication of crystallinity). Interstitial atoms (black; e.g. carbon) may be incorporated into the lattice. The conception of a shared electron 'gas' is illustrated by a blue halo. Metallic iron is covered by a loosely adherent voluminous layer composed of various iron (hydr)oxides (non-ferrous atoms depicted in red).

The nature and physical properties of such surface layers (corrosion products) are amongst the most decisive rate-controlling factors in the progression of iron and steel corrosion.

A.3 Chemical (abiotic) corrosion of iron

The corrosion of iron is, bar from a few exceptions caused by erosion or mechanical stress, principally governed by electrochemical reactions (Whitney, 1903; Revie, 2011). Metallic iron dissolves when submerged into water. Positively charged ferrous ions (Fe^{2+}) from the water-exposed crystal surface transfer into solution, while electrons remain on the metal (Kaesche, 2003; Fig. 5).

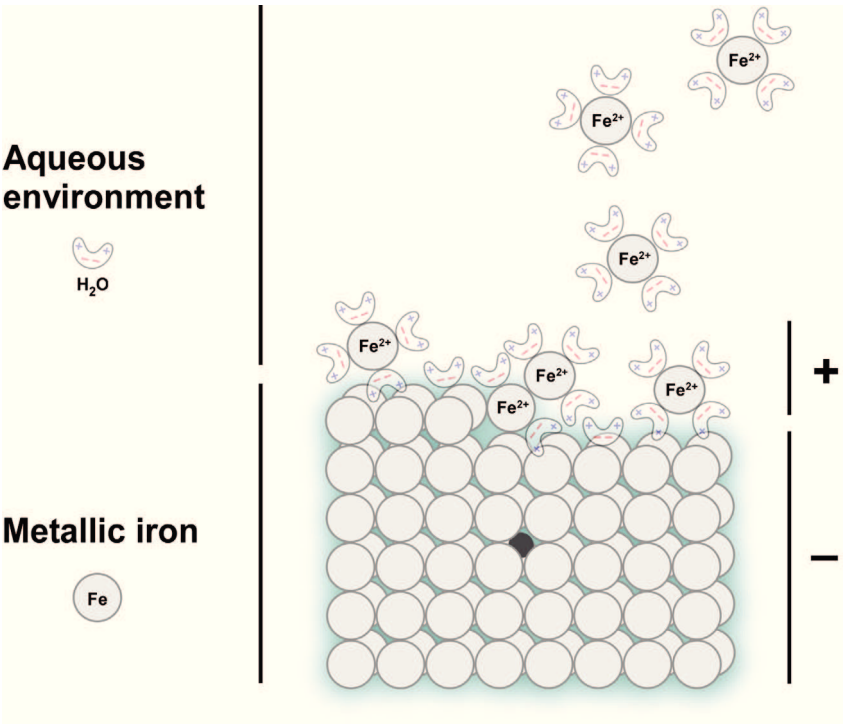

Fig. 5. Schematic illustration of iron dissolution and charge separation in aqueous environments. Positively charged ions (grey) dissolve from the crystal. Electrons cannot dissolve and remain on the metal (valence electrons illustrated by blue halo). This results in a charge separation where the metal assumes a negative charge that counteracts further dissolution of iron and even re-integrates ferrous iron into the crystal. Dissolved ferrous iron forms a hexaqua-complex, $[Fe(H_2O)_6]^{2+}$, with water [blue-red dipole symbols; only four H_2O depicted per $Fe^{2+}(aq)$]. Figure based on Kaesche (2003).

The driving forces of iron dissolution can be envisaged to be the high ionic density within the metal and the tendency of ferrous ions to become hydrated (Widdel, 1992). This leads to a charge separation where positively charged ions accumulate at the metal surface while the metal itself assumes a negative charge that counteracts its further dissolution and even re-integrates ferrous ions into the crystal structure (Fig. 5). The oxidative dissolution of iron and its reductive re-deposition are referred to as the anodic and cathodic reaction, respectively. Under standard conditions ($a_{Fe^{2+}}$ = 1 and T = 298.15 K) iron assumes a redox equilibrium

potential of $E^{\circ}_{Fe^{2+}/Fe^0}$ = −0.47 V vs. SHE (revised value, see *Chapte*r D.1) and no net loss of metal occurs as anodic and cathodic reactions proceed at equal pace.

$$2\,e^- + Fe^{2+} \rightleftarrows Fe^0 \qquad (1)$$

$$E_{Fe^{2+}/Fe^0} = -0.47\ V + 0.0296\ V \cdot \lg a_{Fe^{2+}}$$

The actual redox equilibrium potential E_{Fe^{2+}/Fe^0} in a particular environment can be calculated from the activity of dissolved ferrous ions. However, metallic iron electrochemically interacts with oxidizing and reducing chemical species in its aqueous environment. In the consequence, iron adopts potentials that deviate from E_{Fe^{2+}/Fe^0} and reflect the cumulative contribution of reactions that are in electronic short-circuit with the metal. The resulting mixed potential E_{corr} (also: free corrosion potential) can be measured directly at the metal and is a useful parameter in the understanding of corrosion phenomena (Piron, 1994). When E_{corr} is more negative than the calculated E_{Fe^{2+}/Fe^0} in a particular environment, no net oxidation of metallic iron occurs; the metal is immune to corrosion (Pourbaix, 1990). In certain technical settings this is achieved by cathodic protection, i.e. the establishment of electrical and electrolytic connection of iron to either a more active metal like magnesium, or to a power source (oxidation of water may function as electron-donating reaction in the latter case). However, in aqueous environments, iron readily gets in contact with redox-active chemical species with potentials more positive than E_{Fe^{2+}/Fe^0} and E_{corr} will assume more positive values. Here, corrosion of iron is thermodynamically feasible and the anodic dissolution of iron proceeds as long as suitable electron acceptors are available. The most common electron acceptor in corrosion is molecular oxygen:

$$4\,e^- + O_2 + 4\,H^+ \rightleftarrows 2\,H_2O \qquad (2)$$

$$E_{O_2/2H_2O} = 1.23\ V + 0.0148\ V\ \lg(a_{H^+}{}^4 \cdot a_{O_2})\,.$$

The reduction of electron acceptors such as oxygen at the metal surface likewise represents a cathodic reaction. Owing to the condition of electroneutrality, anodic and cathodic reactions cannot proceed isolated from one another (Kaesche, 2003). Anodic metal dissolution (Eq. 1) combines with cathodic oxygen reduction (Eq. 2) to yield:

$$2\,Fe^0 + O_2 + 2\,H_2O \rightarrow 2\,Fe(OH)_2 \qquad (3)$$

$\Delta G^{o} = -252.6 \text{ kJ (mol Fe}^{0})^{-1}$.

The reduction of protons from or in water, yielding molecular hydrogen, is another thermodynamically feasible reaction at the metal surface:

$$2\ e^{-} + 2\ H^{+} \rightleftarrows H_2 \tag{4}$$

$$E_{2H^{+}/H_2} = 0.00 \text{ V} + 0.0296 \text{ V} \lg(a_{H^{+}}{}^{2} / p_{H_2}) \ .$$

Here, anodic metal dissolution (1) combines with the cathodic half reaction (4) to yield:

$$Fe^{0} + 2\ H^{+} \rightarrow Fe^{2+} + H_2 \tag{5}$$

$\Delta G^{o'} = -10.6 \text{ kJ (mol Fe}^{0})^{-1}$.

This reaction is, however, kinetically impeded and particularly slow at circumneutral *pH* where proton concentrations are low (Widdel, 1992; Cord-Ruwisch, 2000); proton reduction is technically relevant only in acidic surroundings (Piron, 1996). Consequently, in oxygen-free neutral or alkaline waters iron constructions could, in principle, last for centuries.

However, this situation changes dramatically in the presence of weak inorganic and organic acids (Revie, 2011). Such compounds act through the transfer of (uncharged) protons to the metal surface thereby enormously increasing the availability of this electron acceptor. In this context, carbonic acid (H_2CO_3) is a prominent example. Carbonic acid corrosion becomes a serious issue in oil and gas systems where significant amounts of CO_2 and water are present ('sweet' water). Here, the reduction of bound protons in H_2CO_3 is very fast even at slightly acidic *pH* (~ 4.5 − 5) and this leads to rapid iron dissolution (Nešić, 2011).

In summary, iron corrosion largely results from the electrochemical interaction of the metal with its environment, and it is typically the type and concentration of available cathodic reactants that determine the rate of anodic iron dissolution (Fig. 6).

Additionally, corrosion products deposited at the metal surface are, by acting as a diffusion barrier, rate-controlling factors in metal dissolution. Ferrous iron (Fe^{2+}) is always the initial product of iron oxidation. In aerated environments, further oxidation of ferrous iron leads to the formation of various (ferric and ferrous) oxides and hydroxides, poorly soluble deposits commonly referred to as rust. In anoxic environments Fe^{2+} is more stable, particularly at low *pH*. However, at circumneutral or higher *pH*, $Fe(OH)_2$ or, in the presence of carbonate, $FeCO_3$ will form as solid corrosion products. Unlike the oxidation products of many other metals

(including stainless steels), voluminous iron (hydr)oxide or carbonate deposits on pure iron or carbon steel confer only limited protection against corrosion.

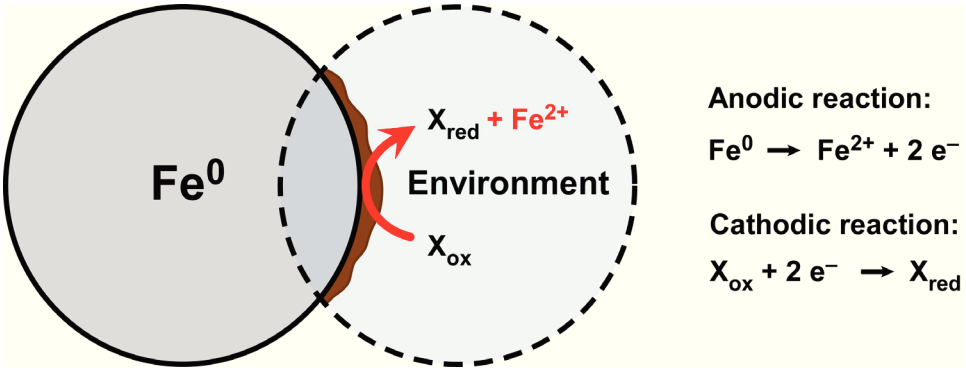

Fig. 6. Schematic illustration of iron corrosion. Corrosion results from the electrochemical reaction of the metal with its abiotic environment. Anodic metal dissolution and the associated deterioration of a ferrous structure are coupled to the reduction of suitable electron acceptors X_{ox} (e.g. 0.5 O_2 or 2 H^+). Solid corrosion products such as iron (hydr)oxides (brown) are formed in the process. Iron (hydr)oxides provide only limited protection against further metal dissolution.

The fundamental electrochemical principles outlined in this chapter also apply to microbially influenced corrosion.

A.4 Microbial corrosion of iron

Microorganisms change their environment, both on a local and on a global scale (Canfield *et al*., 2005). Copious ways are conceivable in which a particular environment may be rendered corrosive towards iron by microbial activity. As corrosion is a surface-associated phenomenon, microbial processes located at the immediate vicinity of the metal are of particular interest. Principally, microorganisms influence corrosion as they change the bordering aqueous phase, transform the solid corrosion deposits or, more directly, as they catalyze particular corrosion reactions (Fig. 7). Both sessile and planktonic microorganisms affect iron corrosion in complex ways by changing the aqueous phase (Fig. 7A); e.g. microbial consumption of oxygen eliminates this effective cathodic reactant (Jayaraman *et al*., 1997), but also affords the development of corrosive anaerobic microorganisms (Lee *et al*., 1993a; Dinh *et al*., 2004) or, potentially, results in differential aeration and pitting of the metal (Little and Lee, 2007). Microbial transformations of inorganic corrosion deposits affect the dissolution rate of the underlying metal (Fig. 7B; Little *et al*., 1998).

Recently, a direct influence on corrosion kinetics has been demonstrated in certain isolates of sulfate-reducing bacteria and methanogenic archaea. These strains apparently couple the oxidation of iron to the reduction of electron acceptors that would not react with iron in the absence of microbial catalysis (Fig. 7C; Dinh *et al*., 2004; Uchiyama *et al*., 2010). Many investigators regard the microbial consumption of cathodic H_2 (Eq. 5) as a central mechanistic prerequisite for the anaerobic corrosion of iron (von Wolzogen Kühr and van der Vlugt, 1934; Booth and Tiller, 1960; King and Miller, 1971; Bryant *et al*., 1991; De Windt *et al*., 2003). The potential role of cathodic H_2 in biocorrosion is therefore also of central interest in the present study.

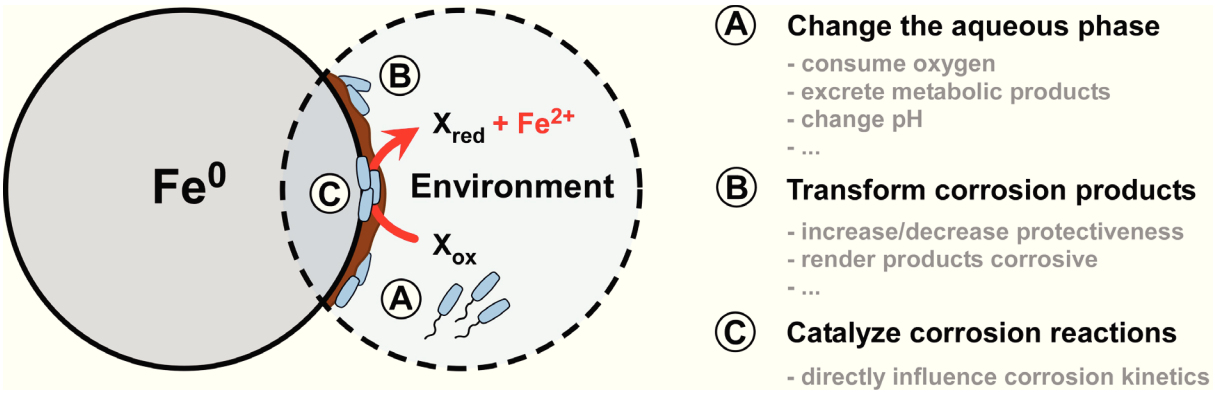

Fig. 7. Schematic illustration of microbial iron corrosion. Microbial corrosion of iron results from the electrochemical reaction of the metal with its biotic and abiotic environment. Microorganisms change the aqueous phase (A), transform corrosion products (B), or directly catalyze corrosion reactions (C). The suggested corrosive actions are not mutually exclusive, and one organism may participate in several of these activities.

A plethora of different microorganisms has been implicated in corrosion. This chapter briefly examines the proposed role of various physiological types of microorganisms in the deterioration of iron and steel constructions. Grouping is based on the terminal electron-accepting process (TEAP; Canfield *et al*., 2005; Heimann *et al*., 2010). From a technical point of view this allows, within certain limits, the prediction of microbial corrosive processes in particular environments where the principal electron acceptors are known. We will successively outline microbial corrosion with oxygen, nitrate, ferric iron minerals, sulfate and CO_2 as the terminal electron acceptor. Extended and comprehensive coverage will be given to the corrosion of iron and steel by sulfate-reducing bacteria, the main subject of the present work.

A.4.1 Corrosion of iron by aerobic bacteria

Molecular oxygen ($E^{o'}_{O_2/H_2O}$ = +0.82 V) is the principal electron acceptor in the microbial utilization of organic and inorganic energy sources in oxygenated habitats. Nevertheless, to this day, no direct coupling of Fe^0 oxidation ($E^{o}_{Fe^{2+}/Fe^0}$ = −0.47 V) to oxygen reduction has been observed in any microorganism (Hamilton, 2003), despite the high energy gain that would be associated with such a reaction. The electrochemical reaction of iron with oxygen (Eq. 5) is instead believed to be a purely chemical (abiotic) process (see *Chapter* A.3).

However, oxygen-consuming microorganisms colonize metallic surfaces and form heterogeneous biofilms of uneven distribution (Lee and de Beer, 1995; de Beer and Stoodley, 2005). This may protect iron against corrosion if, thereby, physical contact between the cathodic reactant oxygen and the metal can be completely prevented, as shown in pure culture experiments with *Pseudomonas fragi* and *Escherichia coli* (Jayaraman *et al*., 1997). If, on the other hand, only certain regions on the metal are shielded from oxygen (e.g. under a microbial colony), these regions will become preferential sites of anodic iron dissolution while cathodic reduction of oxygen continues at aerated sites on the metal (Lee and de Beer, 1995; Little and Lee, 2007). Such so-called differential aeration cells accelerate metal loss and lead to a localized attack (Lewandowski and Beyenal, 2009; Gu *et al*., 2011) which is often viewed as a characteristic of microbial corrosion (Little *et al*., 2006). Furthermore, microbial removal of oxygen affords the establishment of anaerobic microbial populations. Many of the succeeding anaerobes, such as sulfate-reducing bacteria or certain methanogenic archaea, are particularly corrosive towards metallic iron (Hamilton, 1985; Dinh *et al*., 2004; Mori *et al*., 2010).

Also a number of aerobic Fe^{2+}- and Mn^{2+}-oxidizing bacteria have been implicated in corrosion (Gaines, 1910; Iverson, 1987; Li *et al*., 2010; Dang *et al*., 2011; Gu *et al*., 2011). McBeth *et al*. (2011) demonstrated a 1.5-fold increase of corrosion rates in cultures of the abundant steel-colonizing, Fe^{2+}-oxidizing (ferrotrophic) *Mariprofundus* sp., as compared to sterile incubations. Another study reported 5-fold increased corrosion rates in mixed ferrotrophic cultures containing *Sphaerotilus* sp., enriched from the corrosion deposits of a failed heat exchanger (Starosvetsky *et al*., 2001). Differential aeration has been discussed as one possible explanation for the corrosion by ferrotrophic bacteria (Iverson, 1987), but formation of corrosive ferric (Fe^{3+}) minerals as cathodic electron acceptors has also been hypothesized (Starosvetsky *et al*., 2001). Similarly to the latter concept, it is believed that MnOOH and MnO_2 act as powerful cathodic reactants at iron surfaces (Hamilton, 2003; Lewandowski and Beyenal, 2009). Bacterial re-oxidation of Mn^{2+} from abiotic MnOOH and

MnO_2 reduction recycles these cathodic reactants and hence catalyzes rapid metal dissolution with oxygen as the terminal electron acceptor (Shi *et al*., 2002; Hamilton, 2003; Lewandowski and Beyenal, 2009).

Steel may suffer severe destruction in anoxic environments that favor the development of sulfate-reducing bacteria but at the same time are subject to period ingress of oxygen (Nielsen *et al*., 1993; Lee *et al*., 1995; Beech and Campbell, 2008). Secondary oxidation of iron sulfides (FeS), the principle product of SRB-induced corrosion, with oxygen can lead to the formation of elemental sulfur (S^0) deposits on top of the primary corrosion products (von Wolzogen Kühr and van der Vlugt, 1934; Hardy and Brown, 1984; Lee *et al*., 1995):

$$4\,FeS + 3\,O_2 + 2\,H_2O \rightarrow 4\,S^0 + 4\,FeOOH\ . \qquad (6)$$

This may be a purely abiotic process (Hardy and Brown, 1984; Lee *et al*., 1995; Jack *et al*., 1998) or be catalyzed by aerobic lithotrophic microorganisms (compare Fig. 7B). Wet sulfur and its decomposition products are highly corrosive towards metallic iron (MacDonald *et al*., 1978; Schaschl, 1980; Fang *et al*., 2009) and attack the metal according to the following net equation:

$$Fe^0 + S^0 \rightarrow FeS\,. \qquad (7)$$

The involved mechanisms and intermediates of reaction (7) are complex and insufficiently understood (Lee *et al*., 1995). However, there is sufficient evidence to conclude that the coupling of reactions (6) and (7) creates a kinetic path that leads to the rapid oxidation of iron with oxygen as the terminal electron acceptor (Hamilton, 2003). It may be conceived that bacterial disproportionation of sulfur further accelerates reaction (7) by formation of particularly corrosive sulfur species (e.g. HS_2^-).

A.4.2 Corrosion of iron by nitrate-reducing bacteria

Nitrate reduction to molecular nitrogen (denitrification, $E^{O'}_{NO_3^-/0.5N_2}$ = +0.71 V) or ammonium (ammonification, $E^{O'}_{NO_3^-/NH_4^+}$ = +0.36 V) are ecologically important microbial processes in a variety of natural and engineered oxygen-depleted systems (Arrigo, 2005; Canfield *et al*., 2005; Schwermer *et al*., 2008; Gieg *et al*., 2011). Nitrite is an intermediate product in the reduction of nitrate and, depending on environmental conditions, may accumulate in a given system (Gieg *et al*., 2011). Iron reacts in a purely abiotic process with nitrite, which may complicate the investigation of microbial corrosive effects (Kielemoes *et al*., 2000). Chemical

reduction of nitrate with iron was also demonstrated in some studies, but is probably less pronounced (Kielemoes *et al*., 2000). A direct utilization of iron by denitrifying or ammonifying microorganisms has not yet been observed, even though iron oxidation with nitrate, much like with oxygen, is thermodynamically highly favorable. Interestingly, direct electron uptake from solid surfaces occurs in 'electrotrophic' *Geobacter sulfurreducens* grown on graphite electrodes with nitrate as an electron acceptor (Gregory *et al*., 2004; Lovley, 2011a). Pure and mixed anaerobic cultures utilize cathodic H_2 from chemical Fe^0 corrosion (Eq. 5) for nitrate reduction (Till *et al*., 1998; Kielemoes *et al*., 2000; De Windt *et al*., 2003). However, only minor stimulation of metal dissolution was observed in these studies. De Windt *et al*. (2003) demonstrated a 1.3-fold increase in anaerobic corrosion rates by hydrogenotrophic *Shewanella oneidensis* strain MR-1.

Nitrate is being increasingly used in the oil industry as a means to control reservoir souring (biogenic H_2S formation; Reinsel *et al*., 1996; Gieg *et al*, 2011), and potentially MIC (Hubert *et al*., 2005). However, in some cases nitrate addition led to increased corrosion of associated oil production equipment (Hubert *et al*., 2005; Vik *et al*., 2007). In laboratory microcosms, consortia of SRB and nitrate-reducing sulfide-oxidizing bacteria (NR-SOB) produced higher corrosion rates (0.13 mm Fe^0 yr^{-1}) than SRB cultures alone (0.07 mm Fe^0 yr^{-1}; Nemati *et al*., 2001). This observation was explained by formation of corrosive sulfur species (e.g. S^0 and polysulfides) from the incomplete oxidation of H_2S by NR-SOB (Nemati *et al*., 2001). Oxidation of precipitated sulfide in corrosion deposits (FeS) by NR-SOB, on the other hand, has been viewed critically and is unlikely to contribute to sulfur formation in the field (Grigoryan *et al*., 2008; Lin *et al*., 2009).

A.4.3 Corrosion of iron by Fe(III)-reducing bacteria

With the exception of acidic environments ($pH < 4$), ferric iron is poorly soluble under most environmental conditions and readily forms various solid minerals of different crystallinity and redox potential (Weber *et al*., 2006; Bird *et al*., 2011). A variety of anaerobic marine and freshwater microorganisms have adapted to the utilization of these abundant solid electron acceptors (Butler *et al*., 2010). Fe(III)-reducing microorganisms have higher affinity for H_2, and gain more energy from its oxidation than SRB or methanogenic archaea, and hence compete successfully for this ubiquitous electron donor (Lovley and Phillips, 1987; Lovley *et al*., 1994). It was demonstrated that also cathodic H_2 (Eq. 5) could be used by the Fe(III)-reducing isolate *Shewanella putrefaciens*, which increased the corrosion of iron by a factor of 1.5 in pure culture experiments (Dawood and Brözel, 1998). A different study of the same

organism likewise found utilization of cathodic hydrogen, but attributed the observed corrosion rather to a bacterial influence on the anodic reaction, i.e. a change of the iron mineral cover (Obuekwe *et al*., 1981a; Obuekwe *et al*., 1981b). Similarly, a *Pseudomonas* strain isolated from an oil pipeline induced corrosion by dissolution of ferric iron minerals to Fe^{2+}(aq) and partial re-exposure of the underlying metal to oxic seawater (compare Fig. 7B; Obuekwe *et al*., 1981c; Little *et al*., 1998). Other studies reported that the activity of Fe(III)-reducing microorganisms diminished rather than enhanced the corrosion of iron (Potekhina *et al*., 1999; Dubiel *et al*., 2002; Lee and Newman, 2003). This was explained by an effective scavenge of the cathodic reactant O_2 with biologically released Fe^{2+}(aq) from the reductive dissolution of ferric mineral corrosion deposits.

A.4.4 Corrosion of iron by sulfate-reducing bacteria (SRB)

Sulfate-reducing bacteria are the suspected main culprits in microbially influenced corrosion (MIC) and hence have been the focus of most published investigations. There remain, however, considerable uncertainties about the particular corrosive mechanisms and their relative contribution to corrosion damage. This chapter summarizes the physiology and phylogeny of SRB and subsequently explores the various proposed mechanisms of SRB-induced corrosion. Additionally, special consideration is given to microbial hydrogen metabolism as traditionally (cathodic) hydrogen utilization and corrosion are viewed as interconnected abilities of SRB.

A.4.4.1 Physiology and phylogeny of SRB

A sulfate-reducing bacterium (SRB) is defined by its ability to gain energy from the coupling of an oxidative reaction to the reduction of sulfate. Because such dissimilatory reduction of sulfate is not only found in the domain *Bacteria* but also in certain members of the *Archaea*, some authors prefer the term sulfate-reducing prokaryotes or sulfate-reducing microorganisms to refer to this physiological group. We shall, however, use the term SRB throughout this thesis to refer to all microorganisms capable of dissimilatory sulfate reduction, a simplification still commonly made in recent literature (Muyzer and Stams, 2008).

Anaerobic respiration with sulfate as the terminal electron acceptor in the final degradation of organic matter is widespread in natural anoxic environments. SRB are commonly detected in or isolated from marine and freshwater sediments, and from water-logged soils. Additionally, SRB may be found in high numbers in extreme environments such as hydrothermal vents, hydrocarbon seeps, the deep subsurface and in oil fields (Ollivier *et al*.,

2007; Muyzer and Stams, 2008, and references therein). Engineered systems that provide suitable habitats for SRB − and typically suffer from their activity − include but are not limited to oil and gas pipelines, cooling water recirculation systems and certain potable water distribution pipings (Lee *et al*., 1995; Coetser and Cloete, 2005). SRB are most abundant in environments where the availability of sulfate is not limiting (Thauer *et al*., 2007). This is particularly true for the upper layers of anoxic marine sediments (seawater contains approx. 28 mM sulfate). Using fluorescent *in situ* hybridization (FISH), Mußmann *et al*. (2005) found that up to 11% of all cells in an intertidal mud flat of the German Wadden Sea were SRB. Their abundance suggests an important role of SRB in both, the sulfur and the carbon cycle. It has been estimated that sulfate reduction can account for more than 50% of organic carbon mineralization in marine sediments (Jørgensen, 1982).

Extracellular hydrolysis by (primary) fermentative microorganisms renders some of the organic carbon from dead plant and animal biomass (e.g. certain sugars, amino acids) directly accessible to SRB (Sass *et al*., 2002; Muyzer and Stams, 2008). In most ecosystems, however, secondary fermentation processes provide the quantitatively most important substrates for SRB, i.e. molecular hydrogen, alcohols and carboxylic acids. Locally, also hydrocarbons can become important substrates for SRB and the utilization of gaseous, short-chain alkanes, long-chain alkanes and alkenes, and aromatic hydrocarbons has been demonstrated in certain strains (Rabus *et al*., 2006 and reference therein; Kniemeyer *et al*., 2007). In their anoxic habitats, SRB compete with fermentative bacteria, proton-reducing acetogenic bacteria, homoacetogens and methanogens for the common substrates. Amongst these, the hydrogenotrophic homoacetogens and methanogens are rapidly outcompeted (Canfield *et al*., 2005; Muyzer and Stams, 2008). Generally, sulfidogenesis is favored by the more extensive range of substrates available to SRB.

With regard to the oxidation of organic carbon compounds, SRB can be physiologically divided into two groups, the incomplete and the complete oxidizers. Incompletely oxidizing SRB lack a mechanism for the terminal oxidation of acetyl-CoA and hence degrade their substrates only to the level of acetate (Rabus *et al*., 2006). For example the oxidation of lactate, a common substrate, occurs according to

$$2\,CH_3CHOHCOO^- + SO_4^{2-} \rightarrow 2\,CH_3COO^- + 2\,HCO_3^- + HS^- + H^+ \qquad (8)$$

$$\Delta G^{o'} = -160 \text{ kJ (mol sulfate)}^{-1}.$$

Completely oxidizing SRB degrade their substrates entirely to CO_2. This is due to their ability to oxidize acetate, either *via* a modified citric acid cycle, as used by *Desulfobacter postgatei*,

or by the acetyl-CoA pathway, found in for example *Desulfobacterium*, *Desulfotomaculum* and *Desulfococcus* species (Muyzer and Stams, 2008):

$$CH_3COO^- + SO_4^{2-} \rightarrow 2\,HCO_3^- + HS^- \qquad (9)$$

$$\Delta G^{o} = -47.6 \text{ kJ (mol sulfate)}^{-1}.$$

Energy conservation (ATP synthesis) in sulfate-reducing bacteria proceeds *via* oxidative phosphorylation and hence critically depends on the built-up of an electrochemical potential across the cytoplasmic membrane. The associated electron and proton transfer pathways are complex and still insufficiently understood. Terminal reductases are located in the cytoplasm and consequently cannot be involved in proton translocation across the cytoplasmic membrane (Pereira *et al*., 2011). Likewise, the oxidation of most substrates occurs within the cytoplasm, with the important exception of molecular hydrogen and formate (Thauer *et al*., 2007; Pereira *et al*., 2011; see also next chapter). Flavin-based electron bifurcation in the cytoplasm appears to play a more prominent role in energy conservation than previously assumed (Pereira *et al*., 2011). Substrate-level phosphorylation, on the other hand, does not occur in SRB (Rabus *et al*., 2006; Thauer *et al*., 2007).

Although named after their ability to reduce sulfate, SRB can also use other electron acceptors including certain sulfur compounds (e.g. sulfite, thiosulfate), nitrate, nitrite and a number of oxidized metals such as Fe^{3+} (Muyzer and Stams, 2008). Also fermentative and acetogenic growth are widespread among SRB. Even aerobic respiration has been observed, though this is unlikely to support growth of SRB (Thauer *et al*., 2007). In fact, respiratory removal of oxygen is thought to afford subsequent growth at the expense of sulfate reduction, since the latter process is strictly inhibited under oxic conditions (Thauer *et al*., 2007). Hence, sulfate reduction is usually not the exclusive means of energy generation in an organism, but in many natural habitats of SRB provides the energetically most favorable pathway.

Dissimilatory sulfate reduction is found in members of several bacterial and archaeal phyla. Based on the comparative analysis of 16S rRNA gene sequences of known SRB, seven phylogenetic lineages can be distinguished (Fig. 8; Muyzer and Stams, 2008). Most cultivated representatives of the SRB are members of the Gram-negative *Deltaproteobacteria*, followed by the Gram-positive SRB within the *Clostridia*. Most of these microorganisms prefer a neutral *pH* and are inhibited at *pH* values below 5 or 6 and above 9 (Widdel, 1988). However, a small number of alkaliphilic isolates can grow under more alkaline conditions (Zhilina *et al*., 1997; Pikuta *et al*., 1998) and various 16S rRNA gene sequences related to

Desulfonatronum and *Desulfonatronovibrio* have been recovered from hypersaline soda lakes with *pH* values as high as 10.5 (Foti *et al*., 2007).

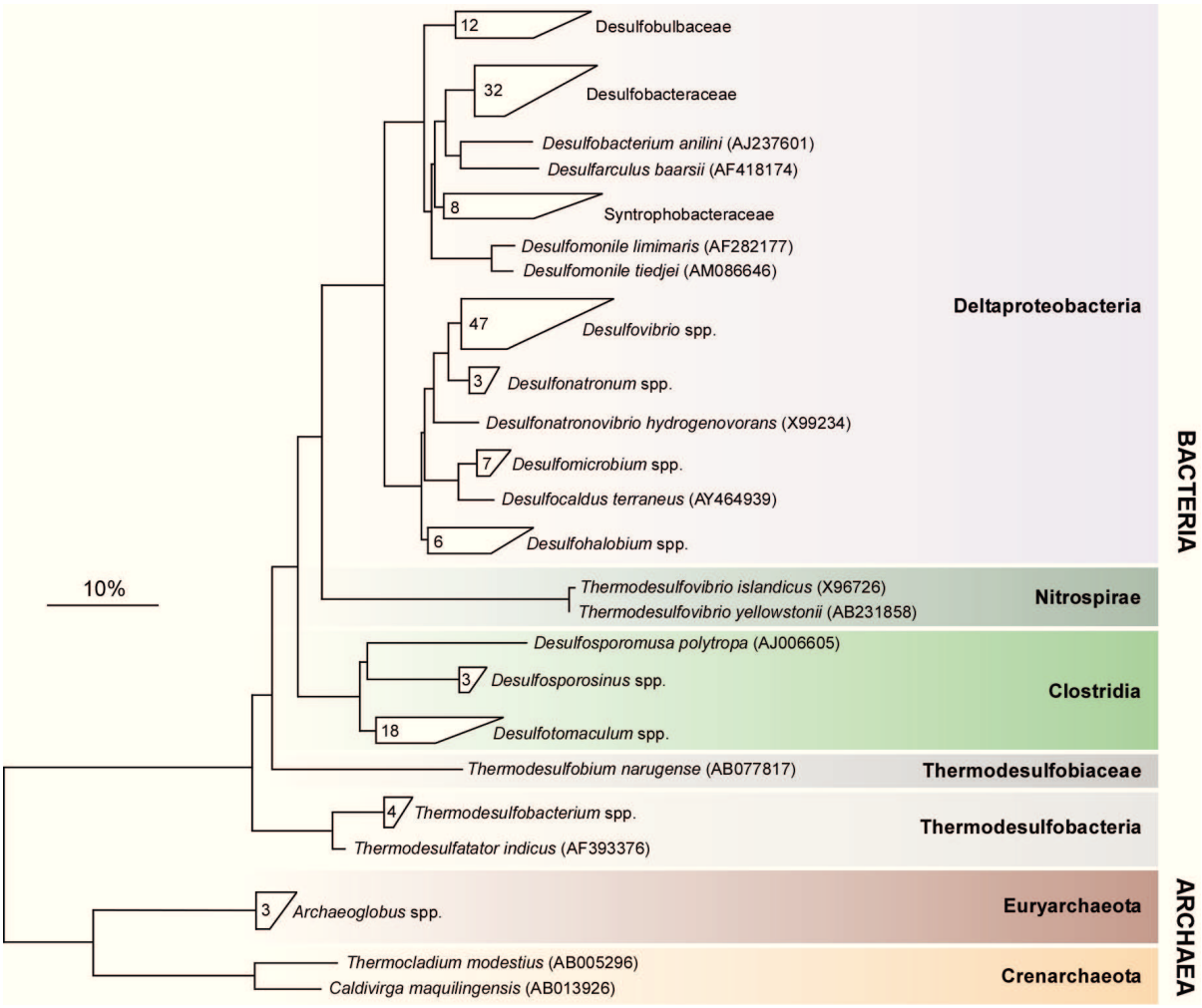

Fig. 8. Phylogenetic affiliation of sulfate-reducing microorganisms based on 16S rRNA sequences. Seven phylogenetic lineages can be distinguished, two within the *Archaea* and five within the *Bacteria*. Bar indicates 10% sequence divergence. Redrawn and modified from Muyzer and Stams (2008).

Most known sulfate-reducing species within the *Deltaproteobacteria* and *Clostridia* are mesophilic with optimal temperatures for growth between 20 and 40°C (Widdel, 1988; Rabus *et al*., 2006). Exceptions include the psychrophilic genera *Desulfotalea*, *Desulfofrigus* and *Desulfofaba* as well as certain moderately thermophilic species within the genus *Desulfotomaculum* (Nilsen, 1996a; 1996b; Knoblauch *et al*., 1999; Sahm *et al*., 1999). Three lineages only contain thermophilic sulfate reducers, i.e. the *Nitrospirae*, the *Thermodesulfobacteria* and the recently described *Thermodesulfobiaceae* (Mori *et al*., 2003; Muyzer and Stams, 2008). Likewise thermophilic or, mostly hyperthermophilic are the sulfate-reducing archaea. In sulfate-rich environments with very high temperatures (>80°C) such as at hydrothermal vents members of the sulfate-reducing genus *Archaeoglobus* (phylum

Euryarchaeota) can be found (Stetter *et al*., 1987; Ollivier *et al*., 2007). Certain *Crenarchaeota* might also grow at the expense of sulfate reduction and two acidophilic species have been isolated from acidic hot springs (Itoh *et al*., 1998; 1999).

A.4.4.2 Hydrogen metabolism in SRB

The use of molecular hydrogen as a substrate for growth is widespread in sulfate-reducing bacteria and best studied in species of the genus *Desulfovibrio*. Members of this genus utilize H_2 rapidly and with high affinity, even at H_2 partial pressures down to 5 − 20 ppm (Cord-Ruwisch *et al*., 1988). The overall reaction can be written as:

$$4\,H_2 + SO_4^{2-} + H^+ \rightarrow HS^- + 4\,H_2O \qquad (10)$$

$$\Delta G^{o'} = -151.9 \text{ kJ (mol sulfate)}^{-1}$$

Typically, H_2 generation *via* fermentative pathways − the natural source of H_2 to SRB − requires the effective scavenge of the gaseous product. H_2 oxidation by SRB creates mutual energetic benefits for the syntrophic partners, an interaction commonly referred to as 'interspecies hydrogen transfer' (Cord-Ruwisch *et al*., 1988; Thauer *et al*., 2007). Both, hydrogen consumption and its generation are catalyzed by the enzyme hydrogenase (Eq. 4: $2\,H^+ + 2\,e^- \rightleftarrows H_2$). Three phylogenetically unrelated types of hydrogenases are known. They differ most importantly in their catalytic metal centers and are hence designated as [FeFe]-, [NiFe]-, and [Fe]-hydrogenases (Vignais and Colbeau, 2004; Matias *et al*., 2005; Pereira *et al*., 2011). In sulfate-reducing bacteria, hydrogenases of the [FeFe]- and [NiFe]-group have been identified (Matias *et al*., 2005; Pereira *et al*., 2011). Additionally, several species contain [NiFeSe]-containing enzymes which represent a sub-group of the [NiFe]-hydrogenases (Matias *et al*., 2005; Pereira *et al*., 2011).

Dissimilatory reduction of sulfate with H_2 involves the oxidation of H_2 in the periplasm, electron transport through the cytoplasmic membrane and the multi-step reduction of activated sulfate in the cytoplasm (Rabus *et al*., 2006; Thauer *et al*., 2007). A proton motive force is established in the process which allows energy conservation via membrane-associated ATP synthases (Fig. 9). Variants of the type I cytochromes c_3 seem to function as general-purpose electron transport proteins (at least in deltaproteobacterial SRB), mediating between periplasmic hydrogenases and the cytoplasmic electron and proton transporting machinery (Matias *et al*., 2005; Pereira *et al*., 2011). *Desulfovibrio vulgaris* strain Hildenborough has four periplasmic uptake hydrogenases (1 x [FeFe], 1 x [NiFeSe], 2 x [NiFe]) that interact with

type I cytochromes c_3 and can functionally replace each other, at least under laboratory conditions with high concentrations of H_2 (Caffrey *et al*., 2007; Thauer *et al*., 2007). Growth rate and expression data suggest that the [NiFeSe]-hydrogenase is important for growth at lower concentrations of H_2, while the [FeFe]-hydrogenase facilitates rapid growth at higher hydrogen concentrations and when lactate serves as the electron donor (Caffrey *et al*., 2007).

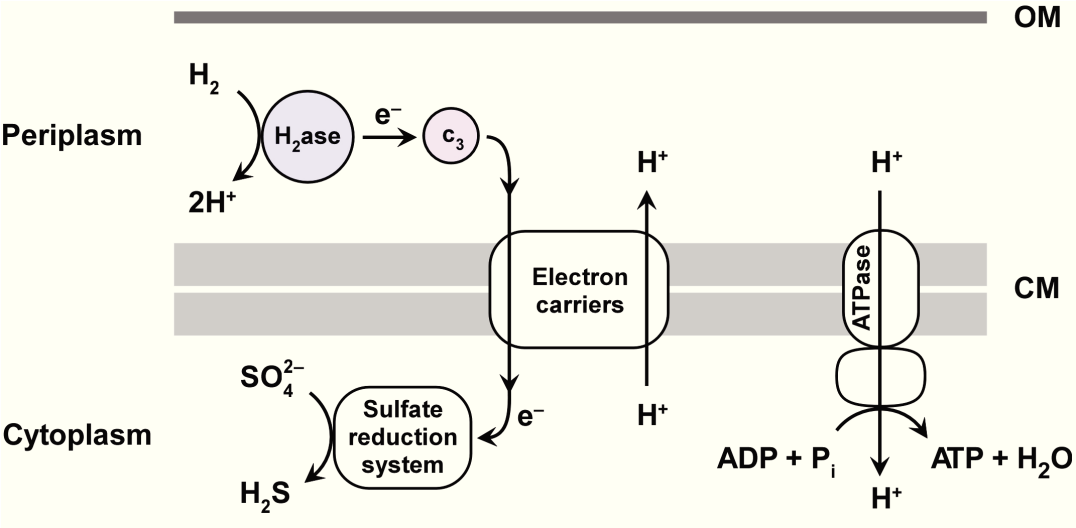

Fig. 9. Simplified scheme of sulfate reduction with H_2 as an electron donor in *Deltaproteobacteria*. Vectorial electron transport, proton translocation and ATP synthesis are indicated. No single organism is represented as there are species-specific differences and general uncertainties about the exact pathway. Reactions are non-stoichiometric. H_2ase: Periplasmic uptake hydrogenase, c_3: Type I cytochromes c_3 (Pereira *et al*., 2011) , OM: Outer membrane, CM: Cytoplasmic membrane.

Hydrogenases, both soluble and membrane-associated, are also found in the cytoplasm of SRB. Many of them catalyze hydrogen formation. Odom and Peck (1981) suggested a coupling of organic compound utilization with the hydrogen metabolism within SRB ('intracellular hydrogen transfer'). Accordingly, reducing power from lactate oxidation in the cytoplasm generates molecular hydrogen which, upon diffusion, is oxidized in the periplasm and thereby contributes to the establishment of an electrochemical transmembrane potential (compare Fig. 9; Odom and Peck, 1981; Matias *et al*., 2005). This hydrogen-cycling mechanism for energy conservation has also been suggested for other substrates such as formate and CO (Voordouw, 2002). However, the absence of hydrogenase-encoding genes in *Desulfococcus oleovorans* strain Hxd3 and in *Caldivirga maquilingensis* implies that hydrogenases are not essential for sulfate reduction in all SRB (Pereira *et al*., 2011). The membrane-associated hydrogenases CooMKLXUHF and EchABCDEF in certain members of the *Desulfovibrionaceae* interact with ferredoxins (Fd) and catalyze the reversible reaction

$$Fd_{red}^{2-} + 2\ H^+ \rightleftarrows Fd_{ox} + H_2 + \Delta\mu_{H^+}, \quad (11)$$

which occurs either at the expense of the proton motive force $\Delta\mu H^+$ or contributes to its generation (Thauer *et al*., 2007; Pereira *et al*., 2011). In the absence of sulfate, several SRB have been demonstrated to grow on organic substrates at the expense of proton reduction in co-cultures with hydrogen-consuming syntrophic partners, e.g. methanogenic archaea (Bryant *et al*., 1977; Nilsen *et al*., 1996). In the absence of both sulfate and a syntrophic partner, hydrogen accumulation is observed in SRB cultures grown on lactate (Thauer *et al*., 2007).

$$CH_3CHOHCOO^- + H_2O \rightarrow CH_3COO^- + CO_2 + H_2 \quad (12)$$

$$\Delta G^o = -8.8 \text{ kJ (mol lactate)}^{-1}$$

Interestingly, it was recently shown that *Desulfovibrio vulgaris* strain G11 evolves hydrogen in sulfate-free media with electrons derived from a poised cathode, a technical set-up referred to as microbial electrolysis cell (MEC; Croese *et al*., 2011).

A.4.4.3 Mechanisms of corrosion by SRB

Despite many studies on SRB-induced corrosion, the exact mechanisms are still insufficiently understood and proposed models are often inconclusive or even contradictory. This chapter examines the various hypothesized mechanisms of corrosion by SRB.

Corrosion of iron by microbial uptake of cathodic hydrogen.

The first comprehensive investigation of anaerobic iron corrosion identified sulfate-reducing bacteria as the main corrosive entity in the anoxic, sulfate-rich soils of North Holland (von Wolzogen Kühr and van der Vlugt, 1934). This study is still highly influential in today's views on microbial corrosion. Von Wolzogen Kühr and van der Vlugt (1934) observed that metallic iron exposed to anoxic sulfate-rich waters with natural populations of SRB suffered from rapid corrosion. No corrosion, on the other hand, was observed if such waters had been previously sterilized by boiling. H_2S as a potential driving force of metal dissolution could be excluded and hence a more direct interaction between bacterial cells and the metal was conceived (von Wolzogen Kühr and van der Vlugt, 1934; von Wolzogen Kühr, 1961). It was assumed that under sterile conditions hydrogen from the cathodic reduction of protons (Eq. 4) accumulated at the metal surface and protected the metal against further dissolution (Eq. 1). In the presence of SRB, however, such 'protective' hydrogen was consumed and served as an

electron donor for sulfate reduction (Eq. 10); progressive metal dissolution was hence driven by microbial hydrogen metabolism (von Wolzogen Kühr, 1961):

$$4\,Fe^0 + SO_4^{2-} + 2\,H_2O + 2\,H^+ \rightarrow FeS + 3\,Fe(OH)_2\,. \qquad (13)$$

Since the accumulation of cathodic hydrogen was assumed to 'polarize' the metal, i.e. decelerate its dissolution rate, bacterial hydrogen consumption and the simultaneous acceleration of iron dissolution were consequently considered a mechanism of cathodic 'depolarization' (Fig. 10). The model which is commonly referred to as the 'classical cathodic depolarization theory' was later expanded to other hydrogenotrophic microorganisms such as methanogenic archaea and nitrate-reducing bacteria (von Wolzogen Kühr, 1961; Daniels *et al*., 1987; De Windt *et al*., 2003).

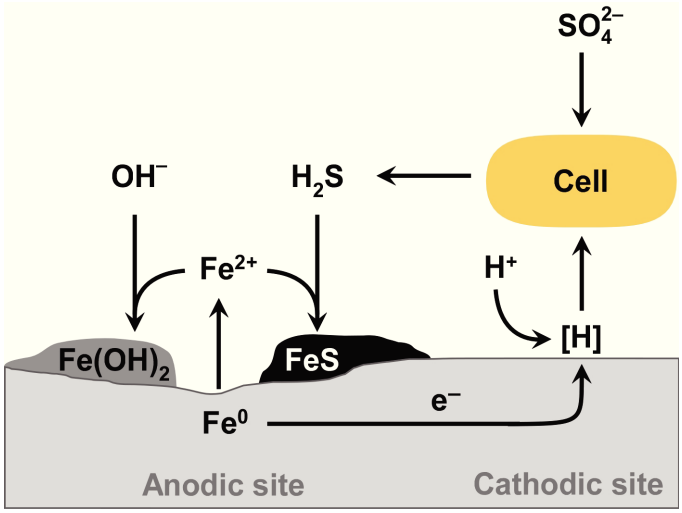

Fig. 10. Scheme of iron corrosion by SRB based on the reactions suggested in the cathodic depolarization theory of von Wolzogen Kühr and van der Vlugt (1934). For convenience, reactions are non-stoichiometric and the bacterial cell is drawn separately from the metal. Hydrogen is formed at cathodic sites in a purely abiotic reaction (no indication whether [H] is atomic or molecular hydrogen). SRB utilize 'polarizing' [H] at the cathode, thereby allowing anodic iron dissolution to proceed ('cathodic depolarization'). Ferrous iron precipitates are FeS and $Fe(OH)_2$. Topological information to their deposition is not provided.

The cathodic depolarization theory is based on thermodynamic principles (von Wolzogen Kühr and van der Vlugt, 1934; von Wolzogen Kühr, 1961; Daniels *et al*., 1987). Formation of H_2 with Fe^0 is only slightly exergonic under standard conditions (Eq. 5). Built-up of the reaction product H_2 at the metal surface increases ΔG and ultimately renders the reaction endergonic. This led to the assumption that progressive hydrogen-producing corrosion was only possible through and directly controlled by the hydrogen uptake activity of SRB (von Wolzogen Kühr and van der Vlugt, 1934; von Wolzogen Kühr, 1961). Interestingly, in this

respect the historic corrosion model resembles the more recent concept of interspecies hydrogen transfer in the syntrophic microbial degradation of organic matter in anoxic environments (Cord-Ruwisch *et al*., 1988; Cord-Ruwisch, 2000; Thauer *et al*., 2007).

The validity of this model is highly controversial (Tiller, 1983; Widdel, 1992; Lee *et al*., 1995; Beech and Sunner, 2007; Lewandowski and Beyenal, 2009). Laboratory tests of the cathodic depolarization theory have been interpreted in its favor by some investigators (Starkey, 1946; Booth *et al*., 1960; Pankhania *et al*., 1986; Daniels et al., 1987; Bryant *et al*., 1991), while others refuted this mechanistic explanation of anaerobic corrosion (Wanklyn and Spruit, 1952; Costello, 1974; Hardy, 1983; Dinh *et al*., 2004).

Corrosion of iron by biogenic H_2S.

Biologically produced H_2S rapidly reacts with metallic iron. Shoesmith *et al*. (1980) suggested the following widely accepted anodic reaction sequence (Lee *et al*., 1995; Hansson *et al*., 2006; Sherar *et al*., 2010):

$$Fe^0 + HS^-_{ads} \rightarrow FeHS^-_{ads} \quad (14)$$

$$FeHS^-_{ads} \rightarrow FeHS^+_{ads} + 2\,e^- \quad (15)$$

Subsequently, the reaction of $FeHS^+_{ads}$ can proceed *via* the release of ferrous iron to the liquid phase (Eq. 16) or the formation of an iron sulfide surface film (Eq. 17).

$$FeHS^+_{ads} \rightarrow Fe^{2+} + HS^- \quad (16)$$

$$FeHS^+_{ads} \rightarrow FeS + H^+ \quad (17)$$

Due to its low solubility in the presence of sulfide at neutral and alkaline *pH*, Fe^{2+} from reaction (16) will rapidly precipitate from solution to form FeS deposits:

$$Fe^{2+} + HS^- \rightarrow FeS + H^+. \quad (18)$$

However, in slightly acidic and alkaline solutions reaction (17) probably dominates over reaction (16) in the first place and tightly adherent FeS films are formed directly at the metal surface (Vera *et al*., 1984; Hansson *et al*., 2006; Sherar *et al*., 2010). Such FeS films can considerably slow down metal dissolution rates, i.e. passivate the metal (Newman *et al*., 1991, 1992; Lee and Characklis, 1993; Lee *et al*., 1995), and may therefore be a desired corrosion product in certain technical operations (Nešić, 2011; Sun *et al*., 2011a; 2011b). However,

local rupture of such FeS films re-exposes iron to the electrolyte and causes rapid pitting corrosion at the uncovered sites (Newman *et al*., 1991; Sun and Nešić, 2007; Sun *et al*., 2011b).

Apart from the catalytic effect on the anodic dissolution of iron, also the cathodic reaction is thought to be stimulated by H_2S (Costello, 1974; Cord-Ruwisch, 2000; Ma *et al*., 2000). H_2S as a weak acid effectively transfers uncharged protons to the metal surface. Hence, protons bound to the sulfide anion react more quickly with iron-derived electrons than do protons from or in water (Wikjord *et al*., 1980; Widdel, 1992; Nešić, 2011), according to the overall net reaction:

$$Fe^0 + H_2S \rightarrow FeS + H_2 . \quad (19)$$

Rapid H_2 evolution from H_2S and Fe^0 has been demonstrated both in the presence (Cord-Ruwisch and Widdel, 1986) and absence (Widdel, 1992; Dinh, 2003) of SRB.

As metal destruction by the above reactions (Eqs 14 – 19) always results from the excretion of a corrosive chemical agent, we here refer to this process as 'chemical microbially influenced corrosion' (CMIC).

Corrosion of iron by biogenic FeS.

Iron sulfides, a natural product of SRB-induced corrosion, are assumed to catalyze the reduction of H^+-ions to H_2 with iron-derived electrons (Booth *et al*., 1968; King and Miller, 1971; Newman *et al*., 1991, 1992, Lewandowski *et al*., 1997):

$$Fe^0 + 2\,H^+ \xrightarrow{FeS} Fe^{2+} + H_2 . \quad (20)$$

Galvanic coupling between Fe^0 and deposited FeS hence accelerates anodic dissolution of the former through stimulation of cathodic H^+ reduction (Fig. 11; King and Miller, 1971; Smith and Miller, 1975; Jack, 2002; Hamilton, 2003). Increased iron weight loss upon galvanic contact to suspensions of certain iron sulfides is evident from abiotic incubation experiments (Booth *et al*., 1968; King *et al*., 1973). However, the effect was transient under sterile conditions (King *et al*., 1973); iron sulfides underwent changes of their crystal structure during incubation and active SRB populations were required for progressive corrosion (King and Miller, 1971; King *et al*., 1973). It was concluded that hydrogen scavenge by SRB is mandatory for the sustained functioning of FeS cathodes and hence for corrosion to proceed (King and Miller, 1971; Tiller, 1983). Other authors, however, attributed the required

presence of active SRB populations to their continuous supply of H_2S and – in the consequence – 'fresh', cathodically active FeS (from Eqs 14 to 19; Newman *et al*., 1991).

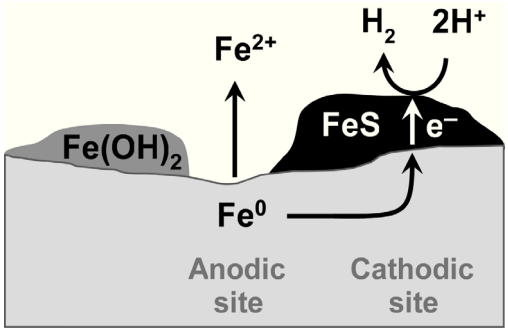

Fig. 11. Suggested galvanic coupling of Fe^0 and FeS. Dissolution of iron at anodic sites is accelerated by the catalyzed reduction of 2 H^+ to H_2 at FeS cathodes.

Iron sulfide deposits on Fe^0 show profound differences in their corrosiveness depending on their crystallinity (Mara and Williams, 1972; King *et al*., 1973; Smith and Miller, 1975) and specific surface area (Lee and Characklis, 1993; Newman *et al*., 1991).

Corrosion of iron by direct electron uptake.

Direct uptake of electrons from iron by SRB has been conjectured as an alternative explanation for corrosion in anoxic environments since this would circumvent the kinetically slow formation of cathodic hydrogen (Ferris *et al*., 1992; Widdel, 1992; von Ommen Kloeke *et al*., 1995; Jack, 2002). Recently, kinetic studies indeed suggested electron uptake from Fe^0 by novel lithotrophic SRB, isolated from enrichment cultures with Fe^0 as the only source of electrons (Dinh, 2003; Dinh *et al*., 2004). The isolated SRB '*Desulfobacterium corrodens*' strain IS4 and '*Desulfovibrio ferrophilus*' strain IS5 reduced sulfate faster with Fe^0 than could be explained by consumption of cathodic H_2 and were more corrosive than 'conventional' hydrogenotrophic strains. Uptake of iron-derived electrons by such specialized SRB according to

$$8\,e^- + SO_4^{2-} + 10\,H^+ \rightarrow H_2S + 4\,H_2O \qquad (21)$$

$$E_{\text{average}} = +0.30\ \text{V} + 0.0074\ \text{V}\ \lg(a_{SO_4^{2-}}\ a_{H^+}{}^{10}\ a_{H_2S}{}^{-1})$$

presumably occurred *via* (unidentified) outer membrane redox proteins upon direct electrical contact with the metallic surface (Fig. 12; Dinh *et al*., 2004). This theory is here referred to as 'electrical microbially influenced corrosion' (EMIC).

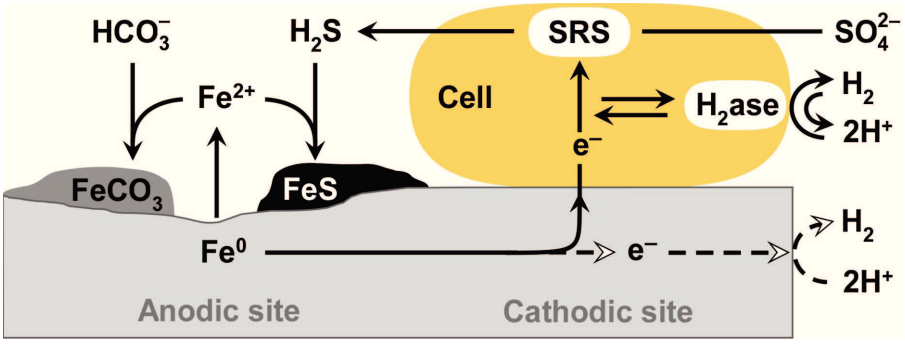

Fig. 12. Suggested electron flow during iron corrosion by specialized SRB such as strain IS4. Stoichiometric equations, cellular components and iron topology are not fully depicted. Electrons flow from metallic iron into the cell *via* an as yet unidentified membrane-associated redox protein. Hydrogen formed during early phases of incubation of strain IS4 is explained by a branched electron transport system that allows disposal of surplus electrons ('overflow') *via* hydrogenase enzyme (H_2ase), and by chemical formation. Ferrous iron precipitates as iron sulfide (FeS) and siderite ($FeCO_3$). SRS: Sulfate reduction system. Figure adapted and modified from Dinh *et al*. (2004).

Molecular hydrogen evolved in one representative of such corrosive SRB, '*Desulfobacterium corrodens*' strain IS4, during early growth phases on metallic iron, possibly as an enzymatic side reaction to divert an initial inflow of surplus electrons (Dinh *et al*., 2004). Biogenic hydrogen formation from metallic iron was also observed in a previous study with membrane fractions of *Desulfovibrio vulgaris* (von Ommen Kloeke *et al*., 1995). These authors suggested the delivery of iron-derived electrons to the cytoplasmic sulfate reduction machinery *via* an outer membrane redox protein and intermediately formed and consumed molecular hydrogen; the latter served as a shuttle of reducing equivalents across the periplasmic space (von Ommen Kloeke *et al*., 1995). Also direct electron transfer between negatively poised stainless steel electrodes and hydrogenase has been observed, though charge transfer was only minor compared with corrosion currents measured in laboratory and field situations (Da Silva *et al*., 2001, 2004). Irrespective of the path of reducing equivalents (hydrogen or electrons) from the metal into SRB, direct corrosion always follows reaction (13). Dinh *et al*. (2004) formulated the equation with precipitation of siderite ($FeCO_3$), which is less soluble than $Fe(OH)_2$ in bicarbonate-rich waters (e.g. seawater).

$$4\,Fe^0 + SO_4^{2-} + 3\,HCO_3^- + 5\,H^+ \rightarrow FeS + 3\,FeCO_3 + 4\,H_2O \qquad (22)$$

Minerals ($FeS/FeCO_3$) deposited on Fe^0 by SRB strains IS4 and IS5 ultimately acted as a process barrier, thus limiting the corrosiveness of the novel isolates (Dinh, 2003; Dinh *et al*., 2004).

Other suggested corrosive mechanisms by SRB.

In addition to H_2S certain other metabolic products of SRB have been proposed to corrode Fe^0. Iverson (1968) suggested the formation of highly reactive reduced phosphorus compounds in cultures of *Desulfovibrio desulfuricans* as the main corrosive mechanism. In this view, reactive phosphorus compounds such as phosphine (H_3P) from bacterial reduction of phosphate ($H_2PO_4^-$, HPO_4^{2-}) combine with iron to yield iron phosphide (Fe_3P) as a black solid corrosion product (Iverson, 1968; Iverson, 2001). Indeed experiments with *D. desulfuricans* demonstrated a positive correlation between phosphate concentration and iron corrosion rate (Weimer *et al*., 1988). However, in this study vivianite ($Fe_3(PO_4)_2 \cdot 8H_2O$) was formed as the main phosphorus-containing corrosion product. Corrosion of iron through biologically reduced phosphorus compounds has been viewed critically (Widdel, 1992; Dinh, 2003). Reduction of phosphate is difficult and requires enormous energy not likely to be available to sulfate-reducing bacteria grown on organic substrates and iron (Widdel, 1992; Roels and Verstraete, 2001). Furthermore, iron phosphide detected in the corrosion products investigated by Iverson (1968) is also naturally found in technical grade steels (Roels and Verstraete, 2001). Hence this corrosion scenario remains ambiguous (Beech and Sunner, 2007).

Furthermore, extracellular polymeric substances (EPS) of SRB have been proposed to influence iron corrosion (Beech *et al*., 1994; Beech *et al*., 1998; Fang *et al*., 2002). The suggested mechanisms include accumulation/entrapment of aggressive microbial metabolic products like FeS (Lee and Characklis, 1993; Newman *et al*., 1991), electronic and ionic conductivity of the EPS matrix (Beech and Sunner, 2004; 2007) and binding/sorption of metal ions (Little *et al*., 1990; Beech *et al*., 1999). Beech and Sunner (2004) conceived a corrosion model of electron transfer from Fe^0 through an anaerobic biofilm to O_2 as the terminal electron acceptor. However, this model of biofilm-assisted electron transfer via EPS-embedded Fe^{2+}- and Fe^{3+}-ions is inherently restricted to partially oxygenated environments (Beech *et al*., 1999; Hamilton, 2003; Beech and Sunner, 2004). Evidence for an involvement of EPS in corrosion is limited and apparently confined to their chelating properties. Cell-free EPS extracts of a marine *Desulfovibrio* strain rapidly dissolved metallic iron in short-term incubations during several minutes (Beech *et al*., 1998), but did only moderately affect corrosion on longer time scales (Beech *et al*., 1998; Fang *et al*., 2002). Generally, EPS may be envisioned to contribute to progressive corrosion through the establishment and functional maintenance of corrosive biofilms (Beech and Gaylarde, 1991; Newman *et al*., 1991).

A.4.4.4 Inorganic products of corrosion by SRB

The most conspicuous products of SRB-induced corrosion are the black iron monosulfides (collectively FeS; Smith and Miller, 1975). FeS may be the only ferrous corrosion product, as in CMIC (Eqs 17 – 19), or may account for only a part of the deposits in case of lithotrophic corrosion (Eqs 13 and 23). The surplus of ferrous iron from lithotrophic corrosion presumably precipitates as $Fe(OH)_2$ or $FeCO_3$ (von Wolzogen Kühr and van der Vlugt, 1934; Jack *et al*., 1995; Dinh *et al*., 2004).

At least seven different solids consisting only of iron and sulfur are found in nature at moderate temperatures (Rickard and Luther, 2007). Of these, mackinawite ($Fe_{1+x}S$) is commonly assumed to be the first corrosion product from reaction of HS^- with Fe^0 (Shoesmith *et al*., 1980; Sun, 2006; Sun and Nešić, 2007). However, also amorphous iron sulfides were detected at anaerobic sites with iron corrosion (Jack *et al*., 1990; Ferris *et al*., 1992). Hansson *et al*. (2006) detected poorly crystalline iron monosulfides in alkaline solutions containing Fe^0 and micromolar concentrations of sulfide.

Most iron sulfides, including mackinawite, are metastable and undergo mineralogical transformations (Smith and Miller, 1975; Anderko and Shuler, 1997; Little *et al*., 2006; Rickard and Luther, 2007). Anderko and Shuler (1997) considered equilibrium thermodynamics and calculated that, in a simulated oil field brine ($a_{Fe^{2+}} = 10^{-4}$; $a_{H_2S} = 4 \cdot 10^{-3}$), the formation of iron monosulfides followed the $FeSH^+ \rightarrow$ amorphous FeS $\rightarrow$ mackinawite $\rightarrow$ phyrrhotite replacement series. Formation of the iron disulfides pyrite and marcasite (FeS_2) is not expected under fully reduced conditions; their formation from FeS requires elemental sulfur or polysulfides (Morse *et al*., 1987; Wilkin and Barnes, 1996).

A.4.5 Corrosion of iron by methanogenic archaea

Methanogenic archaea (methanogens) are strictly anaerobic members of the *Euryarchaeota* that are characterized by the formation of methane in their energy metabolism (Conrad, 1999; Canfield *et al*., 2005). These microorganisms are nutritionally very restricted and depend in their natural habitats on fermentative bacteria that supply suitable substrates. Generally, methane formation in methanogenic archaea results from (i) the reduction of CO_2 with H_2 (or certain alcohols), or (ii) the disproportionation of a limited number of organic fermentation products such as acetate (Garcia *et al*., 2000; Thauer *et al*., 2008). Many SRB have similar nutritional requirements and out-compete methanogens when sufficient quantities of sulfate are accessible (Canfield *et al*., 2005; Thauer *et al*., 2007). Consequently, methanogenesis is

typically restricted to environments that are depleted of sulfate and other thermodynamically more favorable electron acceptors (e.g. metal oxides; Lovley and Phillips, 1987; Lovley *et al*., 1994). In such systems acetate and molecular hydrogen are the quantitatively most important substrates for biological methane production (Conrad, 1999; Garcia *et al*., 2000). Several authors have demonstrated that also cathodic hydrogen (Eq. 5) can serve as an electron donor for a variety of methanogenic archaea (Daniels *et al*., 1987, Deckena and Blotevogel, 1990; Lorowitz *et al*., 1992). In the consequence, methanogens have been implicated in corrosion and their presence could be demonstrated in corroded steel samples *in situ* (Zhang *et al*., 2003; Zhu *et al*., 2005; Larsen *et al*., 2010). Daniels *et al*. (1987) found high corrosion rates of up to 0.37 mm Fe^0 yr^{-1} in thermophilic *Methanococcus thermolithotrophicus* and *Methanobacterium thermoautotrophicum* in short-term culture incubations with metallic iron as the only electron donor. They attributed the observed corrosion to cathodic depolarization of iron by microbial H_2 uptake, a mechanistic model that has been postulated to operate in all hydrogenotrophic microorganisms (see *Chapter* A.4.4.3; von Wolzogen Kühr, 1961). However, other authors challenged this view and found that active hydrogenotrophic methanogens did not significantly stimulate corrosion when compared to sterile incubations (Deckena and Blotevogel, 1990; 1992). Similarly, further studies reported only moderately increased (1.1- to 2-fold) and generally rather low (0.016 to 0.065 mm Fe^0 yr^{-1}) corrosion rates in cultures of several meso- and thermophilic methanogens (Boopathy and Daniels, 1991; Lorowitz *et al*., 1992).

As their metabolic end-product methane is chemically inert towards iron, corrosion by methanogenic archaea must be explained by a different physiological trait. This may be either the effective utilization of cathodic hydrogen (cathodic depolarization) or a direct utilization of Fe^0 (Daniels *et al*., 1987; Dinh *et al*., 2004). Dinh *et al*. (2004) isolated a novel methanogenic archaeon from enrichment cultures with metallic iron as the sole electron donor. The isolated strain IM1, for which no distinct phylogenetic affiliation could be inferred, reduced CO_2 with Fe^0 at a 4-fold higher rate than could be explained by uptake of chemically formed (cathodic) H_2 (Dinh *et al*., 2004; compare Fig. 7C). 'Conventional' hydrogenotrophic methanogens grown with Fe^0 effectively consumed H_2 but did not accelerate corrosion compared to sterile incubations (Dinh, 2003; Dinh *et al*., 2004). Hence, direct uptake of iron-derived electrons was suggested as the mechanism of corrosion in strain IM1 (Fig. 13). Other authors adopted this view and similarly obtained specialized corrosive methanogenic archaea by an enrichment and isolation approach with metallic iron as the sole electron donor (Uchiyama *et al*., 2010; Mori *et al*., 2010). Methanogenesis with iron as the

only source of reducing equivalents always follows equation (23) [Daniels *et al*., 1987; Dinh *et al*., 2004]:

$$4\,Fe^0 + 5\,HCO_3^- + 5\,H^+ \rightarrow 4\,FeCO_3 + CH_4 + 3\,H_2O\,. \qquad (23)$$

Siderite is most likely the sole corrosion product (Dinh *et al*., 2004; Uchiyama *et al*., 2010).

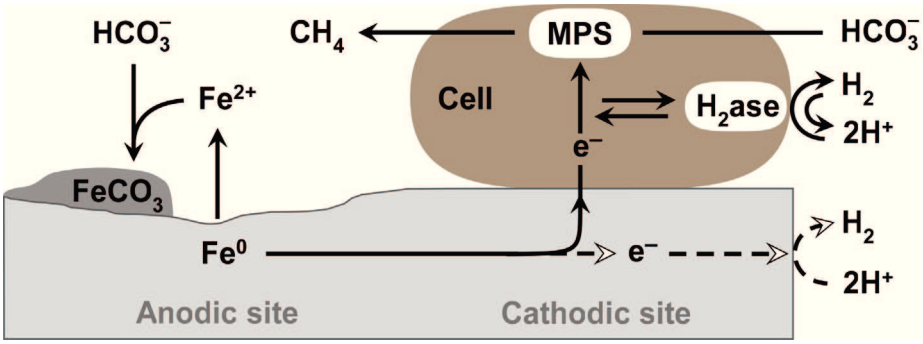

Fig. 13. Suggested electron flow during iron corrosion by specialized methanogenic archaea such as strain IM1. Stoichiometric equations, cellular components and iron topology are not fully depicted. Electrons flow from metallic iron into the cell *via* an as yet unidentified membrane-associated redox protein. Hydrogen formed during early phases of incubation of strain IM1 is explained by a branched electron transport system that allows disposal of surplus electrons ('overflow') *via* the hydrogenase enzyme (H_2ase), and by chemical formation. Ferrous iron precipitates as siderite ($FeCO_3$). MPS: Methane production system. Figure inspired by Dinh *et al*. (2004).

It was concluded that corrosiveness in archaea is a strain-specific physiological trait that depends on the physiological ability of direct electron uptake (Dinh, 2003; Mori *et al*., 2010).

A.4.6 Goals of the present work

Sulfate-reducing bacteria are certainly the main originators of biocorrosion in sulfate-rich anoxic environments. However, as demonstrated by the above considerations, there remain significant uncertainties about the underlying mechanisms and their relative contribution to metal decay. Causal understanding of biocorrosion requires an experimental dissection into individual processes and their study under controlled conditions ('reductionistic' approach). Such approach was followed in the present work in order to obtain an in-depth mechanistic understanding of the recently discovered bioelectrical corrosion of iron by lithotrophic SRB (EMIC), the principle goal of the present work. Obviously, the analysis of the traditional explanations of SRB-induced corrosion was also necessary for reference and comparison with EMIC. The goal of the present work was reached through a combination of the following approaches:

- Kinetic studies of the suggested anaerobic corrosion mechanisms under controlled conditions in axenic microcosms. Many of these experiments required incubation during long, technologically relevant periods of time (~6 months) to demonstrate the practical relevance of the studied mechanisms.
- Electrochemical study of the suggested anaerobic corrosion mechanisms under controlled conditions in pure cultures. These experiments were performed at or in close collaboration with the Max Planck Institute for Iron Research, Düsseldorf (Germany).
- Physicochemical and chemical analysis of biogenic corrosion products. This provided valuable insights into particular corrosion mechanisms. Additionally, such analysis allowed the assessment of the relative contribution of EMIC to total MIC.
- Enrichment and isolation of novel directly corrosive SRB to obtain insights into the phylogenetic diversity of such peculiar lithotrophic microorganisms.

Part B: Results and discussion of the present work

B.1 Mechanistic study of the bioelectrical corrosion of iron by lithotrophic SRB in axenic microcosms

In the present study it is assumed that sulfate-reducing bacteria are the main culprits of oxygen-independent corrosion in sulfate-rich environments and investigated the various proposed mechanisms in axenic microcosm incubations. Such defined incubations facilitate the study of individual corrosion mechanisms that would, under more natural conditions, be masked by the complexity of the various overlaying processes.

B.1.1 Kinetic examination of anaerobic corrosion

We first monitored the temporal progression of Fe^0 oxidation in a sterile anoxic seawater medium. Subsequently, we studied anaerobic corrosion in the same system, but with (i) SRB scavenging cathodic H_2, (ii) SRB growing on lactate and producing large amounts of H_2S, and (iii) novel specialized SRB corroding Fe^0 by the recently proposed mechanism of direct electron uptake. To this end, steel coupons (>99.6% Fe^0; a = 298 cm^2) were incubated in 1.4 l bicarbonate-buffered, sulfide-free artificial seawater medium (ASW) at 22°C.

Abiotic anaerobic corrosion of iron in seawater.

Coupons were exposed to sterile ASW for more than eight months to demonstrate abiotic corrosion reactions during a technologically relevant period of time (Fig. 14). Reduction of H^+-ions to H_2 (Eq. 4) is the only thermodynamically feasible cathodic reaction under the present conditions. Anodic iron dissolution was obvious from increasing concentrations of Fe^{2+}(aq). However, the increase of Fe^{2+}(aq) occurred non-stoichiometrically with regard to hydrogen formation (Eq. 5); later, concentrations of Fe^{2+}(aq) even declined. This is explained by the poor solubility of Fe^{2+}(aq) in bicarbonate-containing environments. During the incubation, large amounts of a white precipitate, presumably $FeCO_3$, were formed. Fe^{2+}(aq) concentrations are occasionally used to quantitatively monitor corrosion (Daniels *et al*., 1987; Rajagopal and LeGall, 1989; Mori *et al*., 2010), but were considered an inappropriate parameter in the present study. Instead, (cathodic) hydrogen concentrations were used to monitor corrosion under the anaerobic conditions. Cathodic H_2 formed on Fe^0 surfaces at an averaged rate of 68.4 nmol H_2 cm^{-2} d^{-1}, corresponding to a corrosion current density (charge transfer) i_{corr} of 0.15 μA cm^{-2}. The rate of H^+ reduction gradually slowed down, most likely a consequence of the slightly increasing pH (ΔpH = 0.3) during incubation.

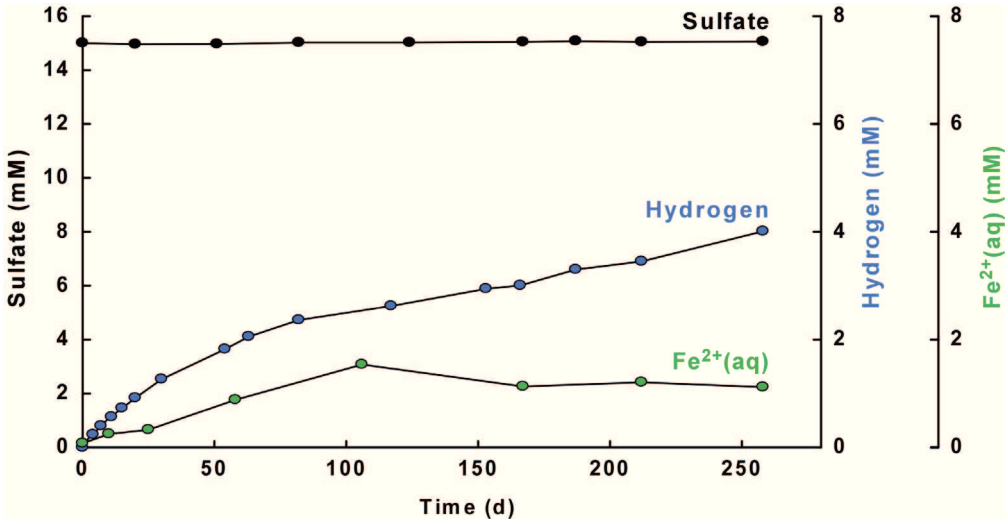

Fig. 14. Corrosion of iron in anaerobic sterile artificial seawater medium. For convenience, hydrogen concentrations refer to the medium. The *pH* increased gradually from *pH* 7.0 to 7.3 (not shown). Error bars were smaller than symbol sizes.

In technology, corrosion rates are often expressed as millimeter metal loss per year (mm Fe^0 yr^{-1}). In the sterile anoxic incubation iron corroded at 0.002 mm Fe^0 yr^{-1}, a metal loss rate with virtually no effect on the integrity of technical iron constructions. The observed rates are, due to the prolonged incubation time, lower than the rates of hydrogen-producing corrosion reported in the literature (Cord-Ruwisch, 2000). Built-up of cathodic hydrogen in the incubations did not stop corrosion (no 'polarizing' effect).

Anaerobic corrosion of iron by hydrogen-consuming SRB.

If the microbial consumption of cathodic H_2 accelerates corrosion, this should be evident from incubation experiments with Fe^0 as the sole source of electrons. We investigated this hypothesis with *Desulfopila inferna* (Gittel *et al.*, 2010), the closest cultivated relative of *Desulfopila corrodens* strain IS4 (formerly *Desulfobacterium corrodens*; Dinh *et al.*, 2004). *D. inferna* did not accelerate corrosion compared to sterile conditions (Figs 14 and 15), despite the effective consumption of H_2 below detection limit (40 ppmv). Apparently, sulfate reduction in this hydrogenotrophic SRB was fuelled by chemically formed H_2, but with no influence on the rate of reaction (5). No accumulation of dissolved sulfide was observed (not shown), probably a consequence of excess amounts of ferrous iron (Eq. 22) and precipitation as FeS according to reaction (18). Steel coupons gradually became covered with a dark grayish mineral crust. The averaged sulfate reduction rate of 20.2 nmol SO_4^{2-} cm^{-2} d^{-1} corresponded to an estimated corrosion rate of 0.002 mm Fe^0 yr^{-1} (0.18 µA cm^{-2}) in this incubation (with q_{Anab} = 0.1; for calculation see appendix to *Chapter* D.1).

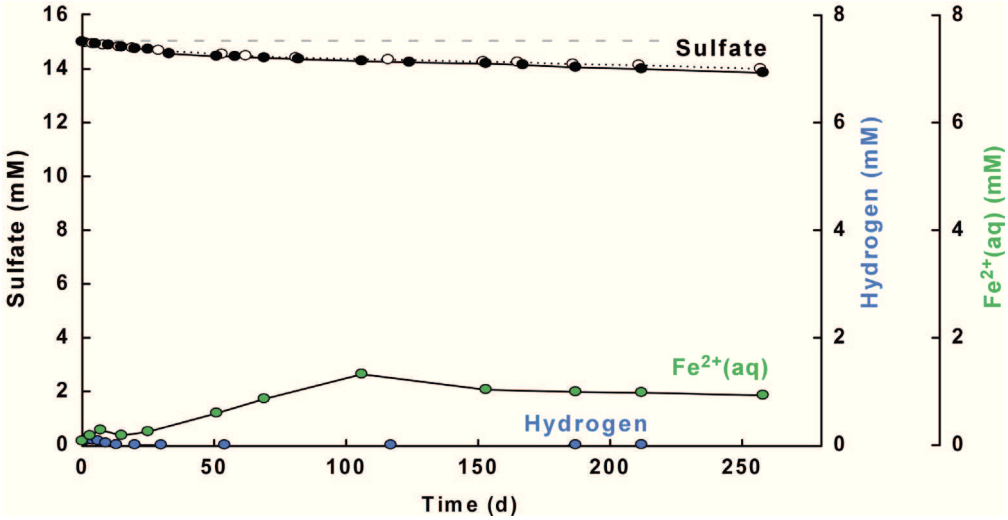

Fig. 15. Corrosion of iron in the presence of hydrogenotrophic *Desulfopila inferna*. Filled black circles indicate sulfate reduction by the strain. Open circles and dotted line indicate expected sulfate reduction from consumption of chemically formed (cathodic) hydrogen. For convenience, hydrogen concentrations refer to the medium. The *pH* increased gradually from *pH* 7.0 to 7.4 (not shown). Dissolved sulfide was below 12 µM during the first month of incubation (not shown). Thereafter, no sulfide was detectable. Error bars were smaller than symbol sizes.

Similar results were obtained with cultures of various other SRB strains, including *Desulfovibrio vulgaris*, *Desulfovibrio aespoeensis*, *Desulfovibrio indonesiensis*, *Desulfobacterium autotrophicum*, *Desulfobacterium vacuolatum* and *Desulfosarcina variabilis* (data not shown). To test the possibility that cathodic depolarization can only be achieved by particularly effective H_2-scavengers that thrive at very low partial pressures of H_2, we isolated three such strains. *Desulfovibrio* sp. strain HS3 was isolated from enrichment cultures with a low diffusive influx of H_2. *Desulfovibrio* sp. strains HS4 and HS5 were isolated directly from enrichment cultures with corroding iron as the only source of hydrogen. Neither of these strains accelerated corrosion, as evidenced by marginal sulfate reduction with Fe^0 and metal weight loss comparable to sterile incubations (Figs S1 and S2). No distinct influence of hydrogen-consuming SRB on iron corrosion was observed in the present study.

Based on thermodynamic and kinetic considerations, consumption of cathodic hydrogen seems an implausible explanation for rapid corrosion in anoxic environments (Widdel, 1992; Cord-Ruwisch, 2000; Dinh *et al*., 2004). The free energy of reaction (5) is $\Delta G^{o'} = -10.6$ kJ mol^{-1} at standard conditions except $a_{H^+} = 10^{-7}$, viz. the reaction is feasible at neutral *pH*. At environmentally relevant activities of $Fe^{2+}(aq)$ that are significantly below standard activity, the Fe^{2+}/Fe^0 redox couple is even more negative, often $E_{Fe^{2+}/Fe^0} < -0.6$ V, so that $\Delta G = <$ -36.7 kJ mol^{-1}. For a thermodynamic halt ($\Delta G \geq 0$) of iron dissolution according to reaction

(5), one would have to assume a 'hydrogen film' with a local fugacity corresponding to $p_{H_2} > 10^{11.4}$ Pa ($10^{6.4}$ atm). Considering the extremely fast diffusion of H_2, such local build-up of a H_2 'film' appears very unrealistic even in the absence of hydrogenotrophic microorganisms.

Formation of molecular hydrogen according to reaction (4) involves a number of discernable steps (Kaesche, 2003). Initially this is the transport of H^+ to the steel surface by electrolytic migration, advection and diffusion

$$H^+ \rightarrow (H^+)_* \tag{24}$$

followed by charge transfer and combination reactions according to

$$(H^+)_* + e^- \rightarrow H_{ads} \quad | \text{Volmer mechanism} | \tag{25}$$

$$H_{ads} + H_{ads} \rightarrow H_2 \quad | \text{Tafel mechanism} | \tag{26}$$

$$H_{ads} + (H^+)_* + e^- \rightarrow H_2 \quad | \text{Heyrowski mechanism} | \tag{27}$$

which proceed either *via* the Volmer-Tafel or the Volmer-Heyrowski reaction sequence (Bockris and Reddy, 1970; Kaesche, 2003). Rate control cannot be easily attributed to any particular of these reactions and depends on factors such as the *pH* of the electrolyte and the material properties of the catalyzing surface (Bockris and Reddy, 1970; Cohen, 1979). However, microbial consumption of H_2, i.e. a reaction behind the kinetic bottleneck, is clearly not expected to accelerate reactions (24) – (27).

In conclusion, experimental and theoretical examinations strongly challenge the view that microbial uptake of cathodic H_2 influences corrosion in anoxic environments.

Anaerobic corrosion of iron with biogenic H_2S (CMIC).

Cultures of *D. inferna* were amended with 20.6 mM lactate as an additional substrate for sulfate reduction to study the corrosion of iron with excess amounts of biogenic sulfides (H_2S, HS^-). Incomplete oxidation of lactate by *D. inferna* can account for a theoretical maximum of 10.3 mM reduced sulfate (Eq. 8; in reality less because of electrons channeled into anabolism). However, the culture reduced 11.5 mM sulfate during the first 40 days of incubation (Fig. 16). The discrepancy can only be explained by the use of reducing equivalents for sulfate reduction from the iron. The required reducing power would be provided by reaction of ≥4.8 mM sulfide with metallic iron and release of hydrogen according to reactions (14) – (19). Indeed, only 5.9 instead of the expected 11.5 mM dissolved sulfide

from sulfate reduction were detected (Fig. 16; the discrepancy is precipitated FeS). Hence CMIC in the present incubation was obvious.

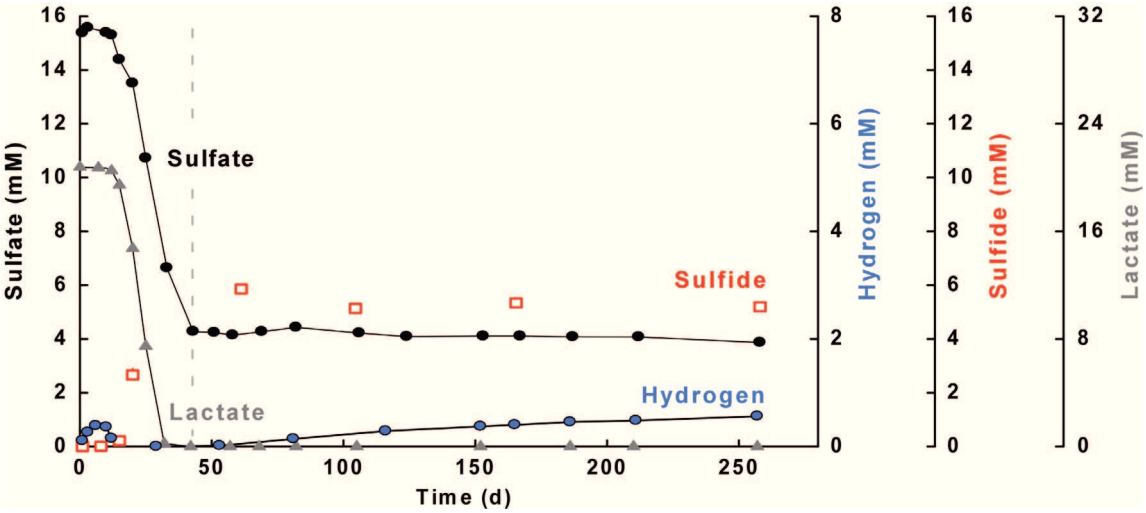

Fig. 16. Corrosion of iron by *D. inferna* grown with lactate as an organic electron donor for sulfate reduction. For convenience, hydrogen concentrations refer to the medium. The *pH* of the medium remained at *pH* ≈ 7.1. Ferrous iron remained below detection limit (3.5 µM) during incubation (not shown). Dotted line indicates stop of sulfate reduction. Error bars smaller than symbol sizes.

Interestingly, sulfate reduction stopped after 40 days and sulfide concentrations remained constant during the following more than 200 days of incubation. Apparently, the iron no longer provided reducing equivalents (viz. H_2) for sulfate reduction and virtually no dissolved sulfide reacted with metallic iron during this time. This is attributed to the formation of a tightly adherent FeS film on the metal. Such FeS films impede corrosion effectively and are a common observation in sulfidic laboratory cultures (Lee and Characklis, 1993; Lee *et al.*, 1995; Sun and Nešić; 2007) and environments (Nešić, 2011; Sun *et al.*, 2011a, 2011b). It has been proposed that iron dissolution is prevented in cases where dissolved H_2S/HS^- concentrations exceed the concentration of $Fe^{2+}(aq)$ at the unreacted metal surface (Newman *et al.*, 1992). Under these conditions the thin and tightly adherent FeS layer (typically mackinawite) is formed and protects the underlying Fe^0 from further corrosion by providing an effective diffusion barrier to $Fe^{2+}(aq)$ [Shoesmith *et al.*, 1980; Newman *et al.*, 1992]. Not surprisingly, high corrosion rates (>0.2 mm Fe^0 yr^{-1}) in culture experiments with SRB have mainly been produced when the formation of such layers was avoided, e.g. by application of artificially high concentrations of ferrous salts in the incubation medium (Adams and Farrer, 1953; Lee and Characklis, 1993). However, the factors that determine the formation and breakdown of protective iron sulfide films are not entirely understood. Aging and rupturing of

such films has been reported to result in rapid localized metal destruction (Newman *et al*., 1991; 1992; Lee *et al*., 1995; Hansson *et al*., 2006).

The corrosion rate in the present long-term incubation was determined from the difference between the expected amount of formed (free) sulfide and the actual amount that could be detected at the end of the incubation. Accordingly, 5.6 mM sulfide reacted with iron corresponding to an overall corrosion rate of 0.0026 mm Fe^0 yr^{-1} (0.22 μA cm^{-2}). Transfer of the FeS-coated steel samples from the flask into separate (sterile) incubators and studying of hydrogen-producing corrosion under these conditions revealed a considerable protectiveness of the FeS film against corrosion (Fig. S3). This supported the assumption that low corrosion rates were due to the surface film.

Accumulation of cathodic hydrogen during the end of the present incubation indicated an inhibition of microbial activity, possibly by the prolonged exposure to sulfidic medium. However, cells remained viable. Cultures could be established in fresh media with hydrogen or lactate. A similar study of CMIC with *Desulfovibrio* sp. strain HS5 grown on Fe^0 and 20 mM lactate showed no such inhibition of microbial activity. Even though the averaged corrosion rate of strain HS5 was higher (0.0057 mm Fe^0 yr^{-1}; 0.49 μA cm^{-2}), again accumulation of free sulfide and hence impediment of corrosion was observed (not shown).

In environments with large amounts of organic electron donors for sulfate reduction, the formed sulfides can severely degrade steel constructions (CMIC) but may also protect the metal through the formation of special forms of tightly adherent FeS films (Newman *et al*., 1992; Lee and Characklis, 1993; Lee *et al*., 1995).

Anaerobic corrosion of iron by direct electron uptake (EMIC).

To study the proposed mechanism of direct electron uptake from metallic iron, we incubated carbon steel coupons with the previously isolated *Desulfopila corrodens* strain IS4 (Dinh *et al*., 2004). Contrary to 'conventional' hydrogenotrophic SRB such as *D. inferna* (Fig. 16), strain IS4 reduced sulfate much faster than could be explained by mere consumption of chemically formed hydrogen (Fig. 17A) and caused pronounced alkalization of the culture medium (Fig. 17B). Furthermore, cultures of strain IS4 initially evolved H_2 rather than scavenged it. This confirmed previous findings (Dinh, 2003; Dinh *et al*., 2004) that demonstrated in similar experiments the ability of strain IS4 to utilize metallic iron effectively, most likely *via* direct electron uptake (Eq. 21).

Compact black crusts gradually formed on the incubated steel coupons. Apparently, precipitation of Fe^{2+}(aq) with inorganic carbon and biogenic sulfide (Fig. 17B) occurred

directly at the corroding metal. This may be due to the pronounced alkalization of the steel surface that is expected from reaction (21) by metal-associated SRB. However, deposition of FeS also at glass walls indicated additional formation and precipitation of sulfide remote from the coupons. This has been explained by the utilization of accumulated hydrogen in such cultures (Fig. 17A; Dinh, 2003).

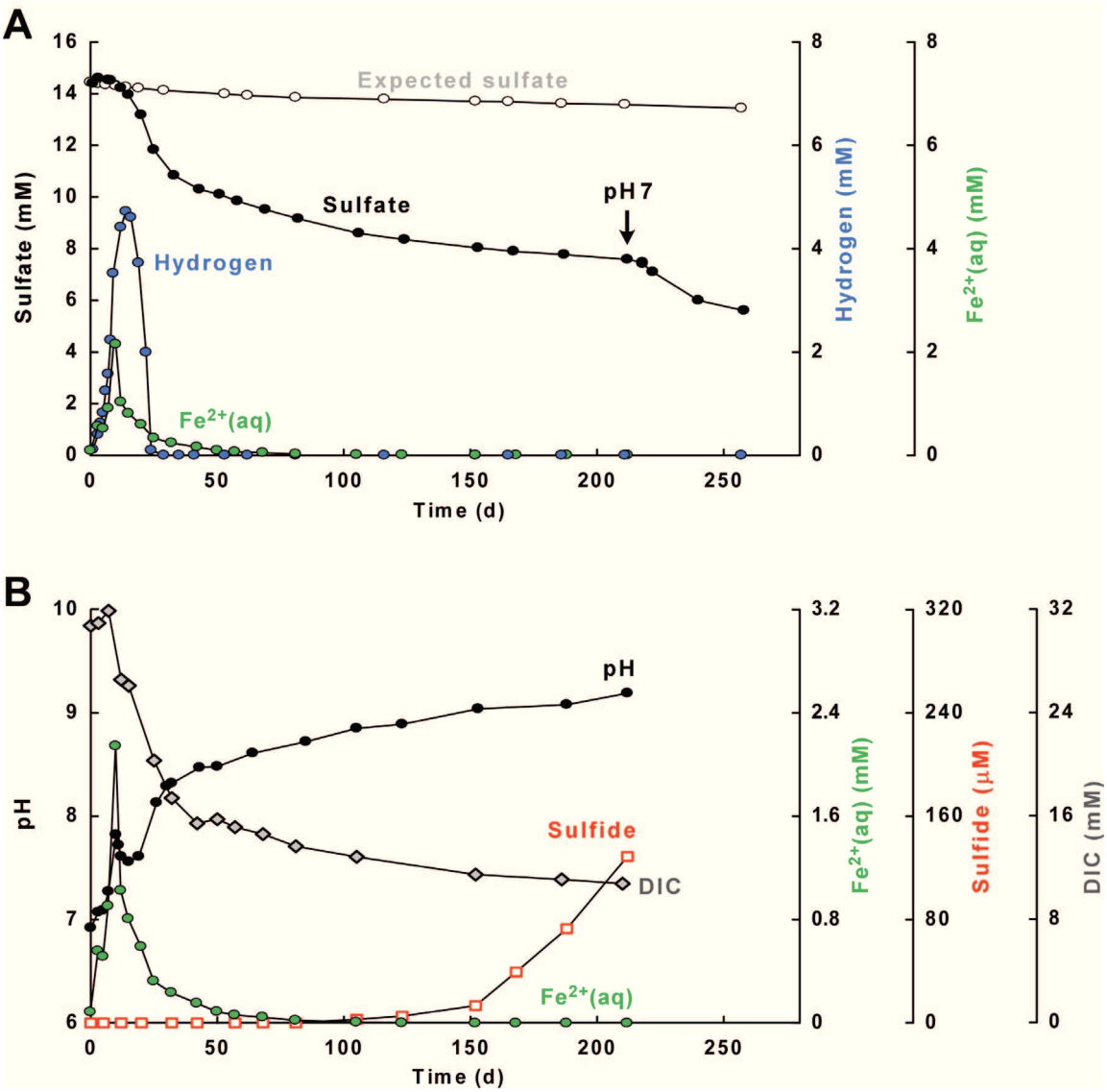

Fig. 17. Corrosion of iron by *D. corrodens* strain IS4.

A. Concentrations of dissolved sulfate, hydrogen and ferrous iron. Expected sulfate reduction from scavenge of cathodic hydrogen is also indicated. Sulfate reduction led to pronounced alkalization (B) according to Eq. (22) and a decrease of culture activity. Activity resumed upon readjustment of the *pH* to 7.0 by addition of HCl (arrow).

B. Increase of *pH* in culture (A) and its effect on dissolved ferrous iron, free sulfide and dissolved inorganic carbon (DIC). Error bars were smaller than symbol sizes.

Rapid formation of molecular hydrogen in cultures of strain IS4 required further investigation. Such formation of H_2 apparently preceded SO_4^{2-} reduction in the present incubation (Fig. 17A). This has been attributed to the disposal, *via* intracellular hydrogenases, of an initial excess of electrons entering strain IS4 during colonization of blank metallic surfaces (Fig. 12; Dinh *et al*., 2004). However, also steel coupons covered with a fully developed biogenic crust rapidly evolved H_2 when transferred into sulfate-free ASW after 8 months of incubation, i.e. when depriving the cultures of the electron acceptor SO_4^{2-} (Fig. S4). To test whether the apparent catalysis of H_2 formation was indeed biological or instead due to FeS (Eq. 20), we incubated washed cell suspensions of strain IS4 with Fe^0 in sulfate- and sulfide-free ASW (Fig. 18). Biological catalysis of H_2 formation by strain IS4 was evident.

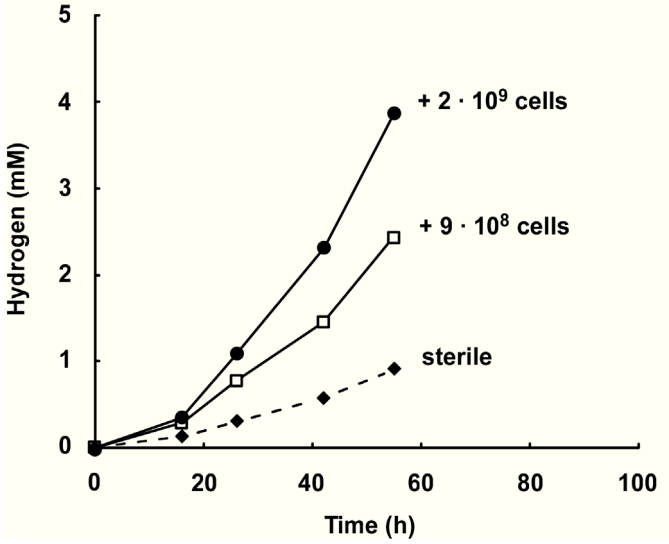

Fig. 18. Catalyzed reduction of H^+-ions to H_2 with Fe^0-derived electrons by resting cell suspensions of *D. corrodens* strain IS4. Washed cell suspensions of strain IS4 (pre-grown on H_2) were incubated with 15 g Fe^0 granules in 100 ml anoxic sulfate- and sulfide-free ASW under rigorous slewing. Hydrogen concentration refers to a 56 mL headspace of N_2/CO_2 (90/10). Error bars were smaller than symbol sizes. The specific H_2 formation rate of strain IS4 ranged between 18 and 45 fmol H_2 $cell^{-1}$ $hour^{-1}$ (errors due to cell aggregation).

Still, no accumulation of H_2 was observed in cultures of other corrosive SRB isolates (*Chapter* B.2.1). Furthermore, *Desulfovibrio ferrophilus* strain IS5 showed no obvious H_2 formation in sulfate-free incubations (Fig. S4). Biogenic proton reduction with iron-derived electrons is an interesting aspect of EMIC that requires further investigation, particularly with regard to its quantitative contribution to corrosion.

Sulfate-reducing activity of strain IS4 (Fig. 17A) gradually decreased during the incubation, resulting in a rather low corrosion rate of approx. 0.016 mm Fe^0 yr^{-1} (1.42 µA cm^{-2}), averaged over the first seven months of incubation. This is in agreement with previous

studies (Dinh *et al*., 2004); inorganic corrosion crusts were considered to act as a process barrier and hence limit the corrosiveness of the novel isolates (Dinh, 2003; Dinh *et al*., 2004). However, EMIC is a strongly alkalizing process (Eq. 22), rapidly exceeding the buffering capacity of batch incubations that provide large metal surfaces (Fig. 17B). Careful readjustment of the present incubation from *pH* 9.2 to *pH* 7.0 by addition of HCl resulted in the rapid resumption of activity despite coverage of steel coupons with the inorganic crust (Fig. 17A). We conclude that the activity of corrosive SRB such as *D. corrodens* in previous experiments (Dinh, 2003; Dinh *et al*., 2004) was mainly limited by the pronounced alkalization.

To examine the destruction of iron by SRB strains IS4 and IS5 under conditions comparable to those *in situ*, the metal surface to culture volume had to be decreased. An appropriate metal surface was $a = 2.4\ cm^{-2}$, which was still large enough to demonstrate macroscopic corrosion phenomena and precisely monitor sulfate consumption in 1.4 l incubation flasks. Indeed, corrosion rates did not significantly decrease over months (Fig. 19A).

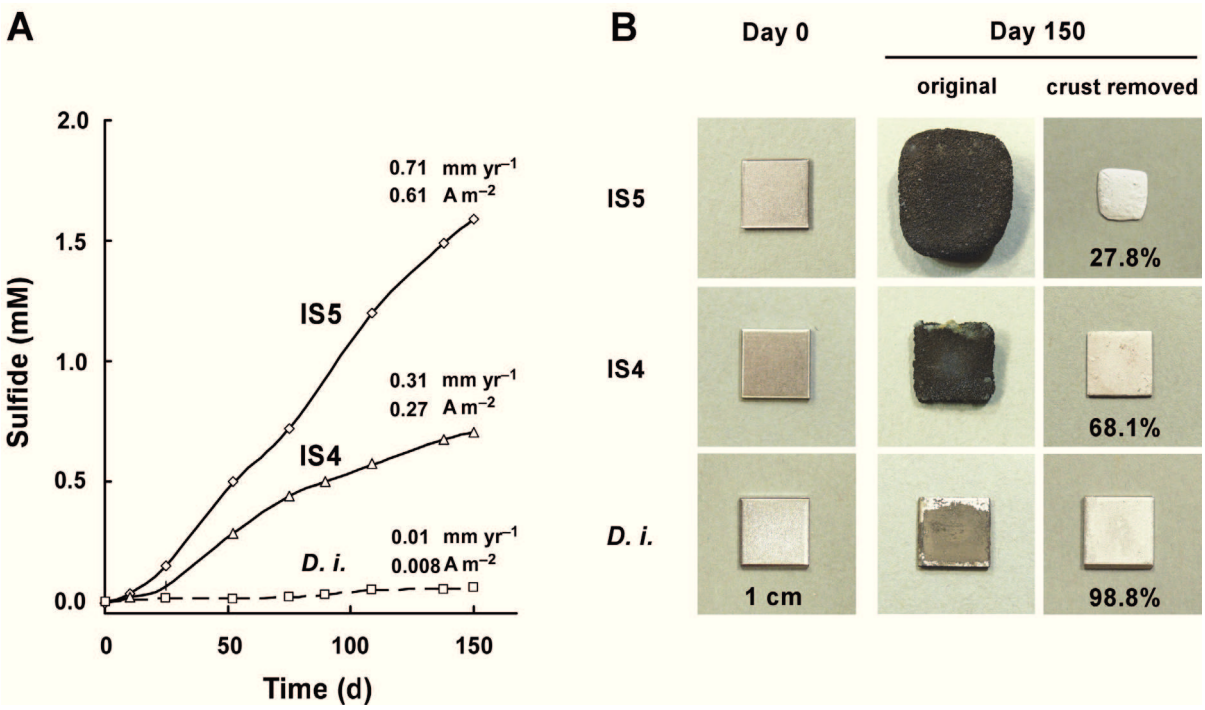

Fig. 19. Corrosive sulfate-reducing bacteria in pure culture.

A. Long-term sulfide formation (calculated from sulfate loss) by *Desulfovibrio ferrophilus* strain IS5 and *Desulfopila corrodens* strain IS4 with iron coupons as the only electron donor. The hydrogenotrophic control culture *Desulfopila inferna* (*D. i*.) was also included in this experiment. Accumulation of hydrogen was not observed in these incubations (not shown).

B. Thick crusts and metal loss in these cultures. Residuary metal (% of initial) became obvious after crust removal with inactivated acid (10% hexamine in 2 M HCl). Inactivated acid did not dissolve metallic iron. Error bars were smaller than symbol sizes.

Corrosive cultures reached values as high as 0.71 mm Fe^0 yr^{-1} (61.2 µA cm^{-2}) and deposited steadily growing black crusts (Fig. 19A and B). After crust removal, severe metal loss was evident (Fig. 19B). In the present experiments, strain IS5 was more corrosive than strain IS4, whereas in the initial physiological characterization (Dinh *et al*., 2004), the latter was more corrosive. This may be due to the higher tolerance of strain IS4 to the significantly increasing *pH* in the previous incubations. In the present experiment, both strains displayed a corrosiveness that matches reported cases of microbially influenced corrosion *in situ* (Jack, 2002), and are hence envisioned as cultivated representatives of the key players in anaerobic iron corrosion (see *Chapter* B.2.3).

No kinetic inhibition of EMIC by the inorganic crust was observed in laboratory microcosms under *in situ*-like conditions. One may speculate that with Fe^0 as the only or main electron donor for sulfate reduction, the resultant surplus of Fe^{2+}(aq) prevents access of H_2S/HS^- to the metal surface and hence the formation of tightly adherent, protective FeS films.

The observed severe bioelectrical corrosion of iron by strains IS4 and IS5 urges upon a more detailed investigation of the underlying mechanisms.

B.1.2 Localization of corrosive SRB and analysis of biogenic corrosion products

The following chapters will focus on EMIC and the cultivated representatives, strains IS4 and IS5. CMIC has been studied extensively (as reviewed e.g. in Booth, 1964; Tiller, 1983; Hamilton, 1985; Lee *et al*., 1995; Lewandowski and Beyenal, 2009) and is treated in this study only where a comparison between the two mechanisms is particularly demonstrative.

Localization of corrosive cells and determination of crust conductivity.

If the pronounced corrosion observed in cultures of strains IS4 and IS5 is due to direct electron uptake, cells must be always electrically connected to their substrate. This would be possible by direct attachment to the metal. However, such localization would implicate increasing coverage by the forming hard corrosion crust (Fig. 19B) and cut-off from the medium supplying sulfate and diminishing the strongly alkalizing 'bio-cathodic' reaction (Eq. 21). The observed progressive utilization of metallic iron despite coverage by the crust could be possible if cells would colonize the medium-exposed crust surface, and if the biogenic crust would be electrically conductive.

Indeed, virtually no planktonic cells could be observed, and scanning electron microscopy revealed a densely colonized crust surface in the corrosive cultures of strains IS4 and IS5

(Fig. 20). Colonized areas of the structurally heterogeneous surface contained the element S in addition to Fe, C and O (details in Fig. 20), as revealed by energy-dispersive X-ray spectroscopy (EDX) of the uppermost (~5 µm) crust. Sulfur-free patches were never colonized, indicating a co-localization of cells with iron sulfide. Iron sulfides are long known semiconducting minerals (Braun, 1875; Pearce *et al*., 2006).

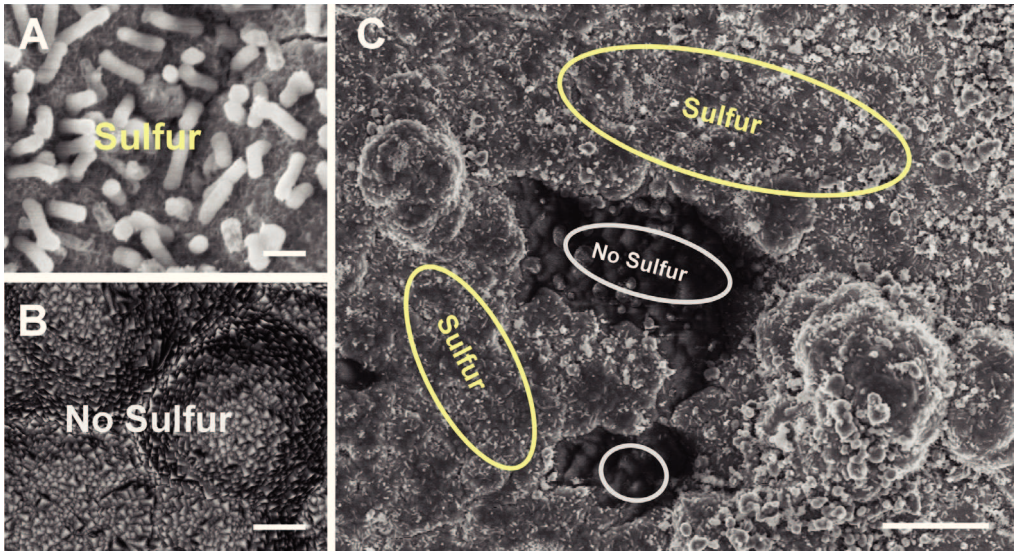

Fig. 20. X-ray microanalysis (EDX) of crust surface in a culture of corrosive strain IS4.
A. Site with microbial colonization (SEM. Bar, 1 µm).
B. Site without microbial colonization (SEM. Bar, 1 µm).
C. Both sites in the same field of view (SEM. Bar, 20 µm). Surface-attached cells of strain IS4 co-localize with the element S. No cells can be detected at S-free sites. Both types of sites include the elements Fe, C and O. Cell-free sites contain in addition Mg and Ca. Thirty point spectra at 10 kV were collected at each site. Resolution (lateral and vertical) is 3–5 µm.

The *in situ* electrical conductivity of the bulk corrosion crust was evaluated as follows. The crust was allowed to cement and bridge two iron coupons fixed at defined distance and connected to monitoring wires protruding the stopper of an anoxic incubation flask (Fig. 21). The mounted coupons were only partly immersed so as to keep iron other than the slot-forming part outside of the medium. The electrical conductivity σ of the biogenic crust measured at a voltage (≤0.2 V) far below that for water electrolysis was around 50 S m^{-1} (Fig. 21, Table S1). Such electrical conductivity is substantial and even higher than that of many typical semiconductors (e.g. pure silicon, $\sigma = 1.6 \cdot 10^{-3}$ S m^{-1}, *Chapter* D.1). Conductivity must be due to iron sulfides within the crust; siderite ($FeCO_3$) and other carbonate minerals likely to be found in the heterogeneous crust, are essentially insulators with $\sigma < 10^{-10}$ S m^{-1}.

With the measured conductivity, the observed metal loss (0.71 mm Fe^0 yr^{-1}) and associated current density (61.2 µA cm^{-2}) would need a potential difference (voltage) of only

$\Delta E = 1.2 \cdot 10^{-4}$ V across a 1 cm crust. The calculated equilibrium potential at the corroding iron surface and the zone of sulfate reduction is around –0.60 and –0.23 V, respectively, viz. $\Delta E = 0.37$ V (see appendix to *Chapter* D.1). Hence, there is significant leeway for the 'self-adjusting' potential difference to drive the corrosion current through the crust. Crust conductivity is apparently not a rate-limiting factor.

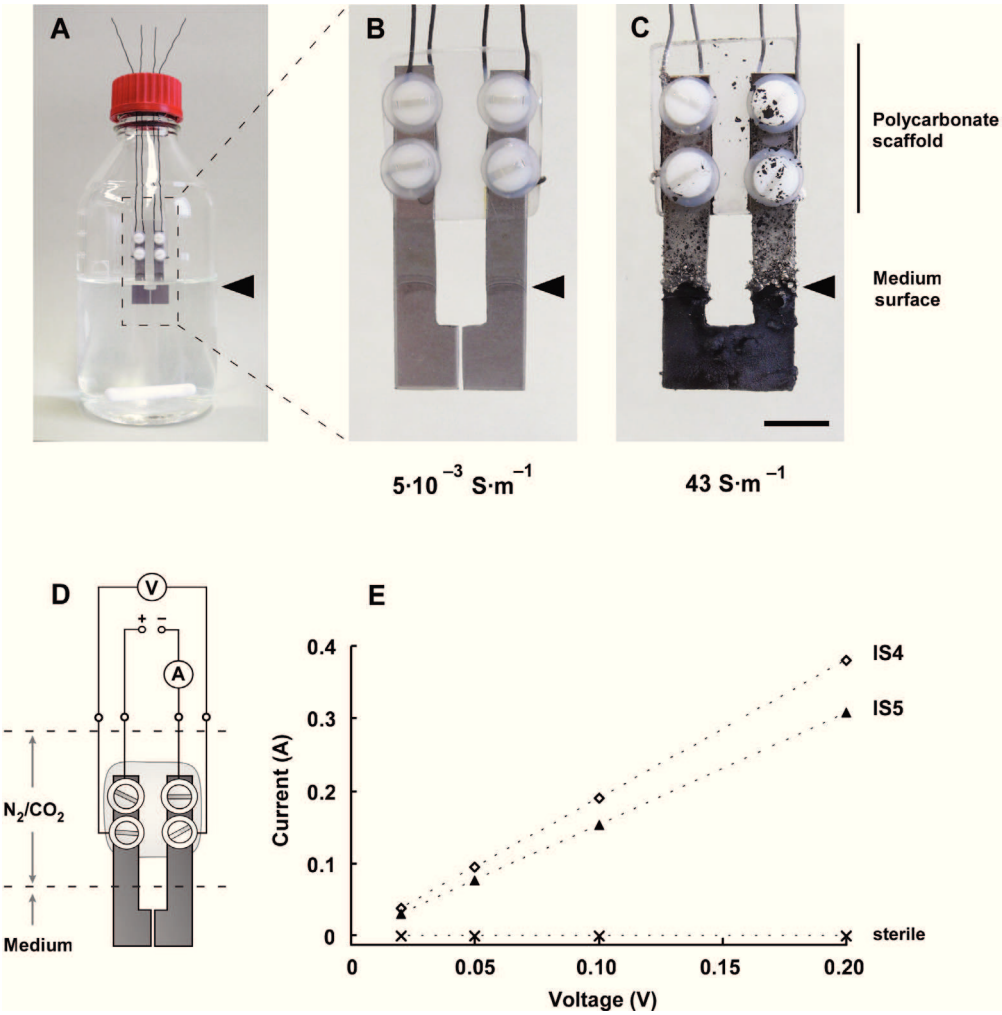

Fig. 21. Determination of the electrical conductivity of the corrosion crust**.**

A. Anoxic incubation flask (600 ml medium) with two specially shaped iron coupons.

B. Coupons after three weeks in sterile medium.

C. Coupons after three weeks in medium with strain IS4. Bar, 1 cm.

D. Schematic illustration of the arrangement of instruments for non-invasive measurement of voltage and current (separate circuits to avoid considerable contact resistances).

E. Linear current response to applied (non-electrolytic) voltage (0.02 – 0.2 V, DC). Instruments were only connected at the end of the incubation.

Quantitative chemical composition and crystalline components of the biogenic crust.

Equations (19) and (22) predict fundamentally different mineral corrosion products as the result of biogenic H_2S (CMIC) and bioelectrical corrosion by SRB (EMIC), respectively. This applies particularly to the relative quantities of contained S and Fe. Quantitative analysis of bulk corrosion products was achieved by combining EDX, X-ray diffraction (XRD), inductively coupled plasma optical emission spectroscopy (ICP-OES) and infrared spectroscopy.

First, we analyzed the black detached precipitates from a culture of *D. inferna* incubated with Fe^0 and 20.6 mM lactate (Fig. 16); collection and quantitative analysis of the thin metal-attached FeS film was not possible. Two thirds (dry mass) of the flocculent precipitated material consisted of the elements S and Fe in approximately equimolar amounts. Expectedly, FeS was the only ferrous corrosion product of CMIC, i.e. the ratio of the amount of sulfidic iron, $n_{FeS,}$ and totally corroded iron, $n_{Fe(II),}$ was $q_{FeS/Fe(II)} = 0.99 – 1.09$ (theoretically $q_{FeS/Fe(II)}$ is always ≤ 1).

Subsequently, we analyzed the hard, mineral-like corrosion crusts formed in cultures of *D. corrodens* strain IS4. Principally, EMIC is predicted to produce FeS as well as additional non-sulfidic ferrous minerals Fe_{NonS} (Eq. 22), so that sulfidic iron accounts for 25% of total corroded iron, or $q_{FeS/Fe(II)} = 0.25$. However, reaction (22) considers catabolic iron oxidation only; additional Fe^0 oxidized for anabolic purposes slightly lowers the ratio to an estimated $q_{FeS/Fe(II)} = 0.23$ (*Chapter* D.1).

In parallel to the purely lithotrophic incubations, some cultures of strain IS4 were supplemented with 3 mM lactate, to investigate the influence of simultaneously occurring EMIC and CMIC on the composition of biogenic crusts. The formed crusts were subjected to a full quantitative analysis (Table 1). Crusts of strain IS4 grown with Fe^0 as the only electron donor contained deposited S and Fe in the expected stoichiometry (Table 1; *Chapter* D.1). Fe^0-independent sulfide formation with lactate led to additional amounts of deposited FeS in the crust, in accordance with reactions (14) – (19), and possibly also by substitution of $FeCO_3$ (Lin *et al*., 2009):

$$FeCO_3 + HS^- \rightarrow FeS + HCO_3^- \qquad (28)$$

Additionally, all analyzed crusts contained considerable amounts of the co-precipitated elements Ca, Mg and P; it is assumed that the pronounced alkalization of the metal

surroundings by the 'bio-cathodic' reaction (21) facilitates the localized deposition of carbonate and phosphate minerals.

Table 1: Quantitative elemental composition of corrosion crusts of strain IS4. Cultures were either incubated with Fe^0 as the only electron donor (IS4 + Fe^0) or with an additional 3 mM lactate (IS4 + Fe^0 + lac).

Element [a], parameter	IS4 + Fe^0		IS4 + Fe^0 + lac	
Fe	29.7	28.0	24.3	26.4
Ca	8.4	9.6	12.8	12.1
C	6.3	6.5	8.3	8.1
S	3.9	4.0	6.5	7.0
P	2.7	2.5	0.7	0.7
Mg	2.1	2.2	2.4	2.2
O [b]	46.9	47.3	45.1	43.6
$q_{FeS/Fe(II)}$ [c]	**0.23**	**0.25**	**0.46**	**0.46**
Detected by XRD [d]	Siderite, calcite		Siderite, calcite	

a. Elements detected in corrosion products by EDX. Quantitative analysis (weight percent) was achieved by infrared spectroscopy for (combusted) C and S. The remaining elements were quantified by ICP-OES.
b. Oxygen was calculated as the remaining fraction in corrosion products. Hydrogen could not be quantified by available instrumentation, but is expected to account for only a minor fraction (weight percent) in dried corrosion products.
c. Molar ratio sulfide to ferrous iron in corrosion products.
d. Detection of crystalline phases by X-ray diffraction.

X-ray diffraction (XRD) analysis of homogenized crust samples showed the absence of crystalline iron sulfides such as mackinawite ($Fe_{1+x}S$), pyrrhotite ($Fe_{1-x}S$), troilite (FeS), greigite (Fe_3S_4) and pyrite (FeS_2). Hence, the iron sulfides formed through bioelectrical corrosion by SRB (Eq. 22) were apparently amorphous. Interestingly, iron sulfides detected in many sulfidic environments and laboratory cultures are usually in the form of crystalline minerals, most notably mackinawite (Shoesmith *et al*., 1980; Jeffrey and Melchers, 2003; Little *et al*., 2006; Sun, 2006; Sherar *et al*., 2010). However, also amorphous iron sulfides have been detected (Jack *et al*., 1990; 1995; Hansson *et al*., 2006). Parameters that possibly influence iron mineral formation such as the concentrations of dissolved sulfide and ferrous iron are intrinsically different in EMIC and CMIC (Figs 16 and 17). It has been speculated that mackinawite forms as a result of direct reaction between Fe^0 and HS^- (Eqs 14, 15 and 17; Shoesmith *et al*., 1980; Sun, 2006), which is less likely in EMIC where a stoichiometric excess of sulfide-scavenging Fe^{2+}(aq) is produced. Accordingly, we found mackinawite as a

corrosion product only in sulfidic cultures of *D. inferna* with lactate as an electron donor for sulfate reduction. Additionally, heterogeneous crusts formed by strain IS4 contained the carbonate minerals siderite and calcite (Table 1).

Its elemental composition and mineral-like appearance suggested that the crust was largely inorganic. Large amounts of detected C in the crust, though possibly indicative of microbial biomass, could be quantitatively accounted for by the (Fe/Ca) carbonate minerals (Venzlaff, 2012). As there is presently no method to precisely quantify biomass in the compact mineral crust, its content was calculated from predicted growth yields (*Chapter* D.1). The estimated biomass content (mass% of dry mass) of the crusts formed by lithoheterotrophic strain IS5 and lithoautotrophic strain IS4 was ≤3.7% and ≤1.3%, respectively. Hence, in accordance with its hard, mineral-like appearance, the crusts were shown to be essentially inorganic and thus differed profoundly from typical biofilms that are composed of cells and an organic matrix.

B.1.3 Surface analysis of biogenic corrosion products

Iron specimens exposed to lithotrophic strains IS4 and IS5 usually blackened within a few days after inoculation. This is in contrast to 'conventional' hydrogenotrophic SRB such as *Desulfovibrio* sp. strain HS3 which did not significantly affect the steel surface even after prolonged incubation periods exceeding one year (Fig. 22).

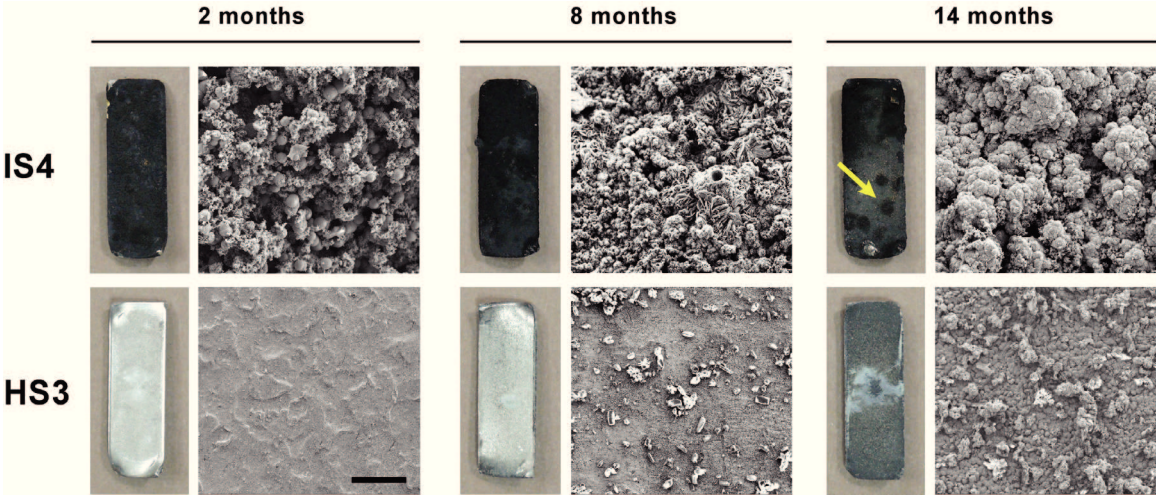

Fig. 22. Scanning electron micrographs of crust surfaces on low carbon steel coupons (photographs; 10 mm · 10 mm · 1 mm) incubated with corrosive strain IS4 or hydrogenotrophic control strain HS3 for 2, 8 or 14 months. Within this incubation period, the *pH* in cultures of strain IS4 (100 ml) reached values above 9 (compared to *pH* 7.3 in sterile controls and in cultures of strain HS3). Arrow indicates 'pustule'-like elevation on crust of strain IS4. Representative scanning electron micrographs of the predominant type of surface cover are shown. EDX identified spherical structures (e.g. IS4, 2 months) as siderite. Crystals on coupons incubated with strain HS3 for 8 months were magnesium phosphate. Bar, 100 µm.

Scanning electron microscopy showed that crusts formed in alkalizing cultures of strain IS4 became gradually more compact (Fig. 22). On the black crusts of cultures with strongly increased *pH*, 'pustule'-like elevations appeared after several weeks of incubation (Figs 22 and 23A, insert). These elevated mineral deposits covered areas of pronounced anodic pitting of the underlying metal, as visualized upon crust removal (Fig. 23A).

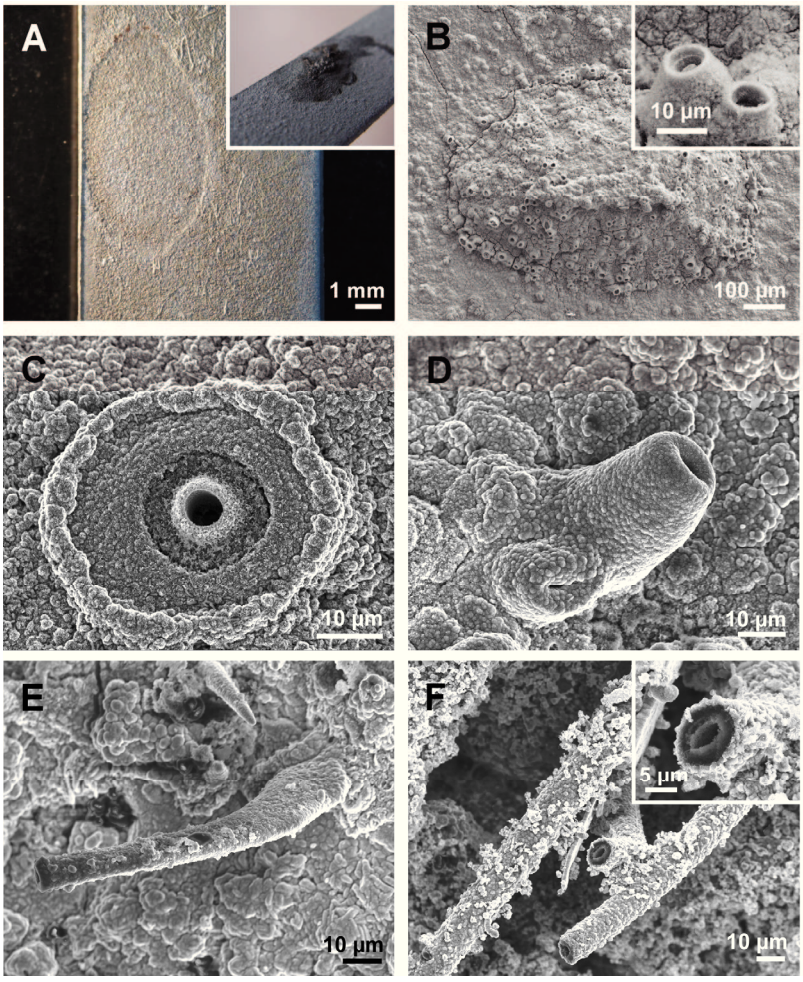

Fig. 23. Scanning electron micrographs of crust surface and micro-chimneys.
A. Anodic iron dissolution (crust removed) underneath a 'pustule' (insert) formed by strain IS4 at high *pH* (~9).
B. 'Pustule' with short micro-chimneys (magnified in insert) in a culture of strain IS4.
C. Micro-chimney developing from a crater-like structure in a culture of strain IS4.
D. Short micro-chimney in a culture of strain IS4.
E. Long micro-chimney in a culture of strain IS4.
F. Long micro-chimney in a corrosive enrichment culture.

Strikingly shaped structures emerged on top of the 'pustules' at pH ≥ 9 (Fig. 23B–F). In such cultures, 'pustules' were perforated and exhibited crater- or chimney-like structures. Various growth stages of these structures were observed (Fig. 23C–F). EDX microanalysis on the

walls of the hollow micro-chimneys detected the elements Fe, S, C and O (data not shown). Electron backscatter diffraction analysis (EBSD) demonstrated an amorphous configuration (Venzlaff, 2012), indicative of rapid formation by precipitation reactions (Hansson *et al*., 2006). Micro-chimneys were observed in strongly alkalizing cultures of strain IS4 and in enrichments but not in cultures of the less alkali-tolerant strain IS5 (*Chapter* D.1). Generally, chimney formation coincided with the drop of Fe^{2+}(aq) below detection limit (3.5 µmol l^{-1}; see Fig. 17B). The observed micro-structures strongly support the model of trans-crustal electron flow. Electrons can only flow from the metal to the crust-attached cells if the crust allows an equivalent ion flow *via* aqueous 'bridges' (maintenance of electroneutrality). These may be tiny interstices or fissures in porous crusts. However, at high *pH*, crusts were more compact and anodic iron dissolution (with 'pustule' formation) occurred at few and apparently random sites only (Fig. 22). Within the 'pustules', precipitation of Fe^{2+}-ions is probably prevented due to their slightly acidic reaction ($Fe^{2+} + H_2O \leftrightarrow Fe(OH)^+ + H^+$, pK_a = 8.8; Lee and de Beer, 1995). Outside the 'pustule', Fe^{2+}-ions precipitate immediately with carbonate or sulfide in the alkaline medium (Fig. 17B), and form mineralized ion bridges of mixed carbonate/sulfide composition.

In conclusion, high-*pH* incubations provided visual proof of the Fe^{2+}-ion flow that necessarily accompanies trans-crustal electron flow to surface-attached SRB.

B.1.4 Electrochemical examination of bioelectrical corrosion of iron

Evidence for biologically enhanced corrosion of iron due to direct electron uptake (Eq. 21) is so far based on the much higher activity of novel SRB with iron than can be explained by mere consumption of cathodic H_2, and the significant electrical conductivity of the colonized corrosion crust. The postulated mechanism of bioelectrical iron corrosion and thus by-pass of the abiotic hydrogen formation urges upon corroboration by electrochemical measurements.

If the slow abiotic reduction of water-derived protons (Eq. 4) is indeed largely overlaid by a faster biological cathodic reaction (Eq. 21), this should be obvious from electrochemical measurements with iron electrodes in cultures of corrosive strains in comparison with non-corrosive, conventional strains and with sterile incubations. We first measured the influence of *D. corrodens* strain IS4 on the free (mixed) corrosion potential (E_{corr}). Subsequently, we characterized the cathodic reaction by recording the external current density in response to potentiodynamic sweeps of the electrodes towards values more negative than E_{corr}. In all these experiments, electrons for sulfate reduction were provided exclusively *via* the iron (lithotrophic growth conditions), i.e. there was no organic electron donor such as lactate.

Influence of lithotrophic corrosive SRB on the free corrosion potential of iron.

If the metal-colonizing SRB strain IS4 accelerates corrosion by direct electron uptake, this would shift the free corrosion potential E_{corr} towards more positive values (with $E_{Fe^{2+}/Fe^0} < E_{corr} < E_{average\ (SO_4^{2-}/H_2S)}$). Scavenge of cathodic H_2 by metal-attached strain HS3, on the other hand, is not expected to shift the mixed potential. We investigated these assumptions with iron electrodes in electrochemical cells incubated with either of the two SRB strains (Fig. 24A). E_{corr} was continuously monitored during incubation of the iron electrodes with strains IS4 or HS3 during eight days (Fig. 24B). Simultaneously, we recorded the microbial activity (Fig. 24C).

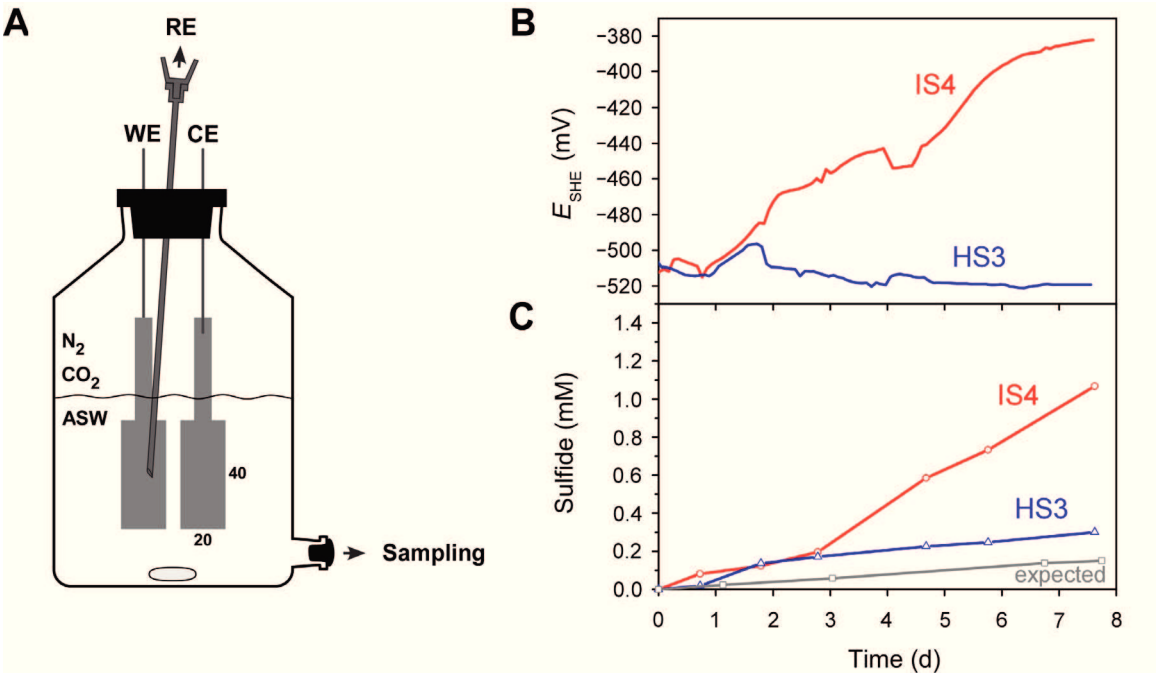

Fig. 24. Study of bioelectrical corrosion by strain IS4 (red) colonizing iron electrodes in an electrochemical cell. Hydrogenotrophic SRB strain HS3 (blue) was incubated as a control.
A. Schematic illustration of the anaerobic electrochemical cell with artificial seawater medium (ASW) and anoxic headspace. WE: Iron working electrode. RE: Ag/AgCl reference electrode with electrolyte-containing stainless steel cannula. CE: Iron counter electrode (not required for E_{corr} measurement; see Fig. 25). A sampling port allowed withdrawal of medium for chemical analysis.
B. Continuous measurement of E_{corr}. Values are expressed vs. standard hydrogen electrode (SHE).
C. Production of sulfide (calculated from sulfate loss) in electrochemical cells with strains IS4 and HS3. Expected values (grey) display calculated sulfide production from usage of chemically formed cathodic H_2 (measured in sterile controls).

The free corrosion potentials in the two cultures began to diverge considerably after two days of incubation. The increasing shift by strain IS4 of E_{corr} towards more positive values is

fully in agreement with an increasing dominance of the (cathodic) biological electron uptake reaction (Eq. 21) over the abiotic proton reduction (Eq. 4). The electron-withdrawing cells of strain IS4 obviously became more and more established and grew during the incubation period. Such a pronounced, steady shift of E_{corr} was not observed with control strain HS3. Only during the second day, strain HS3 caused a transient though rapid increase of E_{corr}. We attribute this to formation of iron sulfide forms with temporary catalytic cathodic activity, i.e. with increased rate of abiotic H_2 formation (details in *Chapter* D.2). This assumption is supported by the initially increased sulfate reduction that must be due to H_2 utilization. In the longer run, E_{corr} in the presence of the non-corrosive strain HS3 became slightly more negative and the rate of sulfate reduction was not higher than the theoretical rate expected from mere utilization of 'cathodic' hydrogen.

In conclusion, the pronounced differences in the development of E_{corr} in cultures of strains IS4 and HS3 were as expected. The positive shift of the mixed potential, E_{corr} in cultures of strain IS4 reflects the postulated direct electrical coupling of the primary anodic reaction (Eq. 1) with biological sulfate reduction (Eq. 21) as the dominant cathodic reaction. Such shifts of E_{corr} are also observed in electrochemical measurements with 'conventional' SRB (Wanklyn and Spruit, 1951; Miranda *et al*., 2006; Kuang *et al*., 2007); however, they are routinely provided with an organic electron donor leading to excessive sulfide. The abiotic shift of E_{corr} by sulfide is attributed to two factors, an accelerated cathodic reaction on the one hand and passivation by a particular type of FeS layer on the other hand (Newman *et al*., 1992). To verify that the strong shift of E_{corr} by strain IS4 is indeed due to the acceleration of the cathodic reaction by direct electron uptake, we investigated this half-reaction by linear sweep voltammetry.

Revealing the microbial cathodic reaction by linear sweep voltammetry (LSV).

Microbial catalysis of a fast cathodic reaction (Eq. 21) at the iron electrodes should become obvious upon imposing more negative electrode potentials than E_{corr} (ΔE) and recording the required external current (expressed as current density i). Such recorded currents should be higher than in sterile control experiments or with non-corrosive SRB that lack the ability to directly derive electrons from iron. Furthermore, inactivation of the electrode-colonizing cells using a biocide can clarify whether an increased consumption of current is indeed biological or rather results from the deposition of catalytically active iron sulfide minerals (according to Eq. 20).

Hence we transferred the colonized electrodes (Fig. 24) into fresh electrolyte and recorded i vs. ΔE curves in potentiodynamic sweeps down to ΔE = −400 mV (LSV; Fig. 25). Subsequently, attached microbial cells were inactivated with glutaraldehyde and LSV was again performed for the 'sterilized' crust-covered electrodes. In cultures of strain IS4, there was a pronounced difference between the cathodic currents before and after glutaraldehyde treatment, viz. obvious biological cathodic activity. This was not observed for the hydrogenotrophic strain HS3 where the cathodic reduction of H^+ ions proceeded essentially uncoupled from microbial consumption of H_2.

The influence of strain IS4 on the recorded current densities was principally restricted to ΔE = −150 to −200 mV (shaded area in Fig. 25). As all enzymatic and living systems, the colonizing sulfate-reducing cells have their maximum (or saturation) activity (known as v_{max}) which was reached while the abiotic reaction came increasingly into play as the electrode potential deviated further from E_{corr}.

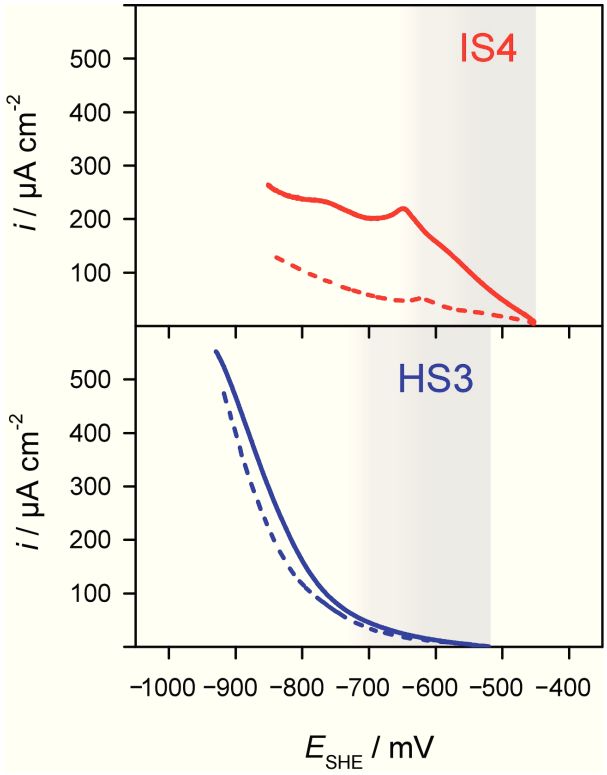

Fig. 25. Current density i vs. applied potential (displayed as E_{SHE}) of iron electrodes incubated for eight days (Fig. 24) with corrosive strain IS4 (red) or non-corrosive strain HS3 (blue). LPV was performed in fresh artificial seawater medium as electrolyte with viable cells (solid line) and after inactivation of cells with glutaraldehyde (dashed line). The potential sweep with 1 mV s^{-1} ranged from the free corrosion potential (E_{corr}; start) to −400 mV below E_{corr}. The shaded area indicates ΔE range with influence on current density i by strain IS4 (for comparison, also indicated in strain HS3).

In conclusion, linear polarization voltammetry showed that acceleration of the cathodic reaction is largely a direct biological effect and not explained by deposition of catalytically active FeS minerals. This strongly supports the model of direct electron uptake by specialized lithotrophic SRB such as strain IS4 through an electroconductive, sulfidic mineral crust. Furthermore, the absence of any cathodic stimulation by hydrogen-consuming strain HS3 clearly challenges the classical 'cathodic depolarization theory', i.e. accelerated corrosion due to microbial H_2 uptake.

B.1.5 Holistic model of the bioelectrical corrosion of iron by lithotrophic SRB

The anaerobic corrosion of iron is profoundly accelerated in the presence of peculiar lithotrophic SRB. These specialized strains directly withdraw electrons from Fe^0 which leads to the deterioration of the technical material, a process referred to as electrical microbially influenced corrosion (EMIC) in the present work. The corrosive effect of lithotrophic SRB such as *D. corrodens* strain IS4 and *D. ferrophilus* strain IS5 is fully independent from the consumption of the abiotically, slowly formed cathodic H_2 on Fe^0 (Fig. 26). In fact, 'conventional' lithotrophic SRB effectively utilize such cathodic H_2, but this does not influence iron corrosion to any significant extent. Hence, lithotrophic iron corrosion is always EMIC.

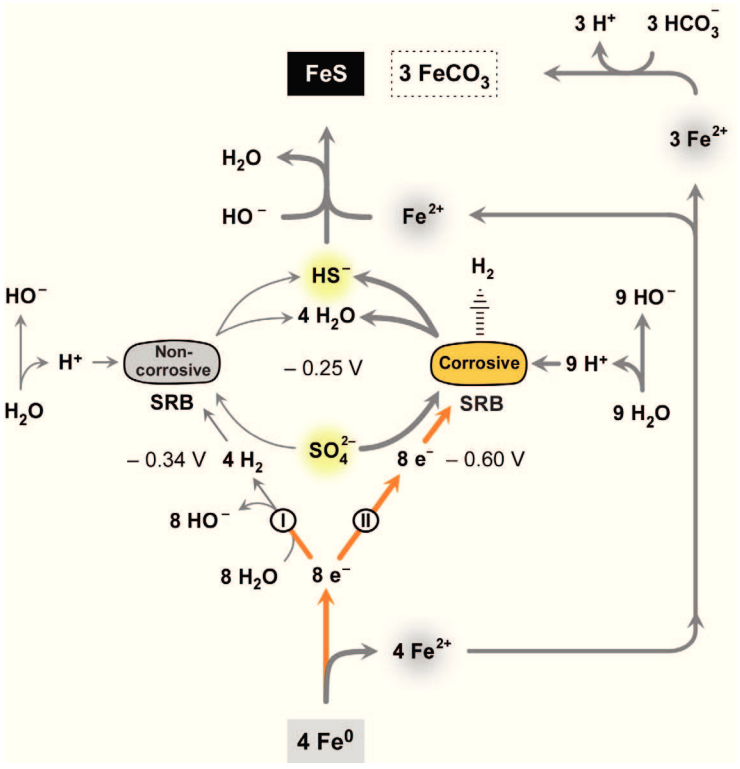

Fig. 26. Scheme of the stoichiometry of direct (lithotrophic) corrosion. Stoichiometry of iron dissolution and channeling of electrons *via* H_2 (I; classical scheme) or directly (II; new model) into sulfate reduction. Bold lines indicate the much faster 'electric' bypass. Redox potentials are indicated for real conditions (see *Chapter* D.1). Direct electron utilization provides a higher metabolic driving force (voltage: ΔE = 0.35 V, compared to 0.09 V *via* H_2 of assumed ≈40 ppmv). Fe^{2+} not precipitated as sulfide may enter solution or precipitate with naturally widespread inorganic carbon as $FeCO_3$.

EMIC leads to the built-up of thick non-passivating mineral crusts on the corroding metal. The largely inorganic, porous crusts (<3.7% biomass by dry weight) are electrically conductive (~50 S m^{-1}), so that electrical contact between the metal and the distant, crust-attached cells is sustained (Fig. 27).

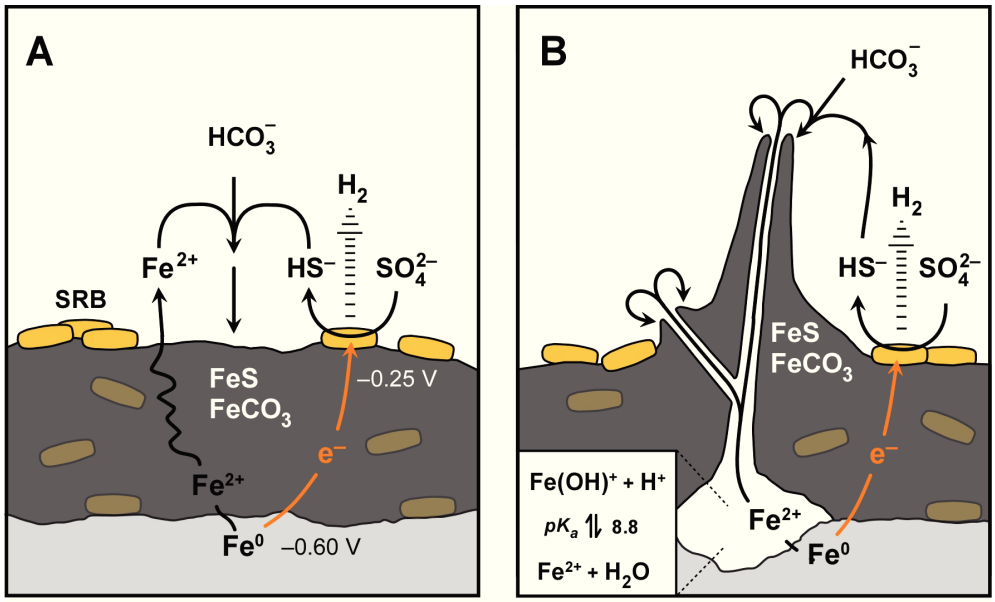

C

Crust properties	
Biomass (mass% of dry weight):	**<3.7**
Content of FeS ($q_{FeS/Fe(II)}$):	**0.23–0.25**
Electrical conductivity (S m^{-1}):	**27–44**
Type of FeS:	**amorphous**
Catalysis of H$^+$ reduction:	**no**

Fig. 27. Scheme of the topology of direct, lithotrophic corrosion (EMIC) and properties of the forming corrosion crust.

A. Electron flow through the crust to attached cells at *pH* = 8 (simplified, non-stoichiometric). The equivalent ion flow may occur *via* aqueous interstices (not depicted).

B. Built-up of chimney-like ion bridges at $pH \geq 9$. Reactions are essentially as in (A). However, there are pronounced spots of anodic iron dissolution. A significant *pH* gradient (low inside, high outside) causes rapid Fe^{2+} precipitation at the rim leading to chimney growth.

C. Properties of the corrosion crusts formed in bioelectrical corrosion of iron by SRB. Crusts may contain additional co-precipitated minerals such as calcite.

Schemes include the possibility of H_2 release (that may foster remote bacterial cells) due to an imbalance between electron uptake and sulfate reduction. Participation of possibly buried (encrusted) cells in sulfate reduction and H_2 release is unknown.

Amorphous iron sulfides were detected in the crusts at the predicted stoichiometries. However, contrary to common views (Smith and Miller, 1975; Ferris *et al.*, 1992), no significant influence of these minerals on the rate of abiotic proton reduction, and hence corrosion, was observed. In fact, electrons flow from the metal ($4\,Fe^0 \rightarrow 4\,Fe^{2+} + 8\,e^-$) through the semiconductive iron sulfides to the crust-attached cells reducing sulfate

($8\,e^- + SO_4^{2-} + 10\,H^+ \rightarrow H_2S + 4\,H_2O$). Such electron flow necessarily involves an equivalent flow of ions. At high *pH* of the surrounding medium the flow of Fe^{2+}-ions is 'visualized' by the formation of strikingly shaped ion bridges (Fig. 27B).

In conclusion, oxidation of iron in anoxic environments can be the direct result of a 'bio-cathodic' reaction, with the type and number of attached cells being important rate-controlling factors. Technologically highly relevant corrosion rates of up to 0.71 mm Fe^0 yr^{-1} (61.2 µA cm^{-2}) were observed in the present work. Hence EMIC is envisioned as a potentially important process in technical settings (*in situ*).

B.2 Diversity, abundance and environmental significance of directly corrosive lithotrophic SRB

Thus far, the present work has focused on the mechanistic aspects of bioelectrical corrosion, the study of which was most appropriate in axenic cultures of the previously isolated corrosive SRB (Dinh *et al*., 2004). In the following we will assess the diversity and abundance of such specialized corrosive SRB in natural environments and the significance of EMIC *in situ*.

B.2.1 Lithotrophic enrichment cultures with Fe^0 and preliminary characterization of novel corrosive SRB isolates

In a previous study of the anaerobic corrosion of iron (Dinh, 2003; Dinh *et al*., 2004) three directly corrosive SRB isolates were obtained from enrichment cultures with Fe^0 as the only electron donor. *Desulfopila corrodens* strain IS4 and *Desulfovibrio ferrophilus* strain IS5 originated from cultures incubated with anoxic marine sediment from Wilhelmshaven, Germany. A third isolate, phylogenetically closely related to strain IS4, was obtained from enrichment cultures established with anoxic marine sediment from Halong Bay, Vietnam (Dinh, 2003). These strains are so far the only SRB that display higher activity on Fe^0 than can be explained by consumption of cathodic H_2. To investigate the possibility of a phylogenetic clustering of directly corrosive SRB, we attempted to isolate further strains.

Lithotrophic enrichment cultures with Fe^0 as the only source of electrons.

Two enrichment cultures (E15 and E20) with iron coupons were inoculated with black sulfidic crusts from a corroded iron structure buried in anoxic sediment of West Coast Park, Singapore. Previous enrichments (Dinh, 2003) had been performed with large amounts of iron which rapidly showed microbial activity but also led to pronounced alkalization ($pH \approx 9$) and hence inhibited microbial activity. Here, we incubated with smaller amounts of iron to minimize such inhibitory effects. Incubation was carried out with 56.6 and 11.4 cm^2 Fe^0 in 150 and 400 ml ASW, respectively, and without addition of an organic carbon or energy source. Activity and hence alkalization of the medium was more pronounced in the culture containing a larger amount of Fe^0 (E15). We transferred parts of the crust-covered coupons from both cultures into fresh media once the culture with less Fe^0 (E20) reached *pH* values close to 8 (Fig. 28). Both enrichment cultures developed black corrosion crusts on Fe^0. However, crusts in culture E15 ($pH \leq 9$) were more compact and contained ‘pustules’ while crusts in culture E20 ($pH \leq 8$) were generally more voluminous and uniform.

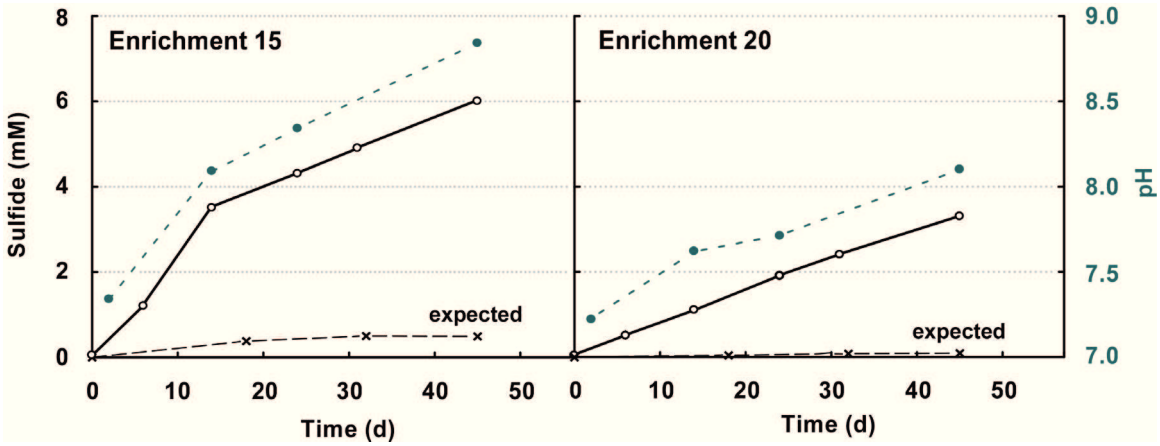

Fig. 28. Sulfide formation (calculated from sulfate loss) and increase of *pH* in sediment-free lithoautotrophic enrichment cultures E15 and E20. Iron coupons (0.38 and 0.03 cm^2 ml^{-1}, respectively) provided the only source of electrons. A part of the crust-covered coupons was transferred into fresh ASW approx. every six weeks when culture E20 had reached a *pH* of 8. Transfer of oxygen-sensitive coupons was carried out in an anaerobic chamber. Expected sulfide formation from consumption of cathodic hydrogen is also indicated.

To investigate the microbial communities that developed under such conditions, we collected crusts from both enrichment cultures (Fig. 28) and constructed bacterial 16S rRNA gene libraries (Fig. 29).

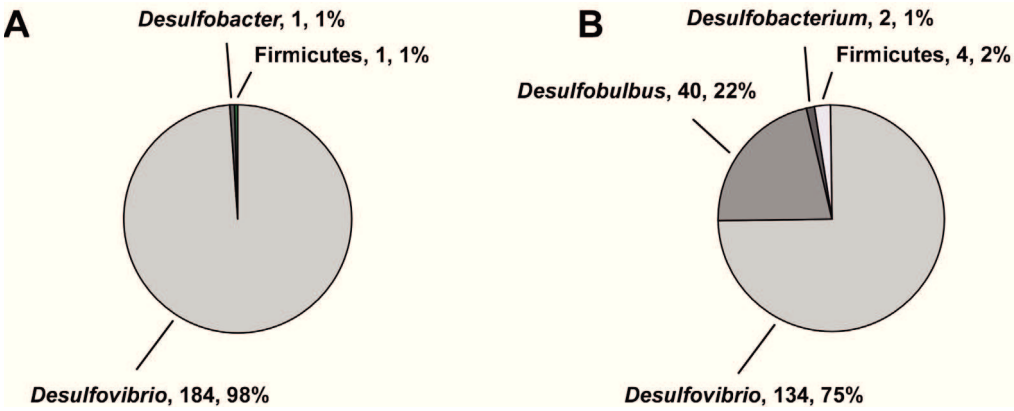

Fig. 29. Bacterial 16S rRNA gene libraries from black sulfidic crusts in anaerobic corrosive enrichment cultures. Affiliation is depicted on the genus level. Numbers indicate number of clones and percent of total clones for any particular genus in the library. Clone libraries are based on partial length sequences and were constructed with RDP SeqMatch.
A. Crust from enrichment cultures E15 ($pH \leq 9$).
B. Crust from enrichment cultures E20 ($pH \leq 8$).

These clone libraries were dominated by sequences affiliating with deltaproteobacterial SRB; only one and four out of 186 and 180 clones in the libraries of cultures E15 and E20, respectively, affiliated with the *Firmicutes*. The dominance of sulfate-reducing bacteria was

as expected in highly enriched cultures that contained iron as the only electron donor and sulfate as the thermodynamically most favorable electron acceptor (Dinh *et al*., 2004). Interestingly, the culture with less pronounced alkalization (E20) contained two dominant genera, indicating that *pH* was a selective pressure.

It was assumed that all or most of the detected SRB were capable of direct electron uptake. However, non-corrosive hydrogenotrophic strains (e.g. strain HS4 and HS5, *Chapter* B.1.1) were frequently and easily isolated from corrosive enrichment cultures by dilution of crust homogenates into agar with H_2 as the electron donor. This may indicate that such crusts sustain hydrogen-consuming, 'secondary' SRB populations, possibly thriving on biogenically formed H_2.

Isolation and preliminary characterization of corrosive SRB strains IS6 and IS7.

To isolate the most abundant corrosive SRB from the enrichment cultures, we carefully homogenized the mineral crust and serially diluted it into glass tubes with ASW and iron granules (three successive dilution-to-extinction series). This yielded SRB isolates IS6 and IS7 from cultures E20 and E15, respectively. The most closely related cultivated organism of strain IS6 is *Desulfobulbus mediterraneus* (90% 16S rDNA sequence similarity; Sass *et al*., 2002), but no distinct assignment to either the *Desulfobulbus* or *Desulfurivibrio* genus could be made and strain IS6 probably represents a separate, new genus (Fig. 30). Strain IS7 was most closely related to *Desulfovibrio aespoeensis* (99% 16S rRNA sequence similarity; Motamedi and Pedersen, 1998), a non-corrosive hydrogenotrophic SRB isolated from deep groundwater.

Cells of strain IS6 were ovoid and sometimes formed chains of several cells while strain IS7 displayed a classical curved morphology that is observed in other *Desulfovibrio* species. Both strains utilized metallic iron as a direct electron donor for sulfate reduction and were corrosive. In fact, strain IS6 displayed the highest recorded corrosion rate of any tested lithotrophic organism (0.88 mm Fe^0 yr^{-1}; Fig. S5). Other substrates tested included acetate, ethanol, propionate, butyrate, succinate, pyruvate, lactate and H_2. Of these, only ethanol and H_2 (± acetate) were used by strain IS6. Strain IS7 grew only with lactate or H_2. Interestingly, *Desulfovibrio* sp. strain IS7 grew lithoautotrophically with H_2 in the absence of acetate and synthesized fatty acids from C^{13}-labeled HCO_3^- (data not shown; G. Wegener, personal communication). Autotrophic carbon fixation is not expected in *Desulfovibrio* sp. and the observed growth could be explained by the presence of a homoacetogenic co-culture supplying acetate (Brysch *et al*., 1987). However, microscopic analysis did only show a single

morphotype, even after repeated purification of the culture by growth in H_2 (+acetate) and subsequent dilution to extinction. Attempts to enrich the putative accompanying organism by incubation in sulfate-free media or with the addition of fructose, a common substrate of homoacetogenic bacteria, were not successful. Autotrophic growth of cultures of strain IS7 requires further investigation.

Phylogenetic affiliation of directly corrosive lithotrophic SRB.

The isolated SRB comprise a limited number of cultivated representatives of the envisioned key players in anaerobic iron corrosion. They are, thus far, all members of the *Desulfovibrionaceae* or *Desulfobulbaceae* (Fig. 30). Within these families there is no obvious phylogenetic clustering. Apparently, corrosive SRB are not necessarily more closely related to each other than to other, non-corrosive SRB that lack the ability of direct electron uptake. It must be concluded that direct corrosiveness in SRB is a polyphyletic trait. Interestingly, direct electron uptake from iron has also been reported for certain methanogenic archaea (Dinh *et a*l., 2004; Uchiyama *et al*., 2010; Mori *et al*., 2010).

This has several practical implications. Most notably, molecular biological tools based on 16S rRNA genes cannot be use to quantify or screen for directly corrosive SRB as a group in the environment. There is currently insufficient information on the biochemical prerequisites for direct electron uptake and hence no general ‘marker’ gene for direct corrosiveness.

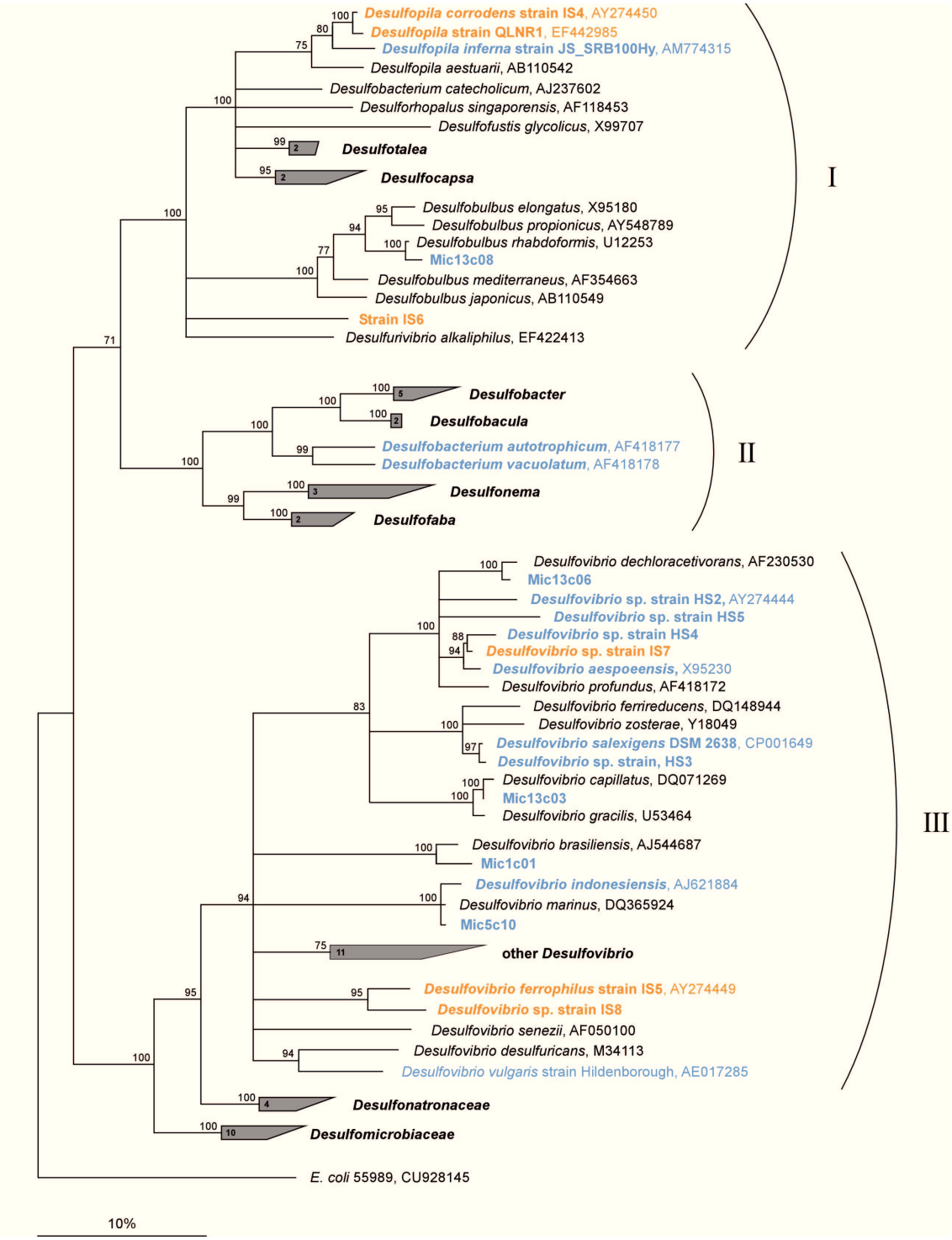

Fig. 30. Phylogenetic tree constructed from full length 16S rRNA gene sequences of cultivated sulfate-reducing bacteria within the *Deltaproteobacteria*. The tree shows SRB isolates capable of direct electron uptake (orange) and hydrogenotrophic, non-corrosive SRB (blue). Other SRB (black) were not tested on Fe^0. 'Mic'-isolates are from Mori *et al.* (2010). Tree does not include all cultivated SRB. I: *Desulfobulbaceae*. II: *Desulfobacteraceae*. III: *Desulfovibrionaceae*. The tree was calculated based on maximum likelihood with the ARB software package and SILVA database (Ludwig *et al.*, 2004; Pruesse *et al.*, 2007). Branching with bootstrap values below 75 is not depicted. The scale bar represents 10% difference in sequence similarity.

B.2.2 Notes on the ecophysiology of directly corrosive lithotrophic SRB

The specific ability to utilize metallic iron as an electron donor is a physiologically striking capacity, the ecological significance of which is presently unknown. Apart from rare cases (meteorites, seldom rocks from deep subsurfaces; Deutsch *et al*., 1977; Haggerty and Toft, 1985), metallic iron has been introduced into the environment on a large scale only by industrialization, viz. very 'recently' from an evolutionary point of view. Yet, counting of corrosive SRB *via* dilution series with anoxic sediment and metallic iron revealed several 10^7 cells per gram wet mass (Fig. 31), despite obvious absence of man-made iron constructions.

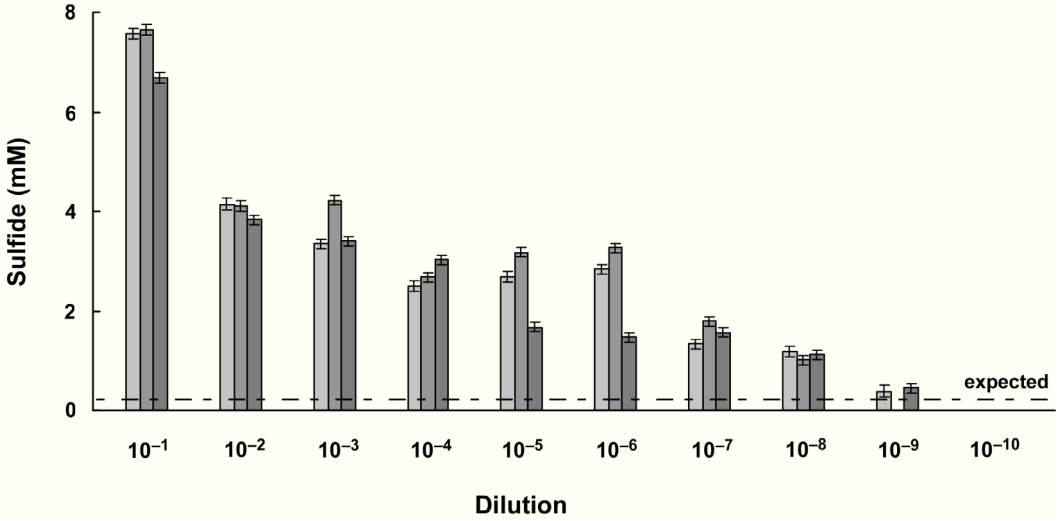

Fig. 31. Dilution series of anoxic marine sediment from a tidal flat (Sylt, North Sea) incubated with iron coupons. Developed sulfide (from sulfate consumption) after six months with native sediment (2 g, wet mass), sampled and immediately diluted on site (three in parallel). The line indicates sulfide expected solely by consumption of H_2 formed from iron and seawater (based on independently measured H_2-formation rates and experiments with merely H_2-scavenging SRB).

One may speculate that corrosiveness represents the promiscuous use of a long-existing physiological trait for environmental electron uptake ('electrotrophy'; Lovley, 2011b) that is suited to also exploit the anthropogenically introduced metal as a substrate. Normally, SRB with such trait may be involved in biogenic electron flow through sulfidic marine sediments and other ecosystems (Nakamura *et al*., 2009; Nielsen *et al.*, 2010; Kato *et al*. 2011). Also, electron gain in direct contact with other bacteria with a surplus of catabolic electrons (Summers *et al.*, 2011; Lovley, 2011a) or from strongly reducing, reactive mineral surfaces such as pyrite being formed from ferrous sulfide and free sulfide ($FeS + H_2S \rightarrow FeS_2 + H_2$ / $FeS_2 + 2H^+ + 2e^-$; Wächtershäuser, 1992) can be envisaged as the genuine role of the electron uptake system underlying direct corrosion. Fig. 32 summarizes a present hypothesis of the *in situ* function of SRB with the ability for electron uptake from external sources. Such SRB

may represent a so far overlooked part of the anaerobic population. Still, more extended examinations of their abundance at various natural sites and physiological studies are needed to unravel their real significance in anaerobic mineralization.

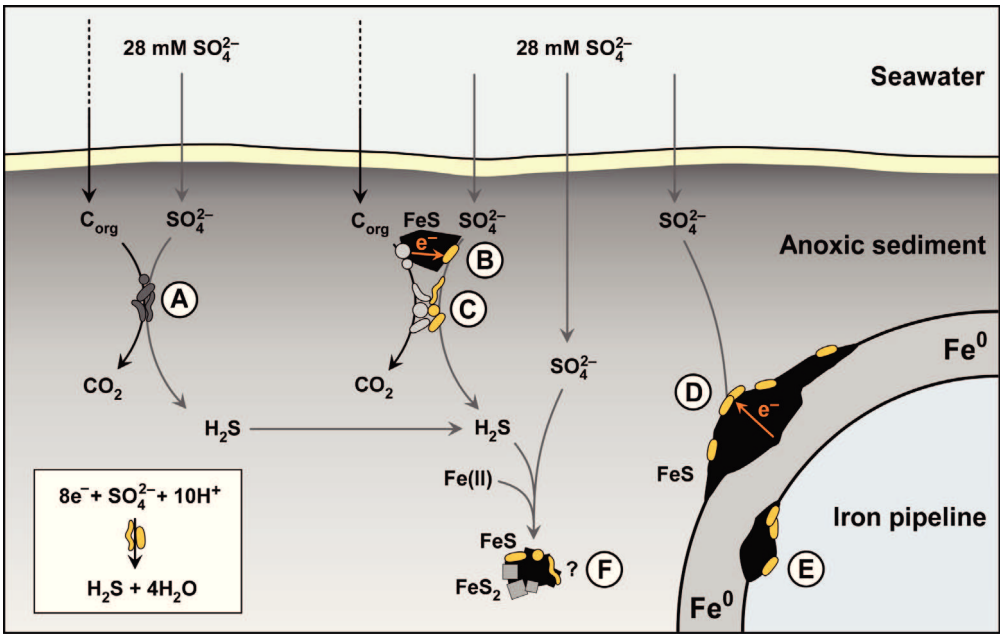

Fig. 32. Present synoptic view on the possible role of sulfate-reducing bacteria with the capability of electron uptake from external sources in anoxic marine sediment.

A. Conventional organotrophic SRB.

B. SRB interacting *via* electroconductive ferrous sulfide with organotrophic electron-donating anaerobic microorganisms.

C. SRB interacting directly with electron-donating organotrophic anaerobic microorganisms.

D. Special SRB exploit metallic iron as an electron source at the outer surface of a buried pipeline.

E. Special SRB exploit metallic iron as an electron source inside of a pipeline.

F. Speculative possibility of pyritization of FeS ($FeS + H_2S \rightarrow FeS_2 + 2\,H^+ + 2\,e^-$).

B.2.3 Quantifying the contribution of electrical microbially influenced corrosion (EMIC) to total microbial corrosion *in situ*

In sulfate-rich anoxic environments, the corrosion of iron is heavily influenced by sulfate-reducing bacteria (Starkey, 1946; Booth, 1964; Hamilton, 1985; Lee *et al.*, 1995). Conventionally, attack by SRB is attributed to three effects, (i) the chemical corrosiveness of sulfide from sulfate reduction (CMIC), (ii) a facilitated abiotic reduction of H^+ to H_2 at galvanically coupled iron sulfides, and (iii) the microbial consumption of chemically formed (cathodic) H_2 from the iron or iron sulfides. Bioelectrical corrosion of iron by specialized lithotrophic SRB (viz., EMIC) offers an alternative explanation for the observed deterioration of iron constructions in anoxic environments.

In the present study we excluded possibility (iii), i.e. microbial hydrogen consumption, as the cause of MIC. This is fully in agreement with several earlier studies (Spruit and Wanklyn, 1951; Costello, 1974; Hardy, 1983; Dinh *et al*., 2004; Mori *et al*., 2010).

Catalysis of the cathodic reaction by FeS (ii) has been demonstrated with fine suspensions of iron sulfide minerals (Booth *et al*., 1968; King and Miller, 1971; King *et al*., 1973). However, the effect was transient and depended on the amount and crystal structure of the investigated iron sulfides (King *et al*., 1973; Smith and Miller, 1975). Newman *et al*. (1991) found the effect to be small upon closer inspection and stated that the increased cathodic surface area provided by FeS was probably more important than its catalytic properties. In the present study, steel coupons with abiotically formed (pure) FeS crusts did not corrode more rapidly than blank metal controls (not shown). Likewise, FeS could be excluded as a reason for the accelerated cathodic reaction in cultures of directly corrosive SRB (*Chapter* B.1.4).

Technologically relevant corrosion rates have been demonstrated in sulfate-reducing, sulfidogenic cultures (Table 2); hence CMIC (i) seems a plausible mechanistic explanation for MIC in natural sulfate-rich environments.

However, iron also corrodes rapidly and progressively in the presence of specialized lithotrophic SRB such as strains IS4 and IS5 (Table 2). Hence, EMIC offers another obvious explanation for anaerobic corrosion in sulfate-rich environments.

We intended to quantify the relative contribution of EMIC vs. CMIC in microbial corrosion *in situ*. Diagnosing EMIC through the detection of the causative organisms is impractical. It is currently impossible in a cultivation-independent approach to distinguish SRB with the capability of EMIC from those that corrode iron simply by excretion of hydrogen sulfide (CMIC). However, because CMIC (Eqs 14–19) leads exclusively to sulfidic iron, whereas EMIC (Eq. 22) leads in addition to non-sulfidic (usually carbonaceous) iron, their measurable ratio in the crust of a corroded iron construction may be used for estimating the extent of EMIC. This is quantitatively expressed as the quotient of the amounts (mol) of iron lost by EMIC, n_{FeEMIC}, and iron lost totally by MIC, n_{FeMIC}, and thus defined as $q_{\mathrm{EMIC}} = n_{\mathrm{FeEMIC}}/n_{\mathrm{FeMIC}}$. Assuming that all ferrous iron in the crust results from metal corrosion, $n_{\mathrm{FeMIC}} = n_{\mathrm{Fe(II)}}$, so that $q_{\mathrm{EMIC}} = n_{\mathrm{FeEMIC}}/n_{\mathrm{Fe(II)}}$. Further calculation so as to substitute the unknown n_{FeEMIC} and introduce the measurable amount of precipitated sulfide, n_{FeS}, leads to the formula (calculation in *Chapter* D.1):

$$q_{\mathrm{EMIC}} = \frac{n_{\mathrm{FeEMIC}}}{n_{\mathrm{FeMIC}}} = \frac{4\,(1 - n_{\mathrm{FeS}} / n_{\mathrm{Fe(II)}})}{3 + q_{\mathrm{Anab}}}\,. \tag{29}$$

Table 2. Compilation of corrosion rates recorded for (anoxic) sulfate-rich natural and engineered environments, and for laboratory cultures of sulfate-reducing bacteria.

Location	Type of environment	Corrosion rate [a] (mm Fe^0 yr^{-1})	Reference
Bohai Bay, China	Marine sediment	**0.03 – 0.09**	Li (2009)
Draugen Oil Field, Norwegian North Sea	PWRI; untreated produced water	**0.12**	Vik *et al.* (2007)
Thames Estuary, UK	Brackish anoxic sediment	**0.03 – 0.23**	Booth *et al.* (1963)
Tonnenlegerbucht, German North Sea	Marine anoxic sediment	**0.12 – 0.28**	This study
South Korea	Gas transmission pipelines; disbanded coating	**0.33 – 0.47**	Li *et al.* (2000)
Gullfaks Oil Field, Norwegian North Sea	Water injection system; biocide treatment	**0.09 – 0.75**	Boedtker *et al.* (2008)
Culture	**Type of medium [b]**	**Corrosion rate [c] (mm Fe^0 yr^{-1})**	**Reference**
Desulfopila inferna	Lactate-based, marine	**0.003**	This study
Desulfovibrio sp., strain HS5	Lactate-based, marine	**0.006**	This study
Desulfovibrio sp.	Lactate-based, freshwater	**0.007**	Hardy and Brown (1984)
Desulfovibrio vulgaris, strain Woolwich	Lactate-based, freshwater	**0.024**	Gaylarde (1992)
Desulfovibrio desulfuricans, strain New Jersey	Lactate-based, marine	**0.094**	Beech *et al.* (1994)
Desulfovibrio desulfuricans	Lactate-based, brackish	**0.285**	Bell and Lim (1981)
SRB bioreactor	Lactate-based, brackish	**0.408**	Hubert *et al.* (2005)
Desulfovibrio vulgaris, strain Hildenborough	H_2, freshwater [d]	**0.500**	Pankhania *et al.* (1986)
Sterile artificial seawater	Fe^0 lithotrophy, marine	**0.010**	This study
Desulfopila inferna	Fe^0 lithotrophy, marine	**0.012**	This study
'Desulfopila corrodens', strain IS4	Fe^0 lithotrophy, marine	**0.311**	This study
'Desulfovibrio ferrophilus', strain IS5	Fe^0 lithotrophy, marine	**0.710**	This study
'Desulfobulbus' sp., strain IS6	Fe^0 lithotrophy, marine	**0.879**	This study

a. Corrosion rate in natural and engineered environments. The recorded range is given. Corrosion must not necessarily be influenced by SRB in these systems.
b. Energy source for SRB metabolism is indicated. All cultures contained iron or mild steel. 'Fe^0 lithotrophy' indicates that metallic iron was the only available source of reducing equivalents. Salt content of media (freshwater, brackish, marine) is also designated.
c. Corrosion rate in cultures of SRB. The maximal reported value is given. The large range of corrosion rates for SRB with external energy source is attributed to the sometimes protective properties of formed FeS films (see text).
d. H_2 from previous polarisation experiment was available in these cultures.

Therefore, besides analysis of sulfidic and total ferrous iron in the crust, only the assumption of a q_{Anab} value, i.e. the partition of anabolic in total (anabolic + catabolic) electron consumption, is needed (*Chapter* D.1). Still, such treatment is only applicable for anoxic conditions and absence of corrosive processes other than sulfate reduction, for instance methanogenesis (Dinh *et al.,* 2004; Mori *et al.*, 2010; Uchiyama *et al.*, 2010).

We buried low carbon steel coupons in an anoxic tidal mud flat of the Wadden Sea (island of Sylt, Germany) as an example of a sulfate-rich environment possibly favoring MIC. Indeed after three months, the coupons were heavily corroded and covered by a black corrosion crust (Fig. 33).

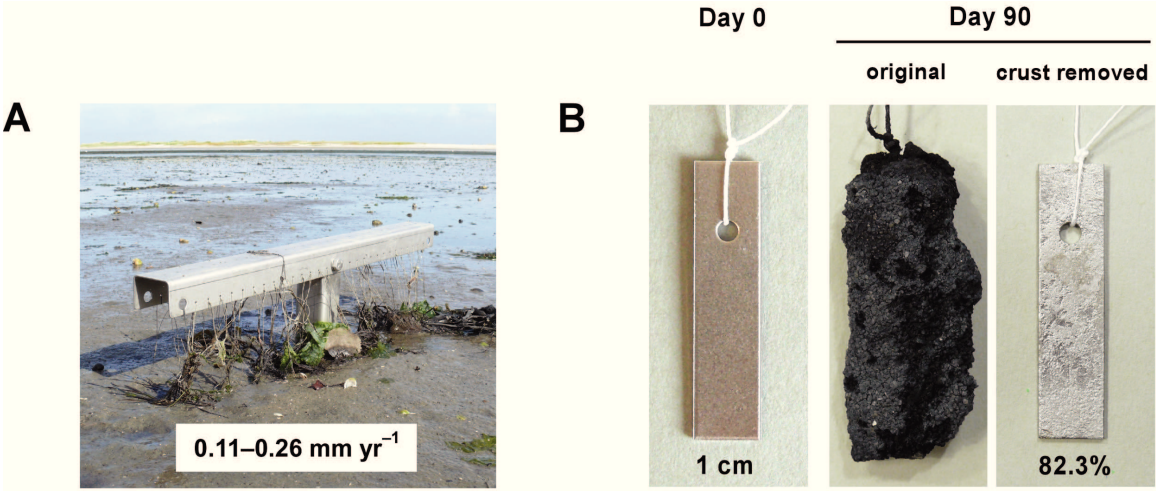

Fig. 33. Anaerobic corrosion of iron in a sulfate-rich anoxic sediment of the Wadden Sea, island of Sylt, Germany.
A. Positioning device (stainless steel). Iron coupons were bound with threads to the device and buried for three months at ≥20 cm. Range of corrosion rates determined for five samples is indicated.
B. Corrosion crusts (with encrusted sand grains) and corroded metal after removal of the crust with inactivated acid. Percent of original weight is indicated.

Analysis of the crust on the coupons recovered from the field study revealed $n_{FeS}/n_{Fe(II)}$ = 0.20 to 0.24 (Table 3). By assuming, for convenience, $q_{Anab} \approx 0.1$, we obtain q_{EMIC} = 0.98 to 1.03 (theoretically, according to Eq. 29, q_{EMIC} always ≤ 1). This strongly suggests that corrosion under the conditions prevailing at the studied marine sediment site was indeed only EMIC, viz. due to SRB capable of direct electron uptake (Fig. 32).

The introduced Fe^0 served as an electron donor to indigenous SRB in marine sediment and was rapidly utilized. Apparently, adaptation of the microbial community to this 'artificial' substrate was not necessary. SRB capable of direct electron uptake were detected at high numbers at the site prior to burial of the coupons (Fig. 31). Sulfate reduction rates per iron

surface area were calculated based on substrate (Fe^0) consumption. Accordingly, crust-attached SRB reduced between 0.4 and 0.9 mmol SO_4^{2-} cm^{-2} yr^{-1}. This at least equals typical depth-integrated sulfate reduction rates in marine coastal sediments (per surface area) with natural input of organic matter (Jørgensen, 1982; Canfield, 1990). Hence sulfate reduction in marine sediments is greatly stimulated by the 'anthropogenic' substrate iron. For the structural integrity of technical iron constructions, this can have dire consequences.

Table 3. Analysis of corrosion crust from Fe^0 incubated with strain IS4 or buried in marine anoxic sediment of the German Wadden Sea.

Element[a], parameter	Fe^0 with strain IS4[b]		Fe^0 buried in sediment[c]		
Fe	29.7	28.0	24.9	21.3	19.8
S	3.9	4.0	2.9	3.0	2.6
C	6.3	6.5	1.9	2.8	2.1
Si	-	-	15.0	14.8	18.3
Ca	8.4	9.6	0.7	1.1	1.1
Mg	2.1	2.2	0.4	0.6	0.5
O[d]	46.9	47.2	51.8	52.3	52.1
Other[e]	2.7	2.5	2.4	4.1	3.5
$q_{FeS/Fe(II)}$[f]	0.23	0.25	0.20	0.24	0.23
$q_{EMIC/MIC}$[g]	**0.99**	**0.97**	**1.03**	**0.98**	**0.99**
Detected by XRD[h]	Siderite, calcite		Quartz, siderite		

a. Elements detected in corrosion products by EDX. Quantitative analysis (weight percent) was achieved by infrared spectroscopy for elements C and S. The remaining elements were quantified by ICP-OES.
b. Corrosion products from two cultures of strain IS4 on iron without exogenous (organic) growth substrate.
c. Corrosion products from three environmental samples. Homogenized ground sample was sieved (150 µm mesh) to remove coarse sand grains.
d. Oxygen was calculated as the remaining fraction in corrosion products. Hydrogen could not be detected and quantified by the applied methodology, but is expected to account for a minor mass% fraction.
e. Sum of other quantified elements. Fe^0 with strain IS4 (rows, from left to right): 2.7 and 2.5% P; Fe^0 buried in sediment: 1.2, 2.5 and 1.7% Al, 0.6, 0.8 and 0.9% K, 0.6, 0.8 and 0.8% Na; 0, 0 and 0.1% P.
f. Molar ratio sulfide to ferrous iron in corrosion products.
g. Share of EMIC in total microbial corrosion.
h. Crystalline phases detected by X-ray diffraction.

B.3 Conclusions and perspectives

Recent views on microbially influenced corrosion emphasize the physiological and phylogenetic diversity of the involved microorganisms (Hamilton, 2003; Coetser and Cloete, 2005; Lewandowski and Beyenal, 2009). MIC is assumed to be seldom if ever a single-species event, but rather results from the cumulative contribution of different microbial physiologies. This view is principally supported by the finding of phylogenetically diverse microbial communities on iron constructions by modern molecular biological technique (Jan-Roblero *et al*., 2004; Neria-Gonzáles *et al*., 2006; Kjieldsen *et al*., 2007; Duncan *et al*., 2009; McBeth *et al*., 2011).

However, the mere presence of a microorganism does not necessarily imply its contribution to the electrochemical processes that drive metal dissolution (Beech and Sunner, 2007). Surface-attached lifestyle is widespread in prokaryotes and the utilization of external (non-Fe^0) energy sources by sessile microbial communities might have little or no influence on the integrity of the metallic substratum. A better understanding of the potentially deleterious interactions between environmental microorganisms and metallic iron is needed. It is particularly important, from a technical point of view, to assess the corrosion rates and relevance of the various microbial candidates. Cord-Ruwisch (2000) concluded that the actual increase in the corrosion rate in laboratory experiments is usually less than a factor of 2 over that of the sterile control. By contrast, the damage caused, for example, in oil production equipment occurs on the order of 10 to 50 times faster than in sterile laboratory tests (Cord-Ruwisch, 2000).

In the present study, recently discovered specialized lithotrophic SRB (Dinh *et al*., 2004) as well as novel isolates accelerated corrosion by factors of up to 85 compared to sterile control incubations upon appropriate adjustment of cultivation conditions. The recorded rates were technologically highly relevant and it is speculated that such strains are cultivated representatives of the key players in anaerobic biocorrosion. Indeed, the corrosion of iron in a marine anoxic sediment was shown to result exclusively from the activity of these or similar SRB. We refer to the novel process as electrical microbially influenced corrosion (EMIC) and investigated its mechanistic underpinnings under much defined conditions. A holistic understanding of this bioelectrical process was achieved. The study of EMIC necessarily entailed experimental comparisons to other suggested mechanisms and explanations of SRB-induced corrosion and some of these were challenged.

Cultivation-based mechanistic studies of biocorrosion in pure or defined mixed cultures are, in the author's view, crucial for a causal understanding of biocorrosion. It is concluded

that bioelectrical corrosion (EMIC) is a so far largely unconsidered, yet obvious mechanistic explanation for the observed rapid deterioration of iron constructions in anoxic, sulfate-containing environments.

Future investigations of EMIC should principally address the following three key issues. Firstly, the natural ecophysiological role of SRB with the capability of direct electron uptake from Fe^0 and FeS is currently still speculative. It seems unlikely that such ability has evolved and spread within the last few millennia. It is therefore desirable to better understand the native physiology and ecological significance of these metabolic specialists in their natural anoxic habitats. Secondly, corrosion by the studied organisms depends on the presence of sulfate. However, also corrosion by certain methanogenic archaea has been demonstrated (Dinh *et al*., 2004; Uchiyama *et al*., 2010; Mori *et al*., 2010) and this likewise represents a form of EMIC. The quantitative importance, particularly in freshwater ecosystems (e.g. water-logged soil), of this sulfate-independent EMIC is so far poorly understood, despite its obvious practical relevance. Thirdly, the remarkable ability of both, specialized SRB and methanogenic archaea to take up electrons from solid surfaces awaits the elucidation of its biochemical and genetic prerequisites. An understanding of the underlying electron transport pathways with particular focus on the initial electron uptake step should be the principal goal of future studies. Besides its obvious ecological importance, an understanding of bioelectrical corrosion on the cellular level may find potential application in biotechnology (e.g. MIC monitoring).

Part C: References and supplementary figures, tables and methods

C.1 References

Adams, M.E., and Farrer, T.W. (1953) The influence of ferrous iron on bacterial corrosion. *J Appl Chem* **3**: 117−120.

Adebayo, A., and Dada, A.S. (2008) An evaluation of the causes of oil pipeline incidents in oil and gas industries in Niger delta in Nigeria. *J Eng Appl Sci* **3**: 279−281.

Aeckersberg, F. (1994) *Anaerober Abbau von Alkanen und 1-Alkenen durch sulfatreduzierende Bakterien*. Aachen: Verlag Mainz.

Anderko, A., and Shuler, P.J. (1997) A computational approach to predicting the formation of iron sulfide species using stability diagrams. *Comput Geosci* **23**: 647−658.

Aroh, K.N., Ubong, I.U., Eze, C.L., Harry, I.M., Umo-Otong, J.C., and Gobo, A.E. (2010) Oil spill incidents and pipeline vandalization in Nigeria. Impact on public health and negation to attainment of Millennium development goal: the Ishiagu example. *Disaster Prev Manage* **19**: 70−87.

Arrigo, K.R. (2005) Marine microorganisms and global nutrient cycles. *Nature* **437**: 349−355.

Beavers, J.A., and Thompson, N.G. (2006) External corrosion of oil and natural gas pipelines. In *ASM Handbook. Corrosion: Environments and Industries (#05145)*. Cramer, S.D., and Covino, B.S.J. (eds). Materials Park, Ohio: ASM International.

Beech, I.B., and Campbell, S.A. (2008) Accelerated low water corrosion of carbon steel in the presence of a biofilm harbouring sulphate-reducing and sulphur-oxidising bacteria recovered from a marine sediment. *Electrochim Acta* **54**: 14−21.

Beech, I.B., Cheung, C.W.S., Chan, C.S.P., Hill, M.A., Franco, R., and Lino, A.R. (1994) Study of parameters implicated in the biodeterioration of mild steel in the presence of different species of sulfate-reducing bacteria. *Int Biodet Biodegr* **34**: 289−303.

Beech, I.B., and Gaylarde, C.C. (1999) Recent advances in the study of biocorrosion - an overview. *Rev Microbiol* **30**: 177−190.

Beech, W.B., and Sunner, J. (2004) Biocorrosion: towards understanding interactions between biofilms and metals. *Curr Opin Biotech* **15**: 181−186.

Beech, I.B., and Sunner, I.A. (2007) Sulphate-reducing bacteria and their role in corrosion of ferrous materials. In *Sulphate-reducing Bacteria: Environmental and Engineered Systems*. Barton, L.L., and Hamilton, W.A. (eds). Cambridge: Cambridge University Press, pp. 459−482.

Beech, I.B., Zinkevich, V., Tapper, R., and Gubner, R. (1998) Direct involvement of an extracellular complex produced by a marine sulfate-reducing bacterium in deterioration of steel. *Geomicrobiol J* **15**: 121−134.

De Beer, D., and Stoodley, P. (2006) Microbial Biofilms. In *The Prokaryotes*. Dworkin, M., Falkow, S., Rosenberg, E., Schleifer, K.-H., and Stackebrandt, E. (eds). New York: Springer, pp. 904−937.

Binnewies, M., Jäckel, M., Willner, H., and Rayner-Canham, G. (2004) *Allgemeine und Anorganische Chemie*. Heidelberg: Spektrum.

Bird, L.J., Bonnefoy, V., and Newman, D.K. (2011) Bioenergetic challenges of microbial iron metabolisms. *Trends Microbiol* **19**: 330−340.

Bockris, J.O.M., and Reddy, A.K.N. (1970) *Modern Electrochemistry*. New York: Plenum.

Boopathy, R., and Daniels, L. (1991) Effect of pH on anaerobic mild steel corrosion by methanogenic bacteria. *Appl Environ Microbiol* **57**: 2104−2108.

Booth, G.H. (1964) Sulphur bacteria in relation to corrosion. *J Appl Bacteriol* **27**: 174−181.

Booth, G.H., Elford, L., and Wakerley, D.S. (1968) Corrosion of mild steel by sulphate-reducing bacteria: an alternative mechanism. *Br Corros J* **3**: 242−245.

Booth, G.H., and Tiller, A.K. (1960) Polarization studies of mild steel in cultures of sulphate-reducing bacteria. *T Faraday Soc* **56**: 1689−1696.

Braun, F. (1875) Über die Stromleitung durch Schwefelmetalle. *Ann Phys* **229**: 556−563.

Bryant, M.P., Campbell, L.L., Reddy, C.A., and Crabill, M.R. (1977) Growth of *Desulfovibrio* in lactate or ethanol media low in sulfate in association with H_2-utilizing methanogenic bacteria. *Appl Environ Microbiol* **33**: 1162−1169.

Bryant, R.D., Jansen, W., Boivin, J., Laishley, E.J., and Costerton, J.W. (1991) Effect of hydrogenase and mixed sulfate-reducing bacterial populations on the corrosion of steel. *Appl Environ Microbiol* **57**: 2804−2809.

Brysch, K., Schneider, C., Fuchs, G., and Widdel, F. (1987) Lithoautotrophic growth of sulfate-reducing bacteria and description of *Desulfobacterium autotrophicum* gen. nov., sp. nov. *Arch Microbiol* **148**: 264−274.

Butler, J.E., Young, N.D., and Lovley, D.R. (2010) Evolution of electron transfer out of the cell: comparative genomics of six Geobacter genomes. *BMC Genomics* **11**: 1−12.

Cabanillas, E.D., and Palacios, T.A. (2006) An hexahedrite meteorite from the Campo del Cielo Fall. *Planet Space Sci* **54**: 303−309.

Caffrey, S.A., Park, H.S., Voordouw, J.K., He, Z., Zhou, J., and Voordouw, G. (2007) Function of periplasmic hydrogenases in the sulfate-reducing bacterium *Desulfovibrio vulgaris* Hildenborough. *J Bacteriol* **189**: 6159−6167.

Canfield, D.E. (1989) Sulfate reduction and oxic respiration in marine sediments - Implications for organic carbon preservation in euxinic environments. *Deep-Sea Res* **36**: 121−138.

Canfield, D.E., Thamdrup, B., and Kristensen, E. (2005) *Aquatic Geomicrobiology*. San Diego: Elsevier.

Cline, J.D. (1969) Spectrophotometric determination of hydrogen sulfide in natural waters. *Limnol Oceanogr* **14**: 454−458.

Coetser, S.E., and Cloete, T.E. (2005) Biofouling and biocorrosion in industrial water systems. *Crit Rev Microbiol* **31**: 213−232.

Cohen, M. (1979) Dissolution of iron. In *Corrosion Chemistry*. Brubaker, G., and Phipps, P.B.P. (eds). Washington DC: ACS Symposium Series.

Conrad, R. (1999) Contribution of hydrogen to methane production and control of hydrogen concentrations in methanogenic soils and sediments. *FEMS Microbiol Ecol* **28**: 193−202.

Cord-Ruwisch, R. (1985) A quick method for the determination of dissolved and precipitated sulfides in cultures of sulfate-reducing bacteria. *J Microbiol Met* **4**: 33−36.

Cord-Ruwisch, R. (2000) Microbially Influenced Corrosion of Steel. In *Environmental Microbe-Metal Interactions*. Lovley, D.R. (ed). Washington, D.C.: ASM Press, pp. 159−173.

Cord-Ruwisch, R., Seitz, H.J., and Conrad, R. (1988) The capacity of hydrogenotrophic anaerobic bacteria to compete for traces of hydrogen depends on the redox potential of the terminal electron acceptor. *Arch Microbiol* **149**: 350−357.

Cord-Ruwisch, R., and Widdel, F. (1986) Corroding iron as a hydrogen source for sulfate reduction in growing cultures of sulfate-reducing bacteria. *Appl Microbiol Biotechnol* **25**: 169−174.

Costello, J.A. (1974) Cathodic depolarization by sulphate-reducing bacteria. *S Afr J Sci* **70**: 202−204.

Croese, E., Pereira, M.A., Euverink, G.J.W., Stams, A.J.M., and Geelhoed, J.S. (2011) Analysis of the microbial community of the biocathode of a hydrogen-producing microbial electrolysis cell. *Appl Microbiol Biotechnol* **92**: 1083−1093.

Dang, H.Y., Chen, R.P., Wang, L., Shao, S.D., Dai, L.Q., Ye, Y. et al. (2011) Molecular characterization of putative biocorroding microbiota with a novel niche detection of

Epsilon- and *Zetaproteobacteria* in Pacific Ocean coastal seawaters. *Environ Microbiol* **13**: 3059−3074.

Daniels, L., Belay, N., Rajagopal, B.S., and Weimer, P.J. (1987) Bacterial methanogenesis and growth from CO_2 with elemental iron as the sole source of electrons. *Science* **237**: 509−511.

Da Silva, S., Basseguy, R., and Bergel, A. (2002) The role of hydrogenases in the anaerobic microbiologically influenced corrosion of steels. *Bioelectrochemistry* **56**: 77−79.

Da Silva, S., Basseguy, R., and Bergel, A. (2004) Electron transfer between hydrogenase and 316L stainless steel: identification of a hydrogenase-catalyzed cathodic reaction in anaerobic MIC. *J Electroanal Chem* **561**: 93−102.

Dawood, Z., and Brözel, V.S. (1998) Corrosion-enhancing potential of *Shewanella putrefaciens* isolated from industrial cooling waters. *J Appl Microbiol* **84**: 929−936.

Deckena, S., and Blotevogel, K.H. (1990) Growth of methanogenic and sulfate-reducing bacteria with cathodic hydrogen. *Biotechnol Lett* **12**: 615−620.

Deckena, S., and Blotevogel, K.H. (1992) Fe^0-oxidation in the presence of methanogenic and sulfate-reducing bacteria and its possible role in anaerobic corrosion. *Biofouling* **5**: 287−293.

Deutsch, E.R., Rao, K.V., Laurent, R., and Seguin, M.K. (1977) New evidence and possible origin of native iron in ophiolites of eastern Canada. *Nature* **269**: 684−685.

De Windt, W., Boon, N., Siciliano, S.D., and Verstraete, W. (2003) Cell density related H_2 consumption in relation to anoxic Fe(0) corrosion and precipitation of corrosion products by *Shewanella oneidensis* MR-1. *Environ Microbiol* **5**: 1192−1202.

Dinh, H.T. (2003) Microbiological study of the anaerobic corrosion of iron. *Ph.D.-thesis*. University of Bremen.

Dinh, H.T., Kuever, J., Mußmann, M., Hassel, A.W., Stratmann, M., and Widdel, F. (2004) Iron corrosion by novel anaerobic microorganisms. *Nature* **427**: 829−832.

Dubiel, M., Hsu, C.H., Chien, C.C., Mansfeld, F., and Newman, D.K. (2002) Microbial iron respiration can protect steel from corrosion. *Appl Environ Microbiol* **68**: 1440−1445.

Duncan, K.E., Gieg, L.M., Parisi, V.A., Tanner, R.S., Tringe, S.G., Bristow, J., and Suflita, J.M. (2009) Biocorrosive thermophilic microbial communities in Alaskan North Slope oil facilities. *Environ Sci Technol* **43**: 7977−7984.

Etkin, D.S. (2001) Analysis of oil spill trends in the USA and worldwide. *International Oil Spill Conference 2001*. Tampa, Florida. pp. 1291−1300.

Fang, H., Young, D., and Nešić, S. (2009) Elemental sulfur corrosion of mild steel at high concentrations of sodium chloride. In *Corrosion*. Houston: NACE International, pp. 1−16.

Fang, H.H.P., Xu, L.C., and Chan, K.Y. (2002) Effects of toxic metals and chemicals on biofilm and biocorrosion. *Water Res* **36**: 4709−4716.

Ferris, F.G., Jack, T.R., and Bramhill, B.J. (1992) Corrosion products associated with attached bacteria at an oil field water injection plant. *Can J Microbiol* **38**: 1320−1324.

Flemming, H.C. (1994) Microbial deterioration of materials − fundamentals − econom-ical and technical overview. *Mater Corros* **45**: 5−9.

Foti, M., Sorokin, D.Y., Lomans, B., Mußman, M., Zacharova, E.E., Pimenov, N.V. et al. (2007) Diversity, activity, and abundance of sulfate-reducing bacteria in saline and hypersaline soda lakes. *Appl Environ Microbiol* **73**: 2093−2100.

Gaines, R. (1910) Bacterial activity as a corrosive influence in the soil. *J Ind Eng Chem* **2**: 128−130.

Garcia, J.L., Patel, B.K.C., and Ollivier, B. (2000) Taxonomic phylogenetic and ecological diversity of methanogenic *Archaea*. *Anaerobe* **6**: 205−226.

Gieg, L.M., Jack, T.R., and Foght, J.M. (2011) Biological souring and mitigation in oil reservoirs. *Appl Microbiol Biot* **92**: 263−282.

Gittel, A., Seidel, M., Kuever, J., Galushko, A.S., Cypionka, H., and Konneke, M. (2010) *Desulfopila inferna* sp. nov., a sulfate-reducing bacterium isolated from the subsurface of a tidal sand-flat. *Int J Syst Evol Microbiol* **60**: 1626−1630.

Grigoryan, A., Lambo, A., Lin, S., Cornish, S.L., Jack, T.R., and Voordouw, G. (2008) Souring remediation by field-wide nitrate injection in an Alberta oil field. In *Canadian International Petroleum Conference*. Calgary, Canada.

Gregory, K.B., Bond, D.R., and Lovley, D.R. (2004) Graphite electrodes as electron donors for anaerobic respiration. *Environ Microbiol* **6**: 596−604.

Gu, J.-D., Ford, T.E., and Mitchell, R. (2011) Microbiological corrosion of metallic materials. In *Uhlig's Corrosion Handbook*. Revie, R.W. (ed). New York: Wiley, pp. 549−557.

Haggerty, S.E., and Toft, P.B. (1985) Native iron in the continental lower crust − Petrological and geophysical implications. *Science* **229**: 647−649.

Hamilton, W.A. (1985) Sulphate-reducing bacteria and anaerobic corrosion. *Annu Rev Microbiol* **39**: 195−217.

Hamilton, W.A. (2003) Microbially influenced corrosion as a model system for the study of metal microbe interactions: a unifying electron transfer hypothesis. *Biofouling* **19**: 65−76.

Hansson, E.B., Odziemkowski, M.S., and Gillham, R.W. (2006) Formation of poorly crystalline iron monosulfides: Surface redox reactions on high purity iron, spectroelectrochemical studies. *Corros Sci* **48**: 3767−3783.

Hardy, J.A. (1983) Utilization of cathodic hydrogen by sulphate-reducing bacteria. *Br Corros J* **18**: 190−193.

Hardy, J.A., and Bown, J.L. (1984) The corrosion of mild steel by biogenic sulfide films exposed to air. *Corrosion* **40**: 650−654.

Heimann, A., Jakobsen, R., and Blodau, C. (2010) Energetic constraints on H_2-dependent terminal electron accepting processes in anoxic environments: a review of observations and model approaches. *Environ Sci Technol* **44**: 24−33.

Hubert, C., Nemati, M., Jenneman, G., and Voordouw, G. (2005) Corrosion risk associated with microbial souring control using nitrate or nitrite. *Appl Microbiol Biotechnol* **68**: 272−282.

Hurt, R.A., Qiu, X.Y., Wu, L.Y., Roh, Y., Palumbo, A.V., Tiedje, J.M., and Zhou, J.H. (2001) Simultaneous recovery of RNA and DNA from soils and sediments. *Appl Environ Microbiol* **67**: 4495−4503.

Itoh, T., Suzuki, K., and Nakase, T. (1998) *Thermocladium modestius* gen. nov., sp. nov., a new genus of rod-shaped, extremely thermophilic crenarchaeote. *Int J Syst Bacteriol* **48**: 879−887.

Itoh, T., Suzuki, K., Sanchez, P.C., and Nakase, T. (1999) *Caldivirga maquilingensis* gen. nov., sp. nov., a new genus of rod-shaped crenarchaeote isolated from a hot spring in the Philippines. *Int J Syst Bacteriol* **49**: 1157−1163.

Iverson, W.P. (1968) Corrosion of iron and formation of iron phosphide by *Desulfovibrio desulfuricans*. *Nature* **217**: 1265−1267.

Iverson, W.P. (1987) Microbial corrosion of metals. *Adv Appl Microbiol* **32**: 1−36.

Iverson, W.P. (2001) Research on the mechanisms of anaerobic corrosion. *Int Biodet Biodegr* **47**: 63−70.

Jack, T.R. (2002) Biological corrosion failures. In *ASM Handbook Volume 11: Failure Analysis and Prevention*. Shipley, R.J., and Becker, W.T. (eds). Materials Park: ASM International, pp. 881−898.

Jack, T.R., Wilmott, A., Stockdale, J., Van Boven, G., Worthingham, R.G., and Sutherby, R.L. (1998) Corrosion consequences of secondary oxidation of microbial corrosion. *Corrosion* **54**: 246−252.

Jack, T.R., Wilmott, M.J., and Sutherby, R.L. (1995) Indicator minerals formed during external corrosion of line pipe. *Mater Perform* **34**: 19−22.

Jan-Roblero, J., Romero, J.M., Amaya, M., and Le Borgne, S. (2004) Phylogenetic characterization of a corrosive consortium isolated from a sour gas pipeline. *Appl Microbiol Biotechnol* **64**: 862−867.

Jayaraman, A., Cheng, E.T., Earthman, J.C., and Wood, T.K. (1997) Axenic aerobic biofilms inhibit corrosion of SAE1018 steel through oxygen depletion. *Appl Microbiol Biot* **48**: 11−17.

Jeffrey, R., and Melchers, R.E. (2003) Bacteriological influence in the development of iron sulphide species in marine immersion environments. *Corros Sci* **45**: 693−714.

Jørgensen, B.B. (1982) Mineralization of organic matter in the sea bed˜ the role of sulfate reduction. *Nature* **296**: 643−645.

Kaesche, H. (2003) *Corrosion of Metals: Physicochemical Principles and Current Problems*. Berlin: Springer.

Kato, S., Nakamura, R., Kai, F., Watanabe, K., and Hashimoto, K. (2010) Respiratory interactions of soil bacteria with (semi)conductive iron-oxide minerals. *Environ Microbiol* **12**: 3114−3123.

Kielemoes, J., De Boever, P., and Verstraete, W. (2000) Influence of denitrification on the corrosion of iron and stainless steel powder. *Environ Sci Technol* **34**: 663−671.

King, R.A., and Miller, J.D.A. (1971) Corrosion by sulphate-reducing bacteria. *Nature* **233**: 491−492.

King, R.A., Miller, J.D.A., and Smith, J.S. (1973) Corrosion of mild steel by iron sulphides. *Br Corros J* **8**: 137−141.

Kjeldsen, K.U., Kjellerup, B.V., Egli, K., Frolund, B., Nielsen, P.H., and Ingvorsen, K. (2007) Phylogenetic and functional diversity of bacteria in biofilms from metal surfaces of an alkaline district heating system. *FEMS Microbiol Ecol* **61**: 384−397.

Kniemeyer, O., Musat, F., Sievert, S.M., Knittel, K., Wilkes, H., Blumenberg, M. *et al*. (2007) Anaerobic oxidation of short-chain hydrocarbons by marine sulphate-reducing bacteria. *Nature* **449**: 898−901.

Knoblauch, C., Sahm, K., and Jørgensen, B.B. (1999) Psychrophilic sulfate-reducing bacteria isolated from permanently cold Arctic marine sediments: description of *Desulfofrigrus oceanense* gen. nov., sp. nov., *Desulfofrigus fragile* sp. nov., *Desulfofaba gelida* gen. nov., sp. nov., *Desulfotalea psychrophila* gen. nov., sp. nov. and *Desulfotalea arctica* sp. nov. *Int J Syst Bacteriol* **49**: 1631−1643.

Koch, G.H., Brongers, M.P.H., Thompson, N.G., Virmani, Y.P., and Payer, J.H. (2001) Corrosion cost and preventive strategies in the United States. In: CC Technologies Laboratories. NACE International.

Kruger, J. (2011) Cost of metallic corrosion. In *Uhlig's Corrosion Handbook*. Revie, R.W. (ed). Hoboken, New Jersey: Wiley, pp. 15−20.

Kuang, F., Wang, J., Yan, L., and Zhang, D. (2007) Effects of sulfate-reducing bacteria on the corrosion behavior of carbon steel. *Electrochim Acta* **52**: 6084−6088.

Larsen, J., Rasmussen, K., Pedersen, K., Sørensen, K., Lundgaard, T., and Skovhus, T.L. (2010) Consortia of MIC bacteria and archaea causing pitting corrosion in top side oil production facilities. *CORROSION 2010*: NACE International. Paper no. 10252.

Lee, W.C., and de Beer, D. (1995) Oxygen and pH microprofiles above corroding mild-steel covered with a biofilm. *Biofouling* **8**: 273−280.

Lee, W., and Characklis, W.G. (1993) Corrosion of mild steel under anaerobic biofilm. *Corrosion* **49**: 186−199.

Lee, W., Lewandowski, Z., Morrison, M., Characklis, W.G., Avci, R., and Nielsen, P.H. (1993a) Corrosion of mild steel underneath aerobic biofilms containing sulfate-reducing bacteria. Part I: At high dissolved oxygen concentrations. *Biofouling* **7**: 217−239.

Lee, W., Lewandowski, Z., Nielsen, P.H., and Hamilton, W.A. (1995) Role of sulfate-reducing bacteria in corrosion of mild steel - a review. *Biofouling* **8**: 165−194.

Lee, A.K., and Newman, D.K. (2003) Microbial iron respiration: impacts on corrosion processes. *Appl Microbiol Biotechnol* **62**: 134−139.

Lewandowski, Z., and Beyenal, H. (2009) Mechanisms of Microbially Influenced Corrosion. In *Marine and Industrial Biofouling*. Flemming, H.C., Murthy, P.S., Venkatesan, R., and Cooksey, K.E. (eds). Berlin: Springer, pp. 35−64.

Lewandowski, Z., Dickinson, W., and Lee, W. (1997) Electrochemical interactions of biofilms with metal surfaces. *Wat Sci Technol* **36**: 295−302.

Li, S., Kim, Y., Jeon, K., and Kho, Y. (2000) Microbiologically influenced corrosion of underground pipelines under the disbonded coatings. *Met Mater* **6**: 281−286.

Li, D., Li, Z., Yu, J.W., Cao, N., Liu, R.Y., and Yang, M. (2010) Characterization of bacterial community structure in a drinking water distribution system during an occurrence of red water. *Appl Environ Microbiol* **76**: 7171−7180.

Lin, S.P., Krause, F., and Voordouw, G. (2009) Transformation of iron sulfide to greigite by nitrite produced by oil field bacteria. *Appl Microbiol Biotechnol* **83**: 369−376.

Little, B.J., and Lee, J.S. (2007) *Microbiologically Influenced Corrosion*. Hoboken: Wiley.

Little, B.J., Lee, J.S., and Ray, R.I. (2006) Diagnosing microbiologically influenced corrosion: a state-of-the-art review. *Corrosion* **62**: 1006−1017.

Little, B., Wagner, P.A., Characklis, W.G., and Lee, W. (1990) Microbial Corrosion. In *Biofilms*. Characklis, W.G., and Marshall, K.C. (eds). New York: Wiley, pp. 635−670.

Little, B., Wagner, P., Hart, K., Ray, R., Lavoie, D., Nealson, K., and Aguilar, C. (1998) The role of biomineralization in microbiologically influenced corrosion. *Biodegradation* **9**: 1−10.

Lorowitz, W.H., Nagle, D.P., and Tanner, R.S. (1992) Anaerobic oxidation of elemental metals coupled to methanogenesis by *Methanobacterium thermoautotrophicum*. *Environ Sci Technol* **26**: 1606−1610.

Lovley, D.R. (2011a) Reach out and touch someone: potential impact of DIET (direct interspecies energy transfer) on anaerobic biogeochemistry, bioremediation, and bioenergy. *Rev Environ Sci Biotechnol* **10**: 101−105.

Lovley, D.R. (2011b) Powering microbes with electricity: direct electron transfer from electrodes to microbes. *Environ Microbiol Rep* **3**: 27−35.

Lovley, D.R., Chapelle, F.H., and Woodward, J.C. (1994) Use of dissolved H_2 concentrations to determine the distribution of microbially catalyzed redox reactions in anoxic groundwater. *Environ Sci Technol* **28**: 1205−1210.

Lovley, D.R., and Phillips, E.J.P. (1987) Competitive mechanisms for inhibition of sulfate reduction and methane production in the zone of ferric iron reduction in sediments. *Appl Environ Microbiol* **53**: 2636−2641.

Ludwig, W., Strunk, O., Westram, R., Richter, L., Meier, H., Yadhukumar *et al*. (2004) ARB: a software environment for sequence data. *Nucleic Acids Res* **32**: 1363−1371.

Ma, H.Y., Cheng, X.L., Li, G.Q., Chen, S.H., Quan, Z.L., Zhao, S.Y., and Niu, L. (2000) The influence of hydrogen sulfide on corrosion of iron under different conditions. *Corros Sci* **42**: 1669−1683.

MacDonald, D.D., Roberts, B., and Hyne, J.B. (1978) Corrosion of carbon steel during cyclical exposure to wet elemental sulfur and atmosphere. *Corros Sci* **18**: 499−501.

Mara, D.D., and Williams, D.J.A. (1972) Polarisation of pure iron in the presence of iron sulfide minerals. *Br Corros J* **7**: 94−95.

Matias, P.M., Pereira, I.A.C., Soares, C.M., and Carrondo, M.A. (2005) Sulphate respiration from hydrogen in *Desulfovibrio* bacteria: a structural biology overview. *Prog Biophys Mol Bio* **89**: 292−329.

McBeth, J.M., Little, B.J., Ray, R.I., Farrar, K.M., and Emerson, D. (2011) Neutrophilic iron-oxidizing "*Zetaproteobacteria*" and mild steel corrosion in nearshore marine environments. *Appl Environ Microbiol* **77**: 1405−1412.

Miranda, E., Bethencourt, M., Botana, F.J., Cano, M.J., Sanchez-Amaya, J.M., Corzo, A. *et al*. (2006) Biocorrosion of carbon steel alloys by an hydrogenotrophic sulfate-reducing bacterium *Desulfovibrio capillatus* isolated from a Mexican oil field separator. *Corros Sci* **48**: 2417−2431.

Mori, K., Kim, H., Kakegawa, T., and Hanada, S. (2003) A novel lineage of sulfate-reducing microorganisms: *Thermodesulfobiaceae* fam. nov., *Thermodesulfobium narugense*, gen. nov., sp. nov., a new thermophilic isolate from a hot spring. *Extremophiles* **7**: 283−290.

Mori, K., Tsurumaru, H., and Harayama, S. (2010) Iron corrosion activity of anaerobic hydrogen-consuming microorganisms isolated from oil facilities. *J Biosci Bioeng* **110**: 426−430.

Morse, J.W., Millero, F.J., Cornwell, J.C., and Rickard, D. (1987) The chemistry of the hydrogen sulfide and iron sulfide systems in natural waters. *Earth Sci Rev* **24**: 1−42.

Motamedi, M., and Pedersen, K. (1998) *Desulfovibrio aespoeensis* sp. nov., a mesophilic sulfate-reducing bacterium from deep groundwater at Äspö hard rock laboratory, Sweden. *Int J Syst Bacteriol* **48**: 311−315.

Mußmann, M., Ishii, K., Rabus, R., and Amann, R. (2005) Diversity and vertical distribution of cultured and uncultured *Deltaproteobacteria* in an intertidal mud flat of the Wadden Sea. *Environ Microbiol* **7**: 405−418.

Muyzer, G., and Stams, A.J.M. (2008) The ecology and biotechnology of sulphate-reducing bacteria. *Nat Rev Microbiol* **6**: 441−454.

Muyzer, G., Teske, A., Wirsen, C.O., and Jannasch, H.W. (1995) Phylogenetic relationships of *Thiomicrospira* species and their identification in deep-sea hydrothermal vent samples by denaturing gradient gel electrophoresis of 16S rDNA fragments. *Arch Microbiol* **164**: 165−172.

Nakamura, R., Kai, F., Okamoto, A., Newton, G.J., and Hashimoto, K. (2009) Self-constructed electrically conductive bacterial networks. *Angew Chem Int Ed* **48**: 508−511.

Nemati, M., Jenneman, G.E., and Voordouw, G. (2001) Impact of nitrate-mediated microbial control of souring in oil reservoirs on the extent of corrosion. *Biotechnol Progr* **17**: 852−859.

Neria-González, I., Wang, E.T., Ramirez, F., Romero, J.M., and Hernandez-Rodriguez, C. (2006) Characterization of bacterial community associated to biofilms of corroded oil pipelines from the southeast of Mexico. *Anaerobe* **12**: 122−133.

Nešić, S. (2011) Carbon dioxide corrosion of mild steel. In *Uhlig's Corrosion Handbook*. Revie, R.W. (ed). New York: Wiley, pp. 229−245.

Newman, R.C., Rumash, K., and Webster, B.J. (1992) The effect of pre-corrosion on the corrosion rate of steel in neutral solutions containing sulfide − Relevance to microbially influenced corrosion. *Corros Sci* **33**: 1877−1884.

Newman, R.C., Webster, B.J., and Kelly, R.G. (1991) The electrochemistry of SRB corrosion and related inorganic phenomena. *ISIJ Int* **31**: 201−209.

Nielsen, P.H., Lee, W., Lewandowski, Z., Morison, M., and Characklis, W.G. (1993) Corrosion of mild steel in an alternating oxic and anoxic biofilm system. *Biofouling* **7**: 267−284.

Nielsen, L.P., Risgaard-Petersen, N., Fossing, H., Christensen, P.B., and Sayama, M. (2010) Electric currents couple spatially separated biogeochemical processes in marine sediment. *Nature* **463**: 1071−1074.

Nilsen, R.K., Beeder, J., Thorstenson, T., and Torsvik, T. (1996a) Distribution of thermophilic marine sulfate reducers in North Sea oil field waters and oil reservoirs. *Appl Environ Microbiol* **62**: 1793−1798.

Nilsen, R.K., Torsvik, T., and Lien, T. (1996b) *Desulfotomaculum thermocisternum* sp. nov., a sulfate reducer isolated from a hot North Sea oil reservoir. *Int J Syst Bacteriol* **46**: 397−402.

Obuekwe, C.O., Westlake, D.W.S., Plambeck, J.A., and Cook, F.D. (1981a) Corrosion of mild steel in cultures of ferric iron reducing bacterium isolated from crude oil: 1. Polarization characteristics. *Corrosion* **37**: 461−467.

Obuekwe, C.O., Westlake, D.W.S., Plambeck, J.A., and Cook, F.D. (1981b) Corrosion of mild steel in cultures of ferric iron reducing bacterium isolated from crude oil: 2. Mechanism of anodic depolarization. *Corrosion* **37**: 632−637.

Obuekwe, C.O., Westlake, D.W.S., Cook, F.D., and Costerton, J.W. (1981c) Surface changes in mild steel coupons from the action of corrosion-causing bacteria. *Appl Environ Microbiol* **41**: 766−774.

Odom, J.M., and Peck, H.D. (1981) Hydrogen cycling as a general mechanism for energy coupling in the sulfate-reducing bacteria, *Desulfovibrio* sp. *FEMS Microbiol Lett* **12**: 47−50.

Ollivier, B., Cayol, J.-L., and Fauque, G. (2007) Sulphate-reducing bacteria from oil field environments and deep-sea hydrothermal vents. In *Sulphate-reducing Bacteria*. Barton, L.L., and Hamilton, W.A. (eds). Cambridge: Cambridge University Press, pp. 305−328.

von Ommen Kloeke, F.V., Bryant, R.D., and Laishley, E.J. (1995) Localization of cytochromes in the outer membrane of *Desulfovibrio vulgaris* (Hildenborough) and their role in anaerobic biocorrosion. *Anaerobe* **1**: 351−358.

Pankhania, I.P., Moosavi, A.N., and Hamilton, W.A. (1986) Utilization of cathodic hydrogen by *Desulfovibrio vulgaris* (Hildenborough). *J Gen Microbiol* **132**: 3357−3365.

Pearce, C.I., Pattrick, R.A.D., and Vaughan, D.J. (2006) Electrical and magnetic properties of sulfides. *Rev Mineral Geochem* **61**: 127−180.

Pereira, I.A.C., Ramos, A.R., Grein, F., Marques, M.C., da Silva, S.M., and Venceslau, S.S. (2011) A comparative genomic analysis of energy metabolism in sulfate reducing bacteria and archaea. *Front Microbiol* **2**: 1−18.

Pikuta, E.V., Zhilina, T.N., Zavarzin, G.A., Kostrikina, N.A., Osipov, G.A., and Rainey, F.A. (1998) *Desulfonatronum lacustre* gen. nov., sp. nov.: A new alkaliphilic sulfate-reducing bacterium utilizing ethanol. *Microbiology* **67**: 105−113.

Piron, D.L. (1994) *The Electrochemistry of Corrosion*. Houston: NACE Press.

Pope, I.D.H. (1991) Microbiologically influenced corrosion in the natural gas industry. *GRI Annual Report 92/0006.* Gas Research Institute, Chicago. pp. 1−105.

Potekhina, J.S., Sherisheva, N.G., Povetkina, L.P., Pospelov, A.P., Rakitina, T.A., Warnecke, F., and Gottschalk, G. (1999) Role of microorganisms in corrosion inhibition of metals in aquatic habitats. *Appl Microbiol Biotechnol* **52**: 639−646.

Pourbaix, M. (1990) Thermodynamics and corrosion. *Corros Sci* **30**: 963−988.

Pruesse, E., Quast, C., Knittel, K., Fuchs, B.M., Ludwig, W.G., Peplies, J., and Glockner, F.O. (2007) SILVA: a comprehensive online resource for quality checked and aligned ribosomal RNA sequence data compatible with ARB. *Nucleic Acids Res* **35**: 7188−7196.

Rabus, R., Hansen, T., and Widdel, F. (2006) Dissimilatory sulfate- and sulfur-reducing prokaryotes. In *The Prokaryotes*. Dworkin, M., Schleifer, K.-H., and Stackebrandt, E. (eds). New York: Springer, pp. 659−768.

Rajagopal, B.S., and LeGall, J. (1989) Utilization of cathodic hydrogen by hydrogen-oxidizing bacteria. *Appl Microbiol Biotechnol* **31**: 406−412.

Reinsel, M.A., Sears, J.T., Stewart, P.S., and McInerney, M.J. (1996) Control of microbial souring by nitrate, nitrite or glutaraldehyde injection in a sandstone column. *J Ind Microbiol* **17**: 128−136.

Revie, R.W. (2011) *Uhlig's Corrosion Handbook*. New York: Wiley.

Rickard, D., and Luther, G.W. (2007) Chemistry of iron sulfides. *Chem Rev* **107**: 514−562.

Roels, J., and Verstraete, W. (2001) Biological formation of volatile phosphorus compounds. *Bioresource Technol* **79**: 243−250.

Sahm, K., Knoblauch, C., and Amann, R. (1999) Phylogenetic affiliation and quantification of psychrophilic sulfate-reducing isolates in marine Arctic sediments. *Appl Environ Microbiol* **65**: 3976−3981.

Sass, A., Rutters, H., Cypionka, H., and Sass, H. (2002) *Desulfobulbus mediterraneus* sp. nov., a sulfate-reducing bacterium growing on mono- and disaccharides. *Arch Microbiol* **177**: 468−474.

Schaschl, E. (1980) Elemental sulfur as a corrodent in deaerated, neutral aqueous solutions. *Mater Perform* **19**: 9−12.

Schwermer, C.U., Lavik, G., Abed, R.M.M., Dunsmore, B., Ferdelman, T.G., Stoodley, P. et al. (2008) Impact of nitrate on the structure and function of bacterial biofilm communities in pipelines used for injection of seawater into oil fields. *Appl Environ Microbiol* **74**: 2841−2851.

Sherar, B.W.A., Power, I.M., Keech, P.G., Mitlin, S., Southam, G., and Shoesmith, D.W. (2011) Characterizing the effect of carbon steel exposure in sulfide containing solutions to microbially induced corrosion. *Corros Sci* **53**: 955−960.

Shi, X.M., Avci, R., and Lewandowski, Z. (2002) Electrochemistry of passive metals modified by manganese oxides deposited by *Leptothrix discophora*: two-step model verified by ToF-SIMS. *Corros Sci* **44**: 1027−1045.

Shoesmith, D.W., Taylor, P., Bailey, M.G., and Owen, D.G. (1980) The formation of ferrous monosulfide polymorphs during the corrosion of iron by aqueous hydrogen sulfide at 21°C. *J Electrochem Soc* **127**: 1007−1015.

Smith, J.S., and Miller, J.D.A. (1975) Nature of sulphides and their corrosive effect on ferrous metals: a review. *Br Corros J* **10**: 136−143.

Starkey, R.L. (1946) Sulfate reduction and the anaerobic corrosion of iron. *A van Leeuw J Microbiol* **12**: 193−203.

Stetter, K.O., Lauerer, G., Thomm, M., and Neuner, A. (1987) Isolation of extremely thermophilic sulfate reducers evidence for a novel branch of archaebacteria. *Science* **236**: 822−824.

Starosvetsky, D., Armon, R., Yahalom, J., and Starosvetsky, J. (2001) Pitting corrosion of carbon steel caused by iron bacteria. *Int Biodet Biodegr* **47**: 79−87.

Summers, Z.M., Fogarty, H.E., Leang, C., Franks, A.E., Malvankar, N.S., and Lovley, D.R. (2010) Direct exchange of electrons within aggregates of an evolved syntrophic coculture of anaerobic bacteria. *Science* **330**: 1413−1415.

Sun, W. (2006) Kinetics of iron carbonate and iron sulfide scale formation in CO_2/H_2S corrosion. *Ph.D.-thesis.* Ohio University.

Sun, W., Pugh, D.V., Ling, S., Reddy, R.V., Pacheco, J.L., Nisbet, R.S. et al. (2011a) Understanding and quantifying corrosion of L80 carbon steel in sour environments. *CORROSION 2011*: NACE International. Paper no. 11063.

Sun, W., Li, C., Ling, S., Reddy, R.V., Pacheco, J.L., Asmann, M. et al. (2011b) Laboratory study of sour localized/pitting corrosion. *CORROSION 2011*: NACE International. Paper no. 11080.

Sun, W., and Nešić, S. (2007) A mechanistic model of H_2S corrosion of mild steel. *CORROSION 2007*: NACE International. Paper no. 07566.

Thauer, R.K., Kaster, A.K., Seedorf, H., Buckel, W., and Hedderich, R. (2008) Methanogenic archaea: ecologically relevant differences in energy conservation. *Nat Rev Microbiol* **6**: 579−591.

Thauer, R., Stackebrandt, E., and Hamilton, W.A. (2007) Energy metabolism and phylogenetic diversity of sulphate-reducing bacteria. In *Sulphate-reducing Bacteria*. Barton, L.L., and Hamilton, W.A. (eds). Cambridge: Cambridge University Press, pp. 1−38.

Till, B.A., Weathers, L.J., and Alvarez, P.J.J. (1998) Fe(0)-supported autotrophic denitrification. *Environ Sci Technol* **32**: 634−639.

Tiller, A.K. (1983) Electrochemical aspects of corrosion: an overview. In *Microbial Corrosion*. Teddington: The Metals Society. pp. 54−65.

Uchiyama, T., Ito, K., Mori, K., Tsurumaru, H., and Harayama, S. (2010) Iron-corroding methanogen isolated from a crude-oil storage tank. *Appl Environ Microbiol* **76**: 1783−1788.

U.S. Geological Survey (2011) *Mineral Commodity Summary 2011. U.S. Geological Survey:* 1−198 [www document]. URL http://minerals.usgs.gov/minerals/ pubs/mcs/2011/mcs2011.pdf

Venzlaff (2012) Die elektrisch mikrobiell beeinflusste Korrosion von Eisen durch sulfatreduzierende Bakterien. *Ph.D.-thesis.* University of Bochum.

Vera, J., Kapusta, S., and Hackerman, N. (1986) Localized corrosion of Iron in alkaline sulfide solutions − Iron sulfide formation and the breakdown of passivity. *J Electrochem Soc* **133**: 461−467.

Vignais, P.M., and Colbeau, A. (2004) Molecular biology of microbial hydrogenases. *Curr Iss Mol Biol* **6**: 159−188.

Vik, E.A., Janbu, A.O., Garshol, F., Henninge, L.B., Engebretsen, S., Kuijvenhoven, C. et al. (2007) Nitrate-based souring mitigation of produced water - side effects and challenges from the Draugen produced water re-injection pilot, paper SPE 106178. *SPE International Symposium on Oilfield Chemistry*. Houston.

Volk, C., Dundore, E., Schiermann, J., and Lechevallier, M. (2000) Practical evaluation of iron corrosion control in a drinking water distribution system. *Water Res* **34**: 1967−1974.

Voordouw, G. (2002) Carbon monoxide cycling by *Desulfovibrio vulgaris* Hilden-borough. *J Bacteriol* **184**: 5903−5911.

Wächtershäuser, G. (1992) Groundworks for an evolutionary biochemistry: the iron-sulphur world. *Prog Biophys Mol Biol* **58**: 85−201.

Wanklyn, J.N., and Spruit, C.J.P. (1952) Influence of sulphate-reducing bacteria on the corrosion potential of iron. *Nature* **169**: 928−929.

Weber, K.A., Achenbach, L.A., and Coates, J.D. (2006) Microorganisms pumping iron: anaerobic microbial iron oxidation and reduction. *Nat Rev Microbiol* **4**: 752−764.

Weimer, P.J., Vankavelaar, M.J., Michel, C.B., and Ng, T.K. (1988) Effect of phosphate on the corrosion of carbon steel and on the composition of corrosion products in 2-stage continuous cultures of *Desulfovibrio desulfuricans*. *Appl Environ Microbiol* **54**: 386−396.

Whitney, W.R. (1903) The corrosion of iron. *J Am Chem Soc* **25**: 394−406.

Widdel, F. (1992) Microbial Corrosion. In *Biotechnology Focus 3*. Finn, R.K., Prave, P., Schlingmann, M., Crueger, W., Esser, K., Thauer, R., and Wagner, F. (eds). Munich: Hanser, pp. 277−318.

Widdel, F. (1988) Microbiology and ecology of sulfate- and sulfur-reducing bacteria. In *Biology of Anaerobic Microorganisms*. Zehnder, A.J.B. (ed). New York: John Wiley & Sons, pp. 469−585.

Wikjord, A.G., Rummery, T.E., Doern, F.E., and Owen, D.G. (1980) Corrosion and deposition during the exposure of carbon steel to hydrogen sulfide-water solutions. *Corros Sci* **20**: 651−671.

Wilkin, R.T., and Barnes, H.L. (1996) Pyrite formation by reactions of iron monosulfides with dissolved inorganic and organic sulfur species. *Geochim Cosmochim Acta* **60**: 4167−4179.

von Wolzogen Kühr, C.A.H. (1961) Unity of anaerobic and aerobic iron corrosion process in the soil. *Corrosion* **17**: 119−125.

von Wolzogen Kühr, C.A.H., and van der Vlugt, L.S. (1934) The graphitization of cast iron as an electrobiochemical process in anaerobic soil. *Water* **18**: 147−165.

Zhang, T., Fang, H.H.P., and Ko, B.C.B. (2003) Methanogen population in a marine biofilm corrosive to mild steel. *Appl Microbiol Biotechnol* **63**: 101−106.

Zhilina, T.N., Zavarzin, G.A., Rainey, F.A., Pikuta, E.N., Osipov, G.A., and Kostrikina, N.A. (1997) *Desulfonatronovibrio hydyogenovorans* gen. nov., sp. nov., an alkaliphilic, sulfate-reducing bacterium. *Int J Syst Bacteriol* **47**: 144−149.

Zhu, X.Y., Ayala, A., Modi, H., and Kilbane II, J.J. (2005) Application of quantitative, real-time PCR in monitoring microbiologically influenced corrosion (MIC) in gas pipelines. *CORROSION 2005*. Houston: NACE International.

C.2 Supplementary figures and tables

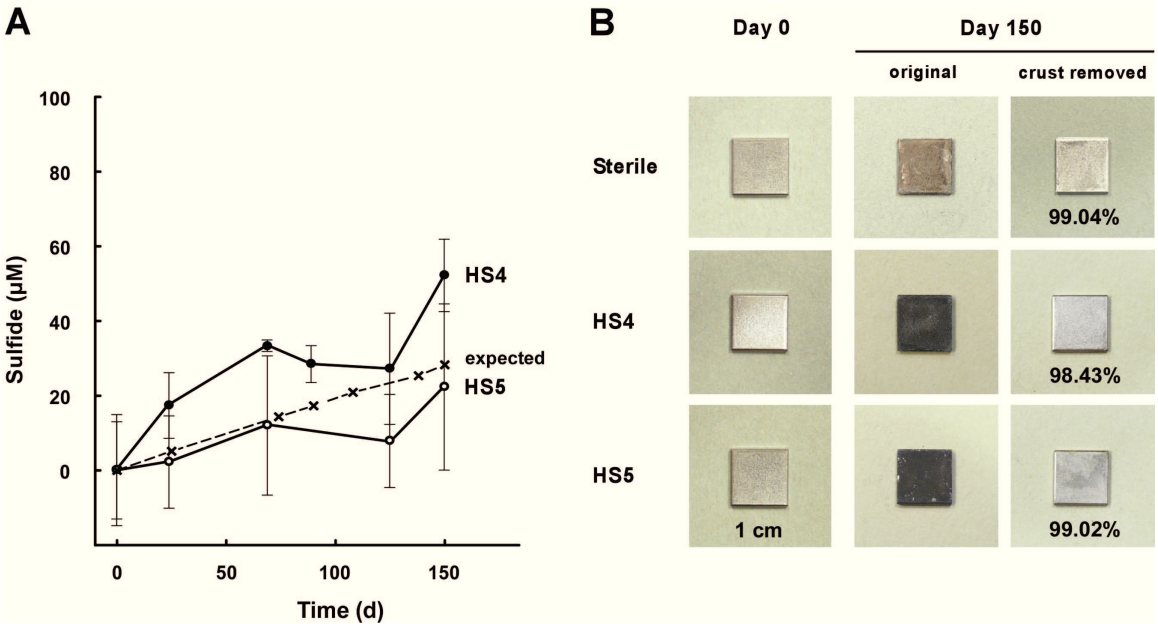

Fig. S1. Non-corrosive, H_2-scavening SRB in pure culture.

A. Long-term sulfide formation (calculated from sulfate loss) by *Desulfovibrio* spp. strains HS4 and HS5 with iron as the only electron donor (a = 2.4 cm^2 in 1.4 l ASW). Data are very imprecise due to only minute changes in sulfate concentration in the present incubation. Expected sulfide production from scavenge of cathodic H_2 is indicated. H_2 is effectively utilized below detection limit (40 ppmv) in cultures of strains HS4 and HS5 (not shown). Weight loss data (B) are more suitable for comparative assessment of corrosion under these conditions.

B. Thin FeS crusts and metal loss in these cultures. Residuary metal (% of initial) became obvious after crust removal with inactivated acid (10% hexamine in 2 M HCl).

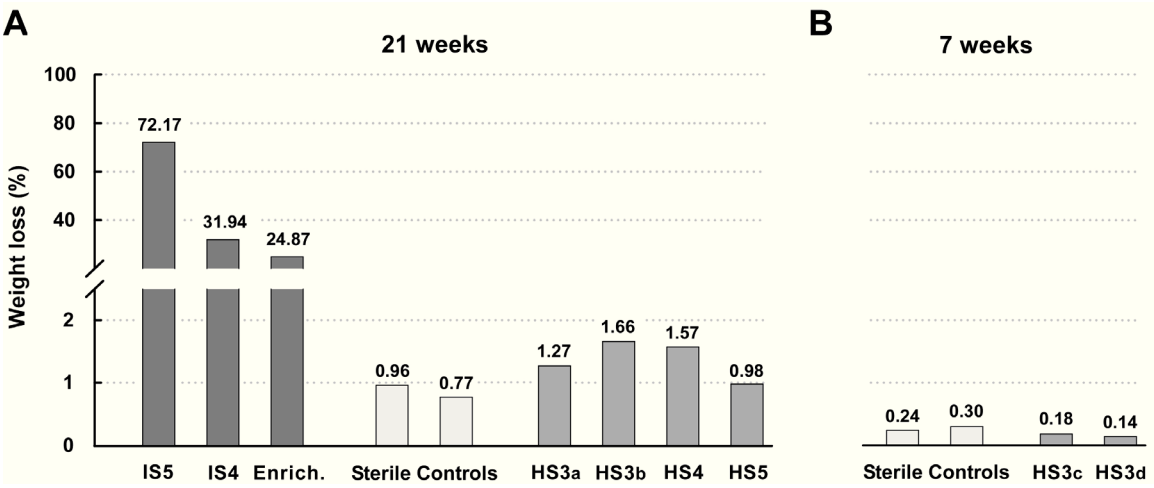

Fig. S2. Weight loss (percent of original) of low carbon steel coupons incubated in cultures of various corrosive and non-corrosive SRB for (A) 21 weeks and (B) 7 weeks. Corrosion due to direct electron uptake (strains IS5, IS4, and enrichment) dissolves Fe^0 far more rapidly than under sterile conditions or in the presence of H_2-scavenging SRB (*Desulfovibrio* sp. strains HS3, HS4 and HS5). Occasionally, hydrogenotrophic cultures have a slightly stimulatory effect on corrosion, presumably *via* deposited FeS.

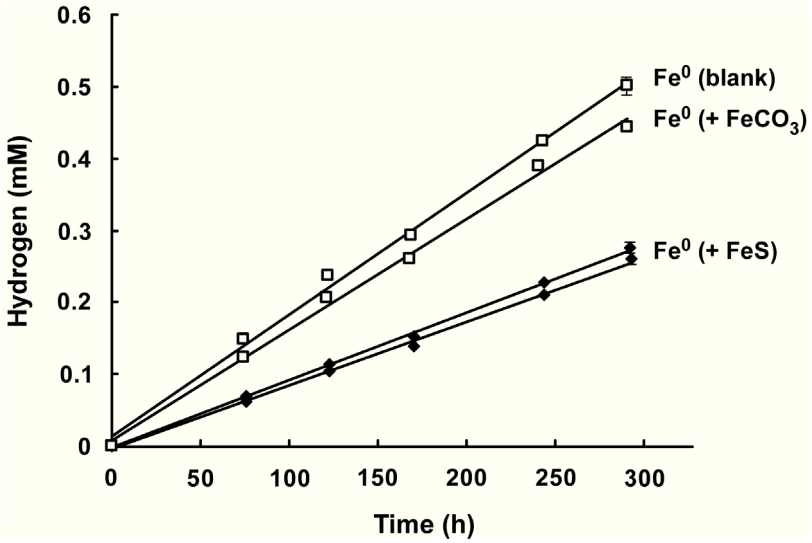

Fig. S3. Formation of cathodic hydrogen from glutaraldehyde-treated steel coupons covered with biogenic FeS or abiotically deposited $FeCO_3$. Coupons (Fe^0 + FeS) were incubated for eight months in a culture of *Desulfopila inferna* with lactate (Fig. 16). Attached cells were subsequently inactivated with glutaraldehyde and coupons were transferred into sterile ASW incubators. The same was done with a coupon with abiotic corrosion products (Fe^0 + $FeCO_3$) after eight months in sterile ASW (Fig. 14). Glutaraldehyde-treated (fresh) blank coupons served as control. For convenience, hydrogen concentrations refer to ASW medium (200 ml). Regression curves are depicted ($R^2 \geq 0.995$). Standard deviation is only indicated where larger than symbol size. H_2 formation rate were as follows. Fe^0 (blank): 0.19 µmol H_2 cm^{-2} d^{-1} (0.43 µA cm^{-2}; 0.005 mm Fe^0 yr^{-1}); Fe^0 (+ $FeCO_3$): 0.16 µmol H_2 cm^{-2} d^{-1} (0.37 µA cm^{-2}; 0.004 mm Fe^0 yr^{-1}); Fe^0 (+ FeS): 0.10 µmol H_2 cm^{-2} d^{-1} (0.23 µA cm^{-2}; 0.003 mm Fe^0 yr^{-1}).

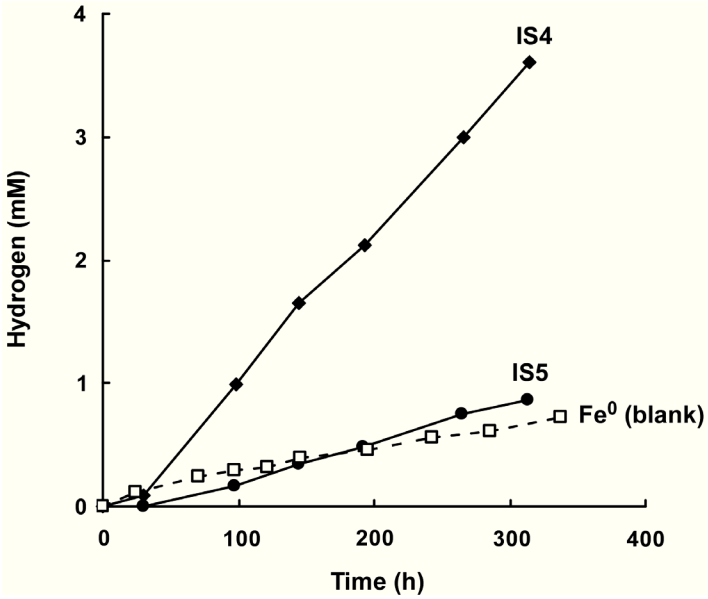

Fig. S4. Formation of hydrogen upon transfer of crust-covered steel coupons into sulfate-free ASW. Coupons had been previously incubated in cultures of strain IS4 (Fig. 17) and IS5 for 37 and 4 weeks, respectively. A blank iron coupon served as control. For convenience, hydrogen concentrations refer to ASW medium (200 ml). Averaged H_2 formation rate were as follows. IS4: 1.28 µmol H_2 cm^{-2} d^{-1} (2.85 µA cm^{-2}; 0.033 mm Fe^0 yr^{-1}); IS5: 0.31 µmol H_2 cm^{-2} d^{-1} (0.69 µA cm^{-2}; 0.008 mm Fe^0 yr^{-1}); Fe^0 (blank): 0.24 µmol H_2 cm^{-2} d^{-1} (0.56 µA cm^{-2}; 0.006 mm Fe^0 yr^{-1}).

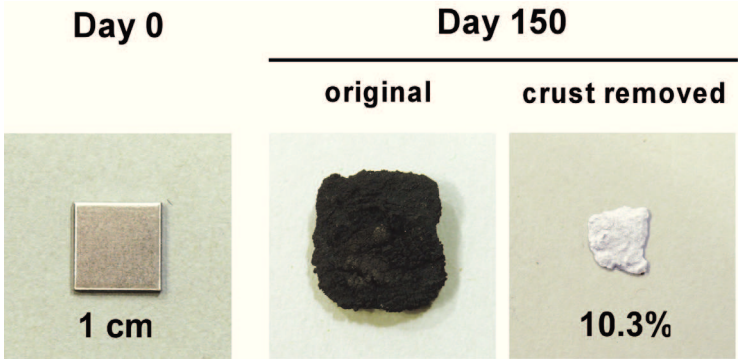

Fig. S5. Corrosion damage by SRB isolate IS6 in pure culture. Thick crust and metal loss after 5 months is depicted. Residuary metal (% of initial) became obvious after crust removal with inactivated acid (10% hexamine in 2 M HCl). The observed metal loss corresponds to an averaged corrosion rate of 0.88 mm yr^{-1} (75.9 µA cm^{-2}).

Table S1. Specific resistance and conductivity determined in split coupon incubations of strains IS4 and IS5.

Strain	e^- - donor [a]	ρ (ohm·m) [b]	σ ($S \cdot m^{-1}$) [c]
IS4a	Fe^0	0.023	43.5
IS4b	Fe^0	0.037	27.4
IS4c	Fe^0	0.028	35.7
IS4d	Fe^0 + lac	0.035	28.6
IS5a	Fe^0	0.024	41.7
IS5b	Fe^0 + lac	0.016	62.5

a. Electron donor in incubations was either metallic iron alone (Fe^0) or metallic iron and lactate (3 mM; Fe^0 + lac).
b. Specific resistance of corrosion products in pre-incubation split dimensions.
c. Conductivity (specific conductance) sigma of corrosion products in pre-incubation split dimension

C.3 Supplementary methods

Full methods in manuscripts. The following contains only supplementary methods.

Chemical analyses

Lactate was quantified in culture filtrates (0.45 µm) *via* reversed phase high performance liquid chromatography (HPLC, Sykam) with UV-vis detector (210 nm). Separation was achieved on an Aminex HPX-87H column (300 mm · 7.8 mm; 60°C) with 5 mM H_2SO_4 as the eluent (4.8 MPa). Dissolved sulfide was quantified after filtration of samples (0.45 µm) to exclude abundant FeS particles. Filtration was performed with much care to minimize out-gassing of H_2S. Quantification of high concentrations of sulfide (>3 mM) was performed in accordance with the photometric method of Cord-Ruwisch (1985). Lower concentrations of sulfide were determined by a modified (Aeckersberg, 1994) version of the photometric method described by Cline (1969). Dissolved inorganic carbon (DIC) was determined by flow injection (carrier: 30 mM HCl; receiver: 10 mM NaOH) and conductivity measurement with an EC Meter Model 1056 (Amber).

Organisms

Several SRB were tested for their ability to corrode iron lithotrophically. *Desulfovibrio vulgaris* strain Hildenborough, *Desulfobacterium autotrophicum* strain HRM2, *Desulfobacterium vacuolatum* and *Desulfosarcina variabilis* were obtained from culture collections within the Max Planck Institute for Marine Microbiology, Bremen. *Desulfovibrio aespoeensis* DSM 10631 and *Desulfovibrio indonesiensis* DSM 15121 were obtained from the Deutsche Sammlung von Mikroorganismen und Zellkulturen (DSMZ).

DNA extraction

Total nucleic acids were extracted following the method of Hurt *et al.* (2001). Briefly, coupons were rinsed with ASW and precipitates were scraped off the iron coupons with a sterile spatula into a mortar containing 1 g of baked sterile sand and 1.5 ml of denaturing solution (4 M guanidine isothiocyanate, 10 mM Tris-HCl [*pH* 7.0], 1 mM EDTA [*pH* 8.0], 0,5% 2-mercaptoethanol). Samples were then frozen in liquid N_2 and ground until thawed (3 x). After addition of 9 ml extraction buffer (100 mM sodium phosphate [*pH* 7.0], 100 mM Tris-HCl [*pH* 7.0], 100 mM EDTA [*pH* 8.0], 1.5 M NaCl, 1% hexadecyltrimethylammonium bromide [CTAB], 2% SDS), samples were incubated for 30 min in a heated water bath (65°C) with gentle mixing and then centrifuged (1,800 g, 10 min, 4°C). The procedure was repeated

twice to maximize extraction efficiency. Supernatants were collected in pre-chilled tubes with 20 ml chloroform-isoamyl alcohol (24:1) and centrifuged (4°C) at 1,800 g for 20 min. The aqueous phase was precipitated with 0.6 volume of 2-propanol (30 min, RT) and centrifuged (4°C) at 53,300 g for 20 min. The pellet was resuspended in 350 µl of RLT lysis buffer from the AllPrep DNA/RNA purification kit (Qiagen). Subsequent steps follow the instructions of the manufacturer. DNA was further purified using the Wizard DNA Clean-up System (Promega).

Cloning and sequencing

16S rRNA gene fragments were amplified in triplicate for each sample using bacterial primers GM3 and GM4 (Muyzer *et al*., 1995). GM3/GM4 PCR-products were pooled with the QIAquick PCR Purification Kit (Qiagen) according to the manufacturer`s instructions. Clone libraries were constructed using the Invitrogen TOPO TA Cloning Kit for Sequencing (Life Technologies). A total of 192 clones per library were picked with toothpicks and grown overnight in microtitre plates containing 300 µl of LB medium with 100 mg ml^{-1} ampicillin. Overnight cultures (1 µl each) were suspended in 10 µl nuclease-free water and freeze-thawed (3 x). Clones were screened for inserts of the expected size by PCR with the vector primers M13F (5'-GTT GTA AAA CGA CGG CCA GT-3') and M13R (5'-GGA AAC AGC TAT GAC CAT G-3') and by electrophoresis on 1.5% agarose gels. Clones containing inserts of the correct size were purified on a Sephadex spin column (Amersham Bioscience) and sequenced. Full-length and partial sequences of approximately 1550 bp or 800 bp length, respectively, were obtained with vector primers M13F/M13R.

Part D: Manuscripts

Overview of the manuscripts

D.1 Marine sulfate-reducing bacteria cause serious corrosion of iron under electroconductive biogenic mineral crusts

Dennis Enning, Hendrik Venzlaff, Julia Garrelfs, Hang T. Dinh, Volker Meyer, Karl Mayrhofer, Achim W. Hassel, Martin Stratmann and Friedrich Widdel

Authors contributions

D.E. and F.W. developed the concept. D.E. performed the growth and corrosion experiments. H.V. and D.E. performed scanning electron microscopy, micro-spectroscopic investigations and mineral analyses. DE designed and performed the conductivity experiments with contributions by V.M.. H.D. and A.W.H. discovered micro-chimneys. D.E. and J.G. designed and conducted the field experiment. K.M. and M.S. contributed electrochemical aspects. All authors discussed the results. F.W. and D.E. wrote the manuscript.

D.2 Accelerated cathodic reaction in microbial corrosion of iron due to direct electron uptake by sulfate-reducing bacteria

Hendrik Venzlaff, Dennis Enning, Jayendran Srinivasan, Karl Mayrhofer, Achim W. Hassel, Friedrich Widdel and Martin Stratmann

Authors contributions

H.V. and D.E. designed the study with support by K.M.. H.V. and D.E. developed a particular type of linear sweep voltammetry. H.V performed electrochemical measurements with contributions of J.S. D.E. and H.V. analyzed microbial activity. H.V. and D.E. performed scanning electron microscopy. K.M., A.W.H. and M.S. contributed electrochemical aspects. All authors discussed the results. F.W., H.V. and D.E. wrote the manuscript.

D.3 Corrosion of iron by sulfate-reducing bacteria - new views of an old problem

Dennis Enning and Julia Garrelfs

Authors contributions

D.E. developed the concept with contributions by J.G.. D.E. produced the contained data. D.E. wrote the manuscript.

Chapter D.1

Marine sulfate-reducing bacteria cause serious corrosion of iron under electroconductive biogenic mineral crusts

Dennis Enning,[1] Hendrik Venzlaff,[2] Julia Garrelfs,[1] Hang T. Dinh,[1] Volker Meyer,[1] Karl Mayrhofer,[2] Achim W. Hassel,[3] Martin Stratmann[2] and Friedrich Widdel[1]*

[1]*Max Planck Institute for Marine Microbiology, Celsiusstraße 1, D-28359 Bremen, Germany.*
[2]*Max Planck Institute for Iron Research, Max-Planck-Straße 1, D-40237 Düsseldorf, Germany.*
[3]*Institute for Chemical Technology of Inorganic Materials, Johannes Kepler University, Altenberger Straße 69, A-4040 Linz, Austria.*

Manuscript *in press* at

Environmental Microbiology (2012)

Summary

Iron (Fe^0) corrosion in anoxic environments (e.g. inside pipelines), a process entailing considerable economic costs, is largely influenced by microorganisms, in particular sulfate-reducing bacteria (SRB). The process is characterized by formation of black crusts and metal pitting. The mechanism is usually explained by the corrosiveness of formed H_2S, and scavenge of 'cathodic' H_2 from chemical reaction of Fe^0 with H_2O. Here we studied peculiar SRB that grew lithotrophically with metallic iron as the only electron donor. They degraded up to 72% of iron coupons (10 mm · 10 mm · 1 mm) within five months, which is a technologically highly relevant corrosion rate (0.7 mm Fe^0 yr^{-1}), while conventional H_2-scavenging control strains were not corrosive. The black, hard mineral crust (FeS, $FeCO_3$, Mg/$CaCO_3$) deposited on the corroding metal exhibited electrical conductivity (50 S m^{-1}). This was sufficient to explain the corrosion rate by electron flow from the metal ($4\,Fe^0 \rightarrow 4\,Fe^{2+} + 8\,e^-$) through semiconductive sulfides to the crust-colonizing cells reducing sulfate ($8\,e^- + SO_4^{2-} + 9\,H^+ \rightarrow HS^- + 4\,H_2O$). Hence, anaerobic microbial iron corrosion obviously bypasses H_2 rather than depends on it. SRB with such corrosive potential were revealed at naturally high numbers at a coastal marine sediment site. Iron coupons buried there were corroded and covered by the characteristic mineral crust. It is speculated that anaerobic biocorrosion is due to the promiscuous use of an ecophysiologically relevant catabolic trait for uptake of external electrons from abiotic or biotic sources in sediments.

Introduction

Iron, the fourth most abundant element in the earth's crust, is the principal redox-active metal in metabolic processes of essentially all living organisms. It is either involved in catalytic quantities as a component of a vast number of proteins, or in much higher, substrate quantities as the external electron donor or acceptor for specially adapted environmental microorganisms referred to as 'iron bacteria' (ferrotrophic bacteria, aerobic or anaerobic) or 'iron-respiring bacteria', respectively. In most biological functions, iron has the +II (ferrous) or +III (ferric) oxidation state. From a physiological point of view it appears astounding that also the native, metallic element (Fe^0) can be involved in a biological process; this is anaerobic microbial corrosion. In technology the process is often referred to as microbially influenced corrosion (MIC).

Iron is the technologically most widely employed metal, due to the abundance of its ores, straightforward melting, and excellent mechanical properties. It is globally produced at a 25-fold higher extent ($9.3 \cdot 10^8$ t yr^{-1}) than the second most widely employed metal, aluminum (U.S. Geological Survey, 2011; data for 2009). Iron corrosion including MIC is thus of significant economic relevance. MIC affects industrial water-bearing systems such as oil and gas pipelines (Hamilton, 1985; Li *et al.*, 2000; Schwermer *et al.*, 2008). It therefore causes, besides economic losses, also failures that are of environmental concern or even hazardous (Duncan *et al.*, 2009; Sherar *et al.*, 2011). A critical feature of MIC is that it is not as visible as the commonly known rusting of iron under air, but usually occurs as a 'hidden' process in the interior of iron pipes or on iron constructions buried in aqueous underground. There is much agreement that sulfate-reducing bacteria (SRB; more generally also sulfate-reducing microorganisms, SRM) are the main culprits of MIC (Hamilton, 1985; Lee *et al.*, 1995). Yet, the underlying mechanisms are apparently complex and insufficiently understood (Beech and Sunner, 2007). Their understanding is expected to contribute to the future development of effective mitigation strategies or causative counter measures.

The principal chemical feature in all models of MIC is that iron as a base metal easily gives off electrons, according to

$$Fe^0 \rightleftarrows Fe^{2+} + 2\ e^- \qquad (1)$$

$$E° = -0.469\ \text{V}$$

(revised redox potential; Appendix S1). In rusting, which to our present knowledge is a purely chemical (abiotic) process, oxygen accepts electrons ($4\ e^- + O_2 + 4\ H^+ \rightleftarrows 2\ H_2O$; $E° = +1.229$

V; $E°'$ = +0.815 V) and finally leads to the formation of brittle ferric oxides/hydroxides. Another ubiquitous electron acceptor are protons yielding hydrogen ($2\ e^- + 2\ H^+ \rightleftarrows H_2$; $E°$ = ±0.000 V; $E°'$ = –0.414 V). However, this is technologically only serious in rare instances of acidic surroundings. Proton reduction in circumneutral H_2O and thus the net reaction

$$Fe^0 + 2\ H_2O \rightarrow Fe^{2+} + H_2(g) + 2\ HO^- \qquad (2)$$

$\Delta G°' = -10.6$ kJ (mol Fe)$^{-1}$

$\Delta H° = +18.4$ kJ (mol Fe)$^{-1}$

are very slow (Fig. S1) so that iron in sterile anoxic water can, in principle, last for centuries. The corrosion risk for iron in the absence of acid or oxygen changes dramatically if constructions are exposed to non-sterile, 'environmental' aqueous surroundings where microorganisms such as SRB can grow and obviously accelerate iron oxidation enormously (Hamilton, 2003). Iron loss rates of 0.2 to 0.4 mm Fe^0 yr^{-1} are typically recorded *in situ* (Jack, 2002; Table S1). Two basically different modes by which SRB act upon iron have been envisaged (Dinh *et al*., 2004).

First, undissociated protons in H_2S from respiratory reduction of natural sulfate (e.g. in seawater) with organic nutrients react more rapidly with iron-derived electrons than do protons from or in (circumneutral) H_2O, according to

$$Fe^0 + H_2S \rightarrow FeS(c) + H_2(g) \qquad (3)$$

$\Delta G° = -72.5$ kJ (mol Fe)$^{-1}$

$\Delta H° = -64.4$ kJ (mol Fe)$^{-1}$

In such way, SRB act indirectly through an excreted chemical agent. We here refer to this process as ‘chemical microbially influenced corrosion’ (CMIC). The net reaction (Dinh *et al*., 2004) can be expressed, for instance with organic carbon of the oxidation state of carbohydrates (‘CH_2O’, viz. the abundant building structure ⟨H-C-OH⟩) as

$$3\ \langle HCOH \rangle + 2\ SO_4^{2-} + 2\ Fe^0 + H^+ \rightarrow 3\ HCO_3^- + 2\ FeS + 2\ H_2O \qquad (4)$$

(details in Appendix S1).

Second, SRB can be involved more intimately in anaerobic iron corrosion by a mechanism that is fundamentally different from the above CMIC. This was first envisaged in a

fundamental study of iron pipe corrosion in anoxic soil (von Wolzogen Kühr and van der Vlugt, 1934). SRB were suggested to use iron as the only source of reducing equivalents for sulfate reduction. The net stoichiometry of this purely lithotrophic process, here with the common carbonate (siderite) precipitation, is

$$4\,Fe^0 + SO_4^{2-} + 3\,HCO_3^- + H_2O \rightarrow FeS\,(c) + 3\,FeCO_3\,(c) + 5\,HO^- \quad (5)$$

$\Delta G°' = -86.2$ kJ (mol Fe)$^{-1}$

$\Delta H° = -190.0$ kJ (mol Fe)$^{-1}$

Still, the bulk equation cannot provide hints as to the actual form of the reducing equivalents channeled from iron into sulfate reduction. It has been appealing to consider H_2 (from H_2O reduction; Eq. 2) as the intermediate (Booth and Tiller, 1960; von Wolzogen Kühr, 1961; Bryant and Laishley, 1990; Coetser and Cloete, 2005), indeed an excellent growth substrate of many SRB. Their high-affinity hydrogen scavenging ($4\,H_2 + SO_4^{2-} + 2\,H^+ \rightarrow H_2S + 4\,H_2O$) is thought to 'pull' the primary oxidation (von Wolzogen Kühr and van der Vlugt, 1934; von Wolzogen Kühr, 1961), an explanation also common in textbooks. On the other hand, accelerated anaerobic corrosion due to H_2 utilization has been viewed critically (Costello, 1974; Hardy, 1983). In several kinetic studies, H_2 scavenging did not accelerate iron oxidation (Spruit and Wanklyn, 1951; Dinh *et al.*, 2004; Mori *et al.*, 2010). Furthermore, novel marine deltaproteobacterial SRB enriched and isolated directly with metallic iron as the only electron donor reduced sulfate much faster than possible by mere scavenge of H_2 and were more corrosive than conventional strains (Dinh *et al.*, 2004). Moreover, they transiently formed much H_2 rather than scavenged it, possibly due to an initial excess of iron-derived reducing power. Therefore, the ability to make use of Fe^0 for sulfate respiration in a kinetically more efficient manner than *via* the slowly formed H_2, viz. through a faster by-pass, was assumed, and direct electron uptake from iron has been suggested (Dinh *et al.*, 2004). This theory is here referred to as 'electrical microbially influenced corrosion' (EMIC).

In this study, we investigated the extent of iron destruction by these strains of SRB as well as the postulated EMIC and its significance in more detail. First, we measured whether corrosion rates as high as observed in industrial settings can be also attained *in vitro* by appropriately adjusted cultivation conditions. Second, we examined whether and in which way the increasing coverage of the metallic substrate by the inorganic black corrosion crust (Dinh *et al.*, 2004) is compatible with progressive corrosion and the hypothesized electron uptake from the metal. Third, we buried iron specimens in a field study in natural marine

sediment to prove whether corrosion phenomena *in situ* were similar as observed in laboratory incubation experiments.

Results

To study the postulated EMIC by the previously isolated strains under experimentally defined conditions, metallic iron was provided in the form of coupons as the sole electron donor for sulfate reduction. The only added organic compounds were trace amounts of vitamins (totally 0.58 mg l^{-1}, Table S2), and acetate (1 mM) provided as a biosynthetic building block to lithoheterotrophic strains IS5, HS3, and to *Desulfopila inferna*. Cultures incubated with 10 mM acetate without iron did not produce any sulfide, indicating that external acetate was not used as an electron donor. Measures of corrosion were the determination of iron mass loss at the end of incubation, a long-established routine method (Booth *et al*., 1967), and quantification of sulfate consumption, a more recently established method (Dinh *et al*., 2004) allowing highly resolved time courses. Consumption of sulfate parallels production of sulfide that cannot be monitored directly due to precipitation as FeS (Eq. 5). An analytical control experiment verified that disappearance of sulfate was only due to reduction and not in addition to a certain co-precipitation in the forming corrosion crust (Fig. S2).

Iron corrosion rates in long-term incubation experiments

Metallic iron represents a very compact, dense form of an electron donor sufficient to reduce dissolved sulfate from a relatively large culture volume. In the initial study (Dinh *et al*., 2004), the culture volume (0.15 l) to metal (30 g) ratio was kept relatively small for clearly revealing the corrosive potential of novel marine SRB within 20 days. In such incubations, the sulfate reduction rate slowed down significantly after a while. Examination in more detail in the present study revealed that this drop in activity was mostly due to the pronounced alkalization and exhaust of counteracting CO_2 (dissolved and gaseous). For the present biocorrosion experiments intended to examine iron destruction under conditions comparable to those *in situ* during much longer incubation, the ratio of the culture (and gas phase) volume to metal mass had to be increased. Because macroscopic corrosion phenomena were of central interest, the iron specimens (10 mm · 10 mm · 1 mm) could not be miniaturized to any extent, thus necessitating much bigger culture volumes. An appropriate medium volume was 1.4 l, which was still small enough for precise monitoring of sulfate consumption. Indeed, corrosion rates did not significantly decrease over months. Corrosive cultures reached values as high as 0.7 mm Fe^0 yr^{-1} and deposited steadily growing black crusts (Fig. 1A and B).

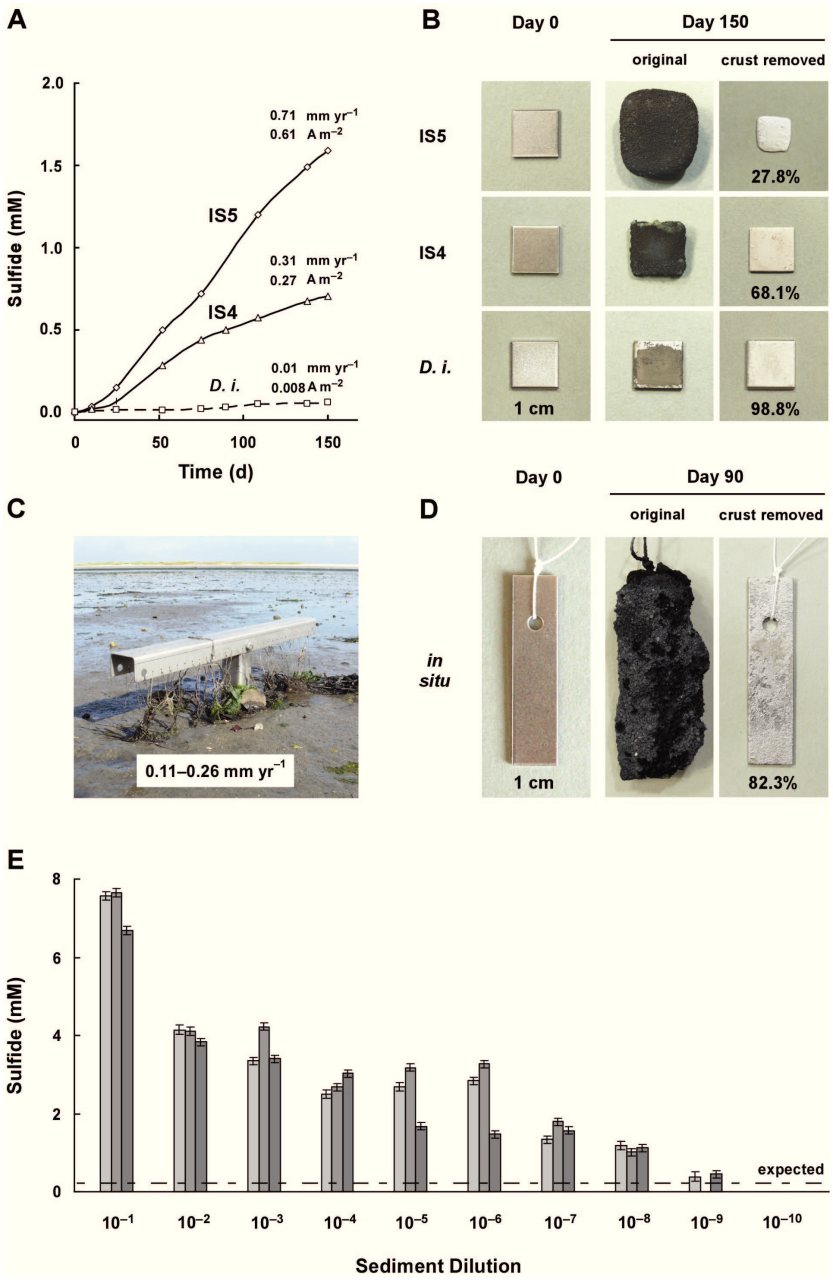

Fig. 1. Corrosive sulfate-reducing bacteria in pure cultures and *in situ*.

A. Long-term sulfide formation by corrosive strains IS5 and IS4 (proposed: *Desulfovibrio ferrophilus* and *Desulfopila corrodens*, respectively) with iron coupons as the only electron donor; hydrogenotrophic control culture, *Desulfopila inferna* (*D. i.*).

B. Thick corrosion crusts and metal loss in these cultures. Residuary metal (% of initial) became obvious after crust removal by HCl-hexamine.

C. Positioning device (stainless steel) for iron coupons in the Wadden Sea, island of Sylt (North Sea). Iron coupons were bound with threads to the device and buried for three months at >20 cm depth in anoxic sediment. Photographed blank and corroded coupon are not identical.

D. Corrosion crust (with sand grains), and eroded metal (after crust dissolution).

E. Developed sulfide (from sulfate consumption) after six months in serial dilutions (three in parallel) with native sediment (2 g, wet mass) from the same habitat. The line indicates sulfide expected solely by consumption of H_2 formed from iron and seawater (based on independently measured H_2-formation rates and experiments with merely H_2-scavenging SRB).

After selective crust removal, severe metal loss was evident (Fig. 1B). In the present experiments, strain IS5 was more corrosive than strain IS4, whereas in the initial physiological characterization (Dinh *et al*., 2004), the latter was more corrosive. This may be due to the higher tolerance of strain IS4 to the significantly increasing *pH* in the previous incubations. 'Conventional' SRB (control strains), which were *Desulfopila inferna* (a phylogenetic relative of strain IS4; Gittel *et al*., 2010), and *Desulfovibrio* strain HS3 (an effective scavenger of H_2 isolated in this study), showed essentially no signs of iron corrosion within the incubation period. Iron in these control cultures was not more affected than in sterile incubations (Fig. 1A and B; Fig. S3). The inability to make more efficient use of iron was not due to sensitivity towards Fe^{2+}-ions. The control strains were able to scavenge H_2 formed from iron and water (Eq. 2) below detection limit (40 ppmv) and grew readily in the presence of iron if H_2 was supplied externally (Fig. S4).

Localization of corrosive cells, and determination of crust conductivity

If the pronounced corrosion is due to direct electron uptake by SRB, cells must be always electrically connected to their metallic substrate. This could be possible by direct attachment to the metal. However, such localization would implicate increasing coverage by the forming hard corrosion crust and cut-off from the medium which supplies sulfate and counteracts the strongly alkalizing effect of iron oxidation (Eq. 5). Progressive utilization of metallic iron despite coverage by crust would be possible if active cells would colonize the medium-exposed crust surface, and if the crust would be electrically conductive.

Indeed, virtually no planktonic (free-living) cells could be observed, and scanning electron microscopy revealed a densely colonized crust surface in the corrosive cultures of strains IS4 or IS5. Colonized areas of the structurally heterogeneous crust contained the element S in addition to Fe, C, and O (details in Fig. 2), as revealed by energy-dispersive X-ray spectroscopy (EDX) of the uppermost (*c*. 5 µm) crust. Sulfur-free patches were never colonized.

Crust conductivity was evaluated as follows. Iron granules employed in previous cultivation (Dinh *et al*., 2004) tended to be cemented by the developing crust. This feature opened a simple way to measure conductivity of the crust in a non-invasive manner if the precipitate was allowed to cement two iron coupons fixed at defined distance and connected to monitoring wires protruding the stopper of the anoxic flask (Fig. 3, Fig. S5). The mounted coupons were only partly immersed so as to keep iron other than the slot-forming part outside

of the medium. The conductivity of the biogenic crust measured at a voltage (< 0.2 V; DC) far below that for water electrolysis was around 50 S m^{-1} (Fig. 3, Tables S3 and S4).

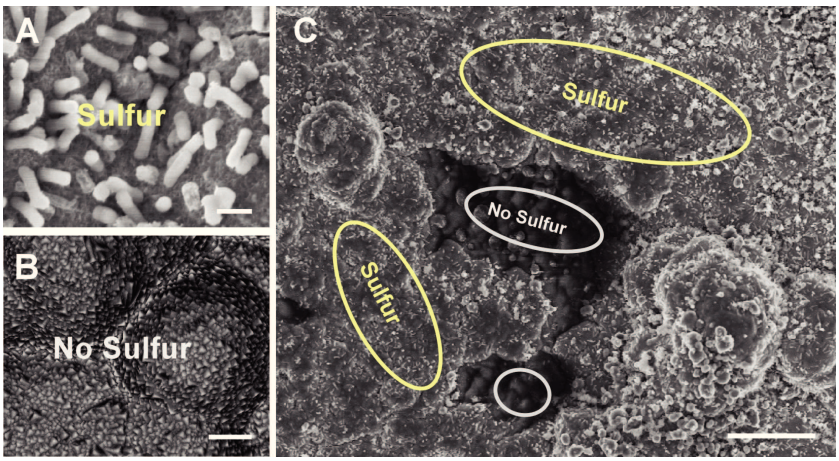

Fig. 2. X-ray microanalysis (EDX) of precipitate surface in a corrosive culture of strain IS4.
A. Site with microbial colonization (Bar, 1 µm).
B. Site without microbial colonization (Bar, 1 µm).
C. Both sites in the same field of view (Bar, 20 µm). Surface-attached cells of strain IS4 co-localize with the element S. No cells can be detected at S-free patches. Both sites contain the elements Fe, C and O. Cell-free sites contain in addition Mg and Ca.
Thirty point spectra at 10 kV were collected for each area. Resolution (lateral and vertical), 3–5 µm.

Bulk composition and surface structures of biogenic corrosion crust

The bulk composition of the crust formed by strain IS4 was analyzed quantitatively by combining EDX, X-ray diffraction (XRD), inductively coupled plasma optical emission spectroscopy (ICP-OES), and infrared spectroscopy. This revealed siderite ($FeCO_3$) and amorphous ferrous sulfide at the expected ratio (Eq. 5; Table 1), and additional co-precipitated minerals such as calcite ($CaCO_3$).

Figure 4 shows various images of the corrosion crust or coupon surface. On the crust covering coupons in cultures with strongly increased *pH* (as often observed in small culture volumes), 'pustule'-like elevations appeared after several weeks of incubation (Fig 4C, insert). The iron located underneath such 'pustules' exhibited a pronounced pitting area, as visualized upon crust removal (Fig. 4C). Strikingly shaped microscopic structures emerged on top of such 'pustules' at $pH \geq 9$. In such cultures, the otherwise irregular crust exhibited round crater- or chimney-like structures (Fig. 4D–H, Figs. S6–S8). Various growth stages of these structures were observed (Fig. 4).

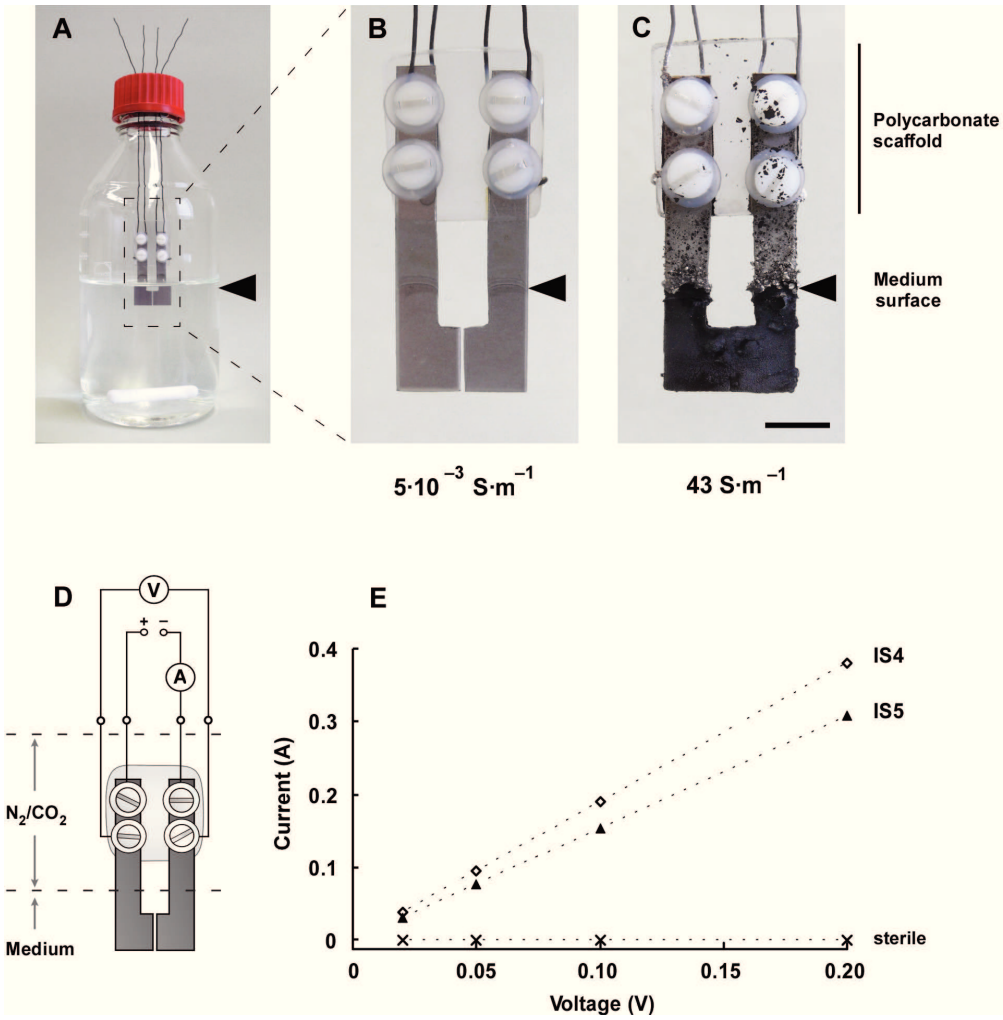

Fig. 3. Determination of the conductivity of the corrosion crust.
A. Anoxic bottle (600 ml medium) with two specially shaped fresh iron coupons
B. Coupons after three weeks of incubation in sterile medium.
C. Coupons after three weeks of incubation in medium with strain IS4. Bar, 1 cm.
D. Scheme of the arrangement with voltage control and current measurement through separate circuits.
E. Linear response of current to (non-electrolytic) voltage (0.05 − 0.2 V; DC).

Field study of iron corrosion in marine sediment

To examine as to which extent the metallic iron used in laboratory experiments undergoes corrosion in a natural environment with sulfate reduction, iron coupons were buried in the dark (anoxic) part of a silty marine mud flat (Wadden Sea, island of Sylt, Germany) at *c.* 20 cm below the surface. Recovery was ensured by fixation *via* threads to a T-shaped positioning device (Fig. 1C). The coupons retrieved after three months were covered by thick black crusts (Fig. 1D). Their enormous thickness was largely due to sedimentary minerals (e.g., sand) cemented with the corrosion crust. Again, a characteristic crust composition of siderite and amorphous iron sulfide (Table 1) as well as surface pitting and mass or thickness loss of the metal were evident (up to 0.26 mm Fe^0 yr^{-1}; Fig. 1D).

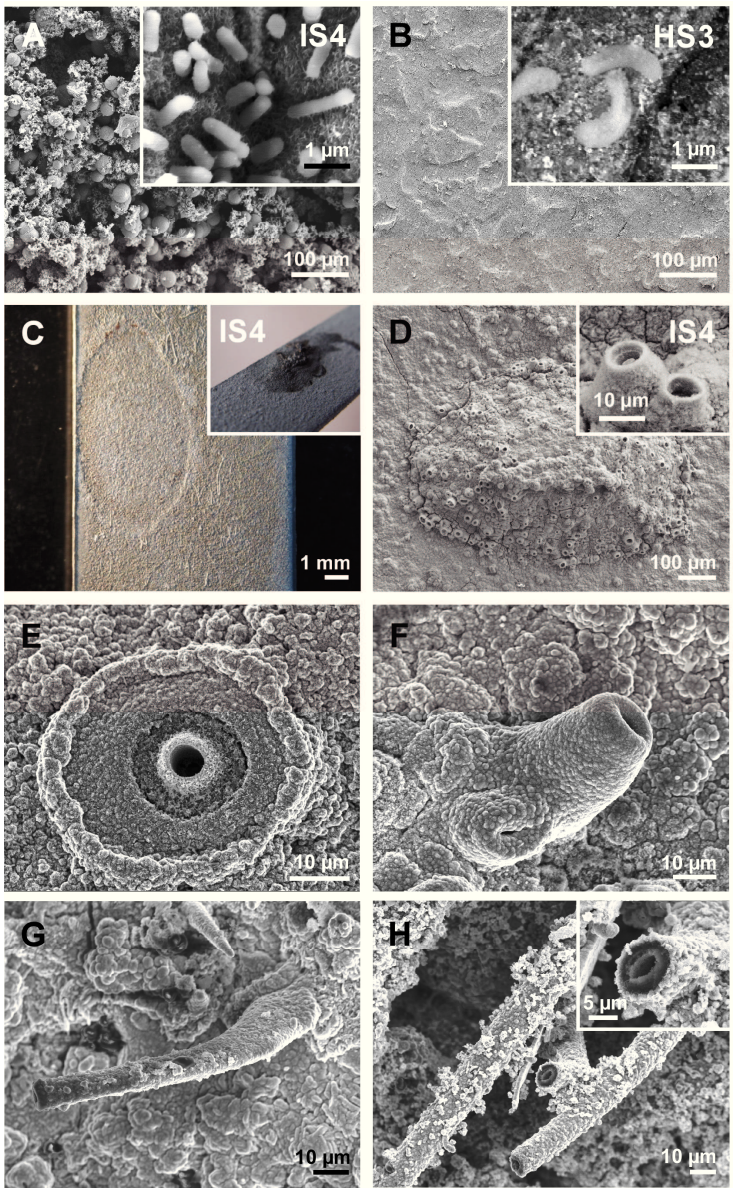

Fig. 4. Scanning electron micrographs of surface colonization and formed micro-chimneys.
A. Cells of strain IS4 on corrosion crust after three months.
B. Cells of non-corrosive hydrogenotrophic SRB control strain HS3 on slightly corroded metal surface after three months.
C. Anodic iron dissolution (crust removed) underneath a 'pustule' (insert) formed by strain IS4 at high *pH* (≈ 9; Fig. 5C).
D. 'Pustule' with short micro-chimneys (magnified in insert) in the crust.
E. Micro-chimney developing from a crater-like structure.
F. Short micro-chimney.
G. Long micro-chimney (IS4).
H. Long micro-chimney (magnified in insert) in an alkalizing corrosive enrichment.

In addition, the natural abundance of SRB with corrosive potential was estimated *via* dilution series in anoxic tubes with iron coupons as the sole electron donor. The examined sediment sample was taken from the same site before the coupons were buried, viz. there was

no artificial pre-enrichment of SRB with metallic iron. Development of sulfate reduction to a higher extent than would be possible by mere scavenging of chemically formed H_2 (known from sterile control incubations) indicated corrosive SRB at numbers of more than 10^7 cells per g wet sediment (Fig. 1E).

Table 1. Analysis of corrosion products of iron coupons from cultures of strain IS4, and from burial in permanently anoxic sulfidic marine sediment (Sylt, North Sea).

	Fe^0 with strain IS4[a]		Fe^0 buried in sediment[b]		
Element (by mass%)[c]					
Fe	29.7	28.0	24.9	21.3	19.8
S	3.9	4.0	2.9	3.0	2.6
C	6.3	6.5	1.9	2.8	2.1
Si	-	-	15.0	14.8	18.3
Ca	8.4	9.6	0.7	1.1	1.1
Mg	2.1	2.2	0.4	0.6	0.5
O[d]	46.9	47.2	51.8	52.3	52.1
Other[e]	2.7	2.5	2.4	4.1	3.5
Parameter					
$q_{FeS/Fe(II)}$[f]	0.23	0.25	0.20	0.24	0.23
$q_{EMIC/MIC}$[g]	**0.99**	**0.97**	**1.03**	**0.98**	**0.99**
Detected by XRD[h]	Siderite, calcite		Quartz, siderite		

a. Corrosion products from two cultures of strain IS4 on iron without exogenous (organic) growth substrate.
b. Corrosion products from three environmental samples. Homogenized ground sample was sieved (150 µm mesh) to remove coarse sand grains.
c. Elements detected in corrosion products by EDX. Quantitative analysis (weight percent) was achieved by infrared spectroscopy for elements C and S. The remaining elements were quantified by ICP-OES.
d. Oxygen was calculated as the remaining fraction in corrosion products.
e. Sum of other quantified elements. Fe^0 with strain IS4 (rows, from left to right): 2.7 and 2.5% P; Fe^0 buried in sediment: 1.2, 2.5 and 1.7% Al, 0.6, 0.8 and 0.9% K, 0.6, 0.8 and 0.8% Na; 0, 0 and 0.1% P.
f. Molar ratio ferrous sulfide to total ferrous iron ($n_{FeS}/n_{Fe(II)}$) in corrosion products.
g. Share of EMIC in total microbial corrosion (Eq. 18).
h. Crystalline phases detected by X-ray diffraction.

Discussion

In the present study, the ability of SRB to utilize metallic iron lithotrophically and thus cause corrosion was even more pronounced than previously expected (Fig. 1; Dinh *et al.*, 2004). Apparently, only particular species of SRB can effectively exploit iron as an electron donor for fuelling their energy metabolism through sulfate reduction, so that distinction between corrosive and non-corrosive ('conventional') strains or species is justified. Corrosive SRB are not necessarily related on the basis of 16S rRNA-based phylogeny; they branch within

distinct lineages of SRB (Dinh *et al*., 2004). Nevertheless, more extended comparative corrosion studies are needed to clarify whether corrosiveness is a genetically fixed trait, or whether also 'conventional' strains, for instance close relatives of strains IS4 and IS5, can gradually adapt to utilize and corrode iron if exposed to the metal over years. The ability to utilize iron directly as an electron donor for sulfate reduction primarily urges upon an understanding of the underlying mechanisms.

Towards an understanding of the corrosion mechanisms

Principal physico-chemical considerations as well as previous (Dinh *et al.*, 2004) and present incubation experiments together with the measured electrical conductivity of the corrosion crust are strongly in favor of the EMIC hypothesis, that is direct electron gain for sulfate respiration from the metal *via* the crust.

The reduction of H^+-ions (strictly, H_3O^+-ions) by Fe^0-derived electrons on the metal surface is a par excellence example of a kinetically 'impeded', slow electrochemical reaction. Availability of H^+-ions at the metal surface and combination of primarily formed atomic hydrogen ($e^- + H^+ \rightarrow H_{(adsorbed)}$) to H_2 are commonly understood as the kinetic 'bottle neck' that also explains the high negative electrochemical overpotential (difference between potential during net reaction and equilibrium potential under the given conditions) of electrochemical H_2-formation on iron (Bockris and Reddy, 1970; Hamann *et al*., 2007). Microbial scavenge of H_2, viz. a product behind the 'bottle neck', is therefore not expected to accelerate the primary iron dissolution (Fig. S1). This is in accordance with experimental findings in evaluations of the 'cathodic hydrogen' theory of MIC (Costello, 1974; Hardy, 1983; Dinh *et al.*, 2004). Some corrosive strains even formed significantly higher amounts of H_2 than sterile incubations during the initial incubation phase with metallic iron. Deposition of some black FeS at the glass walls of the bottles indicated that a part of the SRB population grew distantly from the coupons with such biologically released H_2. The assumption of a direct electron uptake by cells would not only explain the high corrosion rate of special SRB, but also the pronounced initial release of H_2. This is possibly an 'unavoidable' side reaction *via* a hydrogenase because electron uptake from freshly supplied iron may be faster than electron consumption by sulfate reduction (Dinh *et al*., 2004).

Since electrons, unlike chemical compounds such as H_2, cannot diffuse or flow through water, electron-conducting structures would be needed. On the side of the cell, these might be outer membrane and periplasmic membrane proteins investigated in various microorganisms in bioleaching of metals (Appia-Ayme *et al.*, 1999; Auernik *et al.*, 2008), extracellular

iron(III) reduction or microbial fuel cells (Butler *et al.*, 2010). Between cells and the corroding iron, which is being covered by a steadily growing sulfidic corrosion crust, the latter itself is envisaged as the electrical mediator. Metal sulfides are long-known semiconductors (Braun, 1875; Pearce *et al.*, 2006), and some earlier biocorrosion models based on H_2 production and consumption hypothesized about a participation of semiconductive FeS (Booth *et al*., 1968; King and Miller, 1971) in abiotic H^+ reduction.

The undisturbed corrosion crust in cultures of strains IS4 and IS5 indeed exhibited a conductivity of around 50 S m^{-1} (A V^{-1} m^{-1}); this is even higher than that of many typical semiconductors (e.g. pure silicon, $1.6 \cdot 10^{-3}$ S m^{-1}; Table S5) or microbial biofilms with nanowires allowed to form between gold sheets mounted in cultures of *Geobacter sulfurreducens* (0.5 S m^{-1}; Malvankar *et al.*, 2011). Conductivity of the heterogeneous corrosion crust must be due to contained iron sulfides because $FeCO_3$ and $CaCO_3$ are essentially insulating minerals (10^{-10} and 10^{-14} S m^{-1}, respectively; Table S5). This was confirmed in the present study by a conductivity test of siderite mineral (Fig. S9). Even though the measured biocorrosion rates of 0.71 mm Fe^0 yr^{-1} were high and technologically relevant, the corresponding current density of 0.61 A m^{-2} (Appendix S1) would need a voltage (potential difference) of only $V = 1.2 \cdot 10^{-4}$ V across a 1 cm crust. The calculated equilibrium potential at the corroding iron surface and the zone of sulfate reduction is around –0.60 and –0.23 V, respectively, viz. ΔE = 0.37 V (couples $FeCO_3/Fe^0$, and SO_4^{2-}/FeS, respectively; Appendix S1). Hence, there is significant leeway for the 'self-adjusting' potential difference driving the corrosion current through the crust. Crust conductivity is apparently not a rate-limiting factor. The model of corrosive SRB gaining electrons through semiconductive ferrous sulfide is further corroborated by the electron microscopic finding of cells attached mostly to the sulfide-rich islands within the predominantly carbonaceous structure (Fig. 2).

Electrons can only flow to cells if the crust also allows an equivalent ion flow *via* aqueous 'bridges' (maintenance of electroneutrality). These may be tiny interstices or fissures. An apparent, striking ion bridge, also strongly supporting the model of transcrustal electron flow, emerged at $pH \geq 9$. In such cultures, the otherwise irregular crust exhibited round crater- or chimney-like structures (Fig. 4D–H, Figs S6–8). Their formation is presently explained by a lowered, crust-preventing *pH* inside due to slightly acidic Fe^{2+}-ions ($Fe^{2+} + H_2O \rightleftarrows Fe(OH)^+ + H^+$; pK_a = 8.8) and precipitation of Fe^{2+} as soon as it enters the high-*pH* carbonate-containing medium (Fig. 5C, Fig. S10).

In conclusion, anaerobic corrosion caused by the direct, lithotrophic mode of iron utilization according to equation (5) can be only explained by direct electron uptake (Fig. 5), i.e. real occurrence of the electrochemical half-reaction

$$8\,e^- + SO_4^{2-} + 9\,H^+ \rightarrow HS^- + 4\,H_2O \qquad (6)$$

($E°'_{av}$ = –0.218 V, average) coupled to iron dissolution (Eq. 1). Hence, the lithotrophic, direct corrosion is always EMIC.

Comment on direct corrosion by methanogenesis

There is first evidence that also special methanogenic archaea obtained through enrichment with metallic iron as the only source of reducing equivalents can bypass the slow abiotic H_2 formation on iron in water by faster direct use of the electrons (Eq. 1) according to $8\,e^- + HCO_3^- + 9\,H^+ \rightarrow CH_4 + 3\,H_2O$ (Dinh *et al*., 2004; Mori *et al*., 2010; Uchiyama *et al*., 2010). Here, the net reaction, $4\,Fe^0 + 5\,HCO_3^- + 2\,H_2O \rightarrow 4\,FeCO_3\,(c) + CH_4\,(g) + 5\,HO^-$ [$\Delta G°'$ = –35.3 kJ (mol Fe)$^{-1}$], does not lead to a conductive precipitate. One may speculate that in this case cell-metal contact must be sustained so that hindrance by crust coverage may become obvious during long-term incubations (which have not been carried out so far). Nevertheless, the process may play a role in MIC because methanogenic archaea may take advantage of electroconductive FeS precipitated by co-occurring sulfate reduction. In axenic laboratory cultures, there is some FeS precipitation by sulfide added as reductant.

Biosynthesis during direct iron corrosion by sulfate reduction

An understanding of the properties of the precipitate formed during corrosion also requires knowledge of the proportion of formed cell mass that may be embedded. Because there is presently no convenient method for determining cell mass in the solid corrosion crust, its organic content was estimated. According to the principle of bifurcate substrate flow in every chemotrophic organism, the amount (e.g. in mol or mmol) of total iron oxidized in cultures of SRB performing EMIC, n_{FeEMIC}, is the sum of the amount oxidized catabolically by sulfate reduction, $n_{FeCatab}$, and the amount oxidized due to the anabolic need of electrons, n_{FeAnab}, i.e.

$$n_{FeEMIC} = n_{FeCatab} + n_{FeAnab} \qquad (7)$$

(basic scheme in Fig. S11).

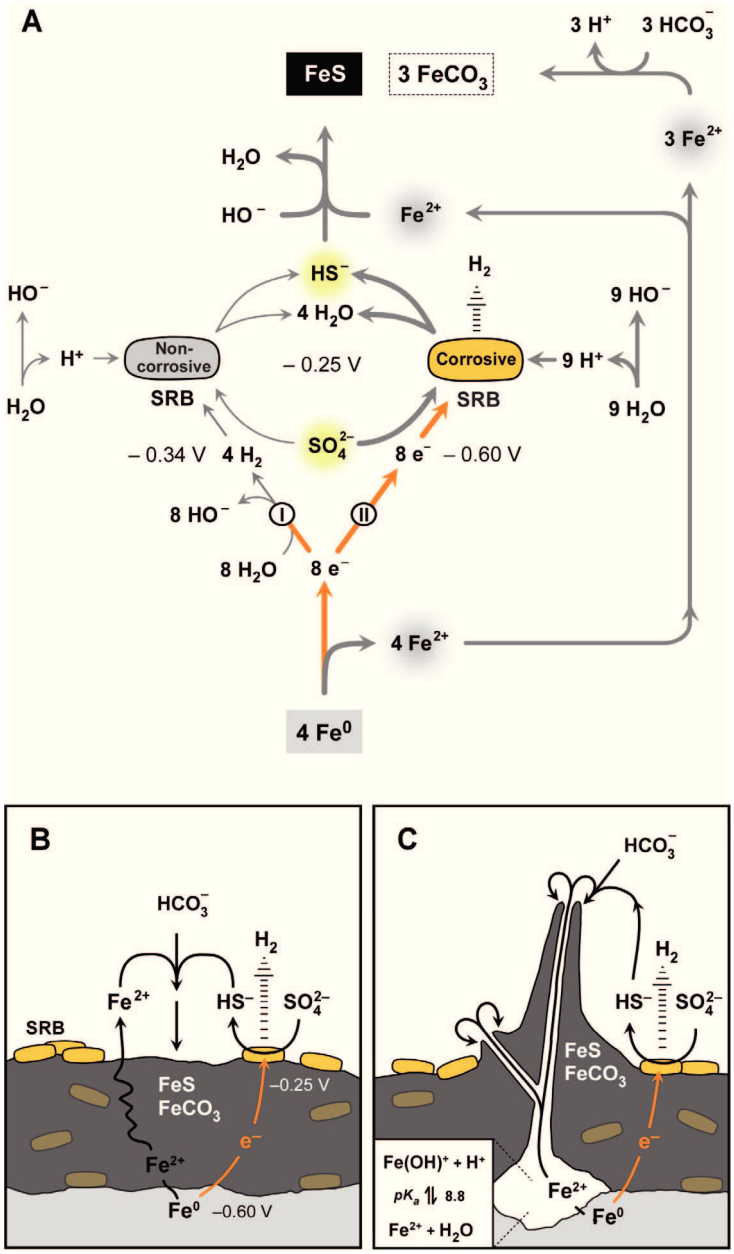

Fig. 5. Stoichiometry and topology of lithotrophic corrosion.

A. Stoichiometry of iron dissolution and channeling of electrons *via* H_2 (I; classical scheme) or directly (II; new model) into sulfate reduction. Bold lines indicate the faster electric 'bypass'. Redox potentials are indicated for real conditions (see Appendix S1). Direct electron utilization provides a higher metabolic driving force (voltage: ΔE = 0.35 V, compared to 0.09 V *via* H_2 of assumed ≈40 ppmv). Fe^{2+} not precipitated as sulfide may enter solution or precipitate with naturally wide-spread inorganic carbon as $FeCO_3$.

B. Electron flow through the crust to attached cells at *pH* = 8 (simplified, non-stoichiometric). Crust may contain co-precipitated calcium and magnesium carbonate, and/or cemented sand. The equivalent ion flow may occur *via* aqueous interstices (not depicted).

C. Build-up of chimney-like ion bridges at $pH \geq 9$ (reactions are essentially as in (B), however, there are pronounced spots of anodic iron dissolution). A significant *pH* gradient (low inside, high outside) results in Fe(II) precipitation at the rim, thus causing chimney growth. Schemes include the possibility of H_2 release (that may foster remote bacterial cells) due to an imbalance between electron uptake and sulfate reduction. Participation of possibly buried (encrusted) cells in sulfate reduction and H_2 release is unknown

If EMIC is the only corrosion process, n_{FeEMIC} is identical with the loss of metallic iron, $n_{\Delta\mathrm{Fe}(0)}$, and n_{FeCatab} is fourfold higher than the amount of sulfate being reduced (Eq. 5), viz. $n_{\mathrm{FeCatab}} = 4\, n_{\mathrm{SR}}$. Hence, anabolic iron oxidation can be expressed as the difference of two measurable parameters according to

$$n_{\mathrm{FeAnab}} = n_{\Delta\mathrm{Fe}(0)} - 4\, n_{\mathrm{SR}}. \tag{8}$$

With this, also a partition coefficient (quotient) or contribution of anabolic iron oxidation to total iron oxidation during EMIC can be formulated as

$$q_{\mathrm{Anab}} = \frac{n_{\mathrm{FeAnab}}}{n_{\mathrm{FeEMIC}}} = \frac{n_{\Delta\mathrm{Fe}(0)} - 4\, n_{\mathrm{SR}}}{n_{\Delta\mathrm{Fe}(0)}} \tag{9}$$

Iron loss is equivalent with ferrous iron formation, i.e. $n_{\Delta\mathrm{Fe}(0)} = n_{\mathrm{Fe(II)}}$. The resulting n_{FeAnab} (Eq. 8) can be translated into formed biomass *via* assimilation equations if an elementary bulk composition and hence a formula mass ('molecular' mass) of bacterial dry mass is assumed. The assimilation equations expresses how much cell mass, m_{Bio} (e.g. in g or mg), is formed per amount of iron used for the anabolism, viz. they allow to formulate an anabolic yield coefficient,

$$Y_{\mathrm{Anab}} = \frac{m_{\mathrm{Bio}}}{n_{\mathrm{FeAnab}}}. \tag{10}$$

Here we used the simplified bulk formula $C_4H_8O_2N$ (van Dijken and Harder, 1975; comments in Widdel and Musat, 2010) with *'M'* = 102.1 g mol^{-1}. Synthesis of cell carbon may occur with CO_2 alone (lithoautotrophic growth; strain IS4), or require in addition an organic substrate such as acetate (lithoheterotrophic growth; strain IS5). The resulting assimilation equations are

$$17\ \mathrm{Fe^0}\ (\equiv 17\ \mathrm{Fe^{2+}} + 34\ \mathrm{e^-}) + 25\ \mathrm{HCO_3^-} + 2\ \mathrm{NH_4^+} + 3\ \mathrm{H_2O}$$

$$\rightarrow 17\ \mathrm{FeCO_3} + 2\ \mathrm{C_4H_8O_2N} + 23\ \mathrm{HO^-} \tag{11}$$

$$Y_{\mathrm{Anab(aut)}} = 12.0\ \mathrm{g\ (mol\ Fe^0)^{-1}},$$

and

$$19\ Fe^0\ (\equiv 19\ Fe^{2+} + 38\ e^-) + 8\ CH_3COO^- + 27\ HCO_3^- + 6\ NH_4^+ + H_2O$$

$$\rightarrow 19\ FeCO_3 + 6\ C_4H_8O_2N + 29\ HO^-, \quad (12)$$

$$Y_{Anab(het)} = 32.2\ g\ (mol\ Fe^0)^{-1},$$

for autotrophic and heterotrophic growth, respectively. The latter equation is based on the observation that *c*. ⅔ of cell carbon in SRB is derived from acetate and *c*. ⅓ from bicarbonate (Sorokin, 1966; Badziong and Thauer, 1978). Through such theoretical assimilation equations and equation (8), the expected biomass can be calculated from n_{FeAnab} as

$$m_{Bio} = Y_{Anab}\ n_{FeAnab} = Y_{Anab}\ (n_{\Delta Fe(0)} - 4\ n_{SR}). \quad (13)$$

The mass of the minerals (FeS, $FeCO_3$, co-precipitated $CaCO_3$ and possibly $MgCO_3$) precipitated during lithotrophic corrosion, m_{Min}, can be calculated from the same measurable parameters as n_{FeAnab} (Eq. 8), viz. from $n_{\Delta Fe(0)}$ (or $n_{Fe(II)}$) and n_{SR} (Appendix S1). This further allows to express the biomass content as a partition coefficient (quotient) relating the biomass, m_{Bio}, to the total mass of precipitated crust, $m_{Min} + m_{Bio}$. For this, the formulas

$$q^m_{Bio(aut)} = \frac{m_{Bio(aut)}}{m_{Min} + m_{Bio(aut)}} \leq \frac{n_{\Delta Fe(0)} - 4\ n_{SR}}{10.66\ n_{\Delta Fe(0)} - 6.33\ n_{SR}} \quad (14)$$

and

$$q^m_{Bio(het)} = \frac{m_{Bio(het)}}{m_{Min} + m_{Bio(het)}} \leq \frac{n_{\Delta Fe(0)} - 4\ n_{SR}}{4.60\ n_{\Delta Fe(0)} - 4.87\ n_{SR}}, \quad (15)$$

can be derived (Appendix S1) for autotrophic and heterotrophic growth, respectively (again with $n_{\Delta Fe(0)} = n_{Fe(II)}$). They are applicable if EMIC is the only process of corrosion, as in our cultures, and if one assumes complete precipitation of ferrous iron (and variable precipitation of $Ca/MgCO_3$).

Strains IS4 and IS5 corroded $n_{\Delta Fe(0)}$ = 4.31 and 9.86 mmol Fe^0, respectively, during reduction of n_{SR} = 0.95 (± 0.06) and 2.14 (± 0.08) mmol SO_4^{2-}, respectively. Hence, the amounts accounting for biosynthesis (Eq. 8) of strains IS4 and IS5 were n_{FeAnab} = 0.51 and 1.3 mmol Fe^0, respectively, which yields the following values for partition of anabolic in total iron oxidation (Eq. 9), and for the biomass content of the crust (Eq. 14, 15):

IS4: $q_{Anab(aut)} = 0.12$ (12%); $q_{Bio(aut)} \leq 0.013$ (1.3%) (16)

IS5: $q_{Anab(het)} = 0.13$ (13%); $q_{Bio(het)} \leq 0.037$ (3.7%) (17)

These results indicate that the bulk of electrons is channelled into the catabolism (sulfate reduction), as common in the strictly anaerobic SRB, and that the corrosion crust is essentially inorganic, in agreement with its hard, mineral-like appearance. The corrosion crust thus profoundly differs from typical biofilms that are largely constituted of cells and an organic matrix.

Practical considerations

Protection of iron against corrosion by alloying or coating is technically and economically not possible at any extent. For instance, the most important alloying metal, chromium, is produced at a 48-fold lesser extent than iron (U.S. Geological Survey, 2011; data for 2009). We therefore expect that advances in the analysis and control of MIC *in situ* will remain a relevant issue.

A long-term goal would be the design of specific counter measures based on detailed understanding of the environmental conditions and mechanisms leading to MIC. Such a 'causative' approach is confronted with a complexity of chemical conditions (e.g. availability of electron acceptors or electron donors in addition to metallic iron) and chemical, electrochemical and microbial reactions in MIC. The most promising research strategy is, in the opinion of the authors, an experimental 'dissection' into individual and elementary processes for later synopsis. In the previous (Dinh *et al*., 2004) and present study, we focused on lithotrophic growth with metallic iron as the only electron donor under strictly anoxic conditions in the presence of sulfate as electron acceptor. Further, more comprehensive microbiological investigations would have to consider contributions to corrosion for instance by lithotrophic methanogenic archaea (Dinh *et al*., 2004; Mori *et al*., 2010; Uchiyama *et al.*, 2010) if sulfate is limiting, or by CMIC due to organotrophic growth of SRB in organic-rich environments. Among the involved inorganic compounds, iron sulfides with their delicate, variable chemical and electrochemical properties are of central interest. They can not only mediate electron flow. Under certain, high-sulfide conditions iron sulfides apparently protect the underlying metal against further rapid corrosion (Smith and Miller, 1975; Lee *et al.*, 1995). Another, different role has been attributed to iron sulfides under intermittent anoxic-oxic conditions where corrosion can be particularly severe. This has been explained mainly by

the reactivity of iron towards chemical oxidation products of ferrous sulfide (Jack, 2002; Hamilton, 2003; Beech and Sunner, 2007).

In view of the present limited understanding of MIC *in situ*, also recommendation of control measures is presently limited. As long as MIC in a particular situation is largely CMIC, prevention would be possible if the organic nutrient of the anaerobic bacteria can be identified and eliminated. If MIC is essentially EMIC, avoidance of sulfate-containing water would be a causative solution. Extended *in vitro* and pilot studies may clarify as to which extent an addition of nitrate, which is applied to control biogenic H_2S (souring) in petroleum reservoirs (Reinsel *et al*., 1996; Gieg *et al*., 2011), is also promising for controlling CMIC and EMIC (Hubert *et al*., 2005; Schwermer *et al*., 2008).

Despite the complexity of anaerobic corrosion processes *in situ*, the presently examined strains IS4 and IS5 are envisaged as representatives of the key players in MIC. These strains caused corrosion rates well matching those reported for the destruction of industrial iron structures in permanently anoxic aqueous surroundings (Table S1). Also, the rates of direct corrosion by strains IS4 and IS5 are as high as rates of chemical iron destruction by sulfide (Lee *et al.*, 1995; Jack, 2002; Beech and Sunner, 2007; Table S1). This raises interest in an estimate of the contribution of EMIC in total MIC (EMIC plus CMIC by organotrophically formed sulfide) in cases of corrosion *in situ*. Because CMIC (Eq. 4) leads exclusively to sulfidic iron, whereas EMIC leads in addition to non-sulfidic (usually carbonaceous) iron, their measurable ratio in the crust of a corroded construction may be used for estimating the extent of EMIC. Such extent is quantitatively expressed as the quotient of the amounts (mol) of iron lost by EMIC, n_{FeEMIC}, and iron lost totally by MIC, n_{FeMIC}, and thus defined as $q_{\mathrm{EMIC}} = n_{\mathrm{FeEMIC}}/n_{\mathrm{FeMIC}}$. Assuming that all ferrous iron in the crust results from metal corrosion, $n_{\mathrm{FeMIC}} = n_{\mathrm{Fe(II)}}$, so that $q_{\mathrm{EMIC}} = n_{\mathrm{FeEMIC}}/n_{\mathrm{Fe(II)}}$. Further calculation so as to substitute the unknown n_{FeEMIC} and introduce the measurable amount of precipitated sulfide, n_{FeS}, leads to the formula (calculation in Appendix S1)

$$q_{\mathrm{EMIC}} = \frac{n_{\mathrm{FeEMIC}}}{n_{\mathrm{FeMIC}}} = \frac{4\,(1 - n_{\mathrm{FeS}}/n_{\mathrm{Fe(II)}})}{3 + q_{\mathrm{Anab}}}\,. \qquad (18)$$

Hence, besides analysis of sulfidic and total ferrous iron in the crust, only the assumption of a q_{Anab} value (see above) is needed. For approximate calculation, q_{Anab} may be omitted (because $q_{\mathrm{Anab}} << 3$). Still, such treatment is only applicable for anoxic conditions and absence of processes other than sulfate reduction, for instance methanogenesis (Dinh *et al.,* 2004; Mori *et al.*, 2010; Uchiyama *et al.*, 2010), and absence of secondary conversion of $FeCO_3$ to FeS by

subsequent sulfidic events. Analysis of the crust on the coupons recovered from the field study revealed $n_{FeS}/n_{Fe(II)}$ = 0.20 to 0.24. By assuming, for convenience, $q_{Anab} \approx 0.1$, we obtain q_{EMIC} = 0.98 to 1.03 (theoretically, according to Eq. 18, q_{EMIC} always ≤ 1). This suggests that corrosion under the conditions prevailing at the studied marine sediment site was indeed only EMIC, viz. due to SRB capable of direct electron uptake. Such crust analysis (von Wolzogen Kühr and van der Vlugt, 1934; Spruit and Wanklyn, 1951), with awareness of its limits in view of additional processes, may be a more promising approach for understanding particular case of corrosion than, for instance, the traditional analysis of aqueous phases (e.g. produced waters in oil fields). Because EDX as a semi-quantitative technique (Goldstein *et al.*, 2003) is not applicable for determining mineral ratios in the crust, chemical analysis is the technique of choice.

A complementary microbiological analysis of instances of MIC would have to examine the presence of SRB with the capability for EMIC, as represented by strains IS5 and IS4. Such SRB may have been overlooked in microbiological monitoring studies of MIC which employ diagnostic methods based on fast growth with organic nutrients such as lactate and samples from water phases. The presently investigated corrosive strains grow relatively slowly and show pronounced surface attachment, so that they are easily out-competed in organic-rich diagnostic media by naturally wide-spread, rapidly growing planktonic SRB. Hence, development of convenient media with Fe^0, inocula scraped off from surfaces, and longer than conventional incubation times should be envisaged.

If molecular, nucleic acid-based analyses of damages by microbial corrosion are of interest, again focus on the microorganisms in precipitated products rather than in aqueous phases is recommended for future studies (Skovhus *et al*., 2011). Still, molecular detection of directly corrosive SRB by long-established markers such as 16S rRNA or its genes are intrinsically limited. Already the first investigations into direct corrosion showed the phylogenetic unrelatedness of corrosive SRB (Dinh *et al.*, 2004).

Physiological and ecological significance of the ability for iron corrosion

The specific ability to utilize metallic iron as an electron donor is a physiologically striking capability, the ecological significance of which is presently unknown. Apart from rare cases (meteorites, seldom rocks from deep subsurfaces; Deutsch *et al*., 1977; Haggerty and Toft, 1985), metallic iron has been introduced into the environment on a large scale only by industrialization, viz. very ‘recently’ from an evolutionary point of view. Yet, counting of corrosive SRB *via* dilution series with anoxic sediment and metallic iron revealed several 10^7

cells per gram wet mass (Fig. 1E), despite obvious absence of man-made iron constructions. One may speculate that corrosiveness represents the promiscuous use of a long-existing physiological trait for environmental electron uptake ('electrotrophy'; Lovley, 2011) that is suited to also exploit the anthropogenically introduced metal as substrate. Normally, SRB with such trait may be involved in biogenic electron flow through sulfidic marine sediments and other ecosystems (Nakamura *et al*., 2009; Nielsen *et al.*, 2010; Kato *et al*. 2011). Also, electron gain in direct contact with other bacteria with a surplus of catabolic electrons (Summers *et al.*, 2011; Lovley, 2011) or from strongly reducing, reactive mineral surfaces such as pyrite being formed from ferrous sulfide and free sulfide ($FeS + H_2S \rightarrow FeS_2 + H_2$ / $FeS_2 + 2H^+ + 2e^-$; Wächtershäuser, 1992) can be envisaged as the genuine role of the electron uptake system underlying direct corrosion. Fig. 6 summarizes a present hypothesis of the *in situ* function of SRB with the ability for electron uptake from external sources. Such SRB may represent a so far overlooked part of the anaerobic population. Still, more extended examinations (such as the above dilution series) of their abundance at various natural sites and physiological studies are needed to unravel their real significance in anaerobic mineralization.

From the viewpoint of mechanistic evolution, merely electron-donating and electron-accepting reactions can be regarded as simple or even primeval. Mere electron transfer does not require extra catalytic mechanisms like cleavage of C–H bonds and rearrangement of bound atoms. With many simple electron donors and acceptors, electron transfer takes place without specific catalysis simply according to redox potentials. This is a classical principle in biochemistry, for instance if electron accepting or donating dyes such as viologens or hexacyanoferrates are used to react unspecifically with various redox proteins. In the cell, cofactors that can transfer electrons as such would be even critical in their free, dissolved form because of unspecific redox reactions. Their reducing or oxidizing power must be controlled for instance by embedding in a protein (heme, FeS clusters, flavins) or by restriction to the lipophilic cytoplasmic membrane (quinones). Outside of the cell, merely electron transferring chemical or biochemical compounds are much less critical, and their use may have been preserved since early evolution to exploit redox active or conductive substances in ecosystems.

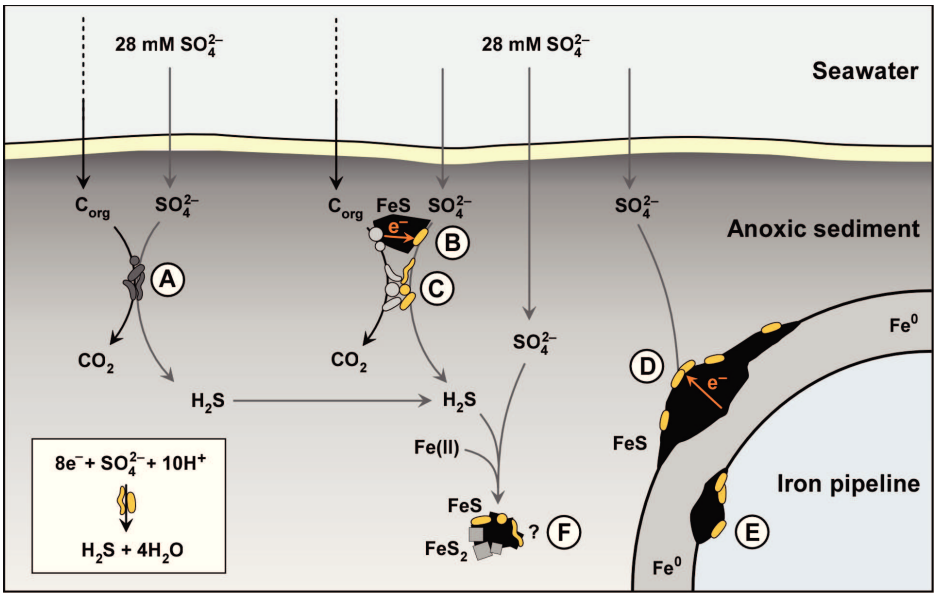

Fig. 6. Present synoptic hypotheses of the role of sulfate-reducing bacteria (SRB) capable of electron uptake from external sources in anoxic marine sediment.

A. Conventional organotrophic SRB.

B. SRB interacting *via* electroconductive ferrous sulfide with electron-donating organotrophic anaerobic microorganisms.

C. SRB interacting in direct contact with electron-donating organotrophic anaerobic microorganisms.

D. Special SRB exploit metallic iron as electron source at the outer surface of a pipeline.

E. Special SRB exploit metallic iron as electron source inside of a pipeline.

F. Speculative possibility of pyritization of FeS ($FeS + H_2S \rightarrow FeS_2 + 2\ H^+ + 2\ e^-$) as a direct electron source for sulfate reduction.

In conclusion, the study of microbial corrosion encompasses interesting mechanistic, ecological and evolutionary aspects, besides its obvious practical significance. It may become, besides microbial fuel cells (Lovley, 2006; Nealson and Finkel, 2011), microbial electrolysis cells for H_2 production from H_2O (Croese *et al*., 2011), and biogenic currents in environments (Nakamuro *et al.*, 2009; Nielsen *et al.*, 2010; Kato *et al*., 2011), a fourth topic in the developing field of 'electro-microbiology' and in this way contribute to future synoptic views.

Experimental procedures

Organisms and Cultivation

Strains IS4 and IS5, tentatively termed *Desulfopila* '*corrodens*' and *Desulfovibrio 'ferrophilus*', respectively, were re-activated from freeze-dried former cultures (Dinh *et al.,* 2004). *Desulfopila inferna* was provided by Antje Gittel [University of Bergen, Norway; (Gittel *et al.*, 2010)]. SRB with high affinity for H_2 were enriched from marine sediment with an H_2-CO_2 mixture (9/1, by volume) provided at growth-limiting rate through a silicon rubber membrane inside an anoxic cultivation device; some acetate (1 mM) was provided for cell synthesis. After two subcultures, the *Desulfovibrio* strain HS3 was isolated *via* agar dilution (Widdel and Bak, 1992).

Cultures were grown in CO_2/bicarbonate-buffered artificial seawater medium (Widdel and Bak, 1992) in butyl rubber-stoppered bottles (routinely 150 ml) under an anoxic N_2-CO_2 (9/1, by volume) headspace at 28°C. SO_4^{2-} was usually provided at 28 mM; exceptions were cultures with 5 mM SO_4^{2-} (not resulting in a noticeable decrease of the growth rate) for precise determination of its consumption. The reductant was usually Fe^0 alone. However, some big cultures (1400 ml) received also 75 µM Na_2S which shortened the lag phase. All strains except strain IS4 were supplemented with 1 mM acetate for heterotrophic cell synthesis. H_2-grown inocula were flushed with N_2-CO_2 to prevent transfer of H_2 substrate and sulfide to Fe^0 cultures. Iron specimens (mild steel EN 1.0330; >99.37% Fe) were degreased with acetone (2 min), freed from oxide layers with 2 M HCl (2 min) and washed in sterile anoxic water (2 · 20 sec). Coupons were then rapidly dried under N_2, weighed (in sterile Petri dishes) and added to cultures. The ratio of medium volume to metal surface was between 15 ml cm^{-2} (for scanning electron microscopy; coupons: 30 mm · 10 mm · 1 mm) and 600 ml cm^{-2} (for corrosion rate determination).

Strain purity was routinely checked microscopically upon growth with H_2 or lactate (+ yeast extract), and sequencing of 16S rRNA genes.

Cells of corrosive SRB in sediment were quantified as most probable numbers *via* triplicate serial 1:10 dilutions with Fe^0 as electron donor and 1 mM acetate as a carbon source. SO_4^{2-} consumption was quantified after six months of incubation at 20°C. Sterile controls were included to calculate sulfate reduction solely based on the measured abiotic H_2 formation. Marginal background sulfate reduction was measured in iron-free controls.

Processing of corroded iron coupons

Corrosion crust for analysis was (inside an N_2 chamber) scraped off the water-rinsed and dried coupons, finely ground in a mortar, and kept under anoxic N_2 until analysis to prevent secondary oxidation. Corrosion coupons for weight loss determination were freed from the crust in aqueous 2 M HCl and 0.7 M hexamethylenetetramine (hexamine). The freed iron was washed in anoxic water and dried under N_2 before weighing.

Determination of corrosion crust conductivity

Shaped and polished mild steel coupons were fixed at exactly defined distance on a polycarbonate support (Figure 2A, B). The four wires protruding the stopper of the anoxic flask (1 liter, 0.6 liter medium) for current and voltage control were also made of iron. Coupon-wire contacts were fixed with plastic screws. The device was sterilized with ethanol (2 h; dried afterwards). The lower, defined slot part was subjected to the pre-treatment of coupons described above and then immersed in artificial seawater medium (Figure 2A, B). The medium was gently stirred during incubation. For conductivity measurement before and after crust formation, the current responding to 20, 50, 100 and 200 mV was measured. The instruments connected for this purpose were a TS3022S precision current (DC) supply (Thandar Instruments), an ammeter (±0.2%, ±10 µA), and a voltmeter (±0.05%, ±10 µV). Electrical conductivity was calculated as $\sigma = I\,d/(V\,a)$; I, current; d, distance between coupons; V, voltage; a, split area (split height × coupon thickness). Additionally, current/voltage curves were recorded with alternating current (AC) from a TOE7741 (Toellner) frequency generator ($5 \cdot 10^{-3}$ – $5 \cdot 10^{4}$ Hz). For photographic documentation, the mounted coupons were transferred to anoxic water.

The specific conductivity of siderite mineral (>85% crystalline siderite with accompanying calcium and magnesium carbonates) was determined with specimens compressed ($9 \cdot 10^{8}$ Pa) to smooth pills in a type 15.011 hydraulic press (Specac Ltd). Impedance was measured *via* a 'piston electrode' (Fig. S9) connected to a Model 1286 potentiostat with a 1255B frequency response analyzer and a 1281 multiplexer (Solartron Analytical).

Field experiment

Mild steel coupons fixed by threads to a T-shaped scaffold (stainless steel; Fig. 1C) were buried during summer 2010 at 20 cm depth in silty black, anoxic sediment of the Wadden Sea (Tonnenlegerbucht, island of Sylt, Germany). Coupons recovered after three months were

immediately transferred to anoxic artificial seawater and further processed as described for other coupons.

Scanning electron microscopy

Crust-covered iron specimens were fixed with 2% (vol/vol) glutaraldehyde in anoxic artificial seawater at 4°C (12 h), washed with anoxic seawater, dehydrated with anoxic ethanol at increasing concentration (25, 50, 75, 90, 100 and again 100%, vol/vol; each step 2 min), pre-dried chemically with hexamethyldisilazane (30 min**;** Araujo *et al*., 2003), and fully dried under N_2. Scanning electron microscopy (SEM) at 5 – 15 kV was performed with a Leo 1550 FE instrument (Zeiss).

Mineral and solute analyses

For element identification, finely ground crust homogenate (see above) was compressed ($9 \cdot 10^8$ Pa) to smooth pills in a type 15.011 hydraulic press (Specac Ltd) and surface-mapped (using triplicate samples) by energy-dispersive X-ray microanalysis (EDX) at 10 kV in combination with SEM. Data were analyzed with the INCA software (Oxford Instruments). C and S were subsequently quantified after combustion (to CO_2 and SO_2, respectively) using a CS-444 infrared spectrometer (Leco). Na, Mg, Al, Si, P, K, Ca, and Fe were quantified by inductively coupled plasma optical emission spectroscopy (ICP-OES) with an IRIS Intrepid HR Duo instrument (Thermo Fisher Scientific). Si was quantified after alkaline pulping. The O-content was calculated as the remaining fraction. H (not detectable with the used instruments) is assumed to constitute a marginal fraction of the dried mineral crust.

Crystalline mineral phases in finely ground corrosion crust were identified by means of X-ray diffraction (XRD) analysis in Bragg-Brentano geometry with CuK_α radiation from 1 µm aperture in a D8 Advance diffractometer (Bruker). The 2θ angle was increased in 0.08° steps with 15 s counting time from 20 to 74.08°; the total scan time per diffractogram was 169 min. Data were analyzed with the EVA software (Bruker).

H_2 was quantified in samples withdrawn (with syringes through hypodermic needles) from the culture headspace *via* a GC-8A gas chromatograph (Shimadzu) equipped with a Porapak Q N80/100 (Machery-Nagel) column (temperature, 40 °C; carrier gas, N_2) and a thermal conductivity detector.

SO_4^{2-} in filtered (0.45 µm pores) FeS-free samples was quantified *via* a 761 Compact Ion Chromatograph (Metrohm) by conductivity detection. Ions were separated *via* a Metrosep A

Supp 5-100 column with an eluent of 3.2 mM Na_2CO_3 and 1 mM $NaHCO_3$ at 0.7 ml min^{-1}. Fe^{2+} dissolved in such filtrates was quantified by ICP-OES (see above).

Acknowledgements

We are indebted to Rebecca Ansorge for technical support. We thank Jens Harder and Thomas Holler for review of the manuscript. Andrea Mingers and Daniel Kurz conducted ICP-OES- and C/S-Analysis, respectively. We thank Bernd Stickfort for support with the bibliography. The authors thank Justus van Beusekom, Ragnhild Asmus and their colleagues at the Alfred Wegener Institute for Polar and Marine Research for support of our field study. This work was supported by the Max Planck Society.

References

Appia-Ayme, C., Guiliani, N., Ratouchniak, J., and Bonnefoy, V. (1999) Characterization of an operon encoding two *c*-type cytochromes, an aa_3-type cytochrome oxidase, and rusticyanin in *Thiobacillus ferrooxidans* ATCC 33020. *Appl Environ Microbiol* **65:** 4781–4787.

Araujo, J.C., Teran, F.C., Oliveira, R.A., Nour, E.A.A., Montenegro, M.A.P., Campos, J.R., and Vazoller, R.F. (2003) Comparison of hexamethyldisilazane and critical point drying treatments for SEM analysis of anaerobic biofilms and granular sludge. *J Electron Microsc* **52:** 429–433.

Auernik, K.S., Maezato, Y., Blum, P.H., and Kelly, R.M. (2008) The genome sequence of the metal-mobilizing, extremely thermoacidophilic archaeon *Metallosphaera sedula* provides insights into bioleaching-associated metabolism. *Appl Environ Microbiol* **74:** 682–692.

Badziong, W., and Thauer, R.K. (1978) Growth yields and growth rates of *Desulfovibrio vulgaris* (Marburg) growing on hydrogen plus sulfate and hydrogen plus thiosulfate as sole energy sources. *Arch Microbiol* **117**: 209−214.

Beech, I.B., and Sunner, I.A. (2007) Sulphate-reducing bacteria and their role in corrosion of ferrous materials. In *Sulphate-reducing bacteria: environmental and engineered systems*. Barton, L.L., and Hamilton, W.A. (eds). Cambridge: Cambridge University Press, pp. 459–482.

Bockris, J.O.M., and Reddy, A.K.N. (1970) *Modern electrochemistry*. New York: Plenum.

Booth, G.H., and Tiller, A.K. (1960) Polarization studies of mild steel in cultures of sulphate-reducing bacteria. *T Faraday Soc* **56:** 1689−1696.

Booth, G.H., Cooper, A.W., and Tiller, A.K. (1967) Criteria of soil aggressiveness towards buried metal. III. Verification of predicted behaviour of selected soils. *Br Corrosion J* **2**: 116–118.

Booth, G.H., Elford, L., and Wakerley, D.S. (1968) Corrosion of mild steel by sulphate-reducing bacteria: an alternative mechanism. *Br Corrosion J* **3:** 242–245.

Braun, F. (1875) Ueber die Stromleitung durch Schwefelmetalle. *Ann Phys* **229:** 556–563.

Bryant, R.D., and Laishley, E.J. (1990) The role of hydrogenase in anaerobic biocorrosion. *Can J Microbiol* **36:** 259–264.

Butler, J.E., Young, N.D., and Lovley, D.R. (2010) Evolution of electron transfer out of the cell: comparative genomics of six *Geobacter* genomes. *BMC Genomics* **11:** 1−12.

Coetser, S.E., and Cloete, T.E. (2005) Biofouling and biocorrosion in industrial water systems. *Crit Rev Microbiol* **31:** 213–232.

Croese, E., Pereira, M.A., Euverink, G.-J.W, Stams, A.J.M., and Geelhoed, J.S. (2011) Analysis of the microbial community of the biocathode of a hydrogen-producing microbial electrolysis cell. *Appl Microbiol Biotechnol* **92:** 1083–1093.

Costello, J.A. (1974) Cathodic depolarization by sulphate-reducing bacteria. *S Afr J Sci* **70**: 202–204.

Deutsch, E.R., Rao, K.V., Laurent, R., and Seguin, M.K. (1977) New evidence and possible origin of native iron in ophiolites of eastern Canada. *Nature* **269:** 684–685.

Dinh, H.T., Kuever, J., Mußmann, M., Hassel, A.W., Stratmann, M., and Widdel, F. (2004) Iron corrosion by novel anaerobic microorganisms. *Nature* **427:** 829–832.

Duncan, K.E., Gieg, L.M., Parisi, V.A., Tanner, R.S., Tringe, S.G., Bristow, J., and Suflita, J.M. (2009) Biocorrosive thermophilic microbial communities in Alaskan North Slope oil facilities. *Environ Sci Technol* **43:** 7977–7984.

Gieg, L.M., Jack, T.R., and Foght, J.M. (2011) Biological souring and mitigation in oil reservoirs. *Appl Microbiol Biotechnol* **92**: 263–282.

Gittel, A., Seidel, M., Kuever, J., Galushko, A.S., Cypionka, H., and Konneke, M. (2010) *Desulfopila inferna* sp. nov., a sulfate-reducing bacterium isolated from the subsurface of a tidal sand-flat. *Int J Syst Evol Microbiol* **60:** 1626–1630.

Goldstein, J., Newbury, D., Joy, D., Lyman, C., Echlin, P., Lifshin, E. *et al*. (2003) *Scanning electron microscopy and X-ray microanalysis*, 3rd edn. New York, USA: Springer.

Haggerty, S.E., and Toft, P.B. (1985) Native iron in the continental lower crust - Petrological and geophysical implications. *Science* **229:** 647–649.

Hamann, C.H., Hamnett, A., and Vielstich, W. (2007) *Electrochemistry*, 2nd edn. Weinheim: Wiley.

Hamilton, W.A. (1985) Sulphate-reducing bacteria and anaerobic corrosion. *Annu Rev Microbiol* **39:** 195–217.

Hamilton, W.A. (2003) Microbially influenced corrosion as a model system for the study of metal microbe interactions: a unifying electron transfer hypothesis. *Biofouling* **19:** 65–76.

Hardy, J.A. (1983) Utilization of cathodic hydrogen by sulphate-reducing bacteria. *Br Corrosion J* **18:** 190–193.

Hubert, C., Nemati, M., Jenneman, G., and Voordouw, G. (2005) Corrosion risk associated with microbial souring control using nitrate or nitrite. *Appl Microbiol Biotechnol* **68**: 272–282.

Jack, T.R. (2002) Biological corrosion failures. In *ASM Handbook Volume 11: Failure Analysis and Prevention*. Shipley, R.J., and Becker, W.T. (eds). Materials Park: ASM International, pp. 881–898.

Kato, S., Hashimoto, K., and Watanabe, K. (2011) Methanogenesis facilitated by electric syntrophy *via* (semi)conductive iron-oxide minerals. *Environ Microbiol*, doi:10.1111/j.1462-2920.2011.02611.x

King, R.A., and Miller, J.D.A. (1971) Corrosion by sulphate-reducing bacteria. *Nature* **233**: 491–492.

Lee, W., Lewandowski, Z., Nielsen, P.H., and Hamilton, W.A. (1995) Role of sulfate-reducing bacteria in corrosion of mild-steel - a review. *Biofouling* **8:** 165–194.

Li, S., Kim, Y., Jeon, K., and Kho, Y. (2000) Microbiologically influenced corrosion of underground pipelines under the disbonded coatings. *Met Mater* **6**: 281–286.

Lovley, D.R. (2006) Microbial fuel cells: novel microbial physiologies and engineering approaches. *Curr Opin Biotech* **17:** 327–332.

Lovley, D.R. (2011) Reach out and touch someone: potential impact of DIET (direct interspecies energy transfer) on anaerobic biogeochemistry, bioremediation, and bioenergy. *Rev Environ Sci Biotechnol* **10:** 101–105.

Malvankar, N.S., Vargas, M., Nevin, K.P., Franks, A.E., Leang, C., Kim, B.C. *et al*. (2011) Tunable metallic-like conductivity in microbial nanowire networks. *Nat Nanotech* **6:** 573–579.

Mori, K., Tsurumaru, H., and Harayama, S. (2010) Iron corrosion activity of anaerobic hydrogen-consuming microorganisms isolated from oil facilities. *J Biosci Bioeng* **110:** 426–430.

Nakamura, R., Kai, F., Okamoto, A., Newton, G.J., and Hashimoto, K. (2009) Self-constructed electrically conductive bacterial networks. *Angew Chem Int Ed* **48:** 508–511.

Nealson, K.H., and Finkel, S.E. (2011) Electron flow and biofilms. *MRS Bulletin* **36:** 380–384.

Nielsen, L.P., Risgaard-Petersen, N., Fossing, H., Christensen, P.B., and Sayama, M. (2010) Electric currents couple spatially separated biogeochemical processes in marine sediment. *Nature* **463:** 1071–1074.

Pearce, C.I., Pattrick, R.A.D., and Vaughan, D.J. (2006) Electrical and magnetic properties of sulfides. *Rev Mineral Geochem* **61:** 127–180.

Reinsel, M.A., Sears, J.T., Stewart, P.S., and McInerney, M.J. (1996) Control of microbial souring by nitrate, nitrite or glutaraldehyde injection in a sandstone column. *J Ind Microbiol* **17**: 128–136.

Schön, J.H. (1996) Electrical properties of rocks. In *Physical properties of rocks: Fundamentals & principles of petrophysics*. Schön, J.H. (ed). Oxford: Pergamon Press.

Schwermer, C.U., Lavik, G., Abed, R.M.M., Dunsmore, B., Ferdelman, T.G., Stoodley, P. *et al*. (2008) Impact of nitrate on the structure and function of bacterial biofilm communities in pipelines used for injection of seawater into oil fields. *Appl Environ Microbiol* **74**: 2841–2851.

Sherar, B.W.A., Power, I.M., Keech, P.G., Mitlin, S., Southam, G., and Shoesmith, D.W. (2011) Characterizing the effect of carbon steel exposure in sulfide containing solutions to microbially induced corrosion. *Corrosion Sci* **53:** 955–960.

Skovhus, T.L., Sørensen, K.B., and Larsen, J. (2011) Rapid diagnostics of microbiologically influenced corrosion (MIC) in oilfield systems with a DNA-based test kit. In *Applied Microbiology and Molecular Biology in Oilfield Systems*. Whitby, C., and Skovhus, T.L. (eds). Dordrecht: Springer, pp. 133−140.

Smith, J.S., and Miller, J.D.A. (1975) Nature of sulphides and their corrosive effect on ferrous metals: a review. *Br Corrosion J* **10:** 136–143.

Sorokin, Y.I. (1966) Role of carbon dioxide and acetate in biosynthesis by sulphate-reducing bacteria. *Nature* **210**: 55̄1552.

Spruit, C.J.P., and Wanklyn, J.N. (1951) Iron sulphide ratios in corrosion by sulphate-reducing bacteria. *Nature* **168:** 951–952.

Summers, Z.M., Fogarty, H.E., Leang, C., Franks, A.E., Malvankar, N.S., and Lovley, D.R. (2010) Direct exchange of electrons within aggregates of an evolved syntrophic coculture of anaerobic bacteria. *Science* **330:** 1413–1415.

U.S. Geological Survey (2011) Mineral commodity summaries 2011. *U.S. Geological Survey*: 1–198, http://minerals.usgs.gov/minerals/pubs/mcs/2011/mcs2011.pdf

Uchiyama, T., Ito, K., Mori, K., Tsurumaru, H., and Harayama, S. (2010) Iron-corroding methanogen isolated from a crude-oil storage tank. *Appl Environ Microbiol* **76:** 1783–1788.

Wächtershäuser, G. (1992) Groundworks for an evolutionary biochemistry: the iron-sulphur world. *Prog Biophys Mol Bio* **58:** 85–201.

Widdel, F., and Bak, F. (1992) Gram-negative mesophilic sulfate-reducing bacteria. In *The Prokaryotes*. Balows, A., Trüper, H.G., Dworkin, M., Harder, W., and Schleifer, K.-H. (eds). New York: Springer, pp. 3352–3378.

Widdel, F., and Musat, F. (2010) Energetic and other quantitative aspects of microbial hydrocarbon utilization. In *Handbook of Hydrocarbon and Lipid Microbiology*. Timmis, K.N. (ed). Berlin: Springer.

van Dijken, J.P., and Harder, W. (1975) Growth yields of microorganisms on methanol and methane. A theoretical study. *Biotechnol Bioeng* **17:** 15–30.

von Wolzogen Kühr, C.A.H., and van der Vlugt, L.S. (1934) The graphitization of cast iron as an electrobiochemical process in anaerobic soil. *Water* **18:** 147–165.

von Wolzogen Kühr, C.A.H. (1961) Unity of anaerobic and aerobic iron corrosion process in the soil. *Corrosion* **17:** 119–125.

List of abbreviations and symbols

CMIC	Chemical microbially influenced corrosion (indirect corrosion)
$\Delta G°$	Change of free energy at standard activities (≈ 1 M, 1 atm)
$\Delta G°'$	Change of free energy, except $\{H^+\} = \{HO^-\} = 10^{-7}$ ($pH = 7$)
$\Delta H°$	Change of enthalpy at 298.15 K
EMIC	Electrical microbially influenced corrosion (direct corrosion)
E	redox potential
$E°$	Redox potential at standard activities (≈ 1 M, 1 atm)
$E°'$	Redox potential at standard activities, except $\{H^+\} = \{HO^-\} = 10^{-7}$ ($pH = 7$)
i	Electrical current density
I	Electrical current
m_{Bio}	Biomass
m_{Min}	Mass of precipitated minerals
MIC	Microbially influenced (usually anaerobic) corrosion (of iron)
$n_{\Delta Fe(0)}$	Amount of metallic iron oxidized (corroded)
$n_{Fe(II)}$	Amount of (total) ferrous iron formed
n_{FeAnab}	Amount of iron oxidized by the anabolism (cell synthesis)
$n_{FeCatab}$	Amount of iron oxidized by the catabolism (sulfate reduction)
n_{FeS}	Amount of ferrous sulfide ($\equiv n_{SR}$)
n_{SR}	Amount of sulfate reduced ($\equiv n_{FeS}$)
q_{Anab}	Partition of anabolic in total (anabolic + catabolic) electron consumption
q_{EMIC}	Contribution (partition) of EMIC to total corrosion by SRB.
Y_{Anab}	Anabolic yield coefficient: cell mass per amount of anabolically oxidized iron

Appendix S1

Costs due to iron corrosion (aerobic, anaerobic)

Several studies have addressed the costs due to metal (iron + other) corrosion, the most comprehensive ones providing data for the United States (Revie, 2011). Here, a recent report (Koch *et al*., 2001) provided annual direct costs due to metal corrosion of $\$ 276 \cdot 10^9$, which is 3.1% of U.S. GDP. 'Indirect' costs to the user were conservatively estimated to be similar, so that total costs due to corrosion to society may be as high as 6% of GDP. Similarly, costs of metallic corrosion in other developed countries have been estimated to range between 2 and 3% of GNP [see (Revie, 2011) for review]. As iron is the by far most widely used metal and particularly prone to corrosion (oxidation crusts of iron provide far less protection than those of other metals), the calculated costs due to metal corrosion are largely those of iron corrosion. Even though aerobic (abiotic) rusting is the most common type of iron corrosion, anaerobic corrosion by microbial activity is a dominant type in particular industrial water systems in the production and transportation of oil, gas and energy carriers (Lee *et al.*, 1995; Jack, 2002; Beech and Sunner, 2007).

Free energy values and redox potentials of dissolved iron

Reactions involving dissolved ferrous iron were based on a revised ΔG_f°-value of Fe^{2+} (aq) of –90.53 kJ mol^{-1} (Rickard and Luther, 2007), the corresponding E° (Fe^{2+}/Fe^0) value being –0.469 V. Other commonly used corresponding values are –84.9 kJ mol^{-1} and –0.440 V (Randall and Frandsen, 1932; Dean, 1992; Dinh *et al*., 2004; Atkins and De Paula, 2006). The least negative corresponding values are –78.87 kJ mol^{-1} and –0.409 V (Patrick and Thompson, 1952).

Indirect corrosion (CMIC) of iron by sulfate-reducing bacteria

Hydrogen sulfide from sulfate reduction with biomass-derived organic carbon (here simplified as ⟨HCOH⟩) according to

$$2\ \langle HCOH\rangle + SO_4^{2-} \rightarrow 2\ HCO_3^- + H_2S \qquad (S1)$$

attacks metallic iron in an abiotic reaction [see also (Dinh *et al.*, 2004)]:

$$Fe^0 + H_2S \rightarrow FeS + H_2. \qquad (S2)$$

The sum reaction is

$$2\ \langle HCOH\rangle + SO_4^{2-} + Fe^0 \rightarrow 2\ HCO_3^- + FeS + H_2. \quad (S3)$$

H_2 from equation (S2) as an excellent electron donor for SRB again leads to H_2S according to

$$H_2 + ¼\ SO_4^{2-} + ½\ H^+ \rightarrow ¼\ H_2S + H_2O, \quad (S4)$$

again attacking ¼ Fe^0. The sum is now

$$2\ \langle HCOH\rangle + 1¼\ SO_4^{2-} + 1¼\ Fe^0 + ½\ H^+$$
$$\rightarrow 2\ HCO_3^- + 1¼\ FeS + ¼\ H_2 + H_2O. \quad (S5)$$

Reduction of ¼ SO_4^{2-} with ¼ H_2 yields $^1/_{16}$ H_2S attacking $^1/_{16}$ Fe^0. Continuing and summing *ad infinitum* yields

$$2\langle HCOH\rangle + \left[\sum_{n=0}^{\infty}\left(\frac{1}{4}\right)^n\right]SO_4^{2-} + \left[\sum_{n=0}^{\infty}\left(\frac{1}{4}\right)^n\right]Fe^0 + \left[\frac{1}{2}\sum_{n=0}^{\infty}\left(\frac{1}{4}\right)^n\right]H^+$$
$$\longrightarrow 2\,HCO_3^- + \left[\sum_{n=0}^{\infty}\left(\frac{1}{4}\right)^n\right]FeS + \left[\sum_{n=0}^{\infty}\left(\frac{1}{4}\right)^n\right]H_2O \quad (S6)$$

The converging geometric series yields

$$\sum_{n=0}^{\infty}\left(\frac{1}{4}\right)^n = \frac{1-\left(1/4\right)^{\infty}}{1-\left(1/4\right)} = \frac{4}{3} \quad (S7)$$

converting equation (S5) to

$$2\ \langle HCOH\rangle + {}^4/_3\ SO_4^{2-} + {}^4/_3\ Fe^0 + {}^2/_3\ H^+ \rightarrow 2\ HCO_3^- + {}^4/_3\ FeS + {}^4/_3\ H_2O\ . \quad (S8)$$

Multiplying by $^3/_2$ yields

$$3\ \langle HCOH\rangle + 2\ SO_4^{2-} + 2\ Fe^0 + H^+ \rightarrow 3\ HCO_3^- + 2\ FeS + 2\ H_2O. \quad (S9)$$

Note that a mere co-oxidation of ⟨HCOH⟩ and Fe^0 can result in the same equation.

Metal loss rates

The rate (velocity) of the loss of metal mass (m) by corrosion is $v^{\theta}_{\mathrm{corr}} = \mathrm{d}m/\mathrm{d}t$ or, if constant during an experimental time interval Δt, also $v^{\theta}_{\mathrm{corr}} = \Delta m/\Delta t$. Division by density, ρ, and surface area, a, yields the thickness (θ) loss rate, $v^{\theta}_{\mathrm{corr}} = \Delta\theta/\Delta t = \Delta m/(a\,\rho\,\Delta t)$. With SI units and $\rho = 7.87$ kg m^{-3} (mild steel EN 1.0330), the thickness loss rate is

$$v^{\theta}_{\mathrm{corr}}\ (\mathrm{m\ s^{-1}}) = 0.1271\ (\mathrm{m^3\ kg^{-1}})\ \frac{\Delta m}{a\,\Delta t}. \tag{S10}$$

If, for convenience, thickness is measured in mm, mass in mg, area in cm^{-2}, and time in yr, the thickness loss rate is

$$v^{\theta}_{\mathrm{corr}}\ (\mathrm{mm\ yr^{-1}}) = 1.27 \cdot 10^{-3}\ (\mathrm{mm\ mg^{-1}\ cm^2})\ \frac{\Delta m}{a\,\Delta t}. \tag{S11}$$

Corrosion current density

The rate (velocity) of the loss of metal amount (n, in mol) by corrosion is derived from mass (m) loss (see above) as $v^{n}_{\mathrm{corr}} = \Delta m/(M_a\,\Delta t)$, with M_a being the atomic mass. With n_e as the number of electrons released per metal atom and the Faraday constant F, the current of electron loss is $i_{\mathrm{corr}} = n_e\,F\,v^{n}_{\mathrm{corr}} = n_e\,F\,\Delta m/(M_a\,\Delta t)$. Division by surface area, a, yields the current density,

$$i_{\mathrm{corr}}\ (\mathrm{A\ m^{-2}}) = \frac{n_{\mathrm{e}}\,F\,\Delta m}{a\,M_{\mathrm{a}}\,\Delta t}. \tag{S12}$$

If the corrosion rate is given as thickness (θ) loss instead of mass loss, the density, ρ, must be included:

$$i_{\mathrm{corr}}\ (\mathrm{A\ m^{-2}}) = \frac{n_{\mathrm{e}}\,F\,\rho\,\Delta\theta}{M_{\mathrm{a}}\,\Delta t}. \tag{S13}$$

With SI units, $n_e = 2$, $M_a = 55.85 \cdot 10^{-3}$ kg mol^{-1} (for iron) and $\rho = 7.87 \cdot 10^{3}$ kg m^{-3} (mild steel EN 1.0330), and $F = 96{,}485$ C mol^{-1}, formulas (S12) and (S13) convert to

$$i_{\mathrm{corr}}\ (\mathrm{A\ m^{-2}}) = 3.455 \cdot 10^{6}\ (\mathrm{A\ s\ kg^{-1}})\ \frac{\Delta m}{a\,\Delta t} \tag{S14}$$

$$i_{corr}\,(\mathrm{A\ m^{-2}}) = 2.72\ \cdot 10^{10}\,(\mathrm{A\ m^{-3}\ s})\ \frac{\Delta\theta}{\Delta t}. \qquad \text{(S15)}$$

If, for convenience, thickness is measured in mm, mass in mg, area in cm^2, and time in yr, the respective corrosion current density is

$$i_{corr}\,(\mathrm{A\ cm^{-2}}) = 1.095 \cdot 10^{-7}\,(\mathrm{A\ yr\ mg^{-1}})\ \frac{\Delta m}{a\,\Delta t} \qquad \text{(S16)}$$

$$i_{corr}\,(\mathrm{A\ cm^{-2}}) = 8.62 \cdot 10^{-5}\,(\mathrm{A\ yr\ cm^{-2}\ mm^{-1}})\ \frac{\Delta\theta}{\Delta t}\ (\text{fraction in mm yr}^{-1}). \qquad \text{(S17)}$$

Crust conductivity and redox potential difference

Electrical current, I, through a cylindrical or cubical body of ohmic behavior is proportional to the applied voltage, V, and area perpendicular to current direction, a, and inversely proportional to length, d, i.e. $I = \sigma V a / d$. The proportionality constant, σ, is the specific conductance or conductivity ($\mathrm{A\ V^{-1}\,m^{-1}}$; $\mathrm{S\,m^{-1}}$, $\Omega^{-1}\,\mathrm{m^{-1}}$). The (argument of the vectorial) electrical field strength sustaining the current I is thus $V / d = I / \sigma a$. With current density $i = I / a$ we can write

$$\frac{V}{d} = \frac{i}{\sigma}. \qquad \text{(S18)}$$

For a corrosion current of $i_{corr} = 0.61\ \mathrm{A\ m^{-2}}$ (calculated from loss of Fe^0) and the determined conductivity of $\sigma = 50\ \mathrm{S\ m^{-1}}$, the field strength between metal and colonized crust would be only

$$\frac{V}{d} = 1.2 \cdot 10^{-2}\ \mathrm{V\ m^{-1}}, \qquad \text{(S19)}$$

which is as low as $1.2 \cdot 10^{-4}$ V across a crust with a realistic thickness of 1 cm. The voltage V is the difference between the operational redox potentials of the electron-accepting sulfate reduction (SR) and the electron-donating iron dissolution (FeDiss), $V = \Delta\phi = \phi_{SR} - \phi_{FeDiss}$. Due to reaction overpotentials, $\Delta\phi$ must be within the difference of the equilibrium redox potentials (E), i.e. $V = \Delta\phi < \Delta E = E_{SR} - E_{FeDiss}$. E_{SR} and E_{FeDiss} are calculated from the half

reactions and free energies of formation[1] (Thauer *et al.*, 1977; Garrels and Christ, 1985), first for standard conditions at $pH = 7$ ($E°'$, here used for $E°_{pH7}$), and subsequently for near-real conditions assuming activities (in seawater) of $\{SO_4^{2-}\} = 3 \cdot 10^{-3}$ and $\{HCO_3^-\} = 1.5 \cdot 10^{-2}$ [from applied concentrations and activity coefficients (Stumm and Morgan, 1996)] and $pH = 8$.

$$SO_4^{2-} + FeCO_3 + 9\ H^+ + 8\ e^- \rightleftarrows FeS + HCO_3^- + 4\ H_2O \qquad \text{(S20)}$$

$E°'_{SR} = -0.175$ V; $E_{SR} = -0.23$ V

$$Fe^0 + HCO_3^- \rightleftarrows FeCO_3 + H^+ + 2\ e^- \qquad \text{(S21)}$$

$E°'_{FeDiss} = -0.62$ V; $E_{FeDiss} = -0.60$ V.

The resulting $\Delta E = -0.37$ V gives more than sufficient leeway for a self-adjusting $\Delta\phi$ during (the irreversible) electron withdrawal by corrosive SRB.

Acidity of Fe^{2+}

The pK_a of an acid, viz. a reaction (acid ⇄ base + proton) with equilibrium constant K_{eq} (also termed K_a) is

$$pK_a = -\lg K_a = -\lg K_{eq} = -(\lg e) \ln K_{eq} = -(\lg e)\frac{-\Delta G^o_{\rightarrow}}{RT} = 0.4343\frac{\Delta G^o_{\rightarrow}}{RT}\ . \qquad \text{(S22)}$$

$\Delta G°_{\rightarrow}$ is the standard free energy of the forward reaction. Hydrated Fe^{2+} ions tend to release a proton from the water shell according to

$$[Fe(OH_2)_6]^{2+} \rightleftarrows [Fe(OH_2)_5(OH)]^+ + H^+, \qquad \text{(S23)}$$

which in thermodynamic data compilations and for calculations is usually simplified as

$$Fe^{2+} + H_2O \rightleftarrows Fe(OH)^+ + H^+ \qquad \text{(S24)}$$

$$K_{eq} = \left(\frac{\{Fe(OH)^+\}\ \{H^+\}}{\{Fe^{2+}\}\ \{H_2O\}}\right)_{eq}$$

[1] Used $\Delta G_f°$-values (kJ mol^{-1}): Fe^0, 0.00; Fe^{2+}, –90.53; $FeCO_3$ (c), –666.7; FeS (c), –100.4; H^+ ($pH = 7$), –40.0; HCO_3^-, –586.8; H_2O, –237.18; SO_4^{2-}, –744.6.

Free energy with revised $\Delta G_f°$–value (Rickard and Luther, 2007) for Fe^{2+} of −90.5 kJ mol^{-1} is $\Delta G°_{\rightarrow}$ = +50.4 kJ mol^{-1}, yielding

$$pK_a = 8.8 \quad (T = 298 \text{ K}). \tag{S25}$$

Free energy with a formerly common $\Delta G_f°$-value for Fe^{2+} of −78.87 kJ mol^{-1} yields $\Delta G°_{\rightarrow}$ = +38.8 kJ and

$$pK_a = 6.6 \quad (T = 298 \text{ K}). \tag{S26}$$

It is possible that also the $\Delta G_f°$-value for $Fe(OH)^+$ (−277.3 kJ mol^{-1}) requires revision (origin of present value not investigated). Hence, the pK_a-values calculated here may be regarded only as upper and lower limits of a range into which a fully revised pK_a-value will fall.

Content of formed biomass in precipitated corrosion products

The fraction of biomass in the precipitated corrosion products is expressed as the quotient

$$q^m_{\text{Bio}} = \frac{m_{\text{Bio}}}{m_{\text{Min}} + m_{\text{Bio}}}, \tag{14, 15, S27}$$

with m_{Bio} indicating the biomass and m_{Min} the mineral mass (superscript '*m*' indicates mass ratio rather than molar ratio in other quotients). Because there is presently no convenient analytical method, the quotient is calculated from the amounts of iron oxidized and sulfate reduced.

The mineral mass, m_{Min}, is that of precipitated FeS and $FeCO_3$, and possibly co-precipitated alkaline earth (Mg + Ca, here Ae) carbonates, $AeCO_3$, i.e. $m_{\text{Min}} = m_{\text{FeS}} + m_{\text{FeCO3}} + m_{\text{AeCO3}}$. This is expressed via molecular masses (M) and amounts (n, mol) as $m_{\text{Min}} = M_{\text{FeS}}\, n_{\text{FeS}} + M_{\text{FeCO3}}\, n_{\text{FeCO3}} + m_{\text{AeCO3}}$. Because FeS precipitation scavenges all formed sulfide, $n_{\text{FeS}} = n_{\text{SR}}$, the amount of sulfate reduced. Assuming that all ferrous iron formed during EMIC and not precipitated as FeS is precipitated as $FeCO_3$, the amount of the latter is total iron loss by EMIC minus sulfidic iron, i.e. $n_{\text{FeCO3}} = n_{\text{FeEMIC}} - n_{\text{FeS}}$ or $n_{\text{FeCO3}} = n_{\text{FeEMIC}} - n_{\text{SR}}$. This yields for the mineral mass

$$m_{\text{Min}} = M_{\text{FeS}}\, n_{\text{SR}} + M_{\text{FeCO3}}\, (n_{\text{FeEMIC}} - n_{\text{SR}}) + m_{\text{AeCO3}}\ . \tag{S28}$$

The biomass (e.g., in g) formed per amount (e.g., in mol) of iron used for (attributed to) the anabolism (biosynthesis) is calculated from the predicted (Eq. 11, 12) yield coefficient Y_{FeAnb}

(biomass per iron oxidized by the anabolism) and the amount of iron needed for the anabolism, $m_{Bio} = Y_{Anab}\, n_{FeAnab}$. Because $n_{FeAnab} = n_{\Delta Fe(0)} - 4\, n_{SR}$ (Eq. 8), the biomass is

$$m_{Bio} = Y_{Anab}\,(n_{\Delta Fe(0)} - 4\, n_{SR}). \tag{S29}$$

With equations (S28) and (S29), the quotient in equation (S27) converts to

$$q^{m}_{Bio} = \frac{Y_{Anab}\,(n_{\Delta Fe(0)} - 4\, n_{SR})}{M_{FeS} n_{SR} + M_{FeCO_3}\,(n_{\Delta Fe(0)} - n_{SR}) + m_{AeCO_3} + Y_{FeAnb}\,(n_{\Delta Fe(0)} - 4\, n_{SR})} \tag{S30}$$

or (with $M_{FeS} = 87.9$ and $M_{FeCO3} = 115.9$ g mol^{-1})

$$q^{m}_{Bio} = \frac{Y_{Anab}\,(n_{\Delta Fe(0)} - 4\, n_{SR})}{115.9\; n_{\Delta Fe(0)} - 28\, n_{SR} + m_{AeCO_3} + Y_{Anab}\,(n_{\Delta Fe(0)} - 4\, n_{SR})}\ . \tag{S31}$$

If $AeCO_3$ is present but not included in equation (S27), it leads to an overestimate of q^{m}_{Bio}, so that

$$q^{m}_{Bio} \le \frac{Y_{Anab}\,(n_{\Delta Fe(0)} - 4\, n_{SR})}{115.9\, n_{\Delta Fe(0)} - 28\, n_{SR} + Y_{Anab}\,(n_{\Delta Fe(0)} - 4\, n_{SR})}, \tag{S32}$$

(for units g, mol). Equations (11) and (12) predict $Y_{FeAna(aut)} = 12.0$ g mol^{-1} for autotrophic and $Y_{FeAna(het)} = 32.2$ g mol^{-1}, yielding

$$q^{m}_{Bio(aut)} \le \frac{n_{\Delta Fe(0)} - 4\, n_{SR}}{10.66\, n_{\Delta Fe(0)} - 6.33\, n_{SR}} \tag{S33}$$

and

$$q^{m}_{Bio(het)} \le \frac{n_{\Delta Fe(0)} - 4\, n_{SR}}{4.60\, n_{\Delta Fe(0)} - 4.87\, n_{SR}}, \tag{S34}$$

respectively.

Calculation of the contribution of direct to total anaerobic corrosion

Whereas CMIC by sulfide leads to FeS as the only product (Eq. 4), EMIC leads in addition to non-sulfidic ferrous iron which tends to precipitate as carbonate (Eq. 5). Hence, the ratio of FeS to total Fe(II) in a crust should allow to calculate the contribution of EMIC to MIC

(EMIC and CMIC), the total corrosion due to the activity of SRB in the environment. The contribution (mol/mol) is expressed as the quotient of the amount of iron corroded by EMIC, n_{FeEMIC}, to the amount corroded by MIC, n_{FeMIC}, the latter being identical with the measurable ferrous iron formed, $n_{\mathrm{Fe(II)}}$, so that

$$q_{\mathrm{EMIC}} = \frac{n_{\mathrm{FeEMIC}}}{n_{\mathrm{FeMIC}}} = \frac{n_{\mathrm{FeEMIC}}}{n_{\mathrm{Fe(II)}}}. \tag{S35}$$

An expression must be found which besides $n_{\mathrm{Fe(II)}}$ includes the amount of formed FeS, n_{FeS}, as the other measurable parameter but no longer the unknown n_{FeEMIC}. This is achieved by including four other equations. Two of these are equations (7) and (9),

$$n_{\mathrm{FeEMIC}} = n_{\mathrm{FeCatab}} + n_{\mathrm{FeAnab}} \tag{S36}$$

and

$$q_{\mathrm{Anab}} = \frac{n_{\mathrm{FeAnab}}}{n_{\mathrm{FeEMIC}}}, \tag{S37}$$

respectively. Equation (8) cannot be applied, because MIC includes also organic electron donors in addition to Fe^0 for sulfate reduction, so that $n_{\mathrm{FeCatab}} < 4\, n_{\mathrm{SR}}$. Furthermore, the characteristic product of EMIC is non-sulfidic iron, its amount being designated n_{FeNonS}. This is ¾ of the amount oxidized by the catabolism (Eq. 5) plus the amount resulting from biosynthesis, i.e.

$$n_{\mathrm{FeNonS}} = ¾\, n_{\mathrm{FeCatab}} + n_{\mathrm{FeAnab}}. \tag{S38}$$

Finally, the amount n_{FeNonS} is iron totally formed by MIC (EMIC + CMIC), $n_{\mathrm{Fe(II)}}$, less sulfidic iron, n_{FeS}, so that

$$n_{\mathrm{FeNonS}} = n_{\mathrm{Fe(II)}} - n_{\mathrm{FeS}}. \tag{S39}$$

The coefficient matrix of equations (S35) – (S39) [order of rows below] arranged by

$n_{\mathrm{Fe(II)}}$, n_{FeS}, n_{FeEMIC}, n_{FeCatab}, n_{FeAnab}, n_{FeNonS},

$$\left(\begin{array}{cccccc|c} q_{\mathrm{EMIC}} & 0 & -1 & 0 & 0 & 0 & 0 \\ 0 & 0 & 1 & -1 & -1 & 0 & 0 \\ 0 & 0 & q_{\mathrm{Anab}} & 0 & -1 & 0 & 0 \\ 0 & 0 & 0 & ¾ & 1 & -1 & 0 \\ -1 & 1 & 0 & 0 & 0 & 1 & 0 \end{array}\right), \tag{S40}$$

is converted to

$$\left([q_{\mathrm{EMIC}}(3+q_{\mathrm{Anab}})-4] \quad 4 \quad 0 \quad 0 \quad 0 \quad 0 \quad | \quad 0\right). \tag{S41}$$

Hence,

$$[q_{\mathrm{EMIC}}(3+q_{\mathrm{Anab}})]\, n_{\mathrm{Fe(II)}} - 4\, n_{\mathrm{Fe(II)}} + 4\, n_{\mathrm{FeS}} = 0 \tag{S42}$$

which is rearranged as

$$q_{\mathrm{EMIC}} = \frac{4\,(1 - n_{\mathrm{FeS}}/n_{\mathrm{Fe(II)}})}{3+q_{\mathrm{Anab}}}. \tag{S43}$$

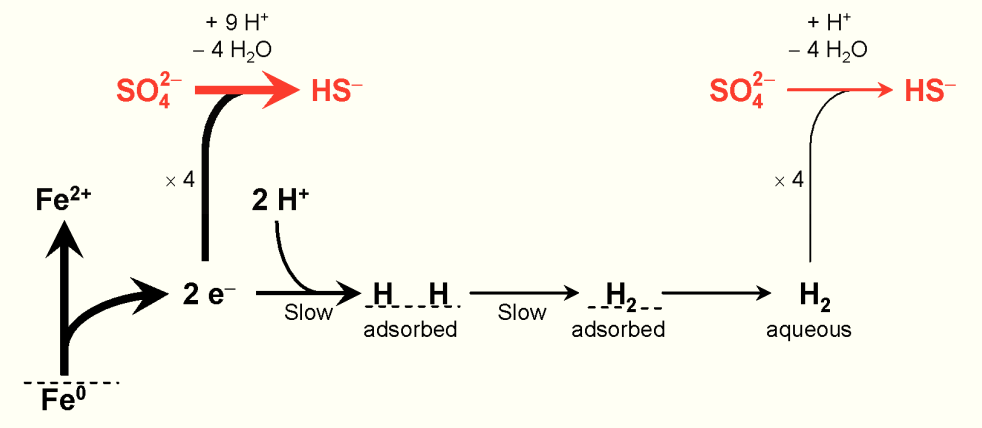

Fig. S1. Kinetic aspects of the abiotic reaction of iron in circumneutral water, and direct (lithotrophic) iron corrosion by SRB. Availability of H^+-ions at the metal surface and combination of adsorbed H-atoms to adsorbed H_2 are assumed to be rate-controlling steps ('bottle necks'), thus also controlling liberation of H_2 into water (Bockris and Reddy, 1970; Hamann *et al.*, 2007). H_2 consumption by SRB behind the bottle neck is therefore unlikely to promote iron dissolution. Direct consumption of electrons can oxidize the iron much faster. Thickness of arrows symbolizes speed. The net reaction is always $4Fe^0 + SO_4^{2-} + 4H_2O \rightarrow FeS + 3Fe^{2+} + 8OH^-$.

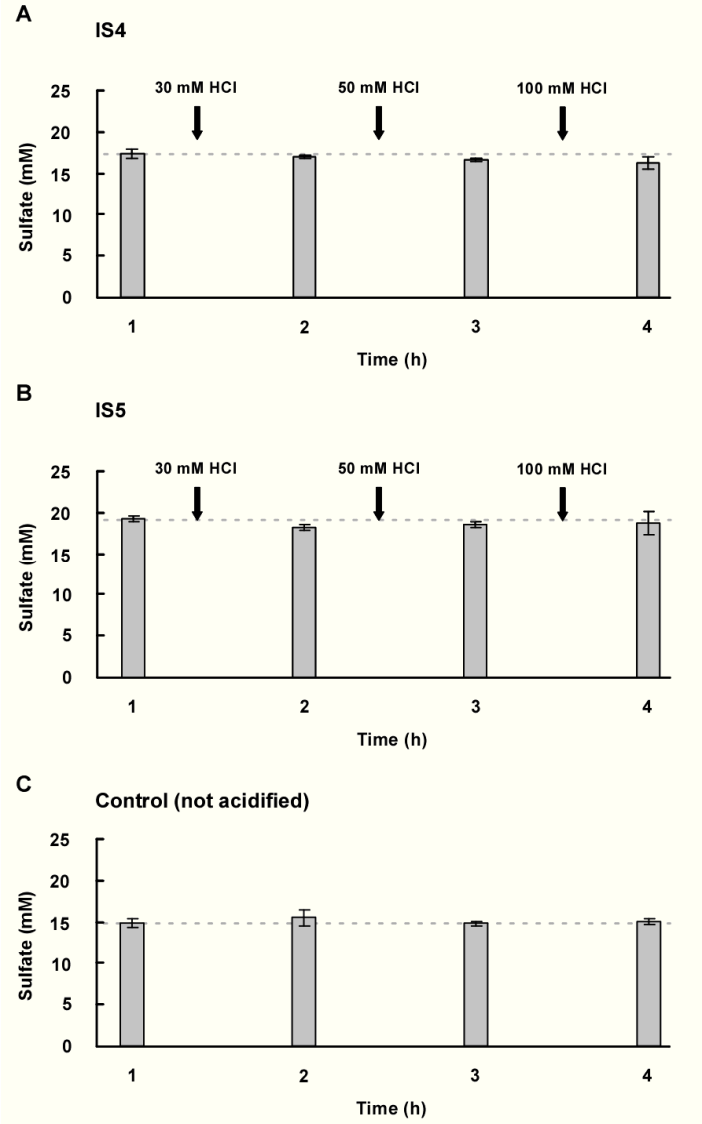

Fig. S2. Excluding disappearance of sulfate due to co-precipitation in the corrosion crust. Grown cultures were step-wise acidified with HCl until formed corrosion products were completely dissolved. Sulfate concentration of medium did not increase.

A. Culture of strain IS4.

B. Culture of strain IS5.

C. Control culture of strain IS4 which was not acidified.

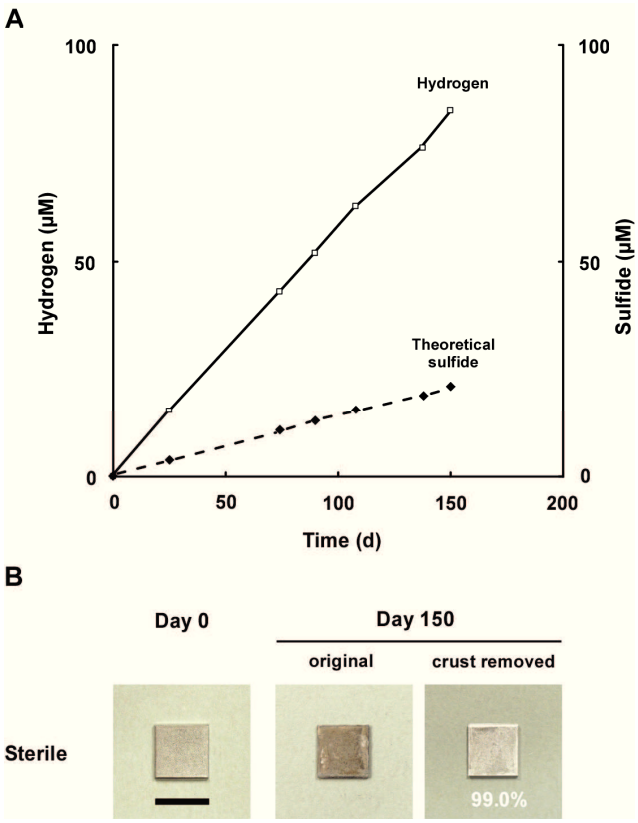

Fig. S3. Abiotic anaerobic iron corrosion in sterile synthetic seawater medium.

A. Production of 'cathodic' hydrogen by reduction of H^+ ions (Fig. S1), and sulfide that could be formed by H_2 utilization by SRB ($4\ H_2 + SO_4^{2-} + 2\ H^+ \rightarrow H_2S + 4\ H_2O$).

B. Original iron specimen (day 0), specimen with precipitate after 5 months (original) and after removal of precipitate (using HCl-hexamine).

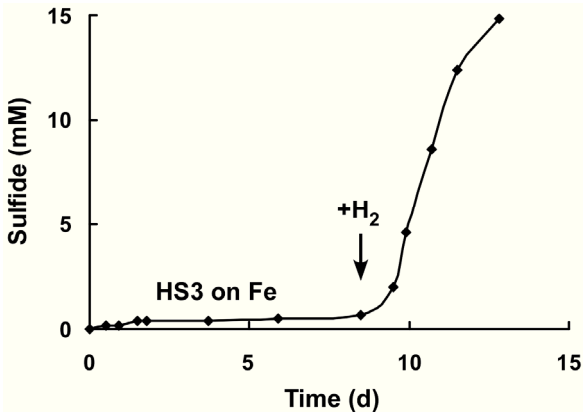

Fig. S4. Insensitivity of non-corrosive control strain HS3 towards Fe^{2+}. Addition of H_2 to the culture including iron granules leads to rapid sulfide production (measured as sulfate loss).

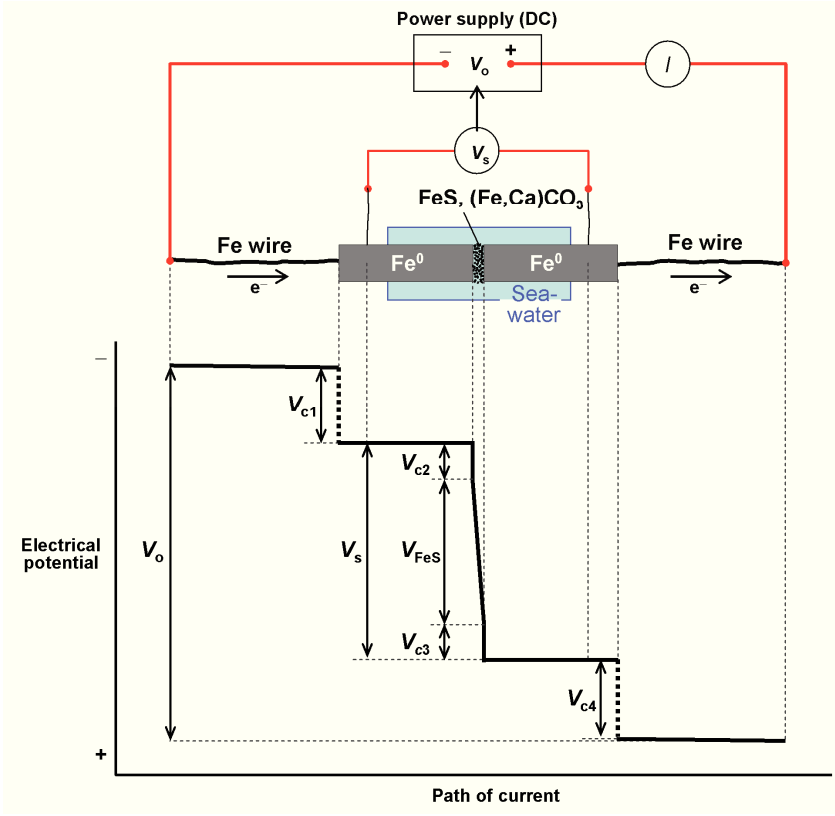

Fig. S5. Electro-technical scheme with approximate voltage drops of the split-coupon incubation device for conductance measurement of the biogenic crust formed on corroding iron. The device circumvents interference by the noticeable contact resistance between the iron wire and the iron coupon inside the incubated bottle (Fig. 3A). The plot in the lower part depicts the voltage drop along current flow. The outer voltage (V_o) is supplied and adjusted such that the voltage across the split (V_s) is kept at 0.20 V while the current (I) is being measured. The adjusted low voltage for measurement avoids electrolysis. Measurement of V_s is carried out with a high-resistance voltmeter. V_{c1} and V_{c4} are the voltage drops due to contact resistance between the iron wire and the iron coupon (around 1 Ω), and V_{c2} and V_{c3} the arbitrarily assumed voltage drops due to the contact resistance between iron and the sulfidic crust. Voltage drop along the iron wire and the iron coupons is negligible (resistance by two and four orders or magnitude lower, respectively, than resistance of wire-coupon contact and the crust).

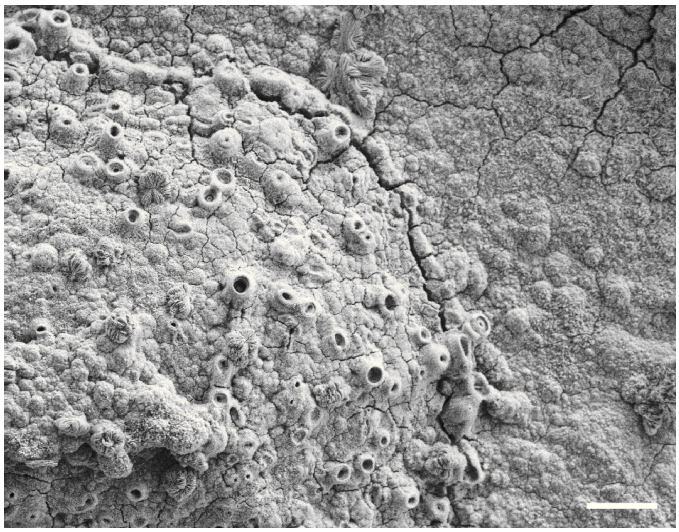

Fig. S6. Pustule (elevated precipitate) with early stage of micro-chimney formation above an anodic site in a culture of strain IS4 after three months of incubation. Bar, 50 µm.

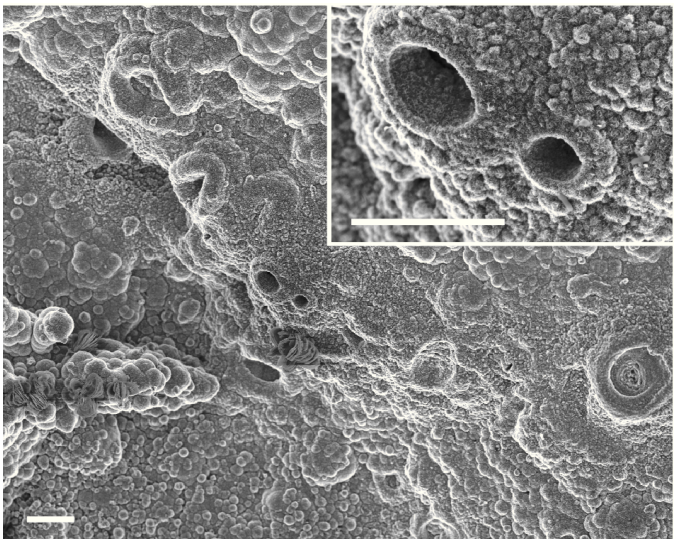

Fig. S7. Early stage of micro-chimney formation above an anodic area in a culture of strain IS4 after three months of incubation. Bar, 10 µm.

Fig. S8. Late stage of micro-chimney formation in a culture of strain IS4 after six months of incubation. Bar, 200 µm.

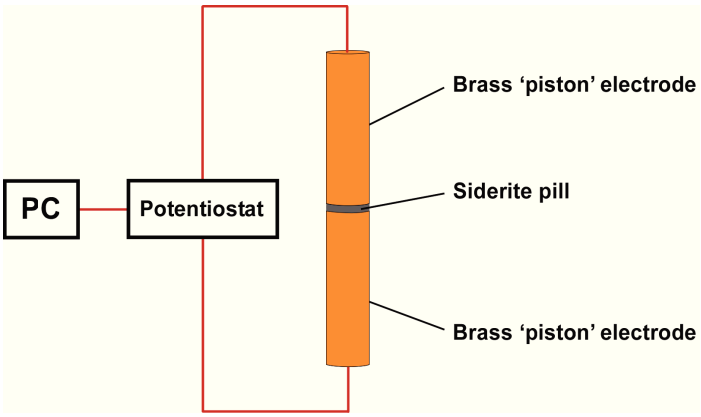

Fig. S9. Piston electrode set-up for measurement of conductivity of a compressed siderite mineral pill.

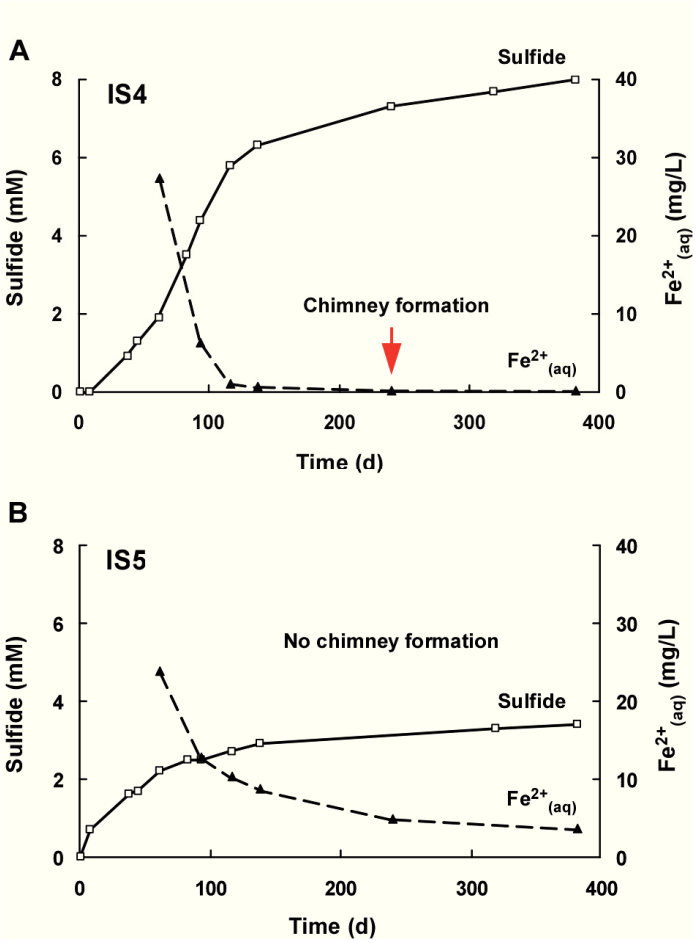

Fig. S10. Sulfide production (determined as sulfate consumption) and decrease of dissolved ferrous iron due to carbonate precipitation in long-term incubations of corrosive SRB. Strain IS4 (A) which was more alkali-tolerant than strain IS5 (B) grew up to higher *pH* [*pH* increase due to equation (5)] thus promoting precipitation according to $Fe^{2+} + HO^- + HCO_3^- \rightarrow FeCO_3 + H_2O$. This favored formation of micro-chimneys (Fig. 5C). Six cultures of each strain were incubated in parallel and sacrificed at different time points for SEM analysis (Fig. 4, Figs S6 to 8). Formation of crater- and chimney-like structures in cultures of strain IS4 coincided with the drop of $[Fe^{2+}_{(aq)}]$ below detection limit (0.2 mg/l). The initial *pH* was 7.3. Strain IS4 reached $pH \approx 9$. Activity of strain IS5 ceased at $pH \approx 8$.

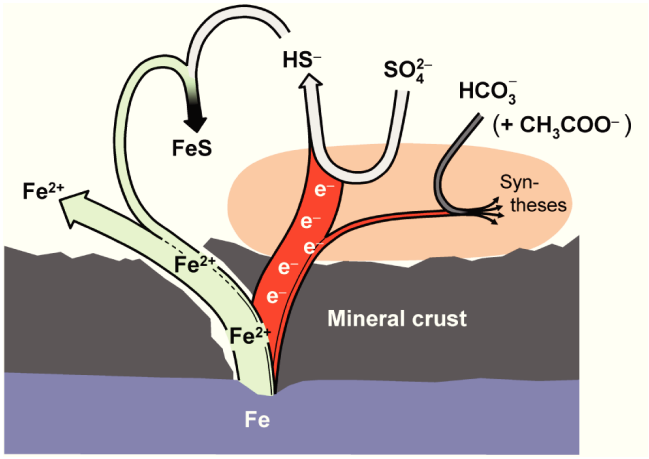

Fig. S11. Electron flow from metallic iron into the catabolism and anabolism.

Table S1. Compilation of corrosion rates recorded for (anoxic) natural and engineered environments, and for laboratory cultures of sulfate-reducing bacteria.

Location	Type of environment	Corrosion rate (mm yr^{-1}) [a]	Method [b]	Reference
Bohai Bay, China	Marine sediment	**0.03 – 0.09**	Weight loss	Li (2009)
Draugen Oil Field, Norwegian North Sea	Produced water re-injection system; untreated produced water	**0.12**	Electrochemical [c]	Vik *et al.* (2007)
Tonnenlegerbucht, German North Sea	Marine anoxic sediment	**0.12 – 0.28**	Weight loss	This study
South Korea	Gas transmission pipelines; disbonded coating	**0.33 – 0.47**	Pit measurement	Li *et al.* (2000)
Gullfaks Oil Field, Norwegian North Sea	Water injection system; biocide treatment	**0.09 – 0.75**	Weight loss	Boedtker *et al.* (2008)
Culture	**Type of energy source, medium [d]**	**Corrosion rate (mm yr^{-1}) [e]**	**Method**	**Reference**
Desulfovibrio sp.	Lactate-based, freshwater	**0.007**	Weight loss	Hardy and Brown (1984)
Desulfovibrio vulgaris, Woolwich	Lactate-based, freshwater	**0.024**	Weight loss	Gaylarde (1992)
Desulfovibrio desulfuricans, New Jersey	Lactate-based, marine	**0.094**	Weight loss	Beech *et al.* (1994)
Desulfovibrio desulfuricans	Lactate-based, brackish	**0.285**	Weight loss	Bell and Lim (1981)
SRB bioreactor	Lactate-based, brackish	**0.408**	Weight loss	Hubert *et al.* (2005)
Desulfovibrio vulgaris, Hildenborough	H_2, freshwater [f]	**0.500**	Electrochemical [g]	Pankhania *et al.* (1986)
Sterile artificial seawater	Fe^0 lithotrophy, marine	**0.010**	Weight loss	This study
Desulfopila inferna	Fe^0 lithotrophy, marine	**0.012**	Weight loss	This study
'Desulfopila corrodens', strain IS4	Fe^0 lithotrophy, marine	**0.311**	Weight loss	This study
'Desulfovibrio ferrophilus', strain IS5	Fe^0 lithotrophy, marine	**0.710**	Weight loss	This study

a. Corrosion rate in natural and engineered environments. The recorded range is given. Corrosion must not necessarily be influenced by SRB in these systems.
b. Method of corrosion rate determination. Weight loss is considered the most accurate technique.
c. A linear polarisation resistance (LPR) probe was used.
d. Energy source for SRB metabolism is indicated. All cultures contained iron or mild steel. 'Fe^0 lithotrophy' indicates that metallic iron was the only available source of reducing equivalents. Salt content of media (freshwater, brackish, marine) is also designated.
e. Corrosion rate in cultures of SRB. The maximal reported value is given. The large range of corrosion rates for SRB with external energy source is attributed to the sometimes protective properties of formed FeS films (see text).
f. H_2 from previous polarisation experiment was available in these cultures.
g. Calculated from slope of cathodic polarisation curve by overvoltage-intercept method.

Table S2. Vitamins in used media.

Vitamin	Concentration (µg l^{-1})
4-Aminobenzoic acid	40
D(+)-Biotin	10
Nicotinic acid	100
Ca-D(+)-Pantothenate	50
Pyridoxine hydrochloride	150
Folic acid	40
Liponic acid	15
Thiamine hydrochloride	100
Riboflavin	25
Cyanocobalamin	50

Table S3. Conductivity values measured in an incubation device with split coupon with corrosive cultures of strains IS4 and IS5, and with sterile artificial seawater. Iron is provided as the sole source of electrons.

	Slot bridged by sulphidic crust [a]	Slot bridged by seawater (control) [b]
Supplied outer voltage (V_O)	0.2 – 0.4 V	0.2 – 0.3 V
Voltage at split coupon (V_S)	0.20 V	0.20 V
Measured current	0.14 – 0.31 A	$0.3 – 0.7 \cdot 10^{-4}$ A
Conductance	0.72 – 1.56 S	$1.5 – 3.5 \cdot 10^{-4}$ S
Conductivity	27.4 – 43.5 S m^{-1}	$0.5 – 1.7 \cdot 10^{-2}$ S m^{-1}
Resistance	0.64 – 1.39 Ω	$2.9 – 6.7 \cdot 10^{3}$ Ω
Resistivity	$2.3 – 3.7 \cdot 10^{-2}$ Ω m	$0.6 – 2.1 \cdot 10^{2}$ Ω m

a. Values refer to data range obtained from 4 biological replicates (3 cultures of strain IS4 and one culture of strain IS5);
b. Values refer to data range obtained from 3 sterile incubations.

Table S4. Electrical conductivity of selected substances.

Material	Conductivity (S m^{-1})	Reference
Iron, 99.98% pure	$1.1 \cdot 10^{7}$	a
Steel, plain	$5.6 \cdot 10^{6}$	b
Graphite	$1.5 \cdot 10^{6}$	b
Steel, stainless	$1.4 \cdot 10^{6}$	b
Troilite (FeS)	$1.0 \cdot 10^{1} – 1.0 \cdot 10^{6}$	Pearce *et al.* (2006)
Pyrrhotite ($Fe_{1-X}S$), mineral	$2.0 \cdot 10^{4} – 1.0 \cdot 10^{5}$	Parasnis (1956)
Pyrrhotite ($Fe_{1-X}S$), ore	$1.0 \cdot 10^{3} – 1.0 \cdot 10^{5}$	Parasnis (1956)
Magnetite (Fe_3O_4)	$1.0 \cdot 10^{4} – 1.0 \cdot 10^{5}$	Schwertmann & Cornell (2003)
Pyrite (FeS_2), mineral	$2.0 \cdot 10^{1} – 2.0 \cdot 10^{4}$	Parasnis (1956)
Pyrite (FeS_2), ore	$1.0 \cdot 10^{-1} – 1.0 \cdot 10^{4}$	Parasnis (1956)
SRB corrosion crust	$\mathbf{2.7 \cdot 10^{1} – 6.4 \cdot 10^{1}}$	**This study**
Germanium	$2.2 \cdot 10^{0}$	b
G. sulfurreducens biofilm	$0.5 \cdot 10^{0}$	Malvenkar et al. (2011)
Silicon	$1.6 \cdot 10^{-3}$	b
Siderite mineral	$\mathbf{1.2 \cdot 10^{-7}}$	**This study**
Goethite (FeOOH)	approx. $1.0 \cdot 10^{-7}$	Schwertmann & Cornell (2003)
Siderite ($FeCO_3$)	$1.2 \cdot 10^{-10}$	Schön (1996)
Calcite ($CaCO_3$)	$2.0 \cdot 10^{-13} – 1.1 \cdot 10^{-14}$	Schön (1996)

a. CRC Handbook of Chemistry and Physics.
b. www.physics.info/electric-resistance/

References

Atkins, P., and De Paula, J. (2006) *Physical Chemistry*. Oxford: Oxford University Press.

Beech, I.B., Cheung, C.W.S., Chan, C.S.P., Hill, M.A., Franco, R., and Lino, A.R. (1994) Study of parameters implicated in the biodeterioration of mild steel in the presence of different species of sulfate-reducing bacteria. *Int Biodet Biodegr* **34**: 289−303.

Beech, I.B., and Sunner, I.A. (2007) Sulphate-reducing bacteria and their role in corrosion of ferrous materials. In *Sulphate-reducing bacteria: environmental and engineered systems*. Barton, L.L., and Hamilton, W.A. (eds). Cambridge: Cambridge University Press, pp. 459−482.

Bell, R.G., and Lim, C.K. (1981) Corrosion of mild and stainless steel by four tropical *Desulfovibrio desulfuricans* strains. *Can J Microbiol* **27**: 242−245.

Bockris, J.O.M., and Reddy, A.K.N. (1970) *Modern Electrochemistry*. New York: Plenum.

Bødtker, G., Thorstenson, T., Lillebø, B.L.P., Thorbjørnsen, B.E., Ulvøen, R.H., Sunde, E., and Torsvik, T. (2008) The effect of long-term nitrate treatment on SRB activity, corrosion rate and bacterial community composition in offshore water injection systems. *J Ind Microbiol Biotechnol* **35**: 1625−1636.

Dean, J.A. (1992) *Lange's Handbook of Chemistry*. New York: McGraw-Hill.

Dinh, H.T., Kuever, J., Mußmann, M., Hassel, A.W., Stratmann, M., and Widdel, F. (2004) Iron corrosion by novel anaerobic microorganisms. *Nature* **427**: 829−832.

Gaylarde, C.C. (1992) Sulfate-reducing bacteria which do not induce accelerated corrosion. *Int Biodet Biodegr* **30**: 331−338.

Hamann, C.H., Hamnett, A., and Vielstich, W. (2007) *Electrochemistry*, 2nd edn. Weinheim: Wiley.

Hardy, J.A., and Bown, J.L. (1984) The corrosion of mild steel by biogenic sulfide films exposed to air. *Corrosion* **40**: 650−654.

Hubert, C., Nemati, M., Jenneman, G., and Voordouw, G. (2005) Corrosion risk associated with microbial souring control using nitrate or nitrite. *Appl Microbiol Biot* **68**: 272−282.

Jack, T.R. (2002) Biological corrosion failures. In *ASM Handbook Volume 11: Failure Analysis and Prevention*. Shipley, R.J., and Becker, W.T. (eds). Materials Park: ASM International, pp. 881−898.

Koch, G.H., Brongers, M.P.H., Thompson, N.G., Virmani, Y.P., and Payer, J.H. (2001) Corrosion cost and preventive strategies in the United States. In: CC Technologies Laboratories NACE International.

Lee, W., Lewandowski, Z., Nielsen, P.H., and Hamilton, W.A. (1995) Role of sulfate-reducing bacteria in corrosion of mild-steel - a review. *Biofouling* **8**: 165−194.

Li, Y.T. (2009) Corrosion behaviour of steel in beach soil along Bohai Bay. *Corrosion Eng Sci Tech* **44**: 91−95.

Li, S., Kim, Y., Jeon, K., and Kho, Y. (2000) Microbiologically influenced corrosion of underground pipelines under the disbonded coatings. *Met Mater* **6**: 281−286.

Malvankar, N.S., Vargas, M., Nevin, K.P., Franks, A.E., Leang, C., Kim, B.C. et al. (2011) Tunable metallic-like conductivity in microbial nanowire networks. *Nat Nanotech* **6**: 573−579.

Pankhania, I.P., Moosavi, A.N., and Hamilton, W.A. (1986) Utilization of cathodic hydrogen by *Desulfovibrio vulgaris* (Hildenborough). *J Gen Microbiol* **132**: 3357−3365.

Parasnis, D.S. (1956) The electrical resistivity of some sulphide and oxide minerals and their ores. *Geophys Propect* **4**: 249−279.

Patrick, W.A., and Thompson, W.E. (1952) Standard electrode potential of the iron-ferrous ion couple at 25°. *J Am Chem Soc* **75**: 1184−1187.

Pearce, C.I., Pattrick, R.A.D., and Vaughan, D.J. (2006) Electrical and magnetic properties of sulfides. *Rev Mineral Geochem* **61**: 127−180.

Randall, M., and Frandsen, M. (1932) The standard electrode potential of iron and the activity coefficient of ferrous chloride. *J Am Chem Soc* **54**: 47−54.

Revie, R.W. (2011) *Uhlig's Corrosion Handbook*. New York: Wiley.

Rickard, D., and Luther, G.W. (2007) Chemistry of iron sulfides. *Chemical Reviews* **107**: 514−562.

Schwertmann, U., and Cornell, R.M. (2003) *The Iron Oxides*. Weinheim: Wiley.

Schön, J.H. (1996) Electrical properties of rocks. In *Physical properties of rocks: Fundamentals & principles of petrophysics*. Schön, J.H. (ed). Oxford: Pergamon Press, p. 379.

Vik, E.A., Janbu, A.O., Garshol, F., Henninge, L.B., Engebretsen, S., Kuijvenhoven, C. et al. (2007) Nitrate-based souring mitigation of produced water - side effects and challenges from the Draugen produced water re-injection pilot, paper SPE 106178. In *SPE International Symposium on Oilfield Chemistry*. Houston.

Symbols used in equations (SI units; and other, convenient units)

a	Area (m^2; cm^2)
d	Distance, length (m)
E_{SR}	Equilibrium redox potential of sulfate reduction (V)
E_{FeDiss}	Equilibrium redox potential of iron dissolution (V)
$E°_{pH7}$, $E°'$	Equilibrium redox potential at pH 7, but otherwise standard conditions (V)
K_{eq}, K_a	Equilibrium constant
F	Faraday constant (C mol^{-1})
ϕ	Operational redox potential (V)
I	Electrical current (A)
i	Current density (A m^{-2})
i_{corr}	Corrosion current density (A m^{-2})
M_a	Atomic mass (kg mol^{-1})
M_A	Atomic mass of substance A (kg mol^{-1}; g mol^{-1})
m_A	Mass of substance A (kg)
m_{Bio}	Biomass (kg; g)
m_{Min}	Mass of minerals in corrosion crust (kg)
m_{AeCO3}	Mass of alkaline earth (Mg, Ca) carbonates (kg)
n	Amount (mol)
n_A	Amount of substance A (mol)
n_{FeAnab}	Amount of iron oxidized anabolically for biosynthesis (mol)
$n_{FeCatab}$	Amount of iron oxidized catabolically by sulfate reduction (mol)
n_{FeEMIC}	Amount of Fe^0 oxidized by EMIC (mol)
n_{FeNonS}	Amount of non-sulfidic iron (mol)
$n_{Fe(II)}$	Amount of total ferrous iron formed, equivalent with $n_{\Delta Fe(0)}$ (mol)
$n_{\Delta Fe(0)}$	Amount of metallic iron lost by anaerobic oxidation, equivalent with $n_{Fe(II)}$ (mol)
n_{FeS}	Amount of sulphidic iron (mol)
n_e	Number of electrons released per metal atom
q	Quotient, molar (mol mol^{-1})
q_{EMIC}	Quotient iron oxidized by EMIC per total iron oxidized by MIC (mol mol^{-1})

q_{Anab}	Quotient iron oxidized for biosynthesis per total iron oxidized by EMIC (mol mol^{-1})
q^{m}_{Bio}	Quotient biomass per total corrosion crusts (kg kg^{-1})
ρ	Density (kg m^{-3})
σ	Electrical conductivity (S m^{-1})
t	Time (s; yr)
θ	Metal thickness (m; mm)
v^{m}_{corr}	Rate of metal mass loss (kg s^{-1}; mg yr^{-1})
v^{n}_{corr}	Rate of metal amount loss (mol s^{-1}; mmol yr^{-1})
$v^{\theta}_{\mathrm{corr}}$	Rate of metal thickness loss (m s^{-1}; mm yr^{-1})
V	Voltage (V)
Y_{Anab}	Growth yield, cell mass per Fe^0 oxidized with sulfate (kg mol^{-1}; g mol^{-1})

Chapter D.2

Accelerated cathodic reaction in microbial corrosion of iron due to direct electron uptake by sulfate-reducing bacteria

Hendrik Venzlaff[1], Dennis Enning[2], Jayendran Srinivasan[1], Karl J.J. Mayrhofer[1], Achim Walter Hassel[3], Friedrich Widdel[2] and Martin Stratmann[1]

[1] Max Planck Institute for Iron Research, Max-Planck-Straße 1, 40237 Düsseldorf, Germany

[2] Max Planck Institute for Marine Microbiology, Celsiusstraße 1, 28359 Bremen, Germany

[3] Institute for Chemical Technology of Inorganic Materials, Johannes-Kepler University, Altenberger Straße 69, 4040 Linz, Austria

Manuscript *submitted* to

Corrosion Science (2012)

Abstract

Microbially influenced corrosion by sulfate-reducing bacteria (SRB) is conventionally attributed to three effects, the chemical corrosiveness of H_2S, a facilitated abiotic reduction of H^+ at deposited FeS, and the biological consumption of chemically formed (cathodic) H_2. Recently, another mechanism, viz. direct electron uptake from iron by specialized lithotrophic SRB, has been demonstrated. Here, we conducted potentiodynamic measurements with iron electrodes colonized by such a highly corrosive SRB. This strain stimulated the cathodic reaction significantly, while a conventional H_2-consuming strain had no effect. Additionally, inactivation of electrode-attached bacteria significantly reduced current stimulation, thus confirming its biological rather than FeS-catalyzed origin.

Highlights:

- Corrosive SRB strain IS4 strongly accelerates the cathodic reaction of iron by direct electron uptake
- Hydrogenotrophic control strain HS3 does not influence the cathodic reaction
- Deposited ferrous sulfides do not stimulate the cathodic reaction
- Deposited ferrous sulfides mediate electrical contact between metal and cells

Keywords: Iron (A); Polarization (B); EIS (B); Microbiological corrosion (C)

1. Introduction

Whereas iron corrosion by oxygen from air is, to our present knowledge, a purely electrochemical process, iron corrosion in neutral media in the absence of air (as, for instance, in aqueous underground or inside iron pipes) is largely biologically influenced. Sulfate-reducing bacteria (SRB) are commonly considered to be the main originators of this microbiologically influenced corrosion (MIC; Hamilton, 1985; Lee *et al*., 1995). SRB gain their biochemical energy for growth by reducing sulfate (SO_4^{2-}) to sulfide (H_2S, HS^-) with natural organic compounds as electron donors that are oxidized to CO_2 (also referred to as sulfate respiration). In addition, many SRB can also utilize molecular hydrogen (H_2), a common product of other bacteria involved in the biological breakdown of organic compounds in oxygen-free aquatic systems such as sewers, sediments and swamps.

The mechanisms by which SRB act upon metallic iron have been controversially discussed in the literature (von Wolzogen Kühr and van der Vlugt, 1934; Costello, 1974; Booth and Tiller, 1960; Hardy, 1983). The basic feature of previously described models is always the low-potential electron release by the metal according to

$$Fe^{2+} + 2\ e^- \rightleftarrows Fe^0 \qquad (1)$$

$$E_{T=298,15K} = -0.47\ V + 0.0296\ V\ \lg(a_{Fe^{2+}})$$

[the common redox potential ($E° = -0.44$ V) revised according to Rickard and Luther (2007)]. The sulfide formed by SRB behaves as a chemically aggressive compound [Costello, 1974; Morris *et al*., 1980; Sherar *et al*., 2011; for review see also Lee *et al*., (1995)], resulting in the bulk equation $Fe^0 + H_2S \rightarrow FeS + H_2$. In this way, SRB act indirectly by chemical reaction of their metabolic end product (chemical microbially influenced corrosion, CMIC).

A fundamentally different, traditional mechanistic proposal is based on the inherent ability of many SRB to utilize H_2 as electron donor ($4\,H_2 + SO_4^{2-} + 2\,H^+ \rightarrow H_2S + 4\,H_2O$). Reduction of protons in water to hydrogen according to

$$2\ H^+ + 2\ e^- \rightleftarrows H_2 \qquad (2)$$

$$E_{T=298,15K} = 0.00\ V + 0.0296\ V\ \lg(a_{H^+}{}^2/a_{H_2})$$

can in principle be linked with iron oxidation (Eq. 1) and results in the net reaction

$$Fe^0 + 2\ H^+ \rightarrow Fe^{2+} + H_2. \qquad (3)$$

Early investigators speculated that in the absence of microorganisms, the H_2 formed builds up a 'hydrogen film' at the metal surface, ultimately impeding reaction (3) and thus iron dissolution to progress (von Wolzogen Kühr and van der Vlugt, 1934; von Wolzogen Kühr, 1961); traditionally, this impediment is often referred to as 'polarization'. In the presence of microorganisms with the capability of H_2 utilization such as SRB, their effective scavenging of H_2 was suggested to lower the local partial pressure and through such 'depolarization' allow iron dissolution to proceed. This proposal became therefore known as 'cathodic depolarization theory'. Because H_2S combines with Fe^{2+} ions from the primary dissolution (Eq. 1), the net reaction (including bicarbonate that is readily available in many water systems) is

$$4\,Fe^0 + SO_4^{2-} + 3\,HCO_3^- + 5\,H^+ \rightarrow FeS + 3\,FeCO_3 + 4\,H_2O\,. \qquad (4)$$

From a merely thermodynamic perspective, however, the above considerations may be questioned. The redox potential of the electron donor (Eq. 1) is more negative than that of the electron acceptor (Eq. 2). Accordingly, the free energy of reaction (3) under standard conditions (except that $a_{H^+} = 10^{-7}$) is $\Delta G^\circ_{pH7} = -10.6$ kJ mol^{-1}, and the reaction can, in principle, proceed spontaneously. At environmentally relevant activities of Fe^{2+}(aq) that are significantly below standard activity, the Fe^{2+}/Fe^0 redox couple is even more negative, often $E_{environ} \leq -0.6$ V vs. standard hydrogen electrode (SHE), so that $\Delta G_{environ} \leq -36.7$ kJ mol^{-1}. For a thermodynamic halt ($\Delta G \geq 0$) of iron dissolution according to reaction (3), one would have to assume a 'hydrogen film' with a local fugacity corresponding to $p_{H_2} > 10^{11.3}$ Pa. Considering the extremely fast diffusion of H_2, viz. of the hydrogen species that is used by bacteria, such local build-up of a hydrogen film appears very unrealistic. If SRB have a direct influence on corrosion, an understanding can be only expected from the viewpoint of electrokinetics, in particular of H^+ reduction to H_2, rather than *via* mere thermodynamic considerations. H_2 formation on iron in circumneutral water is inherently slow, a 'kinetic bottle neck' due to limitations in proton availability and combination reactions forming H_2 (Cohen, 1979; Bockris and Reddy, 2000; Kaesche, 2003). Still, several hydrogenase-positive cultures of sulfate-reducing bacteria apparently stimulated the cathodic current ('depolarization') on mild steel electrodes (Horvàth and Sölti, 1959; Booth and Tiller, 1960; 1962). The authors attributed this to bacterial H_2-uptake from the electrode surface and, hence, interpreted the observation in favor of the 'classical' depolarization theory. The ability of SRB for scavenging H_2 from corroding iron and water has indeed been shown (Hardy, 1983; Cord-Ruwisch and Widdel, 1986; Pankhania *et al*., 1986).

However, an experimental misconception in the early electrochemical study of the postulated direct mechanism involving H_2 with conventional SRB strains was the addition of lactate, a routine, excellent cultivation substrate of SRB (Horvàth and Sölti, 1959; Booth and Tiller, 1960; 1962). Lactate represents a competitive electron donor in addition to 'cathodic' H_2 and, more importantly, leads to excessive concentrations of aggressive sulfide causing chemical corrosion (CMIC) and altering the electrode surface drastically. Costello (1974) and Hardy (1983) therefore omitted lactate and gave proof that cathodic depolarization did not occur in SRB cultures with metallic iron as the only source of electrons for the organisms; rather, acceleration of the cathodic reaction was shown to result from the reactivity of dissolved sulfide. Accelerated corrosion due to bacterial H_2-uptake from the metallic iron surface was consequently questioned by several authors, particularly as SRB incubated with iron alone did not accelerate corrosion (Spruit and Wanklyn, 1951; Dinh *et al*., 2004; Mori *et al*., 2010).

In another model of SRB-induced corrosion, stimulation of H^+-reduction to H_2 by catalytically active ferrous sulfides on the iron electrode was suggested (Booth *et al*., 1968; King and Miller, 1971). Hence, SRB were thought to scavenge H_2 from FeS rather than from the metallic surface. Chemically prepared, fine suspensions of FeS transiently accelerated the cathodic reaction and iron loss even in the absence of bacteria, viz. if H_2 was not consumed (King and Miller, 1971; King *et al*., 1973). However, a variety of both amorphous and crystalline iron sulfides exist which exhibit very different properties with regard to the corrosion of iron. Neither their properties nor the extent of their contribution to anaerobic iron corrosion are completely understood at the moment (Smith and Miller, 1975).

In another approach towards a mechanistic understanding of anaerobic corrosion, SRB were directly enriched and isolated with metallic iron as the only source of electrons (viz. without an organic substrate such as lactate) for sulfate reduction (Dinh *et al*., 2004). They severely corroded the metallic substrate with a rate of up to 0.7 mm Fe^0 yr^{-1}, corresponding to 61 µA cm^{-2} (Enning *et al*., 2012). The corrosion rate could not be explained by dependency on H_2, the chemical formation of which from iron and water was by far too slow (Dinh *et al*., 2004; Enning *et al*., 2012). This and the significant conductivity of the deposited FeS-containing crust (Enning *et al*., 2012) indicated a direct electron uptake (i.e., electrical microbially influenced corrosion, EMIC) by the attached cells according to

$$8\,e^- + SO_4^{2-} + 10\,H^+ \rightarrow H_2S + 4\,H_2O \qquad (5)$$

$$E_{average,\ T=298,15K} = +0.30\ V + 0.0074\ V\ \lg(a_{SO_4^{2-}}\ a_{H^+}{}^{10}\ a_{H_2S}{}^{-1})$$

and thus an effective by-pass of the H_2-formation reaction. The net reaction (combination of Eqs 1 and 5), which is the same as equation (4), results in significant mineral precipitation on the iron.

Such a postulated direct electron uptake urges upon corroboration by electrochemical measurements. If the novel SRB accelerate corrosion by direct electron uptake, this should be obvious from a shift of the free corrosion potential and from an increase of the cathodic current of iron electrodes in potential-controlled experiments. In the present study these effects were investigated using iron coupons colonized and encrusted (Eq. 4) by the corrosive SRB *Desulfopila corrodens* strain IS4 for electrochemical measurements in defined electrolyte. No organic electron donor was added, viz. all electrons for sulfate reduction were provided through the metal. Moreover, to distinguish between the impact of bacterial activity and their deposited iron sulfides, the current-potential relationship was measured prior to and after chemical inactivation of the colonizing bacteria. *Desulfovibrio* sp. strain HS3, an organism similar to SRB investigated in former 'depolarization' studies and growing well with H_2 served as control culture. The expected electrokinetic effects of strain IS4 were indeed observed, thus fully supporting the postulated enhancement of corrosion by direct biological electron uptake rather than by H_2-consumption.

2. Material and methods

2.1. Chemicals and organisms

All solutions and culture media were prepared from p.a. grade chemicals and ultrapure deionised water (Purelab Plus by Elga Labwater, Celle, Germany). Culture liquids were sterilized in an autoclave at 121°C for 25 minutes. Pre-cultures of the two isolated SRB strains used in this study, *Desulfopila corrodens* strain IS4 and *Desulfovibrio sp.* strain HS3 (Dinh *et al*., 2004; Enning *et al*., 2012), were incubated in butyl-rubber-stoppered glass bottles with artificial seawater medium (ASW; Widdel and Bak, 1992) buffered by CO_2/$NaHCO_3$, and provided with an anoxic headspace of CO_2/N_2 (10:90, v/v). ASW contained typically 28 mM sulfate as an electron acceptor and no oxidizable organic substrates. For the experiments including sulfate analysis, the sulfate concentration was lowered to 5 mM for more precise detection of consumption. Pre-cultures of SRB strains were grown on H_2 and subsequently flushed with CO_2/N_2 for 30 minutes to prevent transfer of dissolved sulfide and H_2 into the incubations. The cell density in inocula was determined by acridine orange (0.1 mg/ml) staining and epifluorescent microscopy (Zeiss Axiophot, Carl

Zeiss MicroImaging, Göttingen, Germany), so that all experiments could be started with identical cell numbers.

2.2. Free corrosion potential and potentiodynamic measurements

Electrochemical cell setup and incubation. Electrochemical cells were constructed as follows: Sheets of pure iron (99.877% Fe; < 0.06% Mn, < 0.03% Cu, < 0.01% C, < 0.005% P, < 0.005% N, < 0.005% Co, < 0.005% Sn, < 0.003% S) were mechanically ground, cut into coupons of the dimensions depicted in Fig. 1, and contacted with a silver wire (0.5 mm in diameter). Coupons were then cleaned with alkali soap and pure ethanol, sterilized by complete immersion in pure anoxic ethanol for 90 minutes and subsequently dried in a stream of N_2.

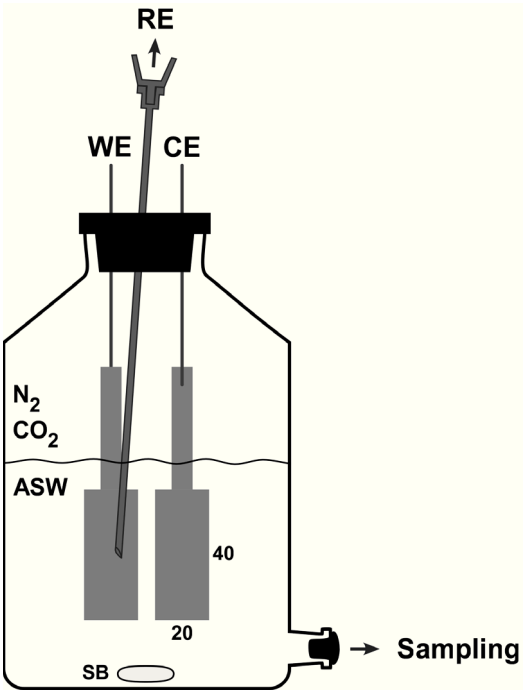

Fig. 1. Electrochemical cell for potential-controlled experiments. WE, working electrode (iron); CE, counter electrode (iron); RE, sterilized steel cannula as contact to the external reference electrode; ASW, artificial sea water medium; SB, magnetic stir bar. Anoxic headspace consists of CO_2/N_2 (10:90, v/v). Dimensions of electrodes (in mm) are identical for WE and CE.

Duran glass bottles (250 mL) filled with 200 mL of anoxic sterile ASW (electrolyte) were used as electrochemical cells (Fig. 1). Sodium sulfide (0.1 mM) was added as reducing agent to remove traces of residual oxygen and shorten the *lag*-phase of cultures. Each bottle was then equipped with a magnetic stir bar and the two sterilized iron coupons (WE and CE) in such a way that only the lower 5 cm of the coupons were immersed. Silver wires providing

electrical contact to the coupons were pierced through the butyl-rubber septum. For connection with the reference electrode, a sterilized steel cannula (13.201 stainless steel; Unimed S.A., Lausanne, Switzerland) of 0.8 mm in diameter was introduced into the cell through the top septum and connected to a glass holder *via* gas-tight butyl rubber tubing (not shown). The glass holder contained two compartments separated by a glass diaphragm. The electrode compartment of the glass holder was filled with 3 M KCl electrolyte and equipped with a standard Ag/AgCl reference electrode (type 6.0750.100 by Metrohm AG, Herisau, Switzerland). To maintain ionic conductivity between the main cell and the reference electrode compartment, ASW was sucked into the compartment so as to establish the ionic connection and held in place by a stopcock. The low volume to electrode surface ratio of around 5 ml cm^{-2} allowed reliable determination of sulfate consumption and ferrous iron formation.

Three electrochemical cells were prepared for each strain, i.e. six in total, and inoculated to initial cell densities of 10^6 cells ml^{-1}. Sodium acetate (1 mM) was added to cultures of heterotrophic strain HS3. Electrochemical cells were gently stirred (250 rpm) during incubation at 28°C. One culture of each strain was used for the potentiodynamic measurements directly after inoculation and a second culture after five days when the coupons with strain IS4 were just completely covered with black precipitate. The third culture of each strain was first used to record the development of the free corrosion potential over eight days and subsequently used for potentiodynamic measurements (see also Fig. S1). All potential-controlled measurements included chemical sterilization and thus sacrificed the colonized electrodes.

Determination of free corrosion potential. The free corrosion potential, E_{corr}, was followed by connecting the electrodes of the electrochemical cells during their incubation with strains IS4 and HS3 *via* a multiplexer (ECM 8 by Gamry Instruments) to a Reference 600 potentiostat (Gamry Instruments, Warminster, PA, USA).

Potentiodynamic measurements – Linear sweep voltammetry. Before measurement, the precipitate-covered electrodes were transferred into fresh electrolyte to avoid an impact of the changes in the electrolyte due to growth so as to ensure reproducible starting conditions. The electrolyte for the measurements was sterile basal ASW without vitamins and trace elements. All transfers were conducted in the N_2 atmosphere of a glove box to prevent oxidation processes at the encrusted electrodes. Electrodes of the electrochemical cell were then connected to a CompactStat potentiostat (Ivium Technologies B.V., Eindhoven, The Netherlands). Once E_{corr} had become constant, a cathodic potential sweep was performed over

a range of ΔE = −400 mV at a rate of 1 mV s^{-1}, starting at E_{corr}. Immediately afterwards, electrodes were disconnected and sterilized with 0.3% (v/v) glutaraldehyde. This concentration had been proven in separate experiments (Fig. S2) to be sufficient for complete inhibition of the activity of strain IS4. To ensure inactivation also of cells inside the possibly protective massive corrosion crust that had been formed after eight days in culture of strain IS4, the glutaraldehyde concentration was doubled for these electrodes. Electrodes were sterilized in the glutaraldehyde-containing medium at 6°C for 12 h, washed twice thoroughly in anoxic basal ASW, and again transferred into fresh anoxic ASW electrolyte. Washing steps and transfers were again performed under N_2 atmosphere in a glove box. Subsequent cathodic potential sweep of the sterilized electrodes was performed and recorded as before.

Control measurements were conducted in two electrochemical cells without inocula. One cell was filled with sterile anoxic ASW as sterile control, while the other cell was filled with anoxic ASW containing 1 mM sodium sulfide. The electrochemical control cells were incubated for four days until dissolved sulfide had completely reacted with the iron electrode and could not be detected any more in the sulfide-amended control. Potentiodynamic measurements were carried out as described above. Another separate electrochemical cell was incubated under aseptic conditions to monitor abiotic hydrogen formation.

2.3. Chemical analyses

A butyl-rubber-stoppered sampling port allowed for anaerobic and aseptic withdrawal of culture medium during incubation of electrochemical cells. Samples were immediately filtered (Acrodisc 13 mm syringe filter with 0.45µm Nylon membrane by Pall Life Sciences, Port Washington, NY, USA) to remove FeS particles and then analyzed for concentrations of sulfate and dissolved ferrous iron. The *pH* was measured in a separate, fresh sample with a SenTix MIC-D *pH*-sensitive electrode (WTW GmbH, Weilheim, Germany). Ferrous iron was quantified by inductively coupled plasma optical emission spectroscopy (ICP-OES; IRIS Intrepid HR Duo by Thermo Fisher Scientific, Waltham, MA, USA). Sulfate was quantified by ion chromatography (Metrohm 761 Compact IC, Metrohm AG, Herisau, Switzerland) with a conductivity detector. Ions were separated *via* a Metrosep A Supp 5-100 column with an eluent of 3.2 mM Na_2CO_3 and 1 mM $NaHCO_3$ at a flow rate of 0.7 ml min^{-1}. Hydrogen was quantified from headspace by gas chromatography with thermal conductivity detection (Shimadzu GC 8A, Shimadzu, Kyoto, Japan) and a Porapak Q N80/100 column (Machery-Nagel, Düren, Germany; 40°C, N_2 as carrier gas). Expected sulfide production from bacterial

scavenge of H_2 in electrochemical cells was calculated assuming the stoichiometry $4\,H_2 + SO_4^{2-} + 2\,H^+ \rightarrow H_2S + 4\,H_2O$.

2.4. Electrochemical impedance spectroscopy

To reveal the dielectric vs. conductive properties of the corrosion crust, electrochemical impedance spectroscopy (EIS) was performed with iron electrodes in the form of wires that were incubated with strains IS4 and HS3, as well as in sterile ASW as electrolyte. The setup of the electrochemical cell was similar as for the potential sweep experiments, except that platinum served as counter electrode. EIS measurements were carried out using a sinusoidal signal from 10^4 to 10^{-3} Hz with an amplitude of 10 mV around E_{corr}. Impedance spectra were fitted to an equivalent circuit using the ZView EIS analysis software (Scribner Associates Inc., Southern Pines, NC, USA).

2.5. Scanning electron microscopy

Iron coupons were incubated for 6 weeks in a batch culture with strain IS4 and HS3, respectively. Specimens were prepared for scanning electron microscopy as described elsewhere (Enning *et al*., 2012). SEM was performed in a Zeiss Leo 1550 FE-SEM (Carl Zeiss NTS GmbH, Oberkochen, Germany) at EHT between 5 and 15 kV.

3. Results and Discussion

Evidence for microbially enhanced corrosion of iron due to direct electron uptake (Eq. 5) and by-pass of the abiotic hydrogen formation was hitherto based on the much faster growth of novel sulfate-reducing bacteria with iron in comparison to conventional H_2-consuming strains (Dinh *et al*., 2004; Enning *et al*., 2012), and the significant electrical conductivity of the mineral crust covering the corroding metal (Enning *et al*., 2012). If the slow abiotic reduction of water-derived protons (Eq. 2) is indeed largely overlaid by a faster biological cathodic reaction (Eq. 5), this should be also obvious from electrochemical measurements with iron electrodes in cultures of corrosive strains and comparison with sterile controls and non-corrosive, conventional strains. First, the influence of *D. corrodens* strain IS4 on the free (mixed) corrosion potential (E_{corr}) was measured. Subsequently, the cathodic reaction (Eq. 5 vs. 2) was characterized by recording the external current density in response to imposed potential shifts towards values more negative than E_{corr}. In all these experiments, the electrons for sulfate reduction were solely provided *via* iron (lithotrophic growth conditions), viz. there was no organic electron donor such as the otherwise frequently employed lactate. Finally, it

was investigated whether the assumption of conductive FeS structures within non-conductive (dielectric) carbonates (Eq. 4; Enning *et al.*, 2012) is corroborated by impedance measurements.

3.1 Influence of corrosive SRB on the free corrosion potential of iron

Fig. 2 visualizes the significant differences in the coverage of the iron surface in cultures of the corrosive and non-corrosive strain. Strain IS4 led to massive deposition of corrosion products while control strain HS3 caused only slight changes of the surface (Fig. 2). Cells of strain IS4 occurred embedded in and attached to corrosion products. The spherical structures (Fig. 2A) represent sulfur-free carbonates surrounded by a mixture of sulfur-containing minerals, as revealed by energy dispersive X-ray spectroscopy (not shown).

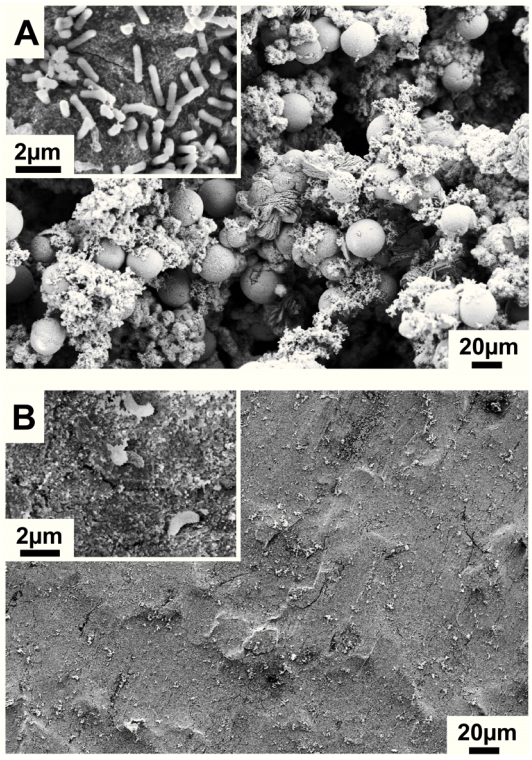

Fig. 2. Scanning electron micrographs of iron specimen surfaces after incubation for six weeks with a culture of (A) corrosive strain IS4 and (B) control strain HS3.

E_{corr} was continuously monitored during incubation of the iron electrodes with strains IS4 and HS3 during eight days (Fig 3A). Simultaneously, the microbial activity was recorded as consumption of the electron acceptor (Fig. 3B), sulfate, that is stoichiometrically converted to and precipitated as ferrous sulfide (Dinh *et al.*, 2012; Enning *et al.*, 2012). The observed sulfate consumption was compared to a calculated (theoretical) sulfate consumption that would occur solely by utilization of the abiotic 'cathodic' H_2 (0.25 mol SO_4^{2-} per mol H_2), the

formation of which was measured with iron in sterile medium. The free corrosion potentials in the two cultures began to diverge considerably after two days of incubation. The increasing shift of E_{corr} by strain IS4 towards less negative values is in full agreement with an increasing dominance of the biological (cathodic) electron uptake reaction (Eq. 5) over the abiotic proton reduction (Eq. 2). The electron-withdrawing cells of strain IS4 obviously became more and more established and grew during the incubation period.

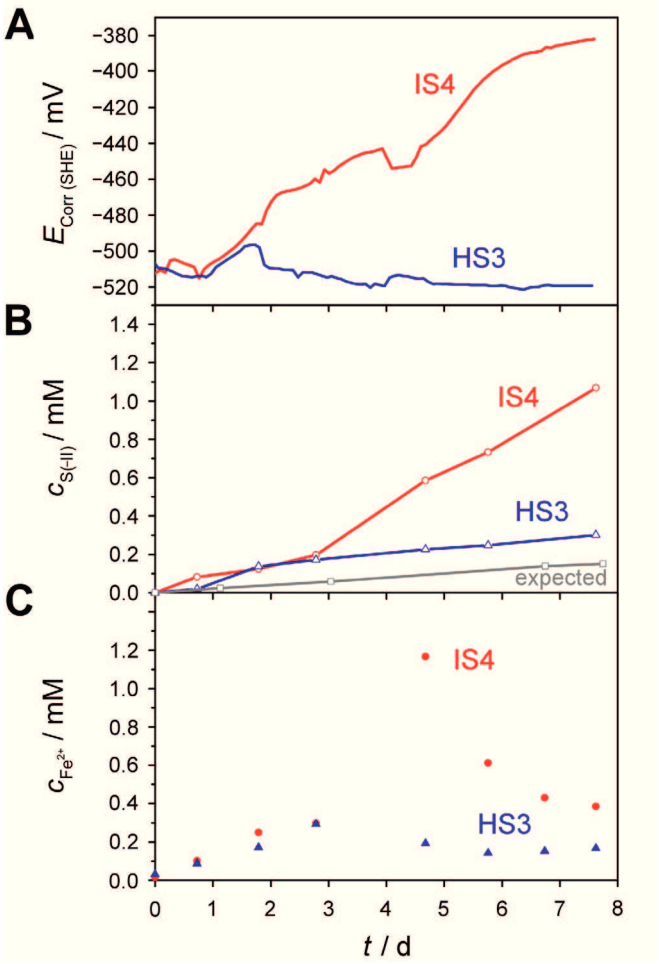

Fig. 3. Study of the corrosiveness of strain IS4 (red) and strain HS3 (blue; control strain) by incubation in electrochemical cells.

A. Continuous measurement of E_{corr}; values vs. standard hydrogen electrode (SHE).

B. Reduction of sulfate displayed as production of sulfide as an indicator of bacterial activity; expected values (grey) display calculated sulfide production solely from usage of chemically formed hydrogen.

C. Concentration of soluble ferrous iron.

Such a pronounced, steady shift of E_{corr} was not observed with control strain HS3. Only during the second day, strain HS3 caused a transient though rapid increase of E_{corr}. This is attributed to the formation of iron sulfide forms with temporary catalytic cathodic activity, i.e. with increased rate of abiotic H_2 formation (details in Fig. S3). This assumption is supported

by the initially increased sulfate reduction that must be due to H_2 utilization. In the longer run, E_{corr} in the presence of the non-corrosive strain HS3 became slightly more negative and the rate of sulfate reduction was not higher than the theoretical rate expected from mere utilization of 'cathodic' hydrogen.

Furthermore, also soluble ferrous iron [Fe^{2+}(aq)] was monitored during the incubation (Fig. 3C) because this is occasionally regarded as another parameter reflecting anaerobic iron corrosion. However, the initial increase of the soluble ferrous iron concentration in the incubation with strain IS4 was rather soon (day 4) followed by a rapid decrease. Even though the strong initial Fe^{2+}(aq) increase by strain IS4 (in comparison to strain HS3) does reflect the high corrosive activity, the effect is after a while masked by precipitation. Because FeS as the most insoluble Fe^{2+}(aq) mineral is assumed to precipitate immediately, the decrease of the Fe^{2+}(aq) concentration must be due to subsequent precipitation of $FeCO_3$ with increasing *pH*. The overall corrosion process according to reaction (4) is proton consuming and leads to an increase of *pH* even in a buffered solution, in particular close to the surface of the electrode (Katsounaros *et al*., 2011; Auinger *et al*., 2011), so that the bulk *pH* in the present incubations of strain IS4 increased from 7.1 to 7.8. Results indicate that Fe^{2+}(aq) monitoring is an ambiguous method for studying MIC, not only because of sulfide but also because of carbonate precipitation.

In conclusion, the pronounced differences in the development of E_{corr} in the cultures of strains IS4 and HS3 were as expected. The positive shift of the mixed potential, E_{corr} in cultures of strain IS4 reflects the postulated direct electrical coupling of the primary anodic reaction (Eq. 1) with biological sulfate reduction (Eq. 5) as the dominant cathodic reaction outcompeting coupling to H_2 evolution. It is true that such shifts of E_{corr} are also observed in electrochemical measurements with 'classical' SRB (Wanklyn and Spruit, 1952; Fonseca *et al*., 1998; Lee *et al*., 2006; Miranda *et al*., 2006); however, they are routinely provided with an organic electron donor leading to excessive sulfide. The abiotic shift of E_{corr} by sulfide is attributed to two factors, an accelerated cathodic reaction on the one hand and passivation by a particular type of the formed FeS layer on the other hand. As the strong shift in E_{corr} alone is no proof for the acceleration of the cathodic reaction (Mansfield and Little, 1991) by direct electron uptake, this assumption was further verified by investigating this half-reaction by potentiodynamic measurements.

3.2. Revealing the microbial cathodic activity by linear sweep voltammetry

If strain IS4 significantly increases E_{corr} towards more positive potentials by catalyzing a fast cathodic reaction, this should become obvious also in the increased cathodic current upon imposing a more negative electrode potential than E_{corr} (ΔE). Such recorded current should be higher than in sterile control experiments or with non-corrosive SRB that lack the ability to directly derive electrons from iron. Furthermore, if increase of the cathodic current is due to biological rather than to abiotic catalysis, e.g. by precipitated ferrous sulfide (Eq. 4), inactivation of the cells should decrease the cathodic current.

The first task was to search for an appropriate sterilizing procedure for the crucial control measurements with inactivated cells. Such a procedure should effectively and specifically inactivate all crust-associated bacterial cells, but should not change the electrokinetic properties of the iron surface or the inorganic crust. Heat treatment or the biocide sodium azide affected the electrokinetic behaviour even of blank and sterile electrodes. Detergents (e.g. Tween-20), on the other hand, did not sufficiently inactivate cells. The best-suited sterilizing agent was glutaraldehyde. It inhibited sulfate reduction (Fig. S2) and had no significant effect on iron electrodes.

The electrodes incubated with the bacteria were transferred to fresh medium for the investigation by linear sweep voltammetry (LSV). In this way, all measurements were conducted in electrolyte of identical composition, which excludes any influence by compositional changes of the electrolyte during incubation. The LSV measurements were performed shortly after inoculation (day 0) and after five and eight days of incubation with strains IS4 or HS3 (Fig. 4). The chosen scan rate of 1 mV s^{-1} is assumed to be slow enough for attached microorganisms to reach their metabolic steady state (Marsili *et al*., 2008; Torres *et al*., 2010). Briefly after inoculation, there was no significant difference in the current response to the applied potential between electrodes before and after treatment with glutaraldehyde. Neither was there a difference between the incubations with strains IS4 and HS3. The short incubation period was obviously insufficient for bacterial attachment to the electrodes. The minor differences before and after the chemical sterilization can be interpreted as a slight effect of glutaraldehyde. After five days of incubation with strain IS4, when the electrode had just been completely covered with black precipitate, there was already a pronounced difference between the cathodic currents before and after glutaraldehyde treatment, viz. obvious biological cathodic activity. After eight days, the cathodic activity of strain IS4 was even more pronounced (Fig. 5A), indicating higher bacterial activity due to further increased cell numbers. However, the voltammograms did not increase continuously,

but rather exhibited irregularities. Apparently, the electrochemically stimulated bacterial sulfate reduction (Faradaic process) was overlaid by non-Faradaic processes, e.g. charging of capacitances in the porous semiconductive crust (King and Miller, 1971; Marsili *et al.*, 2008); such non-Faradaic processes were indicated by supplementary potentiodynamic experiments with different sweep rates (Fig. S4).

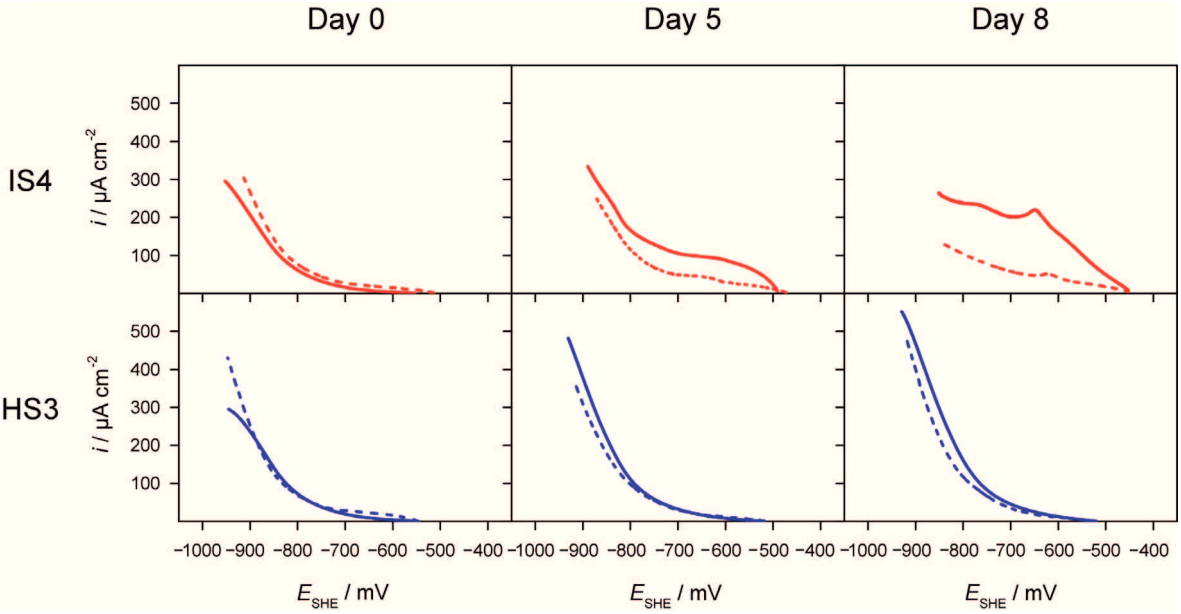

Fig. 4. Cathodic current density (i) vs. applied potential (displayed vs. standard hydrogen electrode, E_{SHE}) of iron electrodes incubated briefly (day 0) and for five and eight days with corrosive strain IS4 (red) and non-corrosive strain HS3 (blue). Measurements were performed in fresh artificial seawater medium as electrolyte with viable cells (solid line) and after sterilization with glutaraldehyde (dashed line). The potential sweep with 1 mV s^{-1} ranged from the free corrosion potential (E_{corr}; start) to −400 mV below E_{corr}.

Additionally, glutaraldehyde-treated electrodes with strain IS4 (Fig. 4, day 5 and 8) showed some residual activity with respect to the cathodic current in comparison to the electrokinetic behaviour at the beginning (day 0) or to the electrodes incubated with control strain HS3. Therefore, residual metabolic activity (including the ability for enzymatic H_2 production (Dinh *et al.*, 2004; Enning *et al.*, 2012) of cells not fully inactivated due to deep burial in the crust cannot be excluded. Neither can some abiotic cathodic catalysis of the thick sulfidic precipitate formed by strain IS4 be excluded at this stage. A certain catalytic effect of ferrous sulfide in cathodic proton reduction could indeed be shown in a purely abiotic experiment. When a sterile, blank iron electrode was allowed to react with 1 mM dissolved sulfide (concentration as produced by strain IS4 after eight days), the cathodic current increased slightly at a given ΔE (Fig. 6).

The electrode colonized by strain IS4 showed an increased current density at potentials down to ΔE = −150 mV (Fig. 4). If ΔE was shifted by more than −150 mV, the voltammograms of the electrodes from different incubation periods approached each other and showed an exponential increase, as characteristic for abiotic H_2 evolution. As all enzymatic and living systems, the colonizing sulfate-reducing cells have their maximum (or saturation) activity (known as v_{max}) which is reached while the abiotic reaction is increasingly coming into play as the electrode potential deviates further from E_{corr}.

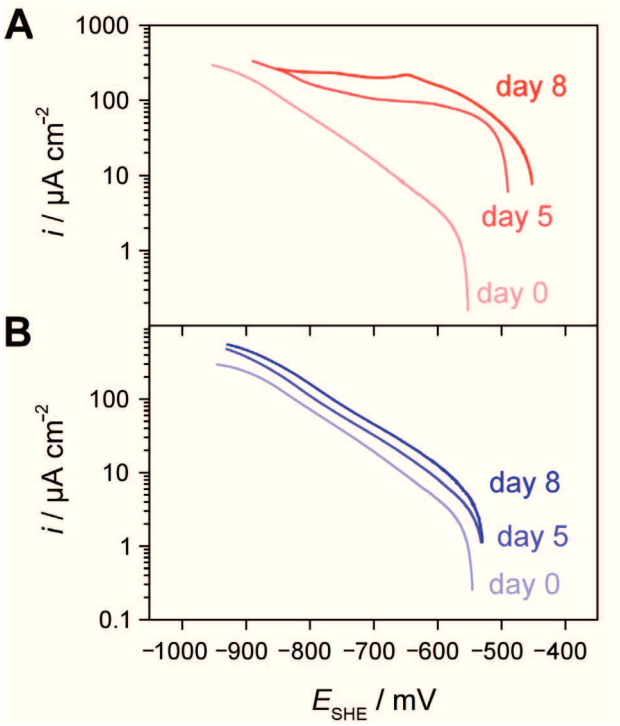

Fig. 5. Comparison of voltammograms displayed in Fig. 4 in a semi-logarithmic plot with viable cells of corrosive strain IS4 (A) and non-corrosive strain HS3 (B).

In conclusion, LSV measurements show that acceleration of cathodic reaction is largely a direct biological effect. This strongly supports the model of direct biological electron uptake by specialized lithotrophic SRB such as strain IS4 through an electroconductive, sulfidic corrosion layer, Furthermore, the absence of any cathodic stimulation by hydrogen-consuming strain HS3 (Fig. 5B) clearly challenges the classical ‘cathodic depolarization theory’, i.e. accelerated corrosion due to microbial H_2 uptake.

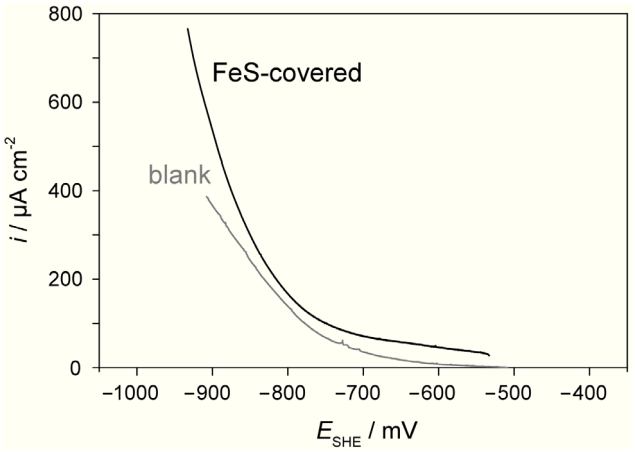

Fig. 6. Voltammograms recorded for a sterile blank and FeS-covered iron electrode in fresh sterile anoxic ASW.

3.3. Electrical impedance spectroscopy of corrosion crust

Based on X-ray microanalyses, the measured conductivity of the corrosion crust formed by strain IS4 was attributed to the presence of FeS (Enning *et al*., 2012), which is a long-known semiconductor. On the other hand, one may envisage that strain IS4 directs crust mineralization such that FeS within the carbonaceous crust assumes particularly conductive forms that do not occur in FeS-$FeCO_3$ co-precipitated unspecifically during mere consumption of 'cathodic' hydrogen. However, the conductivity of the crust formed by strain IS4 could not be compared to that of unspecific co-precipitate because the available quantities of the latter were insufficient for the previous methodological approach (Enning *et al*., 2012). Here, electrochemical impedance spectroscopy (EIS) was employed as a method suitable for small quantities to investigate possible differences with respect to the electronic properties of the precipitates formed on iron wires by the corrosive and non-corrosive strain.

EIS measurements indicated only a single time constant, irrespective of the bacterial strain and incubation time (Fig. S5). The data were fitted to a basic, Randles cell-like equivalent circuit (Fig. 7A). More elaborated equivalent circuits including for example several time constants (representing biofilms or passive layers) or Warburg impedances did not result in better fitting of the spectra. Whilst the fitting routine was more simplistic, the calculated results resemble previous findings (Keresztes *et al*., 2001; Miranda *et al*., 2006; Castenada and Benetton, 2008). An initial steep increase (up to around 45 kΩ cm^2) in the polarization resistance (R_p) of sterile electrodes revealed the formation of a non-conductive, passive layer, probably consisting of iron carbonates and hydroxides (Fig 7B). Incubation of the iron wire with SRB decreased the resistance upon onset of sulfate reduction, indicating conversion of the initial layer to semiconductive (less than 1 kΩ cm^2) sulfides. Conversion to iron sulfides

and their further deposition was much faster and more pronounced in cultures of corrosive strain IS4 than in cultures of the non-corrosive strain HS3. The capacitance (C_d) of the formed layers was estimated using a constant phase element (CPE). In sterile incubations C_d remained at low values of around 0.1 to 0.3 mF cm^{-2}, implying the absence of charge mediation due to the non-conductive layer (Fig. 7C). In both SRB cultures, C_d increased during incubation approaching 4 mF cm^{-2} in culture HS3 and exceeding 40 mF cm^{-2} in culture IS4, thus indicating establishment of a conductive layer, most likely ferrous sulfide, that allows charging.

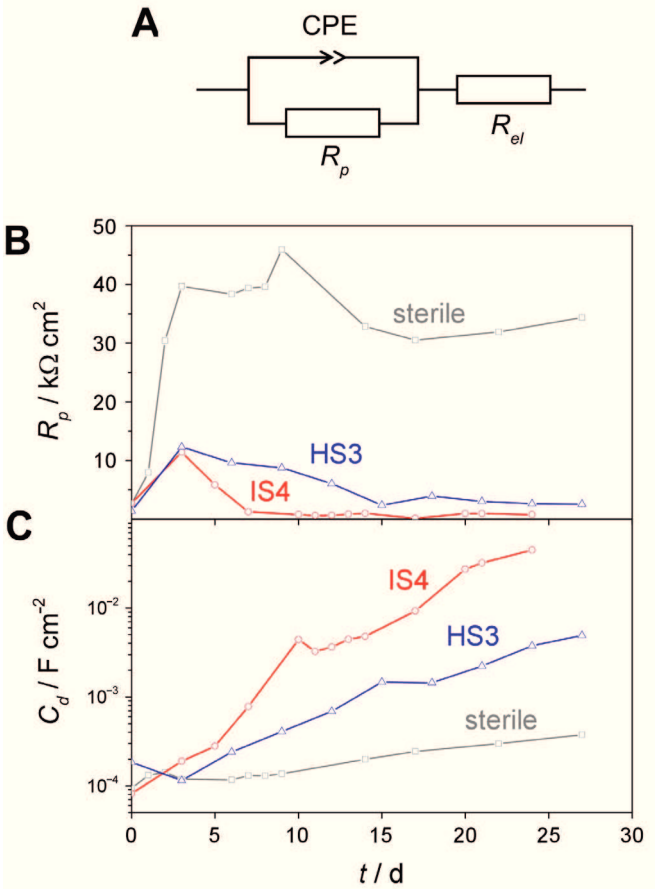

Fig. 7. Revealing the electronic properties of the sulfidic layers formed on iron wires in cultures of strains IS4 (corrosive; red) and strain HS3 (non-corrosive; blue). For comparison, measurements were also carried out with wires incubated in sterile seawater medium (grey).

A. Equivalent circuit used for calculation of polarization resistance, R_p, and capacitance, C_d; CPE, constant phase element.

B. Change of the polarization resistance during incubation.

C. Change of the capacitance during incubation.

In conclusion, EIS allowed some insights into the conductive and dielectric nature of the precipitates, but did not indicate that the corrosive strain formed a crust particularly suited for

mediation of electron flow. Apparently, co-precipitates of FeS and $FeCO_3$ are generally electroconductive.

4. Conclusions

Anaerobic microbial corrosion of iron in technical settings (*in situ*) represents a complexity of processes which are due to chemical effects of metabolites as well as to more intimate physiological microbe-metal interactions. Causal understanding of biocorrosion requires an experimental dissection into individual processes and their study under controlled conditions ('reductionistic' approach). A previously established approach, the (lithotrophic) use of metallic iron as the only electron donor for sulfate reduction and gain of energy for growth, was proven appropriate for gaining first insights into a supposedly central mechanism, the direct uptake of electrons from the metal through a semiconductive corrosion crust. The present study further corroborates this model:

- *Desulfopila corrodens* strain IS4, a representative of specially adapted, highly corrosive SRB, increases the free corrosion potential toward less negative values and enhances the current density at a given electrode potential.
- *Desulfovibrio sp.* strain HS3, which resembles 'conventional' sulfate reducing bacteria, efficiently utilizes molecular hydrogen, including that formed on iron in water, but neither influences the free corrosion potential nor the current density at a given potential. Hydrogen consumption is thus not a decisive factor in microbial corrosion.
- There is no indication for significant catalytic enhancement of the abiotic cathodic proton reduction to hydrogen by deposited ferrous sulfide crusts.
- Rather, deposited ferrous sulfide as a semiconductor plays a significant role in anaerobic corrosion by mediating electron flow from the metal to the cells.

Acknowledgements

We are indebted to Andrea Mingers and Daniel Kurz for ICP-OES measurements. Special thanks to Julia Garrelfs for discussion of the experimental concepts. This study was supported by funding from the Max Planck Society and the Deutsche Forschungsgemeinschaft (Project MA 4819/2-1).

References

Auinger, M., Katsounaros, I., Meier, J.C., Klemm, S.O., Biedermann, P.U., Topalov, A.A., Rohwerder, M., and Mayrhofer, K.J.J. (2011) Near-surface ion distribution and buffer effects during electrochemical reactions. *Phys Chem Chem Phys* **13**: 16384−16394.

Bockris, J.O´M., Reddy, A.K.N., and Gamboa-Aldeco, M. (2000) *Modern Electrochemistry, Vol. 2A: Fundamentals of Electrodics*, 2nd ed., New York: Kluwer Academic Publishers.

Booth, G.H., Elford, L., and Wakerley, D.S. (1968) Corrosion of mild steel by sulphate-reducing bacteria: an alternative mechanism. *Br Corros J* **3**: 242−245.

Booth, G.H., and Tiller, A.K. (1960) Polarization studies of mild steel in cultures of sulphate-reducing bacteria. *T Faraday Soc* **56**: 1689−1696.

Booth, G.H., and Tiller, A.K. (1962) Polarization studies of mild steel in cultures of sulphate-reducing bacteria. Part 3: Halophilic organisms. *T Faraday Soc* **58**: 2510−2516.

Castaneda, H., and Benetton, X.D. (2008) SRB-biofilm influence in active corrosion sites formed at the steel-electrolyte interface when exposed to artificial seawater conditions. *Corros Sci* **50**: 1169−1183.

Cohen, M. (1979) Dissolution of iron. In *Corrosion Chemistry*. Brubaker, G., and Phipps, P.B.P. (eds). Washington DC: ACS Symposium Series.

Cord-Ruwisch, R., and Widdel, F. (1986) Corroding iron as a hydrogen source for sulfate reduction in growing cultures of sulfate-reducing bacteria. *Appl Microbiol Biotechnol* **25**: 169−174.

Costello, J.A. (1974) Cathodic depolarization by sulphate-reducing bacteria. *S Afr J Sci* **70**: 202−204.

Dinh, H.T., Kuever, J., Mußmann, M., Hassel, A.W., Stratmann, M., and Widdel, F. (2004) Iron corrosion by novel anaerobic microorganisms. *Nature* **427**: 829−832.

Enning, D., Venzlaff, H., Garrelfs, J., Dinh, H.T., Meyer, V., Mayrhofer, K., Hassel, A.W., Stratmann, M., and Widdel, F. (2012) Marine sulfate-reducing bacteria cause serious corrosion of iron under electroconductive biogenic mineral crusts. *Environ Microbiol*: *in press.*

Fonseca, I., Feio, M.J., Lino, A.R., Reis, M.A., and Rainha, V.L. (1998) The influence of the media on the corrosion of mild steel by *Desulfovibrio desulfuricans* bacteria: an electrochemical study. *Electrochim Acta* **43**: 213−222.

Hamilton, W.A. (1985) Sulphate-reducing bacteria and anaerobic corrosion. *Annu Rev Microbiol* **39**: 195−217.

Hardy, J.A. (1983) Utilization of cathodic hydrogen by sulphate-reducing bacteria. *Br Corros J* **18**: 190−193.

Horvàth, J., and Sölti, M. (1959) Beitrag zum Mechanismus der anaeroben Korrosion der Metalle im Boden. *Mater Corros* **10**: 624−630.

Kaesche, H. (2003) *Corrosion of Metals: Physicochemical Principles and Current Problems*. Berlin: Springer.

Katsounaros, I., Meier, J.C., Klemm, S.O., Topalov, A.A., Biedermann, P.U., Auinger, M., and Mayrhofer, K.J.J. (2011) The effective surface pH during reactions at the solid-liquid interface. *Electrochem Commun* **13**: 634−637.

Keresztes, Z.; Felhősi, I., and Kálmán, E. (2001) Role of redox properties of biofilms in corrosion processes. *Electrochim Acta* **46**: 3841−3849.

King, R.A., and Miller, J.D.A. (1971) Corrosion by sulphate-reducing bacteria. *Nature* **233**: 491−492.

King, R.A., Miller, J.D.A., and Smith, J.S. (1973) Corrosion of mild steel by iron sulphides. *Br Corros J* **8**: 137−141.

Lee, A.K., Buehler, M.G., and Newman, D.K. (2006) Influence of a dual-species biofilm on the corrosion of mild steel. Corros Sci **48**: 165−178.

Lee, W., Lewandowski, Z., Nielsen, P.H., and Hamilton, W.A. (1995) Role of sulfate-reducing bacteria in corrosion of mild steel - a review. *Biofouling* **8**: 165−194.

Mansfeld, F., and Little, B. (1991) A technical review of electrochemical techniques applied to microbiologically influenced corrosion. Corros Sci **32**: 247−272.

Marsili, E., Rollefson, J.B., Baron, D.B., Hozalski, R.M., and Bond, D.R. (2008) Microbial biofilm voltammetry: direct electrochemical characterization of catalytic electrode-attached biofilms. *Am Soc Microbiol* **74**: 7329−7337.

Miranda, E., Bethencourt, M., Botana, F.J., Cano, M.J., Sánchez-Amaya, J.M., Corzo, A., García de Lomas, J., Fardeau, M.L., and Ollivier, B. (2006) Biocorrosion of carbon steel alloys by an hydrogenotrophic sulfate-reducing bacterium *Desulfovibrio capillatus* isolated from a Mexican oil field separator. *Corros Sci* **48**: 2417−2431.

Mori, K., Tsurumaru, H., and Harayama, S. (2010) Iron corrosion activity of anaerobic hydrogen-consuming microorganisms isolated from oil facilities. *J Biosci Bioeng* **110**: 426−430.

Morris, D.R., Sampaleanu, L.P., and Veysey, D.N. (1980) The corrosion of steel by aqueous solutions of hydrogen sulphide. *J Electrochem Soc* **127**: 1228−1235.

Pankhania, I.P., Moosavi, A.N., and Hamilton, W.A. (1986) Utilization of cathodic hydrogen by *Desulfovibrio vulgaris* (Hildenborough). *J Gen Microbiol* **132**: 3357−3365.

Rickard, D., and Luther, G.W. (2007) Chemistry of iron sulfides. *Chem Rev* **107**: 514−562.

Sherar, B.W.A., Power, I.M., Keech, P.G., Mitlin, S., Southam, G., and Shoesmith, D.W. (2011) Characterizing the effect of carbon steel exposure in sulfide containing solutions to microbially induced corrosion. *Corros Sci* **53**: 955−960.

Smith, J.S., and Miller, J.D.A. (1975) Nature of sulphides and their corrosive effect on ferrous metals: a review. *Br Corros J* **10**: 136−143.

Spruit, C.J.P., and Wanklyn, J.N. (1951) Iron sulphide ratios in corrosion by sulphate-reducing bacteria. *Nature* **168**: 951−952.

Torres, C.I., Marcus, A.K., Lee, H., Parameswaran, P., Krajmalnik-Brown, R., and Rittmann, B.E. (2010) A kinetic perspective on extracellular electron transfer by anode-respiring bacteria. *FEMS Microbiol Rev* **34**: 3−17.

Wanklyn, J.N., and Spruit, C.J.P. (1952) Influence of sulphate-reducing bacteria on the corrosion potential of iron. *Nature* **169**: 928−929.

Widdel, F., and Bak, F. (1992) Gram-negative mesophilic sulfate-reducing bacteria. In *The Prokaryotes*. Balows, A., Trüper, H.G., Dworkin, M., Harder, W., and Schleifer, K.-H. (eds). New York: Springer, pp. 3352−3378.

von Wolzogen Kühr, C.A.H. (1961) Unity of anaerobic and aerobic iron corrosion process in the soil. *Corrosion* **17**: 119−125.

von Wolzogen Kühr, C.A.H., and van der Vlugt, L.S. (1934) The graphitization of cast iron as an electrobiochemical process in anaerobic soil. *Water* **18**: 147−165.

Supplementary data

Scheme for electrochemical cell measurements

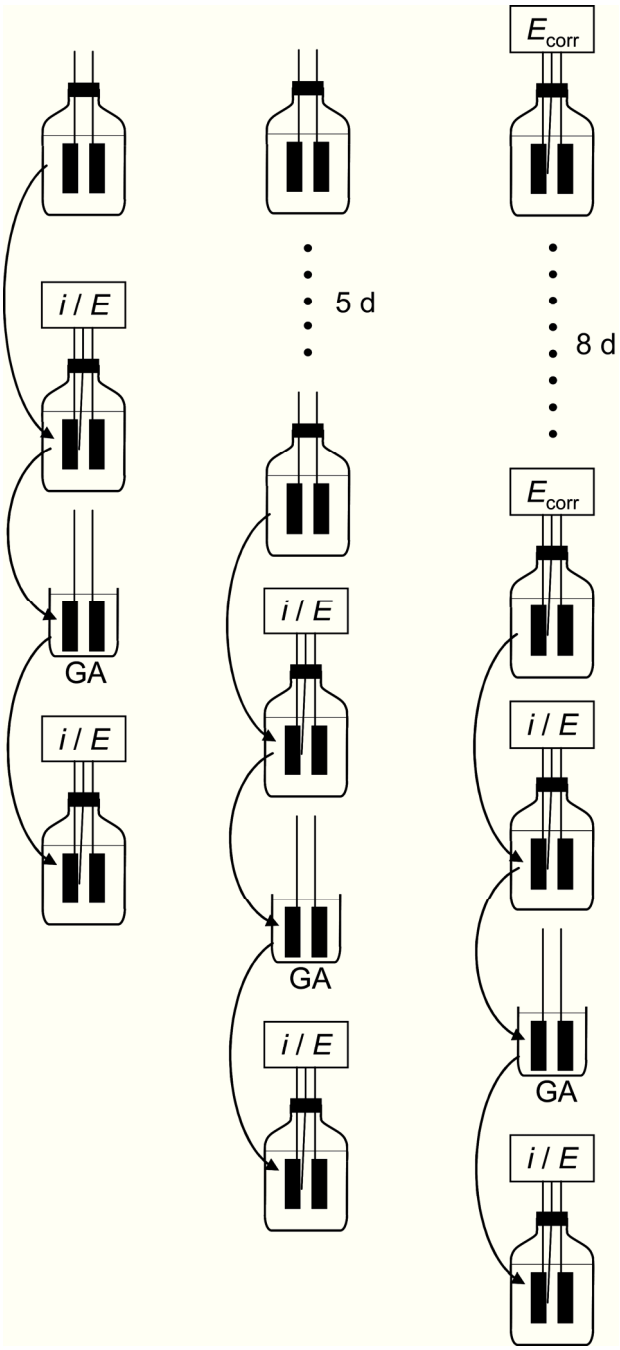

Fig. S1. Three electrochemical cells were prepared for each strain. One cell was used for the LSV measurements ("i / E") directly after inoculation (left column) , the second cell after five days (middle column), the third cell (right column) was first used to record the development of E_{corr} over eight days and subsequently used for potentiodynamic measurements. The first LSV measurements were followed by chemical inactivation, viz. the transfer in glutaraldehyde containing medium and washing steps indicated by "GA". This procedure sacrificed the colonized electrodes. Afterwards the inactivated electrodes were transferred in fresh electrolyte and subsequently investigated by a second LSV measurement.

Efficiency of chemical sterilization procedure

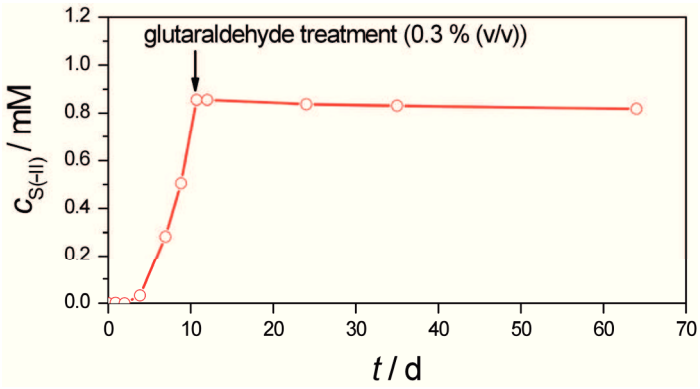

Fig. S2. Production of sulfide (calculated from sulfate loss) in a culture of strain IS4. Corrosion coupon (crust-covered) was treated with 0.3 % glutaraldehyde (v/v) on day 10 and further incubated in fresh ASW.

LSV of strain HS3 after three days

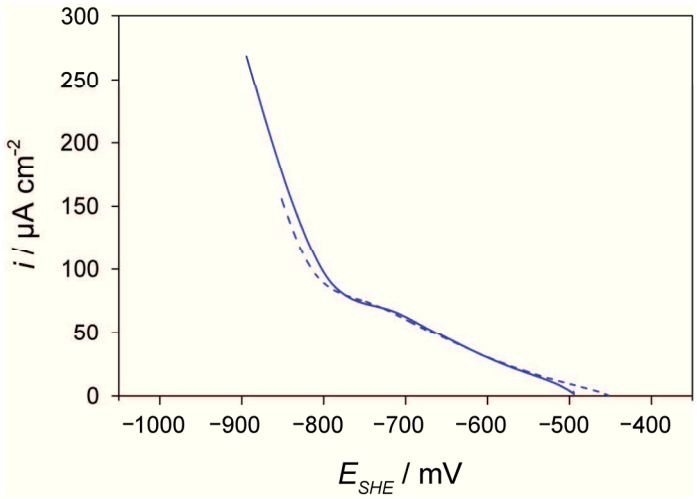

Fig. S3. Voltammograms of an iron electrode incubated in a culture of strain HS3 for three days. Measurements were performed in fresh artificial seawater medium as electrolyte with viable cells (solid line) and after sterilization with glutaraldehyde (dashed line).The potential sweep with 1 mV s^{-1} ranged from the free corrosion potential (E_{corr}; start) to −400 mV below E_{corr}. In the first days of incubation cathodically active iron sulfides with a correspondingly higher rate of H_2 formation may form. These curves support this assumption showing increased corrosion currents independent of the microbial activity.

LSV at different scan rates

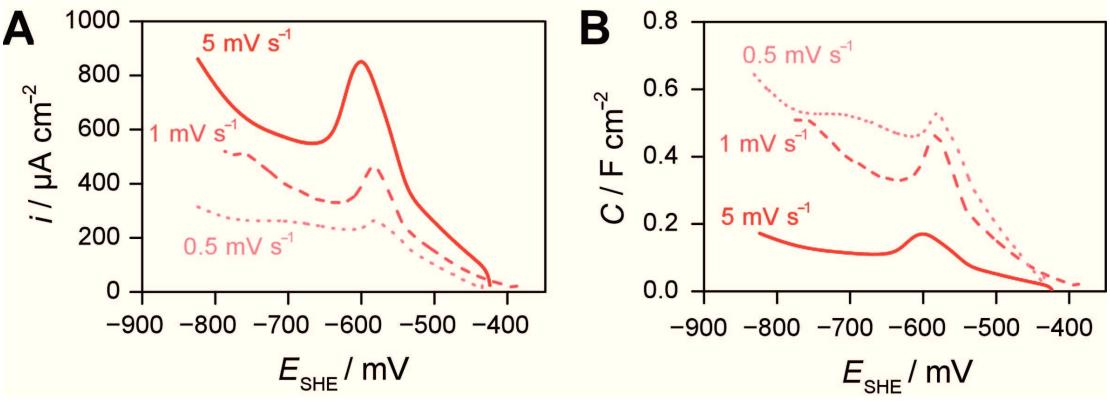

Fig. S4. Voltammograms of an iron electrode incubated in a culture of strain IS4 for twelve days. A thick precipitate crust was established on the surface. The potential sweep ranged from the free corrosion potential (E_{corr}; start) to −400 mV below E_{corr} with a scanrate of 1 mV s^{-1} (first sweep), 0.5 mV s^{-1} (second sweep) and 5 mV s^{-1} (third sweep). A pure Faradaic current would be independent of the scanrate, but actual polarization behaviour (A) indicates an additional non-Faradaic current, e.g. due to charging effects of the semiconductive crust. This current is however also not pure non-Faradaic as the capacitance (current density divided by scanrate, (B)) is not independent of the scanrate. Additional potential sweep experiments had demonstrated that polarization behaviour in general is reproducible for one scanrate.

Impedance spectra (Nyquist plots)

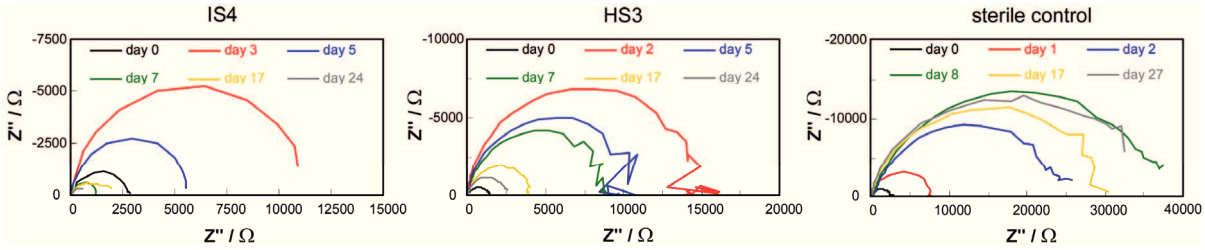

Fig. S5. Impedance spectra (Nyquist representation) of iron wire electrodes incubated in cultures of strain IS4, strain HS3 and without bacteria (sterile control).

Chapter D.3

Corrosion of iron by sulfate-reducing bacteria - new views of an old problem

Dennis Enning[1] and Julia Garrelfs[1]

[1]*Max Planck Institute for Marine Microbiology, Celsiusstraße 1, D-28359 Bremen, Germany.*

Manuscript *in preparation*

Abstract

A connection between the activity of environmental microorganisms and certain cases of serious corrosion of iron was first conceived more than a century ago. Since then, such microbially influenced corrosion (MIC) has gained prominence and its technical relevance is now widely recognized. MIC usually is a 'hidden' process, found in places with no or little access of oxygen such as in oil and gas pipelines, cooling water systems or buried marine constructions. The entailed economic costs are considerable. Sulfate-reducing bacteria (SRB) are commonly considered the main culprits of MIC, a perception that largely stems from three recurrent observations. Firstly, sulfate-rich environments (e.g. seawater) are particularly corrosive. Secondly, SRB and their characteristic corrosion product iron sulfide are ubiquitously associated with anaerobic corrosion damage in the field and thirdly, no other physiological group produces comparable corrosion damage in axenic laboratory cultures. However, there remain several open questions about the underlying mechanisms and their relative contribution to corrosion. Ambiguities and misconceptions of MIC are widespread. The suggested mechanisms of metal attack by SRB include the excretion of corrosive hydrogen sulfide, deposition of catalytically active iron sulfides on the metal and the recently discovered bioelectrical corrosion of iron by peculiar lithotrophic SRB. The latter process (viz. electrical microbially influenced corrosion, EMIC) adds a new perspective to the causes and physiological requirements of MIC *in situ*. This brief review traces the historical twists in the perception of SRB-induced corrosion and critically discusses the most plausible current explanations for the frequently observed corrosion of iron in anoxic, sulfate-rich environments.

Fundamentals of iron corrosion

Iron (Fe^0) is the technologically most widely used metal due to its excellent mechanical properties and the abundance of its ores (US Geological Survey, 2011). It is an indispensable material in transportation, infrastructure and manufacturing. A major drawback is the susceptibility of iron to corrosion. Metallic (iron + other) corrosion causes enormous economic damage. Across all industrial sectors the inferred costs have been estimated to range between 2 and 3% of GDP in developed countries and hence several hundred billion dollars annually (Koch *et al*., 2001; Kruger, 2011). As iron is the most abundant metallic material and due to its particular susceptibility to corrosion, the calculated costs are to a large part those of iron corrosion.

Protection of iron against corrosion can be achieved by coating or painting. However, these measures are technically not always feasible (e.g. inside pipelines or tanks) and often have a limited service life (Grundmeier *et al.,* 2000). Alloying of iron with more active metals such as chromium, nickel and molybdenum yields stainless steels of superior corrosion resistance. Still, their large scale application is economically not achievable to any extent. Instead, inherently corrosion-prone carbon steel (typically ≥98% Fe^0) is used in vast technical infrastructure such as oil and gas pipelines (Koch *et al*., 2001; Sun *et al*., 2011).

Except for a few cases caused by erosion or mechanical stress, the corrosion of iron is mostly an electrochemical process (Whitney, 1903; Revie, 2011). Accordingly, the oxidation of metallic iron is intimately coupled to the reduction of a suitable oxidant, but without a need for the two reactions to occur at the same locality (in contrast to regular redox reactions). Central to iron corrosion is the high tendency of the metal to give off electrons according to

$$Fe^0 \rightleftarrows Fe^{2+} + 2\ e^- \qquad (1)$$

$$E^{\circ}_{Fe^{2+}/Fe^0} = -0.47\ V\ .$$

(revised standard potential; Rickard and Luther, 2007; Enning *et al*., 2012). Hydrated ferrous ions move into solution only as long as electrons, which cannot dissolve into liquid, are removed by suitable chemical reactants. The most common reactant in iron corrosion is molecular oxygen:

$$4\ e^- + O_2 + 4\ H^+ \rightleftarrows 2\ H_2O \qquad (2)$$

$$E^{\circ'}_{O_2/2H_2O} = +0.81\ V\ .$$

Equations (1) and (2) are referred to as an anodic and cathodic half-reaction of corrosion, respectively. Owing to the condition of electroneutrality, anodic and cathodic reactions cannot proceed isolated from one another (Kaesche, 2003). Anodic metal dissolution (Eq. 1) combines with cathodic reduction of oxygen (Eq. 2) to

$$2\,Fe^{0} + O_2 + 2\,H_2O \rightarrow 2\,Fe(OH)_2\,. \qquad (3)$$

Further oxidation yields a complex mixture of ferric oxides and hydroxides, commonly known as rust. The formed rust is an ineffective process barrier, so that corrosion with oxygen proceeds in the absence of appropriate counter-measures.

Another cathodic reactant is protons from dissociated water yielding molecular hydrogen:

$$2\,e^{-} + 2\,H^{+} \rightleftarrows H_2 \qquad (4)$$

$$E^{0'}_{2H^{+}/H_2} = -0.41\,V\,.$$

Reaction (4), however, is 'kinetically impeded' (Bockris and Reddy, 1970; Kaesche, 2003) and particularly slow at $pH > 6$, where proton supply is limiting (Piron, 1994). Hence iron corrosion and the net reaction

$$Fe^{0} + 2\,H^{+} \rightarrow Fe^{2+} + H_2 \qquad (5)$$

are technically insignificant in the absence of oxygen or acid and iron constructions in most anoxic environments (e.g. marine sediment, water-logged soil) could, in principle, last for centuries.

However, the corrosion of iron can be seriously accelerated in the presence of environmental microorganisms. This is particularly true in environments with little or no oxygen, i.e. where from a purely chemical point of view, corrosion should be negligible. In technology, this is referred to as microbially influenced corrosion (MIC) or biocorrosion. Figure 1 depicts a common example of MIC, viz. external corrosion under the disbonded coating of a gas transmission pipeline in anoxic, sulfate-containing soil.

Biocorrosion probably accounts for a significant fraction of total corrosion costs (Booth, 1964; Flemming, 1994; Beavers and Thompson, 2006; Beech and Sunner, 2007) and hence billions of dollars annually, but estimates vary widely and lack a computed basis, so that definite numbers cannot be given with certainty.

One physiological group of environmental microorganisms with a suggested key role in the anaerobic corrosion of iron is the sulfate-reducing bacteria (SRB; Booth, 1964; Lee *et al*.,

1995; Hamilton, 1985; Beech and Sunner, 2007), which are widespread in natural and engineered environments. SRB gain energy for growth by reduction of sulfate to hydrogen sulfide with electrons usually derived from the final degradation of organic matter or from molecular hydrogen, a common fermentation product in anoxic soil and sediment (Muyzer and Stams, 2008).

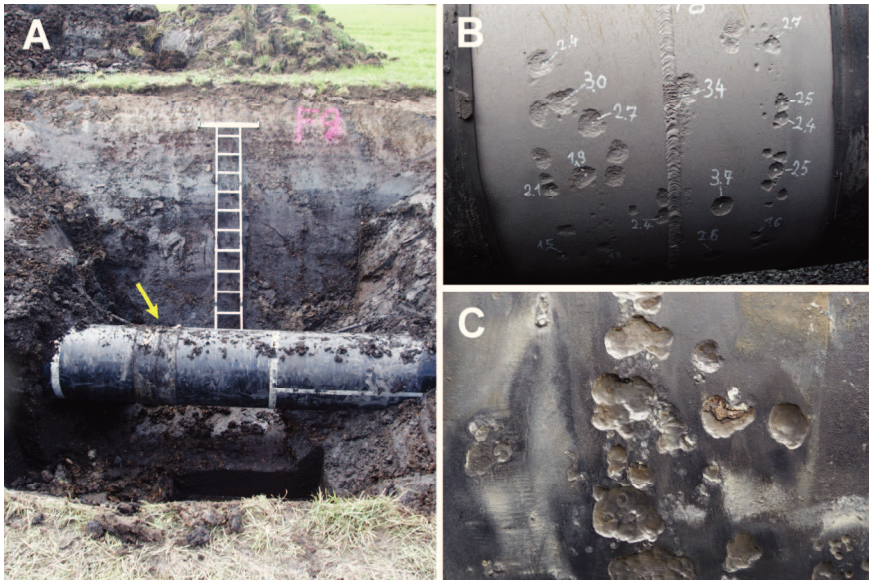

Fig. 1. External corrosion on buried gas transmission pipeline in bog-soil of Northern Germany.
A. Trench with coated carbon steel gas pipeline in water-logged, anoxic soil (1.4 mM sulfate; 17 mM dissolved inorganic carbon, DIC). External corrosion has occurred under disbonded coating at welding sites (arrow).
B. Welding site with corrosion pits. Disbonded asphalt coating and corrosion products (FeS / $FeCO_3$) were removed. Numbers indicate pit depth in millimeters.
C. Higher magnification of corrosion pits from a different site at the same pipeline.

The suggested key function of SRB in biocorrosion is principally grounded on the following three observations. Firstly, iron in anoxic environments containing sulfate, i.e. the electron acceptor of SRB, seems particularly prone to microbial corrosion (Fig. 1; von Wolzogen Kühr and van der Vlugt, 1934; Li *et al*., 2000; Bødtker *et al*., 2008). Secondly, SRB or their characteristic corrosion product FeS, are ubiquitously found at anaerobically corroded metal sites (Ferris *et al*., 1992; Jack *et al*., 1995; Li *et al*., 2000; Zhang and Fang, 2001) and thirdly, SRB in axenic laboratory cultures produce corrosion rates well matching those reported in the field (Bell and Lim, 1981; Pankhania *et al*., 1986; Enning *et al*., 2012). Hence, field data strongly suggest a prominent role of SRB in anaerobic iron corrosion while laboratory investigations provide the plausible mechanistic explanations (Lee *et al*., 1995; Beech and Sunner, 2007; Enning *et al*., 2012). No other physiological group of microorganisms produces

comparable anaerobic corrosion damage of iron in laboratory studies. Besides the assumption that SRB are the main culprits of MIC, there is also an increasing number of reports on sulfate-independent anaerobic corrosion by methanogenic archaea (Daniels *et al*., 1987; Dinh *et al*., 2004; Mori *et al*., 2010; Uchiyama *et al*., 2010; Larsen *et al*., 2011) and this may be of technological importance, particularly in anoxic environments with insufficient supply of sulfate.

This review will first give a brief account of the historical twists in the perception of SRB-induced corrosion before we will then consider the individual mechanisms that are currently believed to most severely affect iron in sulfate-rich environments.

SRB: Long-known key players in anaerobic iron corrosion

Looming evidence for an involvement of SRB in anaerobic corrosion was already provided more than a hundred years ago. In 1910, Gaines reported the analysis of sulfur-rich corrosion products from anaerobically corroded iron constructions and hypothesized about a connection to the bacterial sulfur cycle. Later, it was demonstrated that iron sulfides, when in electrical contact to iron, accelerated metal dissolution (Stumper, 1923).

However, it was the work of von Wolzogen Kühr and van der Vlugt in 1934, who identified SRB as the prime cause of rampant iron pipe failures in the sulfate-rich soils of North Holland. Apparently, most of the observed metal loss resulted from the direct utilization of iron by SRB rather than from the indirect effect of their corrosive metabolic product H_2S. Microbial corrosion was attributed to a single physiological trait, i.e. the oxidation of cathodic hydrogen by lithotrophic SRB (Eq. 5; von Wolzogen Kühr and van der Vlugt, 1934; von Wolzogen Kühr, 1961). The mechanistic explanation, which seemed consistent with the electrochemical nature of corrosion (Whitney, 1903) became famous as the (classical) ‘cathodic depolarization theory’. Much controversy succeeded in the following decades. Most authors initially favored the theory (Starkey, 1946; Butlin *et al*., 1949; Horvath and Sölti, 1959; Booth, 1964), only few rejected the idea that microbial H_2 scavenge would accelerate corrosion (Spruit and Wankyln, 1951; Wanklyn and Spruit, 1952). With the beginning of the 1960s, the hypothesis was subjected to a series of electrochemical investigations (Horvath and Sölti, 1959; Booth and Tiller, 1960; 1962; Tiller and Booth, 1962). Indeed, there seemed a connection between the ability of bacterial cultures to consume cathodic hydrogen (*via* the hydrogenase enzyme) and a stimulation of the cathodic reaction (‘depolarization’) of iron. However, despite the original intention to study the direct interplay between bacteria and their metallic substratum, many of the experiments were performed with lactate as an additional,

organic electron donor for sulfate reduction. This greatly complicated the evaluation of obtained data. Costello (1974) elegantly demonstrated that hydrogen sulfide from sulfate reduction with lactate was a cathodically active compound and hence much of the electrochemical evidence for the 'cathodic depolarization theory' became obsolete. Since then, occasional attempts to resurrect the theory have been made (Pankhania *et al*., 1986; Daniels *et al*., 1987; Bryant *et al*., 1991; Bryant and Laishley, 1991; De Windt *et al*., 2003), but to this day no culture-based experiment could demonstrate that bacterial consumption of cathodic hydrogen accelerates iron weight loss to any significant extent (Spruit and Wanklyn, 1951; Hardy, 1983; Dinh *et al*., 2004; Mori *et al*., 2010; Enning *et al*., 2012).

In the late 1960s and early 1970s an alternative mechanism for SRB-induced corrosion emerged. Several authors demonstrated that biogenic iron sulfides accelerated corrosion when deposited on the metal (Booth *et al*., 1968; King and Miller, 1971; King *et al*., 1973). Interestingly, sustained corrosion by iron sulfides required the presence of active populations of SRB. The exact mechanisms in this corrosion scenario have never been fully resolved (Smith *et al*., 1975; Lee *et al*., 1995). Still, biogenically deposited iron sulfides are assumed to be a contributing corrosive factor in anoxic environments (Tiller, 1983; Ferris *et al*., 1992; Lee and Characklis, 1993).

The other major corrosive compound in these environments is hydrogen sulfide as a powerful cathodic and anodic reactant (Horvath and Sölti, 1959; Costello, 1974; Newman *et al*., 1992). A subject which received considerable attention in the context of H_2S corrosion is the formation of protective ('passivating') iron sulfide films (Newman *et al*., 1991; 1992; Lee *et al*., 1995; Sun and Nešić; 2007). It is generally agreed that these thin iron sulfide layers are amongst the most decisive rate-controlling factors of corrosion (Lee *et al*., 1995; Nešić, 2011; Sun *et al*., 2011).

Hence, until recently, SRB-induced corrosion was viewed as the result of biogenic H_2S and catalytically active iron sulfides, with the ambiguous role of the latter of accelerating corrosion in some cases, while protecting the metal in others. In addition to these indirect effects of SRB, there remained speculation of a direct corrosiveness of SRB, often proposed in the elusive form of a 'regeneration' of 'charged' iron sulfides through microbial hydrogen consumption (King and Miller, 1971; Smith *et al*., 1975; Tiller, 1983; Ferris *et al*., 1992).

In 2004, a novel corrosion mechanism was discovered in peculiar SRB isolates from enrichment cultures with metallic iron as the only electron donor (Dinh *et al*., 2004). Sulfate reduction by these strains was directly fuelled by bacterial uptake and consumption of iron-derived electrons. The mechanism has recently been studied in much detail and the term

electrical microbially influenced corrosion was proposed (EMIC; Enning *et al*., 2012). EMIC can proceed at technologically highly relevant rates and was apparently responsible for serious iron corrosion in anoxic marine environments (Enning *et al*., 2012).

Obviously, there is no single, generalized explanation for SRB-induced corrosion. Yet a causal understanding of the basic underlying mechanisms and principles is possible.

Mechanisms of progressive corrosion by SRB

Corrosion of iron proceeds in two half reactions. This is, on the one hand, the anodic dissolution of metallic iron (Eq. 1) and, on the other hand, a cathodic, electron-consuming reaction. The latter may occur on the metal itself or at an electrically connected site. Anodic and cathodic reactions must proceed at equal pace, hence stimulation of either of them will also accelerate the overall corrosion process.

Sulfate-reducing bacteria (SRB) can principally stimulate both, the anodic and the cathodic reaction, though it is mainly the latter that is affected by their activity (Newman *et al*., 1991; 1992; Enning *et al*., 2012; Venzlaff *et al*., 2012). We will dissect SRB-induced corrosion into its anodic and cathodic half reactions and consider each of them separately in the following.

The anodic half reaction of corrosion by SRB

Dissolution of metallic iron (Fe^0) into ferrous ions (Fe^{2+}) represents the primary oxidation step of corrosion (Fig. 2A; Eq. 1). A common and distinctive characteristic of SRB-induced corrosion is the formation of black corrosion deposits from precipitation of ferrous ions with biogenic, dissolved sulfide ($Fe^{2+} + HS^- \rightarrow FeS + H^+$).

Another reaction leading to the formation of iron sulfide is the chemisorption of dissolved sulfide to metallic iron (Iofa *et al*., 1964) and subsequent oxidation of the metal according to the half reaction $Fe^0 + HS^- \rightarrow FeS + H^+ + 2\ e^-$ (Fig. 2B; details in Shoesmith *et al*. 1980; Newman *et al*., 1992). A transient stimulation of the anodic reaction by SRB has been observed by some investigators (Horvath and Sölti, 1959). We refer to the corrosion of iron by the biologically formed chemical sulfide (H_2S/HS^-) as chemical microbially influenced corrosion (CMIC).

However, biogenic sulfide may also lead, at least temporarily, to the protection of iron against corrosion. This is explained by the formation of tightly adherent FeS films on the metal surface, most likely by direct reaction of dissolved sulfide with metallic iron (Fig. 2B; Shoesmith *et al*., 1980; Newman *et al*., 1992; Sun and Nešić; 2007). Such films act as an effective process barrier by impeding the migration of ferrous ions from the metal anode to the aqueous environment (Newman *et al*., 1992; Hansson *et al*., 2006). Impediment

('polarization') of the anodic half reaction is frequently observed in cultures of SRB (Booth and Tiller, 1960; Tiller and Booth, 1962; Tiller, 1983). Newman *et al*. (1992) stated that formation of such films occurs when dissolved sulfide concentrations exceed the concentration of dissolved ferrous ions at the unreacted metal surface, i.e. usually at high concentrations of dissolved sulfide. Rupture of the FeS film and local re-exposure of metallic iron results in rapid pitting corrosion (localized metal dissolution) unless further sulfide seals the exposed site.

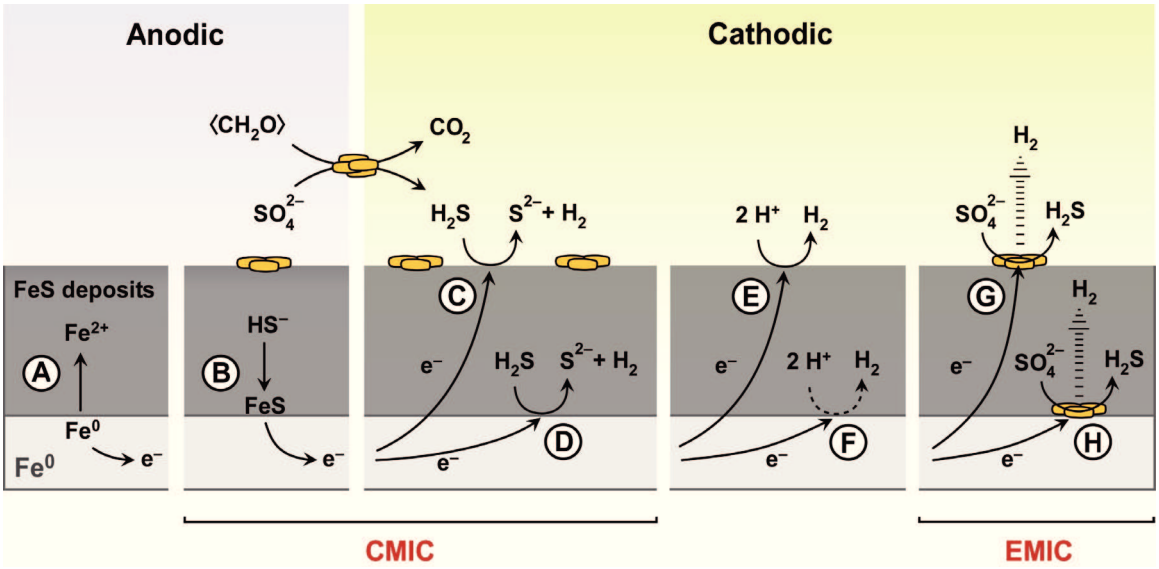

Fig. 2. Schematic illustration of iron corrosion by sulfate-reducing bacteria (SRB) at circumneutral *pH*. Several mechanisms are known which affect the anodic or cathodic half reaction. Reactions are non-stoichiometric for clarity. Anodic and cathodic reactions are drawn separately for overview.

A. Anodic iron dissolution with formation of FeS-containing mineral deposits. Depending on the corrosion mechanism, deposits may contain considerable amounts of other ferrous minerals (e.g. $FeCO_3$).

B. Stimulation of anodic iron dissolution by HS^--ions. Dissolved sulfides (H_2S, HS^-) are formed by sessile and planktonic organotrophic SRB populations.

C. Biogenic, dissolved sulfide (H_2S, HS^-) acts as a cathodic reactant at electroconductive iron sulfides.

D. Biogenic, dissolved sulfide (H_2S, HS^-) acts as a cathodic reactant at the metal surface.

E. Catalytic iron sulfides may accelerate reduction of H^+-ions to H_2. Consumption of such H_2 by SRB does not accelerate the rate of its formation (no 'cathodic depolarization', see text).

F. Slow, kinetically impeded formation of H_2 at the metal. Consumption of such H_2 by SRB does not accelerate the rate of its formation (no 'cathodic depolarization', see text).

G. Specially adapted lithotrophic SRB withdraw electrons from iron *via* electroconductive iron sulfides. Excess of accepted electrons may be released as H_2 (*via* hydrogenase enzyme).

H. Specially adapted lithotrophic SRB withdraw electrons directly from the metal. Excess of accepted electrons may be released as H_2 (*via* hydrogenase enzyme).

CMIC: Chemical microbially influenced corrosion (*via* biogenic, dissolved sulfide). EMIC: Electrical microbially influenced corrosion (direct electron uptake by specialized lithotrophic SRB). Possibly encrusted bacteria not shown for clarity.

Corrosion of iron may initially be accelerated through stimulation of the anodic reaction by hydrogen sulfide (Fig. 2B) but is later driven by an accelerated cathodic, electron-consuming reaction which results either indirectly or directly from the activity of SRB (Newman *et al*., 1991; Enning *et al*., 2012; Venzlaff *et al*., 2012).

The cathodic half reaction of corrosion by SRB

It has been suggested that also the cathodic reaction is stimulated by dissolved sulfides (Costello, 1974; Cord-Ruwisch, 2000; Ma *et al*., 2000; Nešić, 2011). Accordingly, sulfide anions act as a shuttle for bound (uncharged) protons, thereby increasing the availability of this electron acceptor at cathodic sites (Fig. 2C and D; Wikjord *et al*., 1980; Widdel, 1992; Nešić, 2011). The overall net reaction is

$$Fe^0 + H_2S \rightarrow FeS + H_2 . \quad (6)$$

Principally, reduction of protons should occur at the metal and at FeS surfaces alike, but the latter may provide a particularly large cathodic surface area. Rapid hydrogen evolution from 'H_2S reduction' with iron occurs both in the presence (Cord-Ruwisch and Widdel, 1986) and absence (Widdel, 1992; Dinh, 2003; Nešić, 2011) of SRB. The rates of corrosion in sulfidogenic cultures (CMIC) vary widely, but can be high. Particularly severe and progressive CMIC has been demonstrated in lactate-based media with high concentrations of ferrous salts (Adams and Farrer, 1953; Lee and Characklis, 1993); their scavenging of H_2S/HS^- probably prevents formation of the protective FeS film and deposits fine suspensions of cathodically active FeS on the metal.

It has been reported that crystalline iron sulfides also stimulated iron corrosion in sterile, sulfide-free incubations (Booth *et al*., 1968; Mara and Williams, 1971; King *et al*., 1973). This is most likely due to catalysis by FeS of the chemical (abiotic) reduction of protons (Fig. 2E). The role of FeS in SRB-induced corrosion was emphasized by several authors (Booth *et al*., 1968; King and Miller, 1971; Smith and Miller, 1975), but the exact mechanisms are apparently complex and insufficiently understood (Lee *et al*., 1995). Newman *et al*. (1991) found the stimulatory effect of FeS to be small upon closer inspection and stated that the increased cathodic surface area provided by FeS was probably more important than its catalytic properties. Indeed, corrosion by FeS has so far only been reported for chemically prepared fine suspensions of the minerals (Booth *et al*., 1968; King and Miller, 1971; Mara and Williams, 1971; King *et al*., 1973). Venzlaff *et al*. (2012) found the effect of FeS to be

negligible in compact corrosion crusts formed by SRB. Further studies on the exact mechanisms and contribution of FeS to anaerobic corrosion are needed.

The reduction of H^+-ions at the blank metal surface (Fig. 2F) is, as already mentioned before, a very slow process. Von Wolzogen Kühr and van der Vlugt (1934) suggested a microbial acceleration of this reaction through scavenging of the reaction product hydrogen (Eq. 5). The developed theory of 'cathodic depolarization' served to explain the pronounced lithotrophic (H_2S/HS^--independent) corrosion observed in freshwater enrichment cultures with metallic iron (von Wolzogen Kühr and van der Vlugt, 1934). However, culture experiments with hydrogen-consuming SRB (Hardy, 1983; Dinh *et al*., 2004; Enning *et al*., 2012; Venzlaff *et al*. 2012) as well as theoretical considerations (Widdel, 1992; Cord-Ruwisch, 2000; Venzlaff *et al*. 2012) explicitly demonstrated that microbial consumption of cathodic hydrogen does not and can not accelerate anaerobic corrosion.

An alternative explanation for lithotrophic corrosion has been envisioned to be direct electron uptake from metallic iron by SRB (Ferris *et al*., 1992; Widdel, 1992; Jack, 2002). Indeed, this was recently discovered in specialized lithotrophic SRB isolated from enrichment cultures with metallic iron as the only electron donor (Dinh *et al*., 2004). Such 'electron-consuming' sulfate reducers can corrode iron progressively and at very high rates (Enning *et al*. 2012). This remarkable capability is apparently unique to a number of specialized bacteria and archaea (Dinh *et al*., 2004; Uchiyama *et al*., 2010), only few of which have been identified thus far (see below). Here, the anodic dissolution of iron (Fig. 2A) results from electron consumption by microbial sulfate reduction (Fig. 2G and H), i.e. a cathodic reaction that is kinetically impossible in the absence of these microorganisms. We refer to such a process as electrical microbially influenced corrosion (EMIC). The net reaction of sulfate reduction with metallic iron (here written with common carbonate precipitation) is

$$4\,Fe^0 + SO_4^{2-} + 3\,HCO_3^- + 5\,H^+ \rightarrow FeS + 3\,FeCO_3 + 4\,H_2O\,. \qquad (7)$$

The finding of a similar mechanism in certain methanogenic archaea (Dinh *et al*., 2004; Mori *et al*., 2010; Uchiyama *et al*., 2010) demonstrated that the ability to corrode iron lithotrophically is generally independent of iron sulfides, which are not formed in archaeal cultures. Corrosive lithotrophic SRB deposited and colonized steadily growing electroconductive crusts (Eq. 7) on the corroding metal (Enning *et al*., 2012). Linear sweep voltammetry performed prior to and after inactivation of the crust-attached cells with a biocide revealed the biologically stimulated cathodic reaction (Venzlaff *et al*., 2012). In conclusion, sulfate reduction by specialized lithotrophic SRB (Fig. 2G and H) with iron-

derived electrons (Fig. 2A) leads to rapid and progressive anaerobic corrosion. Due to an imbalance between electrons entering such cells and their consumption by sulfate reduction, some of these strains may form molecular hydrogen from iron in a shunt reaction (Dinh *et al*., 2004; Enning *et al*., 2012).

SRB: Indirect or direct catalysts of anaerobic corrosion?

The preceding chapter has discussed the fundamentally different ways in which SRB can influence anaerobic corrosion (Fig. 2). Distinction between indirect and direct catalysis of anaerobic corrosion by SRB is justified and there are species-specific differences in this respect. Principally, every SRB corrodes iron indirectly through the excretion of corrosive sulfide (CMIC). However, only certain lithotrophic SRB can corrode iron also directly by electron uptake, i.e. through the EMIC mechanism. There is currently only a limited number of representative isolates with such capability (Fig. 3). These strains were recently isolated from enrichment cultures with metallic iron as the only electron donor (Dinh *et al*., 2004; Enning, 2012). They have probably evaded earlier discovery as they are rapidly out-competed by 'conventional' SRB in the commonly used media that employ high concentrations of organic substrates.

The causes and physiological requirements of CMIC and EMIC are also fundamentally different. CMIC is principally the result of dissimilatory sulfate reduction by SRB growing on 'natural' (usually organic) substrates. Intracellular oxidation of such substrates by SRB (Rabus *et al*., 2006; Pereira *et al*., 2011) is coupled to sulfide generation which, upon excretion, stoichiometrically reacts with metallic iron (Fig. 2A–D). Hence the presence of sufficient amounts of biodegradable organic matter is a prerequisite for progressive CMIC. For instance, oxidation of 1 g Fe^0 *via* the CMIC mechanism requires the complete oxidation of 0.8 g acetate, a common environmental substrate of SRB (equation in Enning *et al*., 2012). This is different in EMIC, where the metal itself provides the organism with reducing power for sulfate reduction (Eq. 7). Such SRB can corrode metallic iron severely (Fig. 4), even in the complete absence of organic matter (Enning *et al*., 2012).

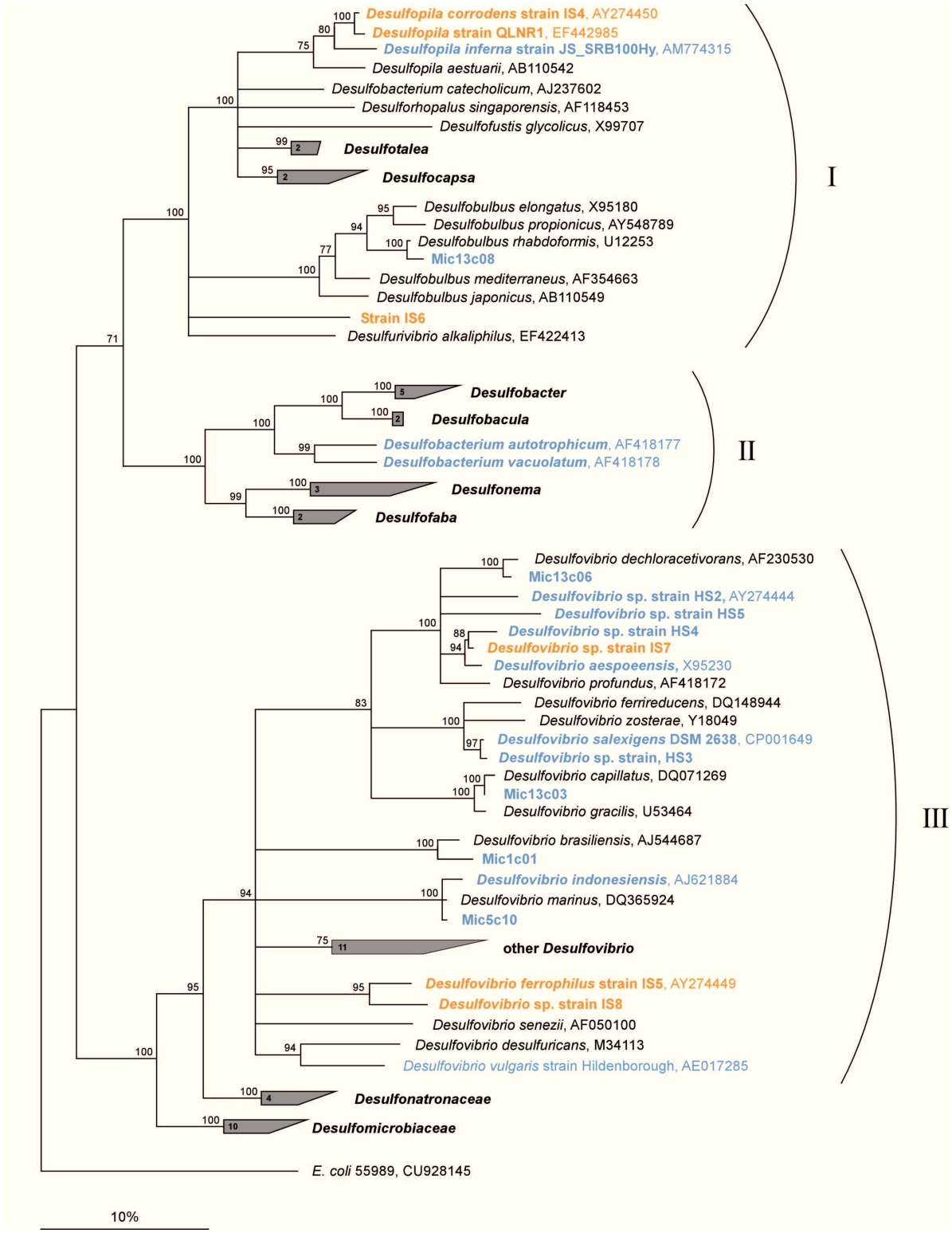

Fig. 3. Phylogenetic tree constructed from full length 16S rRNA gene sequences of cultivated sulfate-reducing bacteria within the *Deltaproteobacteria*. The tree shows SRB isolates capable of direct electron uptake (EMIC; orange) and hydrogenotrophic, non-corrosive SRB (blue). Other SRB (black) were not tested on Fe^0. Tree does not include all cultivated SRB. I: *Desulfobulbaceae*. II: *Desulfobacteraceae*. III: *Desulfovibrionaceae*. The tree was calculated based on maximum likelihood with the ARB software package and SILVA database (Ludwig *et al*., 2004; Pruesse *et al*., 2007). Branching with bootstrap values below 75 is not depicted. The scale bar represents 10% difference in sequence similarity. 'Mic'-isolates are from Mori *et al*. (2010). Figure adapted from Enning (2012).

The molecular mechanisms that enable SRB to withdraw electrons directly from iron are currently unknown. It is assumed that this involves outer membrane redox proteins such as *c*-type cytochromes (Dinh *et al*., 2004), found in other microorganisms that interact with external (extracellular) electron donors (Appia-Ayme *et al*., 1999; Strycharz *et al*., 2011) and acceptors (Butler *et al*., 2010; Shi *et al*., 2007). However, such proteins have not been detected in SRB thus far (Pereira *et al*., 2011) which may further indicate the physiological uniqueness of the novel isolates. Interestingly, these isolates are phylogenetically unrelated on the basis of 16S rRNA genes (Fig. 3). Such organisms with the ability of direct electron uptake from electrically conductive, solid surfaces (e.g. FeS) appear to be widespread (Enning, 2012; Enning *et al*., 2012). It was speculated that these organisms normally use a variety of biotic and abiotic solid electron sources in their natural environments. In fact, from an evolutionary point of view, their utilization of iron and hence EMIC may even be rather accidental. Still, this remarkable catabolic trait has adverse technological consequences.

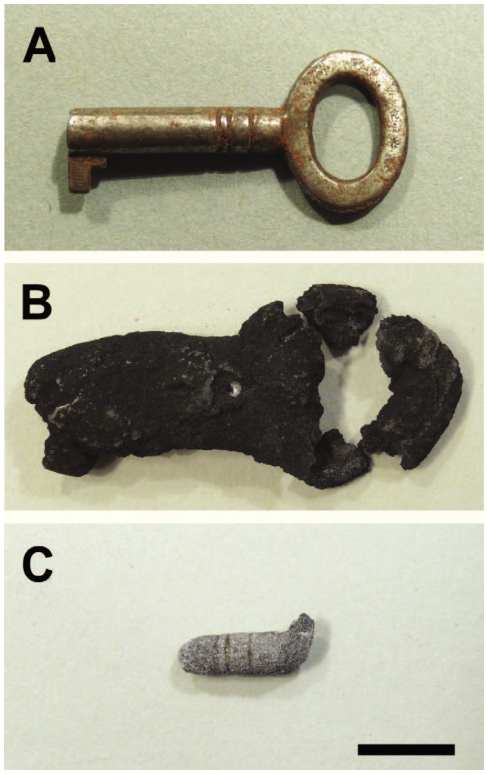

Fig. 4. Electrical microbially influenced corrosion (EMIC) of an iron key. The key was incubated in artificial seawater medium (*pH* 7.5) with *Desulfovibrio ferrophilus* strain IS5 for 9 months. No other electron donor than the iron was provided (lithotrophic growth conditions). Bar, 1 cm.

A. Iron key before incubation.

B. Iron key with corrosion crust after 9 months.

C. Residuary iron after removal of the crust with inactivated acid (10% hexamine in 2 M HCl) revealed 80.3% (2.7 g) iron weight loss. Hexamine-HCl did not dissolve Fe^0.

Relevance of different corrosion processes

A question of considerable interest is the relevance of the individual corrosion processes and their (long-term) rates of anaerobic metal destruction. Typical corrosion rates of unprotected steel in anoxic environments range from 0.2 – 0.4 mm Fe^0 yr^{-1} (Jack, 2002; Enning *et al*., 2012; see also Fig. 1). This can in principle be explained by CMIC; corrosion rates as high as 0.4 mm Fe^0 yr^{-1} were reported in anoxic sulfidogenic cultures of SRB grown with organic substrates (Lim and Bell, 1981; Hubert *et al*., 2005). However, CMIC was usually less pronounced in laboratory tests (Booth, 1964; Gaylarde, 1992; Beech *et al*., 1994; Cord-Ruwisch, 2000), probably due to the formation of protective deposits. The stimulation of corrosion by iron monosulfides, on the other hand, was generally rather low with fine suspensions of the minerals (≤ 0.06 mm Fe^0 yr^{-1}; Booth *et al*., 1968; King *et al*., 1973; Widdel, 1992) and negligible with more compact crusts (Venzlaff *et al*., 2012). Electrical microbially influenced corrosion (EMIC), on the other hand, led to progressive mineralization of metallic iron (Fig. 4) at rates of up to 0.9 mm Fe^0 yr^{-1} (Enning, 2012; Enning *et al*., 2012). However, *in vitro* corrosion rates alone are an insufficient indicator of the relevance of individual corrosion processes *in situ*. The analysis of corrosion products was proposed as another useful indicator (von Wolzogen Kühr and van der Vlugt, 1934). CMIC and EMIC produce corrosion products with inherently different relative amounts of sulfidic and non-sulfidic iron (Eqs 6 and 7, respectively). This was used to quantitatively express the contribution of EMIC to total SRB-induced corrosion (Enning et al., 2012). Indeed it could be demonstrated that serious corrosion damage of buried iron coupons in anoxic marine sediment was solely due to EMIC (Enning *et al*., 2012). Lithotrophic corrosion of iron appears to be widespread and of significant technological relevance. The responsible organisms (Fig. 3) have been largely overlooked so far, but can be enriched for and isolated with metallic iron as the only electron donor (Dinh *et al*., 2004; Sherar *et al*., 2011; Enning, 2012). Evaluation of the original corrosion product data provided by von Wolzogen Kühr and van der Vlugt (1934), reveals that EMIC accounted for 75 to 91% of corrosion damage in their freshwater enrichments. It is tempting to speculate that early researchers already cultivated unidentified lithotrophic SRB capable of direct electron uptake from metallic iron.

Concluding remarks

This review discussed the microbial mechanisms that lead to progressive corrosion of iron in anoxic, sulfate-rich environments. Principally, two scenarios must be distinguished. This is firstly, the chemical microbially influenced corrosion (CMIC) of iron by sulfide from

microbial sulfate reduction with ‘natural’ organic substrates. Secondly, SRB corrode iron lithotrophically, i.e. by direct utilization of the iron itself as an electron donor. This always occurs *via* direct electron uptake and only in a limited number of specialized strains. Still, such electrical microbially influenced corrosion (EMIC) appears to be widespread and of considerable relevance.

CMIC and EMIC are the envisioned primary processes that drive iron corrosion in sulfate-containing anoxic environments. However, there are particular situations in which corrosion can be further exacerbated by ingress of molecular oxygen (Hardy and Brown, 1984; Lee *et al*., 1993; Lee *et al*., 1995; Jack *et al*., 1998) as corrosive sulfur species arise from the secondary oxidation of FeS-containing deposits (MacDonald *et al*., 1978; Schaschl, 1980; Nielsen *et al*., 1993). The amount and composition of such deposits is in turn the result of SRB-induced corrosion (Hamilton, 2003). A better understanding of the primary causes of biocorrosion may hence ultimately aid in the design of better MIC prevention and mitigation strategies in both, fully anoxic and partially aerated sulfate-containing environments.

References

Adams, M.E., and Farrer, T.W. (1953) The influence of ferrous iron on bacterial corrosion. *J Appl Chem* **3**: 117−120.

Appia-Ayme, C., Guiliani, N., Ratouchniak, J., and Bonnefoy, V. (1999) Characterization of an operon encoding two c-type cytochromes, an aa_3-type cytochrome oxidase, and rusticyanin in *Thiobacillus ferrooxidans* ATCC 33020. *Appl Environ Microbiol* **65**: 4781−4787.

Beavers, J.A., and Thompson, N.G. (2006) External corrosion of oil and natural gas pipelines. In *ASM Handbook. Corrosion: Environments and Industries (#05145)*. Cramer, S.D., and Covino, B.S.J. (eds). Materials Park, Ohio: ASM International.

Beech, I.B., Cheung, C.W.S., Chan, C.S.P., Hill, M.A., Franco, R., and Lino, A.R. (1994) Study of parameters implicated in the biodeterioration of mild steel in the presence of different species of sulfate-reducing bacteria. *Int Biodet Biodegr* **34**: 289−303.

Beech, I.B., and Sunner, I.A. (2007) Sulphate-reducing bacteria and their role in corrosion of ferrous materials. In *Sulphate-reducing Bacteria: Environmental and Engineered Systems*. Barton, L.L., and Hamilton, W.A. (eds). Cambridge: Cambridge University Press, pp. 459−482.

Bell, R.G., and Lim, C.K. (1981) Corrosion of mild and stainless steel by four tropical *Desulfovibrio desulfuricans* strains. *Can J Microbiol* **27**: 242−245.

Bockris, J.O.M., and Reddy, A.K.N. (1970) *Modern Electrochemistry*. New York: Plenum.

Bødtker, G., Thorstenson, T., Lillebø, B.L.P., Thorbjørnsen, B.E., Ulvøen, R.H., Sunde, E., and Torsvik, T. (2008) The effect of long-term nitrate treatment on SRB activity, corrosion rate and bacterial community composition in offshore water injection systems. *J Ind Microbiol Biotechnol* **35**: 1625−1636.

Booth, G.H. (1964) Sulphur bacteria in relation to corrosion. *J Appl Bacteriol* **27**: 174−181.

Booth, G.H., Elford, L., and Wakerley, D.S. (1968) Corrosion of mild steel by sulphate-reducing bacteria: an alternative mechanism. *Br Corros J* **3**: 242−245.

Booth, G.H., and Tiller, A.K. (1960) Polarization studies of mild steel in cultures of sulphate-reducing bacteria. *T Faraday Soc* **56**: 1689−1696.

Booth, G.H., and Tiller, A.K. (1962) Polarization studies of mild steel in cultures of sulphate-reducing bacteria. Part 3: Halophilic organisms. *T Faraday Soc* **58**: 2510−2516.

Bryant, R.D., Jansen, W., Boivin, J., Laishley, E.J., and Costerton, J.W. (1991) Effect of hydrogenase and mixed sulfate-reducing bacterial populations on the corrosion of steel. *Appl Environ Microbiol* **57**: 2804−2809.

Bryant, R.D., and Laishley, E.J. (1990) The role of hydrogenase in anaerobic biocorrosion. *Can J Microbiol* **36**: 259−264.

Butler, J.E., Young, N.D., and Lovley, D.R. (2010) Evolution of electron transfer out of the cell: comparative genomics of six Geobacter genomes. *BMC Genomics* **11**: 1−12.

Butlin, K.R., Adams, M.E., and Thomas, M. (1949) Sulphate-reducing bacteria and internal corrosion of ferrous pipes conveying water. *Nature* **163**: 26−27.

Cord-Ruwisch, R. (2000) Microbially Influenced Corrosion of Steel. In *Environmental Microbe-Metal Interactions*. Lovley, D.R. (ed). Washington, D.C.: ASM Press, pp. 159−173.

Cord-Ruwisch, R., and Widdel, F. (1986) Corroding iron as a hydrogen source for sulfate reduction in growing cultures of sulfate-reducing bacteria. *Appl Microbiol Biotechnol* **25**: 169−174.

Costello, J.A. (1974) Cathodic depolarization by sulphate-reducing bacteria. *S Afr J Sci* **70**: 202−204.

Daniels, L., Belay, N., Rajagopal, B.S., and Weimer, P.J. (1987) Bacterial methanogenesis and growth from CO_2 with elemental iron as the sole source of electrons. *Science* **237**: 509−511.

De Windt, W., Boon, N., Siciliano, S.D., and Verstraete, W. (2003) Cell density related H_2 consumption in relation to anoxic Fe(0) corrosion and precipitation of corrosion products by *Shewanella oneidensis* MR-1. *Environ Microbiol* **5**: 1192−1202.

Dinh, H.T. (2003) Microbiological study of the anaerobic corrosion of iron. *Ph.D.-thesis*. University of Bremen.

Dinh, H.T., Kuever, J., Mußmann, M., Hassel, A.W., Stratmann, M., and Widdel, F. (2004) Iron corrosion by novel anaerobic microorganisms. *Nature* **427**: 829−832.

Enning, D. (2012) Bioelectrical corrosion of iron by lithotrophic sulfate-reducing bacteria. *Ph.D.-thesis.* University of Bremen.

Enning, D., Venzlaff, H., Garrelfs, J., Dinh, H.T., Meyer, V., Mayrhofer, K., Hassel, A.W., Stratmann, M., and Widdel, F. (2012) Marine sulfate-reducing bacteria cause serious corrosion of iron under electroconductive biogenic mineral crusts. *Environ Microbiol*: *in press.*

Ferris, F.G., Jack, T.R., and Bramhill, B.J. (1992) Corrosion products associated with attached bacteria at an oil field water injection plant. *Can J Microbiol* **38**: 1320−1324.

Flemming, H.C. (1994) Microbial deterioration of materials − fundamentals − econom-ical and technical overview. *Mater Corros* **45**: 5−9.

Gaines, R. (1910) Bacterial activity as a corrosive influence in the soil. *J Ind Eng Chem* **2**: 128−130.

Gaylarde, C.C. (1992) Sulfate-reducing bacteria which do not induce accelerated corrosion. *Int Biodet Biodegr* **30**: 331−338.

Grundmeier, G., Schmidt, W., and Stratmann, M. (2000) Corrosion protection by organic coatings: electrochemical mechanism and novel methods of investigation. *Electrochim Acta* **45**: 2515−2533.

Hamilton, W.A. (1985) Sulphate-reducing bacteria and anaerobic corrosion. *Annu Rev Microbiol* **39**: 195−217.

Hamilton, W.A. (2003) Microbially influenced corrosion as a model system for the study of metal microbe interactions: a unifying electron transfer hypothesis. *Biofouling* **19**: 65−76.

Hansson, E.B., Odziemkowski, M.S., and Gillham, R.W. (2006) Formation of poorly crystalline iron monosulfides: Surface redox reactions on high purity iron, spectroelectrochemical studies. *Corros Sci* **48**: 3767−3783.

Hardy, J.A. (1983) Utilization of cathodic hydrogen by sulphate-reducing bacteria. *Br Corros J* **18**: 190−193.

Hardy, J.A., and Bown, J.L. (1984) The corrosion of mild steel by biogenic sulfide films exposed to air. *Corrosion* **40**: 650−654.

Horvàth, J., and Sölti, M. (1959) Beitrag zum Mechanismus der anaeroben Korrosion der Metalle im Boden. *Mater Corros* **10**: 624−630.

Hubert, C., Nemati, M., Jenneman, G., and Voordouw, G. (2005) Corrosion risk associated with microbial souring control using nitrate or nitrite. *Appl Microbiol Biotechnol* **68**: 272−282.

Iofa, Z.A., Batrakov, V.V., and Cho-Ngok-Ba (1964) Influence of anion adsorption on the action of inhibitors on the acid corrosion of iron and cobalt. *Electrochim Acta* **9**: 1645−1653.

Jack, T.R. (2002) Biological corrosion failures. In *ASM Handbook Volume 11: Failure Analysis and Prevention*. Shipley, R.J., and Becker, W.T. (eds). Materials Park: ASM International, pp. 881−898.

Jack, T.R., Wilmott, A., Stockdale, J., Van Boven, G., Worthingham, R.G., and Sutherby, R.L. (1998) Corrosion consequences of secondary oxidation of microbial corrosion. *Corrosion* **54**: 246−252.

Jack, T.R., Wilmott, M.J., and Sutherby, R.L. (1995) Indicator minerals formed during external corrosion of line pipe. *Mater Perform* **34**: 19−22.

Kaesche, H. (2003) *Corrosion of Metals: Physicochemical Principles and Current Problems*. Berlin: Springer.

King, R.A., and Miller, J.D.A. (1971) Corrosion by sulphate-reducing bacteria. *Nature* **233**: 491−492.

King, R.A., Miller, J.D.A., and Smith, J.S. (1973) Corrosion of mild steel by iron sulphides. *Br Corros J* **8**: 137−141.

Koch, G.H., Brongers, M.P.H., Thompson, N.G., Virmani, Y.P., and Payer, J.H. (2001) Corrosion cost and preventive strategies in the United States. In: CC Technologies Laboratories. NACE International.

Kruger, J. (2011) Cost of metallic corrosion. In *Uhlig's Corrosion Handbook*. Revie, R.W. (ed). Hoboken, New Jersey: Wiley, pp. 15−20.

Larsen, J., Rasmussen, K., Pedersen, K., Sørensen, K., Lundgaard, T., and Skovhus, T.L. (2010) Consortia of MIC bacteria and archaea causing pitting corrosion in top side oil production facilities. *CORROSION 2010*: NACE International. Paper no. 10252.

Lee, W., and Characklis, W.G. (1993) Corrosion of mild steel under anaerobic biofilm. *Corrosion* **49**: 186−199.

Lee, W., Lewandowski, Z., Morrison, M., Characklis, W.G., Avci, R., and Nielsen, P.H. (1993) Corrosion of mild steel underneath aerobic biofilms containing sulfate-reducing bacteria. Part I: At high dissolved oxygen concentrations. *Biofouling* **7**: 217−239.

Lee, W., Lewandowski, Z., Nielsen, P.H., and Hamilton, W.A. (1995) Role of sulfate-reducing bacteria in corrosion of mild steel - a review. *Biofouling* **8**: 165−194.

Li, S., Kim, Y., Jeon, K., and Kho, Y. (2000) Microbiologically influenced corrosion of underground pipelines under the disbonded coatings. *Met Mater* **6**: 281−286.

Ludwig, W., Strunk, O., Westram, R., Richter, L., Meier, H., Yadhukumar *et al*. (2004) ARB: a software environment for sequence data. *Nucleic Acids Res* **32**: 1363−1371.

Ma, H.Y., Cheng, X.L., Li, G.Q., Chen, S.H., Quan, Z.L., Zhao, S.Y., and Niu, L. (2000) The influence of hydrogen sulfide on corrosion of iron under different conditions. *Corros Sci* **42**: 1669−1683.

MacDonald, D.D., Roberts, B., and Hyne, J.B. (1978) Corrosion of carbon steel during cyclical exposure to wet elemental sulfur and atmosphere. *Corros Sci* **18**: 499−501.

Mara, D.D., and Williams, D.J.A. (1972) Polarisation of pure iron in the presence of iron sulfide minerals. *Br Corros J* **7**: 94−95.

Mori, K., Tsurumaru, H., and Harayama, S. (2010) Iron corrosion activity of anaerobic hydrogen-consuming microorganisms isolated from oil facilities. *J Biosci Bioeng* **110**: 426−430.

Muyzer, G., and Stams, A.J.M. (2008) The ecology and biotechnology of sulphate-reducing bacteria. *Nat Rev Microbiol* **6**: 441−454.

Nešić, S. (2011) Carbon dioxide corrosion of mild steel. In *Uhlig's Corrosion Handbook*. Revie, R.W. (ed). New York: Wiley, pp. 229−245.

Newman, R.C., Rumash, K., and Webster, B.J. (1992) The effect of pre-corrosion on the corrosion rate of steel in neutral solutions containing sulfide − Relevance to microbially influenced corrosion. *Corros Sci* **33**: 1877−1884.

Newman, R.C., Webster, B.J., and Kelly, R.G. (1991) The electrochemistry of SRB corrosion and related inorganic phenomena. *ISIJ Int* **31**: 201−209.

Nielsen, P.H., Lee, W., Lewandowski, Z., Morison, M., and Characklis, W.G. (1993) Corrosion of mild steel in an alternating oxic and anoxic biofilm system. *Biofouling* **7**: 267−284.

Pankhania, I.P., Moosavi, A.N., and Hamilton, W.A. (1986) Utilization of cathodic hydrogen by *Desulfovibrio vulgaris* (Hildenborough). *J Gen Microbiol* **132**: 3357−3365.

Pereira, I.A.C., Ramos, A.R., Grein, F., Marques, M.C., da Silva, S.M., and Venceslau, S.S. (2011) A comparative genomic analysis of energy metabolism in sulfate reducing bacteria and archaea. *Front Microbiol* **2**: 1−18.

Piron, D.L. (1994) *The Electrochemistry of Corrosion*. Houston: NACE Press.

Pruesse, E., Quast, C., Knittel, K., Fuchs, B.M., Ludwig, W.G., Peplies, J., and Glockner, F.O. (2007) SILVA: a comprehensive online resource for quality checked and aligned ribosomal RNA sequence data compatible with ARB. *Nucleic Acids Res* **35**: 7188−7196.

Rabus, R., Hansen, T., and Widdel, F. (2006) Dissimilatory sulfate- and sulfur-reducing prokaryotes. In *The Prokaryotes*. Dworkin, M., Schleifer, K.-H., and Stackebrandt, E. (eds). New York: Springer, pp. 659−768.

Revie, R.W. (2011) *Uhlig's Corrosion Handbook*. New York: Wiley.

Rickard, D., and Luther, G.W. (2007) Chemistry of iron sulfides. *Chem Rev* **107**: 514−562.

Schaschl, E. (1980) Elemental sulfur as a corrodent in deaerated, neutral aqueous solutions. *Mater Perform* **19**: 9−12.

Sherar, B.W.A., Power, I.M., Keech, P.G., Mitlin, S., Southam, G., and Shoesmith, D.W. (2011) Characterizing the effect of carbon steel exposure in sulfide containing solutions to microbially induced corrosion. *Corros Sci* **53**: 955−960.

Shi, L., Squier, T.C., Zachara, J.M., and Fredrickson, J.K. (2007) Respiration of metal (hydr)oxides by *Shewanella* and *Geobacter*: a key role for multihaem c-type cytochromes. *Mol Microbiol* **65**: 12−20.

Shoesmith, D.W., Taylor, P., Bailey, M.G., and Owen, D.G. (1980) The formation of ferrous monosulfide polymorphs during the corrosion of iron by aqueous hydrogen sulfide at 21°C. *J Electrochem Soc* **127**: 1007−1015.

Smith, J.S., and Miller, J.D.A. (1975) Nature of sulphides and their corrosive effect on ferrous metals: a review. *Br Corros J* **10**: 136−143.

Spruit, C.J.P., and Wanklyn, J.N. (1951) Iron sulphide ratios in corrosion by sulphate-reducing bacteria. *Nature* **168**: 951−952.

Starkey, R.L. (1946) Sulfate reduction and the anaerobic corrosion of iron. *A van Leeuw J Microbiol* **12**: 193−203.

Strycharz, S.M., Glaven, R.H., Coppi, M.V., Gannon, S.M., Perpetua, L.A., Liu, A. *et al*. (2011) Gene expression and deletion analysis of mechanisms for electron transfer from electrodes to *Geobacter sulfurreducens*. *Bioelectrochemistry* **80**: 142−150.

Stumper, R. (1923) Inorganic chemistry: The corrosion of iron in the presence of iron sulphuret. *Cr Hebd Acad Sci* **176**: 1316−1317.

Sun, W., and Nešić, S. (2007) A mechanistic model of H_2S corrosion of mild steel. *CORROSION 2007*: NACE International. Paper no. 07566.

Sun, W., Pugh, D.V., Ling, S., Reddy, R.V., Pacheco, J.L., Nisbet, R.S. et al. (2011) Understanding and quantifying corrosion of L80 carbon steel in sour environments. *CORROSION 2011*: NACE International. Paper no. 11063.

Tiller, A.K. (1983) Electrochemical aspects of corrosion: an overview. In *Microbial Corrosion*. Teddington: The Metals Society. pp. 54−65.

Tiller, A.K., and Booth, G.H. (1962) Polarization studies of mild steel in cultures of sulphate-reducing bacteria. Part 2: Thermophilic organisms. *T Faraday Soc* **58**: 110−115.

Uchiyama, T., Ito, K., Mori, K., Tsurumaru, H., and Harayama, S. (2010) Iron-corroding methanogen isolated from a crude-oil storage tank. *Appl Environ Microbiol* **76**: 1783−1788.

U.S. Geological Survey (2011) *Mineral Commodity Summary 2011. U.S. Geological Survey:* 1−198 [www document]. URL http://minerals.usgs.gov/minerals/pubs/mcs/2011/mcs2011.pdf

Venzlaff, H., Enning, D., Srinivasan, J., Mayrhofer, K., Hassel, M., Widdel, F., and Stratmann, M. (2012). Accelerated cathodic reaction in microbial corrosion of iron due to direct electron uptake by sulfate-reducing bacteria. *submitted*.

Wanklyn, J.N., and Spruit, C.J.P. (1952) Influence of sulphate-reducing bacteria on the corrosion potential of iron. *Nature* **169**: 928−929.

Whitney, W.R. (1903) The corrosion of iron. *J Am Chem Soc* **25**: 394−406.

Widdel, F. (1992) Microbial Corrosion. In *Biotechnology Focus 3*. Finn, R.K., Prave, P., Schlingmann, M., Crueger, W., Esser, K., Thauer, R., and Wagner, F. (eds). Munich: Hanser, pp. 277−318.

Wikjord, A.G., Rummery, T.E., Doern, F.E., and Owen, D.G. (1980) Corrosion and deposition during the exposure of carbon steel to hydrogen sulfide-water solutions. *Corros Sci* **20**: 651−671.

von Wolzogen Kühr, C.A.H. (1961) Unity of anaerobic and aerobic iron corrosion process in the soil. *Corrosion* **17**: 119−125.

von Wolzogen Kühr, C.A.H., and van der Vlugt, L.S. (1934) The graphitization of cast iron as an electrobiochemical process in anaerobic soil. *Water* **18**: 147−165.

Zhang, T., and Fang, H.H.P. (2001) Phylogenetic diversity of a SRB-rich marine biofilm. *Appl Microbiol Biotechnol* **57**: 437−440.

Acknowledgements

First, I wish to thank my academic supervisor, Prof. Dr. Friedrich Widdel, for all his support during the last years and for giving me the opportunity to work on this exciting topic in the first place. I appreciated the 'scientific independence' you granted me at some times, while there was always so much to learn for me when we worked together on the principles and problems of microbial corrosion. Thank you for all the time and enthusiasm that you have dedicated to this project.

A special thank goes to my thesis evaluation committee. Prof. Dr. Karl-Heinz Blotevogel, who agreed to be my second reviewer and thus again delve into corrosion science. Thanks also to Prof. Dr. Ulrich Fischer for his involvement and Prof. Dr. Bo Thamdrup who has agreed to come all the way from Odense to attend my thesis defense.

I am very indebted to everybody involved in the microbial corrosion project. Particularly, thank you, Julia, for great team work, relentless support and a fantastic working atmosphere! I will never forget our lively discussions about microbial corrosion and tropical fish. Much of the work was performed with Hendrik Venzlaff at the MPI for Iron Research in Düsseldorf. Thank you, Hendrik, for the fruitful collaboration. I really had a great time during all those hours performing SEM and XRD and always enjoyed lunch with you at McMensa. Also thank you, Rebecca, for all your support during the last two years. I hope you will stay involved in the project.

I further appreciated the collaboration with our colleagues in Düsseldorf: Dr. Karl Mayrhofer, Pascal Beese, Prof. Dr. Achim W. Hassel and Prof. Dr. Martin Stratmann.

Special thanks go to Dr. Thomas Holler, without whom the Department of Microbiology just would not be the same. I very much enjoyed your high spirits and learned a lot from you, Thomas. Thanks to PD Dr. Jens Harder who was always supportive and keeps our department running. Special thanks for technical support to Ramona Appel, Kirsten Imhoff, Volker Meyer, Andrea Mingers and Daniel Kurz. There are so many supportive people at our institute and in Düsseldorf, at the MPI for Iron Research. I also wish to thank Karina van der Heijden for help with ARB.

My work was very much supported by Bernd Stickfort who always found all the right literature I needed.

I am also grateful to all my students and lab assistants, particularly to Juliane Wippler, Jessika Füssel, Robert Marmulla, Rebecca Ansorge and Johanna Radziejewski.

The time here in Bremen would not have been the same if it were not for my MarMic class 2010 (+ Ivo). I found friends for life.

Thanks to all friends at the MPI and also to all former and current members of my office.

Zum Ende hin gilt mein ganz besonderer Dank natürlich meiner Familie. Ich danke meinen Eltern für die jahrelange Unterstützung und den Rückhalt, den sie mir gegeben haben. Ich möchte mich auch bei meinen Brüdern Philipp und Simon dafür bedanken, dass sie über manche Eigenheiten des „Forschers“ hinweggesehen haben. Mein Dank gilt auch meinem engsten Freund Richard Dehn. Ein sehr schöner Nebenaspekt meiner Arbeiten am MPI in Düsseldorf waren die damit verbundenen Besuche bei meinen Großeltern. Danke an Euch, dass ihr mich während unzähliger Dienstreisen beherbergt und so gut umsorgt habt.

Zum Abschluss danke ich besonders Dir, Julie, für all Dein Verständnis und Deine Unterstützung während der letzten Jahre.